TECHNISCHE UNIVERSITÄT DRESDEN

Faculty of Environmental Sciences

Title of the dissertation

Methodology for High Resolution Spatial Analysis of the Physical Flood Susceptibility of Buildings in Large River Floodplains

Dissertation for awarding the academic degree
Doctor Engineer (Dr.-Ing.)

Submitted by:
M.Sc. Ángela Blanco-Vogt
Born on 31st October 1979 in Bogotá, Colombia

Thesis supervisors:
Prof. Dr. rer. nat. Jochen Schanze
Chair of Environmental Development and Risk Management
Faculty of Environmental Science
Technische Universität Dresden

Prof. Dr.-Ing. Norbert Haala
Institute for Photogrammetry
University of Stuttgart

Dissertation defense: 17th December 2015, Dresden

Declaration

This is to certify that this copy is fully congruent with the original copy of the thesis with the topic:

“Methodology for High Resolution Spatial Analysis of the Physical Flood Susceptibility of Buildings in Large River Floodplains”

Stuttgart, 5th April 2015

TECHNISCHE UNIVERSITÄT DRESDEN

Fakultät Umweltwissenschaften

Thema der Dissertation

Methodik für eine räumlich hochauflösende Analyse der physischen Anfälligkeit von Gebäuden gegenüber Hochwasser in großen Flussgebieten

Dissertation zur Erlangung des akademischen Grades

Doktoringenieur (Dr.-Ing.)

vorgelegt von

M.Sc. Ángela Blanco-Vogt

geboren am: 31.10.1979 in: Bogotá, Kolumbien

Gutachter:

Prof. Dr. rer. nat. Jochen Schanze

Professur für Umweltentwicklung und Risikomanagement

Fakultät Umweltwissenschaften

Technische Universität Dresden

Prof. Dr.-Ing. Norbert Haala

Institut für Photogrammetrie

Universität Stuttgart

Dissertationsverteidigung: 17.12.2015, Dresden

Erklärung des Promovendin

Die Übereinstimmung dieses Exemplars mit dem Original der Dissertation zum Thema:

„Methodik für eine räumlich hochauflösende Analyse der physischen Anfälligkeit von Gebäuden gegenüber Hochwasser in großen Flussgebieten“

wird hiermit bestätigt.

Stuttgart, 5. April 2015

Acknowledgement

I wish to express my thankfulness and appreciation to people and organisations, who have contributed significantly to the creation of this thesis by helping me to select and evaluate the resources.

First of all, I am grateful to IPSWaT (International Postgraduate Studies in Water Technology – supported by the Federal Ministry of Education and Research, BMBF) for funding my fellowship. To my supervisor Prof. Dr. Jochen Schanze, who permitted me to pursue a PhD at the TU Dresden: Thank you for encouraging me and teaching me how to organise ideas and create well-structured concepts and for all the time, patience and the valuable supervision. I am also grateful to my second supervisor Prof. Dr. Haala for guiding me in the fields of photogrammetry and building extraction. To Dr. Behnisch, Dr. Schinke, Dr. Nikolowski and Dr. Naumann of the IÖR for listening to my ideas and giving me valuable comments. I also want to thank my colleagues in the chair Urbone, Velazquez, Trümper, Burmeister, Szajda-Birnfeld and Mercado for discussing ideas and for many amusing coffee breaks and lunches.

I would like to thank the Geobasisinformation und Vermessung in Dresden, IGAC, DATUM Ing and GeoEye for providing the data for this application. I would like to express my appreciation to Carlos Andrés Perea for helping me to develop the web and mobile applications. Thanks to Alexander Martínez and Yadira Torres in the UNGRD, Prof. José Manuel Abello of the Fundación Santo Domingo, Prof. Manuel Alvarado, and Ciro Parrado for fruitful discussions and advice on my research in the pilot sites in Colombia. A special thanks to Armando Mora Serpa, Alberto Rojano, Gustavo Rojano and Nancy López for supporting me during my field works.

I am very grateful to my family: my mother, sister, uncles, aunts and family in law for their moral support and Melanie Vogt for the time and patience for the English corrections and for assisting me in every circumstance. Most importantly, I would like to thank my husband for his love, for taking photographs in the field, for his patience and optimistic ideas.

Abstract

The impacts of floods on buildings in urban areas are increasing due to the intensification of extreme weather events, unplanned or uncontrolled settlements and the rising vulnerability of assets. There are some approaches available for assessing the flood damage to buildings and critical infrastructure. To this point, however, it is extremely difficult to adapt these methods widely, due to the lack of high resolution classification and characterisation approaches for built structures. To overcome this obstacle, this work presents: first, a conceptual framework for understanding the physical flood vulnerability and the physical flood susceptibility of buildings, second, a methodological framework for the combination of methods and tools for a large-scale and high-resolution analysis and third, the testing of the methodology in three pilot sites with different development conditions.

The conceptual framework narrows down an understanding of flood vulnerability, physical flood vulnerability and physical flood susceptibility and its relation to social and economic vulnerabilities. It describes the key features causing the physical flood susceptibility of buildings as a component of the vulnerability. The methodological framework comprises three modules: (i) methods for setting up a building topology, (ii) methods for assessing the susceptibility of representative buildings of each building type and (iii) the integration of the two modules with technological tools.

The first module on the building typology is based on a classification of remote sensing data and GIS analysis involving seven building parameters, which appeared to be relevant for a classification of buildings regarding potential flood impacts. The outcome is a building taxonomic approach. A subsequent identification of representative buildings is based on statistical analyses and membership functions.

The second module on the building susceptibility for representative buildings bears on the derivation of depth-physical impact functions. It relates the principal building components, including their heights, dimensions and materials, to the damage from different water levels. The material's susceptibility is estimated based on international studies on the resistance of building materials and a fuzzy expert analysis. Then depth-physical impact functions are calculated referring to the principal components of the buildings which can be affected by different water levels. Hereby, depth-physical impact functions are seen as a means for the interrelation between the water level and the physical impacts.

The third module provides the tools for implementing the methodology. This tool compresses the architecture for feeding the required data on the buildings with their relations to the building typology and the building-type specific depth-physical impact function supporting the automatic process.

The methodology is tested in three flood plains pilot sites: (i) in the settlement of the Barrio Sur in Magangué and (ii) in the settlement of La Peña in Cicuco located on the flood plain of Magdalena River, Colombia and (iii) in a settlement of the city of Dresden, located on the Elbe River, Germany. The testing of the methodology covers the description of data availability and accuracy, the steps for deriving the depth-physical impact functions of representative buildings and the final display of the spatial distribution of the physical flood susceptibility.

The discussion analyses what are the contributions of this work evaluating the findings of the methodology's testing with the dissertation goals. The conclusions of the work show the contributions and limitations of the research in terms of methodological and empirical advancements and the general applicability in flood risk management.

Kurzfassung

In vielen Städten nehmen die Auswirkungen von Hochwasser auf Gebäude aufgrund immer extremerer Wetterereignisse, unkontrollierbarer Siedlungsbauten und der steigenden Vulnerabilität von Besitztümern stetig zu. Es existieren zwar bereits Ansätze zur Beurteilung von Wasserschäden an Gebäuden und Infrastrukturknotenpunkten. Doch ist es bisher schwierig, diese Methoden großräumig anzuwenden, da es an einer präzisen Klassifizierung und Charakterisierung von Gebäuden und anderen baulichen Anlagen fehlt. Zu diesem Zweck sollen in dieser Arbeit erstens ein Konzept für ein genaueres Verständnis der physischen Vulnerabilität von Gebäuden gegenüber Hochwasser dargelegt, zweitens ein methodisches Verfahren zur Kombination der bestehenden Methoden und Hilfsmittel mit dem Ziel einer großräumigen und hochauflösenden Analyse erarbeitet und drittens diese Methode an drei Pilotstandorten mit unterschiedlichem Ausbauzustand erprobt werden.

Die Rahmenbedingungen des Konzepts grenzen die Begriffe der Vulnerabilität, der physischen Vulnerabilität und der physischen Anfälligkeit gegenüber Hochwasser ein und erörtern deren Beziehung zur sozialen und ökonomischen Vulnerabilität. Es werden die Merkmale der physischen Anfälligkeit von Gebäuden gegenüber Hochwasser als Bestandteil der Vulnerabilität definiert. Das methodische Verfahren umfasst drei Module: (i) Methoden zur Erstellung einer Gebäudetypologie, (ii) Methoden zur Bewertung der Anfälligkeit repräsentativer Gebäude jedes Gebäudetyps und (iii) die Kombination der beiden Module mit Hilfe technologischer Hilfsmittel.

Das erste Modul zur Gebäudetypologie basiert auf der Klassifizierung von Fernerkundungsdaten und GIS-Analysen anhand von sieben Gebäudeparametern, die sich für die Klassifizierung von Gebäuden bezüglich ihres Risikopotenzials bei Hochwasser als wichtig erweisen. Daraus ergibt sich ein Ansatz zur Gebäudeklassifizierung. Die anschließende Ermittlung repräsentativer Gebäude beruht auf statistischen Analysen und Zugehörigkeitsfunktionen.

Das zweite Modul zur Anfälligkeit repräsentativer Gebäude beruht auf der Ableitung von Funktion von Wasserstand und physischer Einwirkung. Es setzt die relevanten Gebäudemerkmale, darunter Höhe, Maße und Materialien, in Beziehung zum erwartbaren Schaden bei unterschiedlichen Wasserständen. Die Materialanfälligkeit wird aufgrund internationaler Studien zur Festigkeit von Baustoffen sowie durch Anwendung eines Fuzzy-Logic-Expertensystems eingeschätzt. Anschließend werden Wasserstand-Schaden-Funktionen unter Einbeziehung der Hauptgebäudekomponenten berechnet, die durch unterschiedliche Wasserstände in Mitleidenschaft gezogen werden können. Funktion von Wasserstand und physischer Einwirkung dienen hier dazu, den jeweiligen Wasserstand und die physischen Auswirkung in Beziehung zueinander zu setzen.

Das dritte Modul stellt die zur Umsetzung der Methoden notwendigen Hilfsmittel vor. Zur Unterstützung des automatisierten Verfahrens dienen Hilfsmittel, die die Gebäudetypologie mit der Funktion von Wasserstand und physischer Einwirkung für Gebäude in Hochwassergebieten kombinieren.

Die Methoden wurden anschließend in drei hochwassergefährdeten Pilotstandorten getestet: (i) in den Siedlungsgebieten von Barrio Sur in Magangué und (ii) von La Pena in Cicuco, zwei Überschwemmungsgebiete des Magdalenas in Kolumbien, und (iii) im Stadtgebiet von Dresden, das an der Elbe liegt. Das Testverfahren umfasst die Beschreibung der Datenverfügbarkeit und -genauigkeit, die einzelnen Schritte zur Analyse der. Funktion von Wasserstand und physischer Einwirkung repräsentativer Gebäude sowie die Darstellung der räumlichen Verteilung der physischen Anfälligkeit für Hochwasser.

In der Diskussion wird der Beitrag dieser Arbeit zur Beurteilung der Erkenntnisse der getesteten Methoden anhand der Ziele dieser Dissertation analysiert. Die Folgerungen beleuchten abschließend die Fortschritte und auch Grenzen der Forschung hinsichtlich methodischer und empirischer Entwicklungen sowie deren allgemeine Anwendbarkeit im Bereich des Hochwasserschutzes.

Resumen

El impacto de las inundaciones sobre los edificios en zonas urbanas es cada vez mayor debido a la intensificación de los fenómenos meteorológicos extremos, asentamientos no controlados o no planificados y su creciente vulnerabilidad. Hay métodos disponibles para evaluar los daños por inundación en edificios e infraestructuras críticas. Sin embargo, es muy difícil implementar estos métodos sistemáticamente en grandes áreas debido a la falta de clasificación y caracterización de estructuras construidas en resoluciones detalladas. Para superar este obstáculo, este trabajo se enfoca, en primer lugar, en desarrollar un marco conceptual para comprender la vulnerabilidad y susceptibilidad física de edificios por inudaciones, en segundo lugar, en desarrollar un marco metodológico para la combinación de los métodos y herramientas para una análisis de alta resolución y en tercer lugar, la prueba de la metodología en tres sitios experimentales, con distintas condiciones de desarrollo.

El marco conceptual se enfoca en comprender la vulnerabilidad y susceptibility de las edificaciones frente a inundaciones, y su relación con la vulnerabilidad social y económica. En él se describen las principales características físicas de la susceptibilidad de edificicaiones como un componente de la vulnerabilidad. El marco metodológico consta de tres módulos: (i) métodos para la derivación de topología de construcciones, (ii) métodos para evaluar la susceptibilidad de edificios representativos y (iii) la integración de los dos módulos a través herramientas tecnológicas.

El primer módulo de topología de construcciones se basa en una clasificación de datos de sensoramiento rémoto y procesamiento SIG para la extracción de siete parámetros de las edficaciones. Este módulo parece ser aplicable para una clasificación de los edificios en relación con los posibles impactos de las inundaciones. El resultado es una taxonomía de las edificaciones y una posterior identificación de edificios representativos que se basa en análisis estadísticos y funciones de pertenencia.

El segundo módulo consiste en el análisis de susceptibilidad de las construcciones representativas a través de funciones de profundidad del impacto físico. Las cuales relacionan los principales componentes de la construcción, incluyendo sus alturas, dimensiones y materiales con los impactos físicos a diferentes niveles de agua. La susceptibilidad del material se calcula con base a estudios internacionales sobre la resistencia de los materiales y un análisis a través de sistemas expertos difusos. Aquí, las funciones de profundidad de impacto físico son considerados como un medio para la interrelación entre el nivel del agua y los impactos físicos.

El tercer módulo proporciona las herramientas necesarias para la aplicación de la metodología. Estas herramientas tecnológicas consisten en la arquitectura para la alimentación de los datos relacionados a la tipología de construcciones con las funciones de profundidad del impacto físico apoyado en procesos automáticos.

La metodología es probada en tres sitios piloto: (i) en el Barrio Sur en Magangué y (ii) en la barrio de La Peña en Cicuco situado en la llanura inundable del Río Magdalena, Colombia y (iii) en barrio Kleinzschachwitz de la ciudad de Dresden, situado a orillas del río Elba, en Alemania. Las pruebas de la metodología abarca la descripción de la disponibilidad de los datos y la precisión, los pasos a seguir para obtener las funciones profundidad de impacto físico de edificios representativos y la presentación final de la distribución espacial de la susceptibilidad física frente inundaciones

El discusión analiza las aportaciones de este trabajo y evalua los resultados de la metodología con relación a los objetivos. Las conclusiones del trabajo, muestran los aportes y limitaciones de la investigación en términos de avances metodológicos y empíricos y la aplicabilidad general de gestión del riesgo de inundaciones.

Contents

Abbreviations

The following abbreviations are used in this dissertation:

APFM:	Associated Programme on Flood Management
ASPRS:	American Society for Photogrammetry and Remote Sensing
BMZ:	Federal Ministry for Economic Cooperation and Development – Germany
BMBF:	Federal Ministry of Education and Research – Germany
CRED:	Centre for Research on the Epidemiology of Disasters
CEDIM:	Center for Disaster Management and Risk Reduction Technology – Germany
DEFRA:	Department for Environment, Food & Rural Affairs – UK
DEM:	Digital Elevation Model
DSM:	Digital Surface Model
DTM:	Digital Terrain Model
DSS:	Decision Support System
EERI:	Earthquake Engineering Research Institute
EEA:	European Environment Agency
EVDAB:	European database of vulnerabilities to natural hazards
FEMA:	Federal Emergency Management Agency of the USA
FLEMO:	Flood Loss Model
GEF:	Global Environment Facility
GFDRR:	Global Facility for Disaster Reduction
GIS:	Geographic Information System
GWP:	Global Water Partnership
HAZUS:	Hazards United States
HOWAD:	Flood Damage Simulation Model
ICDE:	Infraestructura Colombiana de Datos Espaciales
IOER:	Leibniz Institute of Ecological Urban and Regional Development – Germany
IDEAM:	Instituto de hidrología, metereología y estudios ambientales – Colombia
IDM:	Internal Displacement Monitoring Centre
IFRC:	International Federation of Red Cross And Red Crescent Societies
ISPRS:	International Society for Photogrammetry and Remote Sensing
IPCC:	Intergovernmental Panel on Climate Change
LiDAR:	Light Detection And Ranging
LISFLOOD:	Rainfall-Runoff Model
NIBS:	National Institute of Building Sciences
NDVI:	Normalized Difference Vegetation Index
RADAR:	Radio Detection And Ranging
SDD:	Standard Distance Deviation
SIAC:	Sistema de Información Ambiental de Colombia
SMS:	Surface Water Modelling
UNISDR:	United Nations International Strategy for Disaster Reduction
UNFPA:	United Nations Population Fund
UNOCHA:	United Nations Office for the Coordination of Humanitarian Affairs
UST:	Urban Structure Types
WAVOS:	Water Level Prediction System
WMO:	World meteorological organization

1 Introduction

1.1 Background

Floods are natural events which may cause fatalities and injuries to people, negative physical impacts to buildings and infrastructure and economic losses worldwide. The WMO (2014) reports based on global data from 1970 to 2012 by natural hazard type that flood caused 44 % of the amount of disasters, 34 % of the economic losses and 14 % of deaths. The 10 worst disasters in terms of lives lost occurred primarily in least developed and developing countries and the economic losses originated predominantly in developed countries and in countries with economies in transition. The IDMC (2014) reveals that 57% of the displacements have been initiated by floods. Munich Re (2013, p. 1) states that "floods dominate natural catastrophe statistics in the first half of 2013 […] being one of the devastating natural hazards in terms of occurrence and impacts". In fact, "[…] the number of victims from hydrological disasters increased by 98.9 % compared to the yearly average of the last decade" (CRED et al., 2010, p. 21). The rainy season 2010 in Colombia, for example, has affected more than 4 million people and over 400 persons lost their lives in 561 municipalities in 28 departments and the capital settlement of Bogotá (OCHA, 2010). "A rescue operation over 200,000 people due to floodings has been launched in India during 2014" (IFRC, 2014).

Settlements have often grown in flood-prone areas and they have changed the morphology of the landscape, leading to an increase of impervious areas heavily affecting the surface runoff (Ashley et al., 2007). Flood-prone areas are flat, which facilitates the development of infrastructure and economic activities. Moreover, half of the world's population lives in urban areas (UNFPA, 2008). This increases the chance that human settlements are located in hazardous areas along rivers, lakes or reservoirs or even inside dried up river beds, where floods are only a matter of time (APFM, 2008). Indeed, "[…] more than half of all deaths from natural disasters occur in underdeveloped countries, especially in dangerous locations with increasing uncontrolled urban growth and slum building" (BMZ, 2010, p. 14). Additionally, the combination of human activities in floodplains and extreme natural events may trigger complex social, economic and ecological impacts, for which the analysis should include concepts, methods and technical tools supporting the assessments of their impacts. Jha et al. (2012) point out the need to integrate a specific set of solutions in urban flooding areas.

Analyses of the flood susceptibility of buildings are scarce, which may negatively infer the proper and efficient allocation of risk reduction measures (e.g. UNISDR, 2004). Various approaches are available for assessing the flood damage to buildings and critical infrastructure based on field data collected after an event, such as FLEMO (Flood Loss Estimation Model) by (Kreibich et al., 2010), as well as synthetic approaches for assessing the damage prior to a future event, as e.g. HAZUS (HAZards United States) by Scawthorn et al. (2006) and HOWAD (Flood Damage Simulation Model) by Neubert et al. (2014).

However, up to now these methods cannot be applied when information about built structures is missing and extensive field surveys are unfeasible. Analyses of the flood susceptibility of buildings are scarce as well, which may negatively infer the proper and efficient allocation of risk reduction (UNISDR, 2004). Experts often manage the flood risk while lacking observational data on flood plain areas on the local level and they have to solve this by surveying basic information. UNISDR (2007) argues that there is a need for a depth analysis of detailed scales on structures in large river floodplains in order to identify specific activities for disaster prevention, mitigation, preparedness and vulnerability reduction. Merz et al. (2004, p. 162) demonstrate the need to improve the refinement, standardisation and validation of data collection for a flood damage estimation. Beyond, Schanze (2006) states that the analysis of damages in buildings caused by floods may not only be carried out post-event; it should also be used prospectively as an issue in science and practice.

Hence, there are many challenges regarding the flood impact assessment of buildings located in flood plains as information about the building structure is lacking, the scales of land use maps are not sufficient, surveys are time-consuming and expensive or cadastral data is not available or outdated. What is more, the challenges are much bigger in developing countries because of unplanned or uncontrolled urban development; permanent changes; buildings were erected at different periods with heterogeneous structures, often without any urban regulation or defined patterns in blocks or streets. There is a need for methods that assist in standardised data collection on the building susceptibility on an overview level. Not least, detailed damage analyses should be advanced to improve the validity of local in-depth investigation and hence enable simulation of future vulnerabilities and risks.

1.2 State of the art

Existing definitions of flood vulnerability and flood susceptibility based on previous studies and the methods for their assessment are examined in this subchapter, which helps to identify the gaps and challenges in theory and practice.

Regarding to definitions of *vulnerability*, Thywissen (2006) found out that there are 35 different definitions of the term and demonstrated the different points of view and interpretations of the term depending on the expert and the relation to one or several hazards. These definitions are provided by international agencies for disaster assessment, research institutes, governmental agencies as well as medical sciences that have added specific factors to the definition.

Some definitions include social and demographic factors, others economic and environmental components. Some of these factors belong to the same dimension or they are not organised in a structured hierarchy, neither have shown any connection between them. Most of these definitions do not include the factors of buildings or infrastructure. However, the definition of vulnerability tends to focus on the constant changing in time and space of the factors: What is currently vulnerable does not need to be so in the future, and vice versa.

Some of these definitions are given as a formula, or have been expressed as an index, or a degree of loss in qualitative or quantitative models. Hollenstein (2005), who found different types of variables to express vulnerability – namely: as a Boolean variable, a semi-quantitative variable, a fully quantitative variable or an interpolated variable – proposes a generic impact description for vulnerability assessments.

In the compendium of definitions of vulnerability presented by Thywissen, four include the term of susceptibility, six include the term of cope and two the term of resilience. Recent vulnerability definitions have incorporated susceptibility and resilience as relevant components. For instance, Brauch and Oswald Spring (2011, p. 73) describe susceptibility as lack of resilience and in depth as principal variables for the physical components vulnerability. The term of resilience has been frequently incorporated in the definition of vulnerability and applied at different receptors such as communities, buildings, neighbourhoods, urban areas, landscapes and regional areas. It has been discussed by many authors in natural and social sciences (e.g.: Berks et al., 2003; Müller, 2011; Schwarz et al., 2011; Birkmann, 2013).

Further definitions of vulnerability include the institutional dimension (e.g.: Kuhlicke et al. (2011)) or a detailed description and classification of physical factors (e.g.: Douglas (2005); Messner et al. (2007); APFM (2008); BMZ (2010)). The need to unify the term has existed due to the wide range of interpretations (Brauch, 2011; Cardona, 2011; Cutter and Finch, 2008), as stated by Mesjasz (2011, p. 155), "the basic terms are used in a completely uncoordinated manner".

Füssel, 2007 (p. 155) points out that an "[…] appropriate definition of vulnerability is a frequent cause for misunderstanding in interdisciplinary research". He has offered a conceptual framework for describing differences between alternative definitions of vulnerability and provided a comprehensive classification of their factors. Green et al. (2011, p. 22) describe vulnerability as "[…] the chain of interrelationships between the initial points at which the perturbation impacts the system", i.e. an element can trigger the vulnerability of another element in the holistic system. This definition is presented as a guidance to assess flood losses for taking decisions. The conceptual and methodological review of vulnerability provided by Villagrán (2006) provides many different views on vulnerability, describing how the trend to develop models, indicator and indices has increased allowing the comparison of the vulnerability factors. Schanze (2006, p. 16) presents a basic framework, which provides "[…] a mental map for the systematisation of the main components and their relations", and this framework can be extended in detail for each component of the flood risk system.

Additionally, the connection of vulnerability with concepts of adaptation, reduction, recovery, resistance, resilience, perception, coping capacities and mitigation has been emphasised by Janssen and Ostrom (2006); Messner and Meyer (2006); Villagrán (2006); UNISDR (2007); Brauch and Oswald Spring (2011). The concept of vulnerability has also been linked to poverty (GTZ et al., 2008; UNISDR, 2008) and exposure (Fedeski and Gwilliam, 2007) and Leichenko R.M. and O'Brien K.L. (2002) suggest the term 'dynamic vulnerability', that considers the relation between the levels.

We can see that the initial approaches of defining vulnerability are focused on listing the factors which may be impacted, harmed or damaged by a hazard. However, the purpose of recent definitions is to find the relation between these factors, also called 'receptors' and their properties. Moreover, the concept of vulnerability concentrates on the macro, meso or micro level, analysing the intrinsic and contextual properties of the factors. In addition, international agencies such as UNISDR, UNOCHA, IPCC, EEA, GEF, APFM, GFDRR, governmental agencies such as FEMA, CEDIM, DEFRA and research institutes such as CRED and IÖR have developed guidelines for including vulnerability into the flood risk concept.

The term of *susceptibility* is represented as the "[…] sensitivity and exposure of an object to exogenous disturbing forces" (Mesjasz, 2011, p. 129). Susceptibility is also related to preparedness (Messner and Meyer, 2006). It is described as a synonym for "[…] sensitivity, limitations, incapacities or deficiencies" (Villagrán, 2006, p. 11), which are just as important as coping capacity, resistance, resilience or exposition for defining vulnerability. There are many terms linked to *vulnerability* and *susceptibility* from different approaches, hence there is a clear need to differentiate between the various dimensions of vulnerability, their components and their relation.

Regarding to the methods for assessing physical vulnerability and physical susceptibility, Douglas, 2007 (p. 283) expresses the challenges of implementing the methods due to a "[…] lack of observation data, various causes of damage, complexity of the modelling effect of an event on an element" among others. Kasperson et al. (1995), Büchele et al. (2006), Samuels et al. (2006) state that the methods for assessing vulnerability should be in constant improvement and should also be implemented for detailed spatial information after significant change.

Badilla (2002), Büchele et al. (2006), Forte et al. (2006), Messner et al. (2007), EXCIMAP (2007), Cutter and Finch (2008) López (2009), Winsemius et al. (2013) have developed methods for mapping flood vulnerability based on spatial analysis, GIS, remote sensing data; Neubert et al. (2014) develop methods for modelling flood vulnerability; (Balica, 2012) creates flood vulnerability indices as well Cardona et al. (2009) define susceptibility indicator. Hollenstein (2005) suggests that the methods for analysing vulnerability can be autonomously implemented for any type of hazard. Furthermore, Villagrán (2006) provides different methods for a vulnerability assessment at national, megacity and local scales and shows methods, indicators and indices for its assessment.

Flood susceptibility methods have been implemented at regional, urban and building levels. One example at urban scale is the approach of Santangelo et al. (2011), who classify the flood susceptibility based on hydraulic network conditions and the location of the road in relation to the catchment. At the building scales, the study of Cançado et al. (2008) includes social variables such as the poverty index, the residents' employment, education situation, age and house density; economic variables such as the householders' income and physical variables such as the relative vulnerability of the constructions. What Majlingová and Lubinszká (2011), Mourato et al. (2013) consider is population, economic activities, public services, utilities, infrastructure, building height and age. These studies combine social, economic and physical variables.

Qualitative approaches for describing flood impacts on buildings have also been developed. For instance, Kelman (2002) develops the damage scale for a hazard threshold event and defines a boundary between non-failure and failure. Douglas (2007) measures the impacts of flood hazard as low, significant and high or as undamaged, light, moderate, severe, near collapse, collapse impact. Blong (2003) establishes the central damage values and damage classes as light, moderate, heavy, severe and collapse. Maiwald and Schwarz (2009) propose a damage degree for building types based on the building materials and susceptibility class. Other authors such as Green et al. (2011) express susceptibility as a percentage of the total value of the assets, based on the empirical approach using ex-post damages assessment values.

Further methods focusing upon economic damage have been developed for large areas. For instance, the German HOWAD model (Neubert et al., 2014) includes water depth and urban structure types; HAZUS-MH of FEMA Scawthorn et al. (2006) takes into account water depth and flood duration as well as synthetic data of the construction; Japan's numerical model includes flood duration (Dutta et al., 2003; Dutta and Tingsanchali, 2003); the Australian ANUFLOOD considers water velocity, water depth and building types; and the British Multi-Colored Manual (Penning-Rowsell, 2010) presents numerous depth-damage functions for typical buildings, for which information is collected from real events. Velasquez (2011) summarises relevant information of models for damage estimations developed for different institutions in some countries, showing the difference of the models in terms of variables, source of data, type of damage, measurement process, units and tools (see Appendix A). Additionally, these methods cannot be adapted until now where detailed data from the classification and characterisation of the built structure is lacking and extensive field surveys are unfeasible.

Some other approaches just carry out post-event analyses estimating the flood damages inventories in different sectors. The UNGRD (2008) in Colombia uses forms in order to set up an inventory of damages, divided into infrastructure of transport, hospitals, aqueducts, sewage systems, electricity supply, residential buildings and communication sectors. However, these methods have the disadvantage that they increment the degree of uncertainty in the evaluation of damages. The results of those surveys do not cover: any spatial reference for each element, they are not interrelated or the forms are filled by experts who have different levels of knowledge about the damage assessment. Previous impacts or losses during past floods may help to estimate whether the element is exposed or not, whether it can resist or can be impacted. This information may be gathered through questionnaires, field surveys, interview, and the judgment of experts or through information from databases of insurance companies. Fieldworks and the validation of interviews often present an uncertainty and rising costs, which should be avoided, which also makes a systematic analysis of exposure and vulnerability a challenge. Moreover, it is common to observe that in developing countries the focus is put on post-event measures.

Operational tools have been created for the analysis of vulnerability. For instance, CEDIM provides different stage-damage functions for individual objects and an estimation for standardised damages without explicitly specifying the damage in monetary units for residential buildings (Kron, 2007). ReVA (Regional Vulnerability Assessment) "[…] is designed to produce the methods needed to understand a region's environmental quality and its spatial pattern in large scales". EVDAB (European database of vulnerabilities to natural hazards) integrates relevant geo-datasets on urban areas for the identification and the evaluation of vulnerabilities.

Technological approaches such as the one from Levy (2005) integrate multicriteria decision making, remote sensing, GIS, hydrologic models and real-time flood information systems. Qi and Altinakar (2011) present an interactive tool, which combines remote sensing image layers and other GIS feature layers like zoning layer, survey database and census block boundaries for flood damage calculations and the estimation of loss of life. Yi et al. (2010) combine the hydraulic model and the flood damage assessment in a GIS model to estimate economic losses through depth-percentage damage relationships. Fedeski and Gwilliam (2007) describe a process for physical survey and GIS mapping techniques in order to rely on a resource consuming field-work through analysis of secondary data. Eleutério and Martinez (2010) describe the main advantages of using GIS for the evaluation of flood damages analyses as a possibility of "easily" realising the analyses several times, in order to compare different scenarios and study uncertainties. The generation of datasets could be used any time in future to support territorial decision making and the possibility of adding information over time to update the dataset and make other analyses. They present a GIS tool in ArcGIS 9.2 for evaluating potential damages of future floods and damage potential estimations, the assessment of expected annual damage calculations as well as the analysis and interpretation functions. However, new tools must be developed which include the process of data collection of the building characteristics, building materials and building susceptibility in order to improve the damage analysis and to reduce uncertainties.

1.3 Problem statement

Thieken et al. (2010) demonstrate the heterogeneity of data availability, survey methods and results between the models. Freni et al. (2010) state that the uncertainty of the depth-damage functions depend on the data availability and on the quality of the collected data. Moreover, Merz et al. (2004) identify the need for an improved refinement and standardisation of data collection for flood damage estimation, and state that current depth-damage functions may have a large uncertainty. Additionally, these functions present relevant differences for damage assessment in terms of "[…] damage categories considered, the degree of detail, the scale of analysis, the application of basic evaluation principles (e.g. replacement cost, depreciated cost) and the application or non-application of results in benefit-cost and risk analyses" Meyer and Messner (2005, p. 1). Green et al. (2011, p. 39) reveal that "the major problems arise when there is no market price to take as a starting point for deriving an estimate of the economic cost of an undesirable change […]". Jongman et al. (2012) prove the difference of the models for the calculation of flood damages in terms of scale, input data and damage calculation as well as their uncertainties in their outputs. Jongman et al. also identify the need to develop an "[…] advanced differentiation on the basis of observable factors such as assumed building material, type, quality and age, and the average value of content compared to structure value, in combination with artificial inundation scenarios, expert judgement and an improving empirical damage database" (Jongman et al., 2012, p. 3748).

The methods to evaluate susceptibility in buildings are very fuzzy. Therefore, it is necessary to improve their certainty for the assessment of physical susceptibility, which deepens into the intrinsic properties of the building material and structure. Then, the following research question is presented: How can a methodology for the physical flood susceptibility analysis be developed for a large scale, using reliable data sources in order to support the flood damage assessment?

1.4 Objectives

The purpose of this research is to enhance the understanding and to develop and test methods for the analysis of the physical flood susceptibility of buildings on a large scale. To fulfil this aim, the following objectives are addressed:

Advance in a conceptual framework that fosters an in-depth understanding of key features that shape the physical flood vulnerability and susceptibility of buildings in order to reduce the vagueness between the two terms and provide a coherent terminology.

Develop a systematic, transferable and standardised methodological framework that supports pre-event assessment of the physical flood susceptibility at a large scale. This involves derivation of approaches for a building typology, depth-physical impact functions for representative buildings and technological tools facilitating the physical susceptibility analysis.

Test the methodology in areas with different socio-economic conditions to provide proof of general applicability. Hereby, implementation and testing in real sites is seen as a means of empirical data collection and practical flood susceptibility assessment.

Findings will be discussed also considering the interface to subsequent more detailed vulnerability analysis with methods from civil engineering.

1.5 Approach and outline

To achieve these objectives, a conceptual and a methodological framework is developed to ensure the consistency of the methodology that support the flood damage assessment. Frameworks enable the integration and understanding of the theoretical knowledge into practice. The main steps for the development of these frameworks are described as follows:

The development of a conceptual framework is based on the reviewed literature associated with the definition of flood risk system. The definitions of the terms of physical vulnerability and physical susceptibility are clarified in regard to previous studies. The new terminology is framed by an in-depth understanding of the physical aspects of vulnerability and its influence on social and economic vulnerabilities. Additionally, the principal variables used in different methods for the assessment of building susceptibility are analysed. This analysis reveals the relevant variables and sources for the proposed methods. The conceptual framework is presented in *Chapter 2*.

Once the principal key features or variables are identified, field works are carried out in order to check and validate these variables and to find new key features. The methodological framework is shaped, showing how these features could be extracted, parameterised, validated and transferred, based on expert judgements and trial and error testing, asking if these features fit with the proposed susceptibility assessment. Methods for an automatic extraction of building types by using remote sensing data and for the integration of the physical susceptibility assessment methods gathering data from field will be tested. The assessment follows the numerical order of the modules ensuring a generic applicability under different conditions, containing guidance for its operability including the development of tools. The methodology guarantees that the methods are structurally interchangeable with others. Moreover, the methodological framework should support the automation and standardisation of data collection and its assessment in order to improve the empirical knowledge. The development of this framework is presented in *Chapter 3*.

The methods are tested in order to ensure their validity and operationalisation and to find weaknesses. Three pilot sites are selected for testing the methodology: Two in the Magdalena River in a settlement of the city of Magangué, Colombia, as well as the Elbe River in a settlement of the city of Dresden, Germany. What is included is a description of the pilot sites, reasons for the selection, data availability and their accuracy. The result of the testing and the empirical findings are depicted in *Chapter 4,* revealing the applicability, limitation and features which should be improved in the methodology.

In *Chapter 5*, the discussion of both the conceptual and methodological framework links the proposed objectives with the observed results of the testing in the three pilot sites with the literature review.

In *Chapter 6*, the contribution of the research in terms of methodological and empirical results of the physical flood susceptibility and a description of potential challenges for future research demands are argued.

2 Conceptual framework

The state of the art confirms the vagueness of the terms physical vulnerability and physical susceptibility and the need to advance in an in-depth understanding of these entities. Continuing with the basic framework of *flood risk management* developed by Schanze (2006), the two terms will be clarified by including them into a conceptual frame. To accomplish this aim, (i) a condensed review on *flood vulnerability* as part of flood risk with a generic description of its dimensions and its components will be given; (ii) the aspects of *physical flood vulnerability* will be disclosed and (iii) the details about *physical flood susceptibility* and its relations with other levels of vulnerability as well as the common variables for its analyses will be explained. Obviously, it will not be possible to elaborate a unique terminology, but the present framework intends to establish guidelines for the analysis of the physical flood susceptibility in buildings. To begin with the conceptual framework, a brief description of the general concepts of flood risk will be condensed. Flood risk is understood as the interaction of flood hazard and flood vulnerability (see Figure 1).

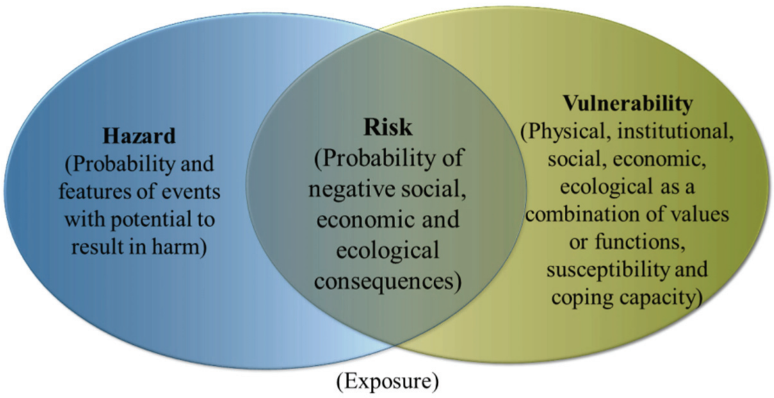

Figure 1: “Risk” in terms of floods (Schanze, 2006)

Flood risk can be defined as the “probability of negative consequences due to floods and depends on the exposure of vulnerable elements to a flood hazard […]” (Schanze, 2006, p. 9). Flood risk can also be defined as the “probability and magnitude of expected losses resulting from interactions between flood hazard and vulnerable conditions” (UNISDR, 2004).

Flood hazard is defined as “the probability and features of events with the potential to cause harm” (Schanze, 2006). “It can exist with or without the presence of people [..]”(FEMA, 2004, p. 1). Flood hazards are defined and characterised according to their features. Some studies on the characteristics of floods are available e.g. for plain floods (OAS, 1991), urban floods (Ashley et al., 2007), flash floods (Egli and Wehner, 2002; Büchele et al., 2006; Adedeji and Salami, 2008), coastal floods, estuarine floods (Dean and Dalrymple, 2001; Carley et al., 2011), groundwater floods and fluvial floods. Floods can be caused by winter rainfalls, summer convectional storms, snowmelt, sea surge and tides, urban sewers, tsunamis, dam breaks or reservoir controls (Schanze, 2006; Ashley et al., 2007). A flood can trigger different types of damages depending on its features such as salinity (Jha et al., 2012), water height, flow velocity, contamination, debris flow deposition, duration etc.

Exposure includes what lies in the area (e.g. people, property, systems or functions) which could be affected by a hazard (FEMA, 2004). Exposure is clearly described by Fedeski and

Gwilliam (2007). The exposure of a building depends on its topological relation with the hazard; the geographic position of buildings is considered as a feature of exposure and hence is not part of the applied vulnerability definition.

2.1 Flood vulnerability

Flood vulnerability is a component of flood risk and may be analysed according to the principle of sustainability, namely in social and cultural, economic and ecological dimensions, held by institutional and physical dimensions, which provide mechanisms and instruments for a balanced system maintenance (UNISDR, 2004; Jha et al., 2012). Beyond that, it can be considered as “a combination of the aspects of *susceptibility, value or function* and *coping capacity”* (Schanze, 2006). Relations between the aspects and the dimensions of vulnerability may exist in the system, which should be analysed as well.

Social flood vulnerability

Social susceptibility is related to a community's predisposition to experience harm by a flood in function of its inherent characteristics, such as living conditions, the inhabitants' occupation, the residential period in the prone zone, the number of sick people as well as the amount of children and social networks. Social susceptibility is shaped by physical and psychological health and indicated by age, gender, education level and physical ability etc. (Samuels et al., 2006; Manyena, 2006; Cutter and Finch, 2008; Lein et al., 2009; Kuhlicke et al., 2011).

The *social function* within a community may be disrupted by a flood event in terms of e.g. disturbances of classes at school, failures of primary services such as water supply, communication, energy system etc. A *social function* is to provide systematic and appropriate means and rules for a communication between their members to ensure the control and continuity of their activities (Lasswell, 1948). The *social value* depends on individual and collective perception and varies substantially within the society (Schanze, 2006).

Social coping capacity may be related to the community’s resilience. How the community may face adverse consequences and make the appropriate choices within the context of its environments to manage the disaster through attitude and motivation. Magsino et al. (2009, p. 3) define community resilience as “[…] a response to stress, and it can be considered as (i) a theory that guides the understanding of stress response dynamics; (ii) a set of adaptive capacities that call attention to the resources that promote successful adaptation capacity in the face of adversity; and (iii) a strategy for disaster readiness against unpredictable and difficult to prepare for dangers”.

The community is able to ensure basic needs with the help of the family, friends, community self-protection teams, which support the cohesion of social systems and access to basic needs. “The coping capacity of communities living in a flood plain with frequent inundation events is probably higher than of persons who have never experienced a flood event” (Samuels et al., 2009). Moreover, Samuels (1999 p. 12) points out that the “vulnerability of a community to flood loss can be mitigated through changing or regulating land use, through flood warning and an effective emergency response”.

Subsequently, floods may cause negative social consequences depending on their characteristics of susceptibility, function and coping capacity*,* such as loss of life, health impacts (injuries, diseases, deterioration of the mental status), loss of vitality, stress, social impacts, loss of personal articles, loss of cultural heritage, loss of archaeological sites, migration processes, change of neighbourhoods (Samuels et al., 2006).

Methods for measuring social vulnerability have been developed by Samuels et al. (2006), Messner et al. (2007), Tapsell (2008), Cutter and Finch (2008), Kuhlicke et al. (2011). Fekete (2009) creates a Social Susceptibility Index (SSI) that includes among others demographic data and socio-economic conditions. Schwarz et al. (2011) for example present a method to measure social vulnerability through interviews and statistical analyses.

The susceptibility of communities might be measured through a *depth-resident function*, considering the negative social consequences in a community for different water depths based on a detailed census of communities located in prone zones.

Economic flood vulnerability

Economic flood vulnerability refers to potential direct and indirect financial losses in industry, agriculture, trades and public services through a damage to property assets, a decrease of productivity, relief efforts, absence of works, a reduction in family incomes etc. (APFM, 2008; Messner et al., 2007).

Economic susceptibility is related to the financial system's inability to provide resources in order to overcome the losses in terms of capital assets, financial obligations, income, limited financial capabilities to respond to that external impact etc. The *economic value* refers to the monetary values. The *economic function* concerns "[…] production, distribution, exchange and consumption" (Mesjasz, 2011, p. 140). *Financial resilience* means how households or communities have the ability to prevent, sustain, compensate or recover from financial shocks or impacts, and depend on flood insurance schemes and financial reserves.

In order to calculate economic losses in buildings, *depth-damage functions* or *stage-damage* functions have been widely implemented, such as linear functions, square root functions, point-based power functions which relate to monetary or perceptual damage losses to the inundation depth using basic information of buildings or structure types, statistical data, indices, non-invasive field surveys, interviews and/or questionnaires or detailed engineering surveys. Depth-damage functions have been broadly implemented (e.g. Smith, 1994; Merz et al., 2004; Kang et al., 2005; Büchele et al., 2006; Messner et al., 2007; Pistrika, 2010; Yi et al., 2010; Naumann et al., 2010; Neubert et al., 2014). But these functions may contain a large uncertainty (Merz et al., 2004).

Depth-damage functions have been implemented and adapted in different areas on the basis of specific criteria or variables, such as the type of damage and hazard, measurement process, units, tool and data source availability. Reese and Ramsay (2010) state that the damages in buildings are normally expressed in terms of monetary costs, such as repair costs or depreciation value; or expressed as a percentage, such as repair cost relative to replacement cost damage or a percentage of real economic values of the building. Depth-damage functions can be derived from estimations of expert assessors (synthetic data) and/or from empirical flood damage data (survey data) (Messner et al., 2007). Depth-damage functions are applied to calculate floods related to damage in buildings by water / moisture, structural impacts and contamination (Naumann et al., 2010). Middelmann-Fernandes (2010) summarises the characteristics of depth-damage function approaches in terms of harm features and characteristics of the building construction used in different countries.

The calculation of the precise economic vulnerability requires both reliable socio-economic information from flood insurances and financial reserves provided by government agencies or insurance companies. This information depends on people's income and tenancy, which may support the analysis of economic losses and compensations. Therefore, this calculation cannot be applied in those parts of the world where detailed information on economic data and rebuilding costs is not available.

Ecological flood vulnerability

Ecological susceptibility refers to the predisposition of ecosystems or species to experience harms caused by flood features. For instance, a high susceptibility of endemic or endangered species could be inferred due to the fact that they may not be able to support saturation or dispersion of heavy metals transported by the flood.

The ecological function of ecosystems such as mangroves, swamps, estuaries, beaches, forests, habitats and species may be disturbed by inundations because they have to face the impacts generated by anthropogenic pollution from sewage, chemicals, heavy metals and other toxic substances. These substances are potentially hazardous and can contaminate the soil and the air or cause landslides, erosion, deterioration and morphological changes (Krapesch et al., 2011; Kruger et al., 2005).

The *ecological coping capacity* refers to the regeneration of the ecosystem's function through a possible biological adaptation of plants to survive an inundation. Hence, floods are hypothesised to have positive impacts as well due to the replenishment of groundwater and the maintenance of a high biological diversity or soil fertility in flood plains (Merz et al., 2004; Penning –Rowsel et al., 2005).

A method for measuring the impact of inundations on specific species, habitats or ecosystems might be developed through a *depth-ecological impact function,* which relates the ecological effects through different features of hazards (contamination, sediments, debris load etc.).

Institutional flood vulnerability

Institutional susceptibility is related to the ability of institutions or governmental agencies to conceptualise, formulate and implement policies, legislation, strategies and programmes for the integration of flood risk management elements. Institutions should engage and build consensus among all stakeholders and the capacity to mobilise information and knowledge (GEF, 2005). They must respond to the flood risk management in a coordinated way. This includes forecasting processes, warning plans, evacuation plans, reaction capability, rescue tasks, financial aids and the preparedness for all legal services. Additionally, "they should establish rules or norms for the definition of roles, rights and responsibilities of actors"(Young, 2002). The *institutional function* in flood risk management might be analysed in terms of availability and reliability of data and information for decision making.

The *coping capacity of institutions* includes prevention and emergency services through technical, financial capacities and the promotion of knowledge enhancements about raising awareness within the community in order to overcome organisational shortcomings. Examples of measures taken for improving the institutional strategies in order to overcome flood losses have been implemented by e.g. Hansson et al. (2008).

Negative consequences in ineffective institutions may potentially lead to a destabilisation of the political climate, to mistrust by the authorities and emergency services, corruption etc. Institutions should also avoid irreversible climate changes as fails of the institution may trigger social, ecological or economic effects (Galaz et al., 2008, p. 145).

2.2 Physical flood vulnerability

In this subchapter the components of the physical flood vulnerability are analysed. Physical vulnerability depends on function or value coping capacity and susceptibility. The term *function* is the purpose for which the building is designed or exists determined by its "assigned duty or activity" and its "specific occupation or role" (Thefreedictionary, 2013). 'V*alue'* refers to "the importance, worth, or usefulness of something". Coping relates to a building's resilience (Brauch and Oswald Spring, 2011) and it is understood as how an "element can deal effectively with something difficult" (Oxford Dictionaries, 2013). *Susceptibility* is understood as the "[…] propensity of buildings to experience harms" (Samuels et al., 2009) as well as "the state or fact of being likely or liable to be influenced or harmed by a particular thing" (Oxford Dictionaries, 2013). These aspects could be analysed for any element within a system.

Buildings and infrastructures are made by men to fulfil a *function* within a particular territory, and this has transformed the landscape. The basic functions of a building are to support "dead loads, live loads and environmental loads […]" (Ochshorn, 2010, p. 39), to protect their inhabitants from rainwater, rough weather, to safeguard them against invaders and enemies, to provide a static structure for their activities or to demonstrate social status or lifestyle through the inventory, furniture or design. Moreover, a building is composed of a "complex system of elements and materials whose construction is based upon physical laws and empirical knowledge, achieving a function for the inhabitants or occupants" (ICE, 2010). Beyond, "[…] the function of building materials determines the performance of the proposed building elements as shelter from heat, cold, noise, sunlight" (Ward-Harvey, 2009, p. x). The combination of components and materials creates a variety of possible building types.

It must also be clarified that a building's use is different from its function. If a building is erected to support a heavy charge, for example, it requires a special structure and design but could just as well be used as a storage warehouse or for institutional activities. For instance, some historical buildings like castles or battalions have changed their use to museums. The use of an individual building can vary through the time, but its function tends to be preserved. However, the function of the buildings has changed with the development of the societies, i.e. each epoch has formed the landscape and brought up different challenges for the construction of buildings as well as the diversity of different styles including a variety of materials, the inclusion of new components and structures for the construction.

An analysis of the principal purposes of buildings in different epochs in Europe is presented by Boults and Sullivan (2010) and reflects how the function of the buildings has changed. In medieval times, for example, castles and walled gardens were built to seek the protection of nature, from enemies or diseases, as well as to construct sacred elements. During the Renaissance, one function of a building was to express the power and authority of humans over nature using creative forms, geometry and figures. During the 20th century, huge buildings and modern malls were built, new equipment and technologies for heating, refrigeration, huge bridges and factories were developed, new modes of transportation were established, and communication systems transformed the way people interacted with the natural world. On the one hand, the 20th century saw the industrial revolution, which brought new construction materials (such as iron, steel and concrete) leading to new elements in the landscape; on the other hand, the slums in cities expanded. In the 21st century, the function of buildings is to face the global climate change, population growth and new paradigms of reducing, reusing and recycling resources.

The *coping capacity or resilience of a building* is considered as "the ability to quickly and efficiently regain the initial state in similar conditions after a hazard". "The vulnerability of physical elements depends on resistance**,** which is the ability to withstand an impact without relevant changes to the system's status" (Naumann et al., 2010). Evans et al. (2006) define "the physical resilience of these buildings as protective elements that allow the constructions to recover quickly and easily". Zevenbergen et al. (2008) point out that resilience in an urban environment should be improved in two aspects: technical aspects on the one hand and political aspects like regulation, decision making and engagement at different levels on the other.

The resilience of a building can be directly related to reconstruction activities meant to overcome the effects caused by a flood and restore the building's original function. These refurbishments could be generalised coarsely as cleansing, drying, painting/repair and replacement activities. Additionally, the refurbishments may be associated to the required personal and the type of financial resources they need including the stress that is required. The estimation of refurbishments of building structures and contents (fixed/mobile inventory) can vary for each country depending on socio-cultural and financial factors, cost estimations are uncertain and data is not updated systematically (Downton and Pielke, 2005). Before economic damages can be calculated, information on the materials and their properties is required, regardless of the monetary units (euros, U.S. dollars or pesos), in order to compare the flood's effects without explicitly calculating the monetary damage.

UNISDR (2004) associates physical vulnerability in accordance with the broader social, economic and environmental requirements of a society. Physical flood vulnerability is not only understood as a mere component of risk management, but it can also be seen as a basic element for determining with better precision the interaction of people with the safety of their environment and their constructions. Because constructions (buildings and infrastructure) are "[…] cultural products representing their inhabitants' ideals and values, situated within a unique social, economic and political environment" (Boults and Sullivan, 2010, p. xi). Physical vulnerability is strongly linked to social and economic vulnerability as the disturbance of the physical elements immediately interrupts or disjoins social and economic activities. Then its interactions with physical and existing social and economic conditions need to be analysed in a holistic approach.

2.3 Physical flood susceptibility

The physical flood susceptibility of buildings "is determined by their structural design, intrinsic properties and the choice of material […]" (Naumann et al., 2010). The susceptibility is related to fragility, weakness, sensibility or instability, here applied to a building which can suffer a physical impact, degradation, failure, loss of structural integrity or deformation of its materials and its components generating incapacity in the building functionalities.

Susceptibility of physical elements depends on their intrinsic properties such as materials, use, condition, size, form, age or structure. Some construction materials of buildings can resist for a maximum of some hours after they have contact with water or flow. After a certain time, these materials will lose their physical properties and can have irreversible failures. In this way, materials can resist certain types of hazards. For example, an element remains unaffected by a plain flood, but not necessarily by flash floods, sediment, debris load or contamination.

A huge variety of intrinsic properties of a building can be analysed, such as the technical constructions, which vary from building to building. Moreover, these techniques are changing and those changes cannot always be predicted. Field surveys for collecting these attributes in large areas for flood physical impact assessments can be very expensive. Therefore, it is necessary to collect the relevant characteristics of the building and classify them for a systematic analysis in order to reduce costs. Building material and technique of the construction define essentially the grade of deterioration of a building caused by the flood. FEMA (2008), Escarameia et al. (2006), Committee and Resources (2006) and BMVBS

(2006) have analysed the performance of materials in the case of floods. However, there is a lack of methods for analysing other material properties in other regions of the world, as the majority of analyses of building materials are carried out after the event in order to find repair solutions and for improving its resilience. Therefore a method for assessing the physical impact on the materials by different water depths should be derived. Here, it is proposed the method: *depth-physical impact function*.

Velasquez (2011) synthesises the principal key features of eight damage flood models that require building characteristics as input: HAZUS (Scawthorn et al., 2006), HOWAD (Neubert et al., 2014) FEMOps and FLEMOcs (Kreibich et al., 2010), Multicolored Manuals (Penning-Rowsell, 2010), ANUFLOOD (Middelmann-Fernandes, 2010), Numerical Model (Dutta et al., 2003) and Synthetic Database (Kang et al., 2005) as well as a post-event assessment presented by Corzo (2010) (see Appendix A). What we see in this review is that most models use synthetic data of the building structure for assessing building damage at large scale and building typologies. This synthetic data is represented in building typologies, as this is a good means for transmitting the analysis of flood impacts in buildings located in large river floodplains. In this section, the building variables are analysed in order to find their applicability for flood physical susceptibility analysis.

Urban Structure Type (UST) seems to be a good approach for grouping buildings with similar characteristics. Blum and Gruhler (2011, p. 46) define "urban structure types as basic urban spatial units with homogenous morphological and functional characters, defined by characteristic structures and development patterns of buildings, infrastructures and open spaces". Haggag and Ayad (2002) define UST as "the relation between built-up areas and constructed and open spaces. Urban structure in its physical sense is significantly influenced by the structure of blocks and their spatial relation to surrounding streets and public accesses". Heiden et al. (2012) define UST as "urban configurations of built-up areas, impervious open spaces, urban green spaces and infrastructure".

UST has worked in a huge variety of fields, and many methods and processes have been developed for its implementation. The urban structure type is used to analyse transportation networks, urban growth, population density, urban changes and impacts (Jiang and Yao, 2010). It is applied in the analysis of surface water networks, the implementation of building regulations, urban blocks or environmental space designs, the connections and interconnections to adjacent structures (Moon et al., 2009), climate change, energy consumption, commonalities and adaptation strategies in urban areas (Blum and Gruhler, 2011). UST patterns of land use, open space and street shape are used to qualify land, air, water and land use and evaluate the implications and opportunities of each for the quality and vitality of neighbourhoods. Thereby, physiognomic or morphological urban characteristics could serve for the identification of building types for different purposes.

Neubert et al. (2014) point out that "urban structure types can also be used to assess the vulnerability of the building environment exposed to flood risks in the context of adaptation to climate change". Füssel (2007) identifies the use of urban structure types as a core indicator for the vulnerability assessment in a spatial procedure. Additionally, Storch (2009) notices that urban structure allows indicators which differentiate between the building complexes and key factors affecting the vulnerability and adaptive capacity of a settlement in a mega-urban region. An example of the implementation of UST is the work of Wieland et al. (2012) who estimate building inventories for a rapid seismic vulnerability assessment. The principal components of UST are: blocks, street patterns and open urban spaces.

Blocks are a central element of urban planning and urban design. Blocks and street patterns are tied up with the functionality and development of the spatial framework and urban structure, which influence the inhabitants' lives as well as the adaptation to new challenges in terms of e.g. public transport, circulation routes for pedestrians and cyclists, vehicular traffic systems or the simple feeling of belonging to a community (Galster et al., 2001).

Street patterns could also be included in the analysis. There are numerous typologies for analysing block and street variables, including shape, dimension, connectivity, public areas, density, distribution, green spaces, age of construction, urbanism regulations, uses etc. Marshall (2005) presents for example a detailed description of different typologies of hierarchy, patterns, connectivity and complexity of route structures which influence the form and structure of urban arrangements. For instance, squares and roundabouts are very important elements for a city's morphology. He concludes that there is not just one way to achieve desired patterns through certain generating processes or particular kinds of design guidance.

Open urban spaces include green spaces and water bodies, which reflect the quality of life, as well as the quality of a city's land, air and water, and they contribute significantly to public health and enjoyment of a community. Open spaces may be categorised in terms of size (e.g. small, medium, large), purpose (e.g. parks, common green areas, private yards, pedestrian paths, protected areas, wildlife habitats or gardens) and distribution (e.g. concentrated or dispersed). Water bodies in urban areas may be categorised in terms of morphological origin (natural, artificial), quality (e.g. polluted or drinking water) and function (e.g. navigation, recreation or wetlands). Many studies evaluate different assessment criteria for natural areas in urban spaces; as is the case in the City of Ottawa (2006) with nine criteria and their respective classification: connectivity, absence of disturbance, habitat maturity, natural communities, regeneration, representative flora, significant flora and fauna, size and shape of the habitat.

Some building properties can be inferred from spatial attributes of the surrounding landscape (Galster et al., 2001). Nevertheless, there are many other relevant building structure attributes such as construction characteristics that cannot be inferred from the spatial attributes of the surrounding landscape. Therefore, the recognition of these building attributes based on the urban structure types in terms of block, street patterns and open areas is a complex task that may not be systematically processed with just one method and the result must be a combination of many typologies for each variable. Block patterns or street patterns are levels of information that interfere with the direct analysis of an intrinsic classification of the building structural characteristics. Even an automatic gathering, characterisation or comparison of the UST criteria in many urban areas in the world can be a strenuous task, which appears unfeasible in areas where buildings have been erected at different periods, with heterogeneous structures, according to different urban regulations and without defining patterns of blocks and streets. In such conditions, there is no clear method for a damage evaluation using only the classification of urban structure types.

Building age reflects and determines the style, material properties and construction technique; it also reflects the processes of adaptation to natural hazards, wars, technological inventions or even construction types according to the socio-political systems. A building's age returns the successes which have marked the way in which the inhabitants of a society interrelate with their landscape. Building age is a principal parameter for flood assessment within the approach of Naumann et al. (2010).

Reasons why these methods for gathering a building’s age cannot always be implemented are the inhabitants' ignorance of the year of construction or the fact that they are just tenants and do not know the process of construction or refurbishment of the buildings. The building age may be determined through the remote or direct use of methods for multi-temporal time series of images, through non-invasive methods comparing urban growth maps, questionnaires and literature or through the inspection of components. Gromicko and London (2011) give some recommendations for the estimation of a building's age, taking into account the shape of the nails, wiring, electrical receptacles, structural panels, meter readers, the toilet, sewer grates as well as architectural styles. The age of the building construction can be categorised by centuries or epochs (e.g. colonial epoch, before or after a war, period after construction of a port). However, these categories cannot be compared to other areas with different periods of development.

Building use is doubtlessly an important variable for the analysis of flood impacts on a building as it allows to get information about the estimation of the inventory and its potential damage calculation. The building use may change temporally and its collecting is laborious and time-consuming and requires techniques combining more than one classification procedure and fieldwork verification. The building use may be collected from urban land use and urban land cover maps. CORINE Land Cover at a scale of 1:25,000 (Bossard et al., 2000) contains standardised methods and techniques for capturing land cover and land uses. Nevertheless, the scale of these maps in urban areas is not detailed enough for heterogeneous and dense areas. Although the building use is an important characteristic, its collection always requires a validation for individual buildings. The classification of building use can vary from region to region. Douglas (2005) for example proposes categories of building uses for the assessment of vulnerability.

Building occupancy reflects the household composition of the building, for example: single building for one household, double building with separate entrances for two households or multi-family buildings with multiple separate housing units within one building or several buildings. Those categories are normally determined in urban plans. Nevertheless, these categories are not clearly defined in areas without an urban regulation, such as slums, or with a mixed building use within the same building.

Building condition can influence the assessment of the damage caused after the flood, but its determination is generally resource-intensive, subjective, time-consuming and costly (Singh Ahluwalia, 2008) and it has not been systematically used up to now for supporting damage calculation. In Colombia, for example, civil engineers evaluated the damages six months after the inundation in the 2010/2011 flood and they could not distinguish between the direct damages caused by the flood and the conditions of the buildings before the flood. A characterisation of building conditions using five classes is proposed by Abbott et al. (2007).

Building density is without doubt an important variable in urban planning and land management, but also an indicator of a city's development (Pan et al., 2008). Brauch (2011, p. 73) states that "physical factors include the location and the susceptibility of the built environment and are often influenced by the 'density levels', 'remoteness of a settlement', 'its sitting design and materials' used for critical infrastructure and for housing". Low density, medium density or high density are categories that can define a building typology. It may be calculated based on the relation of the inhabitants and the lot size of the buildings or the relation between height and size.

Many questions should then be explored about the generation of a building typology for assessing flood impacts in buildings, such as: Which of the above-mentioned variables can be acquired in a systematic process for large areas? Can the variables of urban structure types be automatically collected and implemented for the analysis of flood physical susceptibility? Which other parameters are required for creating a building typology in the analysis of flood physical susceptibility in large flood plains? What are the principal characteristics distinguishing one building from another at the floodplain scales? How should the grouping of building characteristics generally or in detail be done? In addition, how can a building be identified as typical or representative for the analysis in an area or settlement?

A *building typology* results in combining different intrinsic variables collected from different sources and at different scales, such as use, density, condition or inventory for a settlement. For example a combination of variables provides the following categories: 'high density, very high standard, apartment blocks' or 'open structure, low density'. But not all of these variables are always available in many areas of the world. The variables of UST, i.e. building age, building use, building condition and type of occupation, are not always collectable and its typology can vary from region to region. This makes a systematic analysis and the comparison of the huge variety of methods for a classification of the built structures a challenge.

As mentioned in the previous section, the interdependencies between building flood vulnerability and social and economic vulnerabilities are not yet clearly explained due to their inherent systemic complexity. This is an attempt to clear up the relation between them. How can the relation of a building typology and susceptibility of buildings be analysed with the other dimension of vulnerability. A schematic drawing (see Figure 2) describes the complexity of the relation between physical flood vulnerability, economic and social vulnerabilities in terms of susceptibility, function and coping capacity. Figure 2 should be read from bottom to top, illustrating that physical flood vulnerability supports social and economic flood vulnerability.

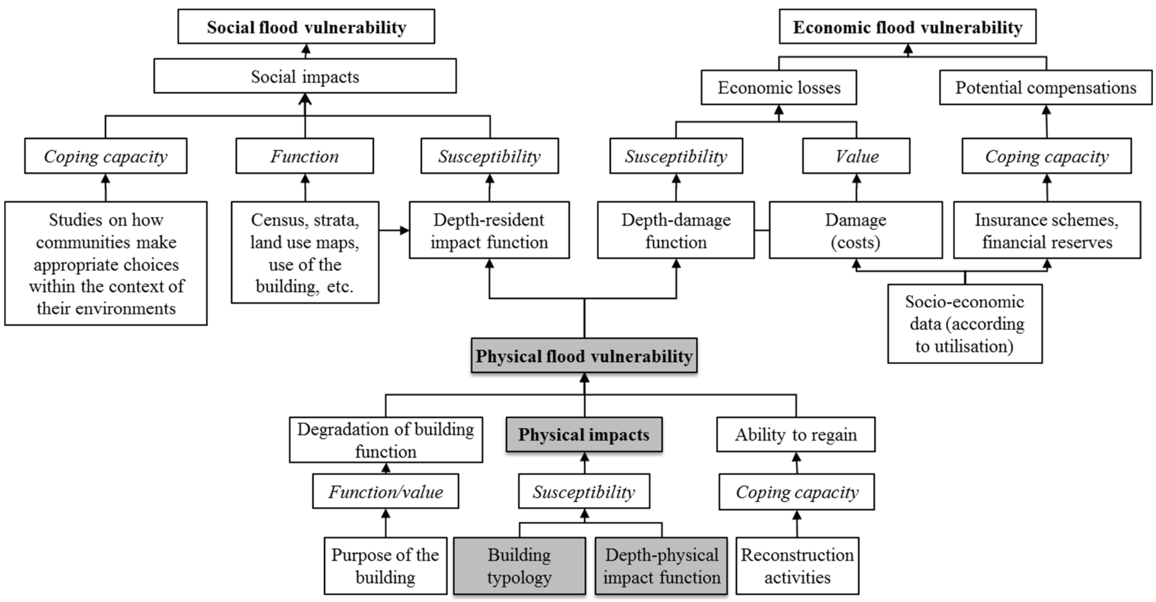

Figure 2: Relation between building vulnerability and social and economic flood vulnerabilities

The physical flood vulnerability is depicted at the bottom of Figure 2 supporting the economic and social flood vulnerabilities. The analysis of the *physical flood susceptibility* of buildings can be simplified through the creation of a *building typology* and for the selection of representative buildings for the analysis of potential impacts of different water depth. This analysis could be carried out using a *depth-physical impact function.* Information about reconstruction activities allows us to infer the ability to regain after a flood (i.e. *physical coping capacity or physical resilience*). Furthermore, as a hypothesis, if the purpose of the building is not altered after a flood event, a degradation of the building function does not exist and vice versa. Further research must be carried out for these last two aspects: the physical flood coping capacity (or resilience) and the physical flood function.

The *social flood vulnerability* analysis may be supported by an evaluation of flood impacts on buildings. For example, it could be inferred that people living in houses with moisture are susceptible to particular diseases, infections or allergic reactions. The WHO (2009) finds sufficient evidence to link health problems to building moisture and biological agents, caused for example by sanitary sewer lines to back up into buildings through drain pipes or contaminated water from fuel tanks. Allergies or respiratory diseases may be potentially triggered in the inhabitants by the presence of mould, muck, insects or toxic sludge in the building materials after a flood. Garvin et al. (2005) describe the direct and indirect health effects caused by flood risk factors in buildings, including guidance for their prevention and restoration. These health issues affect the normal socio-economic activities of families and communities. Moreover, structural impacts on buildings might be a reason for people to migrate or temporally or permanently move to other neighbourhoods.

Additionally, building materials and building structures in a settlement can reflect the social condition of the people living there, e.g. how are they prepared to deal with external sudden disturbances, i.e. if their infrastructure and buildings can protect them against a flood and if they are developing means to protect their activities against potential negative stressors. Building materials and building structures also reveal if the community establishes rules and patterns of constructions and if the construction regulations have been fulfilled to support external impacts. Moreover, the definition of the building's use depends first on its physical characteristics in terms of structure and materials, the regulation of the building's codes established by institutions, the requirements of inhabitants or owners and the market.

The analysis of the social coping capacity requires studies on how communities respond to crises and how they make appropriate choices within the context of their environments in terms of social cohesion, external support provided by family, friends, access to basic needs, community (Thieken et al., 2014). The social function can be determined through land use maps, information of strata and census, which allows us to identify the use of the social variables for the potential of social impacts. The combination of the physical flood vulnerability with the information of the social variables permits us to infer the resident impact function.

The estimation of the *economic flood susceptibility* might be assessed according to the analysis of the building susceptibility in combination with economic data. For instance, the analysis of physical susceptibility may provide the basis for economic feasibility studies, the calculation for rebuilding costs, economic losses in stocks as well as for depth-damage functions. This information might likewise support the analysis of a potential compensation for losses definitely depending on the quality of socio-economic information. Hence, the potential consequences are categorised by a diverse typology, e.g. "[…] direct and indirect impacts or damages, which can be tangible or intangible: Tangible damages can be specified in monetary terms; intangible damages are usually recorded by non-monetary measures" (Messner et al., 2007, p. 11). As an inference, negative consequences on the receptors (buildings) are determined by the degree of the experienced harm, the deterioration of their physical functions and the resilience of constructions regarding to the refurbishment of damage.

A building cannot recover or reconstruct itself after it was harmed, but it requires the engagement of its inhabitants as well as economic resources. The World Bank (2008, p. 142) states that "the vulnerability to flooding is particularly increased where inappropriate or inadequately maintained infrastructure, low-quality shelters and lower resilience of the urban poor intertwine". Those resources are not directly related to the building's internal properties.

The components and material properties of a building should guarantee at most that the building does not suffer cracks, flaking, strain, brittleness, shrinkage, deflection, bending stress, buckling, shearing, expansion or residual stress that affect its proper functionality after an event of inundation. For example, the successive collapse of the walls affects the roof and doors or the moisture load may cause cracks in panels. Then the building's functionality and the potential activities taking place in the building can be affected once one of its element flaws.

Moreover, the study of GTZ et al. (2008) states that the economic aspect has a strong influence on people’s vulnerability to disasters. Additionally, poverty or low incomes make a community particularly vulnerable (BMZ, 2010). Reciprocally, economic vulnerability has a dynamic relationship with social and physical factors. It proves that countries with low incomes suffer most from natural events.

Interventions to strengthen the characteristics of the building and infrastructure can reduce social and economic vulnerabilities, seeking for the lowest disturbances of the system due to an external impact. Hence, it is necessary to develop methods for measuring those interventions or, in other words, increasing flood resilience in regard to the refurbishment of the damage. Detailed information on socio-economic variables could be based on a strata characterisation of the population. For instance, social strata reflect the income of a house's inhabitants in Colombia. Moreover, reference information such as strata maps, which reflect the tenure of certain social groups, could also help to define the inventory. It could be inferred that a group of buildings with similar structural characteristics may possess similar social and economic characteristics. A building typology may therefore simplify the analysis.

Moreover, if information on the living conditions, the inhabitants' occupations, financial obligations or incomes is not available, the physical susceptibility may help to infer these variables. Hereby, the physical flood susceptibility is always a component of the physical flood vulnerability with both belonging to a flood risk system (cf. Schanze, 2006).

Table 1 summarises the relevant definition of the five dimensions of flood vulnerability for all three components, as described in the conceptual framework. The table also shows the proposed method for the assessment and the potential negative consequences for each dimension. The last row gives the potential negative consequences if the element has had contact with flood water. The highlighted cell corresponds to the component this thesis has put its focus on.

Table 1: Summary - scheme of the definition of flood vulnerability

The highlighted cell in this table corresponds to the focused component on this thesis.

	Social	Economic	Ecological	Institutional	Physical
Susceptibility	People's predisposition to experience harm in function of social conditions in terms of occupation, age, residential period, number of sick people based on census population.	The susceptibility of the financial system's inability to provide resources to overcome the losses in terms of capital assets, financial obligations, income etc.	An ecosystem's or species' propensity to experience harm, e.g. protected ecosystems, endemic or endangered species, dispersion of heavy metals in soil, water, vegetation.	An institution's inability in terms of its capacity to conceptualise, formulate and implement policies, legislation, strategies and programmes for FRM, e.g. access to information, legal services.	Propensity of buildings or infrastructure to experience harm depending on its intrinsic properties such as material resistance, structure, age, geometrical characteristics etc.
Value or function	It can be understood as the degradation of the social system in terms of health, education, drinking water supply, wastewater treatment, communication systems, energy etc.	It can be understood as the loans that weaken the system in terms of monetary value and the economic function is concerning “to production, distribution, exchange and consumption”.	It can be understood as the incapacity of an ecosystem to recover its biological and habitat functions, e.g. the mangroves’ incapacity to collect fine sediments to prevent the high-energy wave action.	Weakening of the institutional system in terms of efficiency of prevention and emergency services, data and information supplies for decision making.	Function is defined as the purpose for which the building or infrastructure is designed. A building is designed to support dead loads, live loads and environmental loads such as snow, wind, seismic loads and - for this analysis - flood water contact. Value of the building in terms of quality, status, inventory etc.
Coping capacity or resilience	Social coping capacity is related to a community's skills to make appropriate choices within the context of their environment in terms of social cohesion, external support provided by family, friends, access to basic needs, community.	Financial resilience can be understood as a household's or community's ability to prevent, sustain or recover from financial shocks; depends on flood insurance schemes and financial reserves.	Biological adaptation or regeneration of e.g. plants or animals to survive an inundation or features of the flood.	It can be analysed in terms of technical and financial capacities of institutions, promotion of knowledge enhancements about raising awareness.	Resilience of a building is considered as “the ability to quickly and efficiently regain the initial state in similar conditions after a hazard” and it depends on the social and financial resilience.
Method	Depth-residential impact function	Depth-damage function	Depth-ecological impact function		Depth-physical impact function and building typology
Negative consequences	Flood can cause stress in people, loss of lives, diseases, loss of cultural heritage, change of neighbourhoods, loss of archaeological sites etc.	Can be manifested in terms of economic losses in industry, agriculture, trades, transportation, number of days absent from work etc.	Flood can generate pollution in ecosystems, change of habitats, artificial effects on flora and fauna, morphological degradation etc.	Potential destabilisation of the political climate, mistrust of the authorities and emergency services, corruption etc.	Damage types: moisture/water, structural or contamination (Naumann et al. 2010).

3 Methodological Framework

The previous chapter developed a framework for understanding the wider concepts of flood physical vulnerability and flood physical susceptibility and some of their relations. Schanze (2006) proposes to see vulnerability as a "mathematical" function of susceptibility, value or function and coping capacity of a system considering the physical, ecological, economic, social and institutional dimensions (see Figure 3). This framework bears the development of the methodological framework. The operationalisation of the conceptual framework focuses on the physical dimension of sustainability on the one hand and on susceptibility as one of the components of vulnerability on the other hand.

The previous chapter also demonstrated that the analysis of flood physical susceptibility on buildings in large areas requires a building typology, a method to calculate its physical impacts and tools that support its operation and implementation. These three elements can be divided into separate modules, which comprise methods and algorithms. The modules can deal with alternative methods allowing that the connection of modules should point to the general objective. Figure 3 displays the frameworks of the methodology with dimensions of vulnerability (outer circle), components of vulnerability (middle circle) and modules (inner circle).

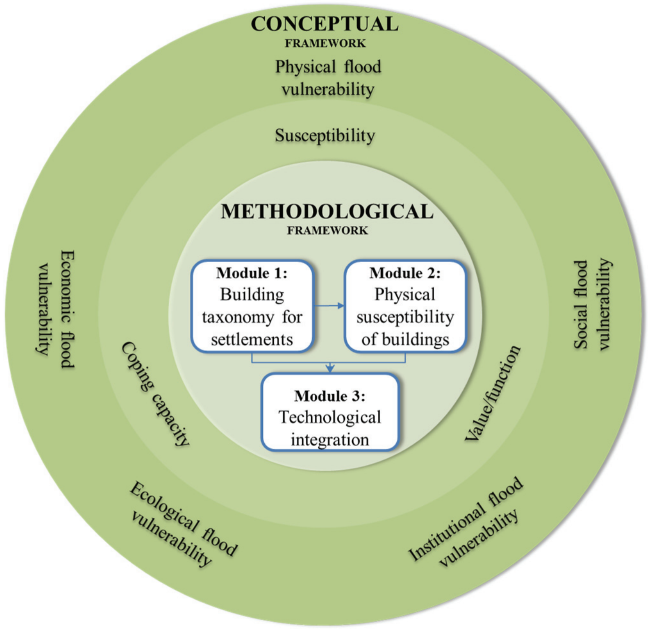

Figure 3: Frameworks of the modules of the methodology (Blanco-Vogt and Schanze, 2014)

In section 2.3 is identified the advantages of a building typology, as it allows us to synthesise the process in a coherent analysis. Since the surveys must not be done one by one as that would be very expensive and information can be transferred to other buildings with similar characteristics. The methods and algorithms for developing a building typology are put together in Module 1. The building typology is called here building taxonomy, which includes the methods for the selection of representative buildings, and the process for a building extraction from a high resolution spatial data and GIS analysis.

The second module of the methodology identifies the interrelations between the water level and the physical impacts using a method called depth-physical impact function. It relates the relevant building components, including their heights, their dimensions and their materials to the susceptible volume of the building materials at different water levels. The material's susceptibility is estimated on the basis of literature research and/or expert judgments. Depth-physical impact functions are derived from interrelations between the water level and the susceptible volume.

The two previous modules are joined through technological integration module. It involves software design, programming and the testing of a consisting tool, a database and GIS tools. The tools allow the user to collect, store, share and transfer the detailed spatial information. This module can be later integrated into a Decision Support System (DSS) according to a schema proposed by (McGahey et al., 2009).

3.1 Module 1: Building taxonomy for settlements

Based on findings from the Earthquake Engineering Research Institute (Brzev et al., 2011), which is creating an initial (beta) version for building taxonomy into World Housing Encyclopedia (WHE), a building typology for the analysis of flood susceptibility assessment is generated. The presented approach modifies the EERI's proposal, which contains only parameters describing the *contextual information, geometric and roof surface* characteristics, which have been initially identified by observing different buildings and they can distinguish one building from another.

If the sources for obtaining these building features are not available in the government agencies, then they should be extracted from reliable data, such as remote sensing data or calculated from GIS analysis. Once the building features are extracted, parameters or attributes may be discretised into classes called categories. A compendium of all categories can then be arranged into codes identifying a building typology. Finally, some representative buildings of each building type are selected for a posterior analysis. Figure 4 shows the scheme of the workflow for the derivation of this building typology called *building taxonomy*.

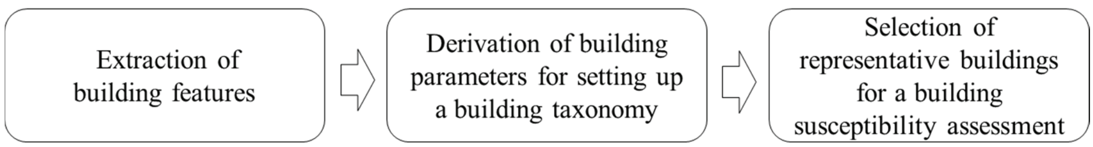

Figure 4: Components of Module 1: "Building taxonomy for settlements"

3.1.1 Extraction of building features

The aim of this section is to define the principal building features and building parameters, which describe the building characteristics needed for the characterisation of them. Additionally, those parameters should be identified through remote processing; whose automatic calculation makes the method transferable. To fulfil this aim, a synthesised analysis of the principal sources and aspects that intervene in a building feature extraction as well as a generic workflow are developed.

3.1.1.1 Relevant factors that intervene in building feature extraction

This section deals with faithful data sources and standardised processes, based on fast, objective and economical methods to identify the features for a building typology for the analysis of building flood susceptibility. Factors, such as (i) data sources, (ii) data quality, (iii) data processing level, (iv) level of result, (v) features to be extracted, (vi) grade of automation and (vii) accuracy are taken into account for the analysis.

i. Data Sources: Benefits of data provided by different sources are described as follows:

Cadastral data in vector format is definitely a good source for deriving building shape, size and length as well as contextual information characteristics, such as adjacency, agglomeration between polygons or distance to other geographic objects. Moreover, cadastral data sets should contain the boundaries of the walls separating properties, parcels, lot blocks, zones, towns, counties or states as well as additional attributes, such as ownership, past ownership, type of ownership, uses, current activities, permits, licenses, rights and restrictions, transactions, land value, purchase price, taxation, legal description, monument description, owner name, administering agency etc. Updated and well-structured cadastral data helps to facilitate the damage inventory and to avoid double reports of the affected building. However, in many countries, the availability of cadastral data for research implies constricting procedures in cadastral agencies or local councils, and it is a time-consuming task to obtain them. In some countries, cadastral data is not accessible due to severe restriction policies and normally this data is collected through field surveys in terrain without spatial reference.

Commercial map vendors sell building footprint data, but often at a price which is too high for risk management institutions. *Land use maps* could also provide information about buildings, but they are usually specific to a particular region and country or their information scale is not sufficient for the extraction of detailed building characteristics.

Elevation information such as DEM is also an essential source for the estimation of building heights as well as for the calculation of spatial relationships between buildings and the hazards measuring the vertical and horizontal distance from water bodies. Terrain and elevation models have improved their accuracy, processing, mean of display and applications. For example, the accuracy of DTMs is more and more overcome by an increasing availability of high resolution digital terrain models from airborne surveys (e.g. Laser scanner, aerial photographs unmanned sensors).

High resolution remote sensing data denotes that the image has a higher separability of features of urban and suburban information. “The definition of high resolution satellite imaging systems is not fixed, it depends upon the application […]” (Jacobsen, 2004). High resolution data has been used for the separation of different urban features and the classification of building types. Spectral data constitutes a much more flexible source, providing a comprehensive coverage at multispectral wavelengths, which is captured across multitemporal intervals and globally available at relatively low costs (Mesev, 2010) compared to expensive field work.

The definition of the ground sampling distance (GSD) for a high resolution, a very high resolution, or an extremely high resolution depends on which type of feature needs to be extracted. Jensen and Cowen (1999) define a very high spatial resolution for aerial photography data, providing details of urban/suburban infrastructure or from space-borne sensors with resolutions of < 1 by 1 m, which may satisfy some of these urban data requirements.

High resolution images and digital surface models are used as data sources for a semi-automatic extraction depending on the resolution of data, especially of the “high data, on the selected method, on the scene complexity and incomplete cue extraction” (Sohn and Dowman, 2007). They are supposed to capture vast multidimensional information on settlement features in an instant of time and allow for a high efficiency through principal global availability and relatively low costs compared to surveying the parameters on the ground (Navulur, 2006; Vu and Ban, 2010). They are provided by a huge range of sensors, which may be categorised by the type of energy used, by the means that they need for the data capture or by the type of sources that they generate in terms of radiometric, spectral or geometric characteristics. By the type of energy, they can be categorised in passive or active sensors, both can be subdivided into ground, airborne or space borne platforms and they provide a huge range of spectral, geometrical and radiometric resolutions. Additionally, the increment of new sensors in the mark allows us to apply these images in the evaluation of phenomena in urban areas, deriving directly many different levels of information for many phenomena. Additionally, the temporal changes in an area can also be investigated with the help of this data source.

The extraction of features from images has been the subject of many disciplines, such as pattern recognition, processing images and applied mathematics. Theses disciplines have contributed to the methodical process of building extraction from remote sensing. Since the apparition of sensors for capturing the characteristics of the earth’s surface, the availability of computing resources, methods, algorithms, instruments, sensors, applications as well as spatial, radiometric, spectral and temporal resolutions of the imaging system has been evolved to capture urban characteristics too (Fugate et al., 2010).

Examples of passive sensors: ground-based platforms (e.g. terrestrial stereo photography, street view), airborne platforms (e.g. UltraCAM, ADS-40 cameras or balloon systems, unmanned aerial vehicles (UAV), colloquially known as drones), space-borne (e.g. satellite images Rapideye, Ikonos, Quickbird, which supply panchromatic, multispectral or hyperspectral images). Examples of active sensors: terrestrial, airborne or spaceborne. An advantage of building extraction from satellite imagery is its high temporal resolution; however, airborne imagery has the advantage of a high spatial resolution. The geometric resolution is not only expressed in terms of ground sample distance, but also in the capture of the 3D surface provided by e.g. aerial stereo, multistereo or oblique imagery photogrammetry data, LiDAR data and interferometry from SAR. This data can be supported and edited through a special-purpose software for object extraction, such as InterImages, e-cognition, Objective and Expert Classifier of ERDAS Imagine, LidarAnalyst, TerraSolid, AFE of SOCET GXP, ENVi, Ilwis, Feature AnalystTM of Visual Learning Systems or Matlab, Numenta, Genie Pro etc.

ii. **Data quality** comprises the measurement and assessment in terms of thematic and temporal accuracy, spatial, spectral, radiometric and temporal resolutions, consistence and completeness (Veregin, 1998). Additionally, the data quality is influenced by sun shadow, low contrast, shadow overcast, occlusion effects, relief displacement of high building illumination, viewpoint and scale changes (Kluckner, 2011; Zhang et al., 2006).

iii. Data processing levels are arranged by the Earth Observing System (Panel et al., 1986) from routine pre-processing to levels 0 and 1A, to higher level data reductions and to mainframe modelling capabilities. Level 0 is the most fundamental of the data record and increases the level with radiometric and geometric calibration coefficients and georeferenced parameters, continuing with the derivation of geophysical variables, mosaics of the data and ending with level 4, which includes the model output or results from analyses of lower level data.

Additional levels of processing data from different sources must also be taken into account, such as digital datasets prepared by national mapping agencies, ground survey data (e.g. ALKIS - Authoritative Real Estate Cadastre Information System), data updated by many users on the Internet (Open Street Map) or GIS-ready information. Depending on the processing level, each set of data requires pre-processing methods before the building extraction is started.

iv. Level of result is defined by Brenner (2010) in three levels: (i) building detection as a classification separating a building from other objects; (ii) delineation of the outlines of footprints used for an automatic update of cadastral maps or a semantic interpretation of the elements; and (iii) building reconstruction or building modelling implemented for a better visualisation and representation of the urban space.

The products of building extraction can be represented in 3D cities or in digital urban mapping. For example, the project CityGML developed levels of a 3D object representation, which can be applied to large areas and small regions. The levels are: terrain-only (LoD0), extruded polygons upon a terrain (LoD1), the addition of roof structures and roof textures (LoD2), the addition of external architectural details such as balconies (LoD3) and the addition of internal rooms (LoD4) (Gröger et al., 2012). The LoD4 level could support evacuation plans.

For the application of this building typology, the focus is put on the delineation of the outlines of footprints. Buildings could be represented at least as a block in the LoD2 level according to CityGML standard. In LoD1, the positional and height accuracy of points should be 5 m or less, while all objects with a footprint of at least 6 x 6 m should be considered. For this typology, the LoD2 level should be preferred for more details in city settlements. The positional and height accuracy of LoD2 is proposed to be 2 m or better. In LoD2, all objects with a footprint of at least 4 × 4 m should be considered (Gröger et al., 2012). The building's height is extracted from the DSM. Data with a low resolution evidently enables us to detect only building regions, whereas a higher resolution allows for a building reconstruction.

v. Features to be extracted such as building outline, building facades, roof structure, roof material and building height can be extracted with the help of a variety of data provided by different sensor types. Publications on feature extraction have been classified in the literature according to the type of sources, object representation or grade of automation as well as the achieved accuracy (see e.g. Rutzinger et al. 2009, Kailasrao et al. 2012, Brito and Quintanilha, 2012).

A condensed literature review of approaches for the extraction of a building's outline, height and roof surface characteristics with different types of data and methods is presented below. This review can serve as a guide for the implementation of the building extraction in other regions with these types of data characteristics:

- *Building outline* or building boundary extraction depends on the average size of the objects in urban areas and the spatial resolution from high resolution data (Schöpfer et al., 2010; Sliuzas et al., 2010). Normally, the exact building footprint area cannot be seen directly from the image, because there is a spatial displacement in the image capturing. This is why the roof boundary may be used as building outline.
    - Airborne platforms: Ahmadi et al. (2010) use active contours for extracting shapes and boundaries form aerial images, similar to

Kabolizade et al. (2010), who use snake and active contours in aerial images and LiDAR data. Gerke et al. (2001) present the generic scene model and invariant geometric moments in aerial colour infrared images GSD (ground sample distance) of 10 cm and a digital surface model DSM with a resolution of 20 cm. Cheng et al. (2011) use multi-view aerial imagery and LiDAR data for determining footprints and 3D building boundaries. They introduced an algorithm, which serves to determine a building's principal orientation in order to improve the correctness and robustness of boundary segment extraction in aerial imagery. Xiao et al. (2012) detect building outlines from multi-view oblique images with the assistance of a point cloud derived from image matching, and the AdaBoost (adaptive boosting) is implemented to integrate geometric and radiometric attributes for the refinement of the roof area. One of the last advance in spatial resolution has been reached by Interspect Kft (2012) with orthoimages in a resolution of 0.05 m.

- Airborne LiDAR data: Michelin et al. (2012) extract building edge from airborne full-waveform LiDAR accessing of the information related to the emitted and backscattered laser signals. Zhang et al. (2006) use region growing and local plane-fitting techniques in LiDAR data. (Dash et al., 2004) create a method for height variation along the periphery and modified standard deviation of the LiDAR data. Haithcoat et al. (2001) generate building footprints based on general knowledge about buildings and geometric characteristics such as size, height and shape to separate buildings from other objects. The extracted building outlines are simplified using an orthogonal algorithm to obtain a better cartographic quality. Rutzinger et al. (2009) use airborne laser scanning for building footprints by Dempster-Shafer Fusion based on Hydrological Raster GIS Tools.
- Spaceborne sensors*:* Grigillo et al. (2012) use an ISODATA classification and mask in stereo panchromatic images of IKONOS and DSM. Awrangjeb et al. (2010) developed an automatic building detection based on masks using LiDAR data and multispectral imagery. Sirmacek et al. (2010) developed a building shape detection algorithm and segments in panchromatic satellite images and DEM. (Sohn and Dowman, 2007) present the binary space partitioning (BSP) method for the polygon cue generation and grouping process relying on straight lines extracted from monocular Ikonos images and LiDAR DEM. Zhang and Maxwell (2007) extract big buildings using fused multi-resolution optical methods and an object-oriented classification. Chai et al. (2012) combine Markov random fields and marked point processes to represent both low-level information and high-level knowledge; they present a combined framework for the modelling and estimation of building extraction from single images.
- Kundra et al. (2010) use a swarm optimization for object extraction in urban areas from high resolution satellite images (Google Earth). Tian and Reinartz (2013) developed an approach for the boundary detection of buildings by a fusion of panchromatic images, multispectral images

and DSM generated from WorldView-2 stereo imagery. An educational tool developed by the (ICIS, 2009) called *SpaceEye* allows for the processing of the visible Google Earth window with simple functions on the imagery such as segmentation and edge extraction. This tool was tested in the pilot sites giving as result a preliminary detection of the buildings with just defining a threshold (e.g. Figure 5).

Figure 5: Building detection from a Google Earth view (segmentation threshold 120)

- SAR: Wegner et al. (2011) use conditional random fields in interferometric SAR (InSAR) data. Michaelsen et al. (2008) use the GESTALT system and grouping evidence for the treatment of alternatives within a layered task-solver in high resolution SAR data. (Guillaso et al., 2013) present an extraction procedure from Lband SAR tomograms dedicated to building area analysis. The above-mentioned methods show that the elevation information data may be a primary component for the building outline extraction.

- *Building height:* The delta Z value from the ground to the top of a building's roof is calculated from the difference between the street level and the highest point of the building. An automatic calculation requires digital terrain models and digital surface models supplied by e.g. LiDAR data, stereo, multi-stereo or omnidirectional images. Persistent Scatterer Interferometry (PSI) is most useful in urban areas with a high number of permanent structures, 3D topographic mapping using TerraSar, 3D city maps, GPS elevation points which can supplement a DEM (or create small ones) or projecting building shadows onto the image space from a single image. Besides the data, Mercer (2001) presents a relation between costs and vertical accuracy in DEM products. He shows that the prices in U.S. dollars/km2 may increase considerably when the vertical accuracy is enhanced. Further approaches or algorithms for generating a DSM and DEM extraction of building height have been implemented as follows:

  - Single images: Kim et al. (2007) present a semi-automatic calculation method for the building height by projecting the building shadow onto the image space from the elevation and azimuth angles of the sun and the camera provided in the metadata. (McGlone and Shufelt, 1994) estimate the building height by projecting the object space geometry in nadir and oblique imagery.

  - Radar data: Soergel et al. (2009) use the GESTALT system for calculating the building height in orthogonal high resolution SAR images. Ender and Brenner (2003) use a procedure based on the corresponding data for delimiting height and roof structure. Liu and Yamazaki (2013) developed a method to detect building heights automatically using 2D GIS data and a single high resolution TerraSAR-X (TSX) intensity image. Additional, they resume briefly other methods for the extraction of building height from SAR data sources.

- Stereo or multi-stereo images: Haala and Rothermel (2012) demonstrate the semi-global matching (SGM) stereo method for the generation of DEM with multi-stereo images. Kim and Habib (2009) use stereo images and LiDAR data with automatic object-based hierarchical processing for obtaining complex polyhedral building models. Jarvis (2008) uses photogrammetry and LiDAR data to obtain height information and to create building models. Van Essen (2008) generates photogrammetric elevation models in CityGML format. Taubenböck et al. (2013) estimate the average height of buildings for delimiting central business settlements in a case study using Cartosat-1 imagery.
- Omnidirectional imaging: Wieland et al. (2012) introduced an omnidirectional camera system for an automated estimation of building height. Zhou et al. (2013) developed omnidirectional laser vision sensors by adopting plane mirrors instead of curved mirrors for the 3D measurement in order to use the simple traditional camera model.
- 3D models: Google maps (2012) present 3D models for entire metropolitan areas to Google Earth on mobile devices based on the combination of new imagery rendering techniques and computer vision that automatically creates complete 3D cityscapes including buildings, terrain and landscaping from a 45-degree aerial imagery. Tack et al. (2012) create 3D models using highly automated photogrammetric methods in satellite images, surface models and cadastral data. Haala and Kada (2010) create 3D models and building facades from DSM and construct polyhedrons. Lafarge et al. (2008) create 3D city models from DTM.
- Sensor orientation: Sarabandi and Kiremidjian (2007, p. 38) explain a method for measuring the height of objects using the sensor orientation model, the collection azimuth or the off-nadir viewing angle as well as the image plane configuration.

▪ *Building roof surface* may be extracted with the following methods:

- Stereo images: Fraser et al. (2002) use photogrammetric processes for delimiting the roof structure. Song and Shan (2005) present the edge flow-driven active contour and JSEG algorithm. (Rottensteiner et al., 2003) use airborne laser scanner data and aerial imagery for building detection, roof plane detection and the determination of roof boundaries. The approach is based on the Dempster-Shafer theory for data fusion. Roof plane detection is improved by using digital images, and the geometric quality of the roof plane boundaries is improved at step edges by matching the object's edges of the polyhedral models with image edges.

- LiDAR: Schuffert (2013) presents an automatic approach to extract suitable single roof planes from airborne laser scanning data. Porfírio Dal Poz (2013) proposes a photogrammetric method for refining 3D building roof contours extracted from airborne laser scanning data. Awrangjeb et al. (2012) reconstruct building roofs by integrating LiDAR and multispectral imagery using 'ground mask' and non-ground points, which are then used to generate initial roof planes. The structural lines are extracted from the grey-scale version of the orthoimage and divided into several classes such as 'ground', 'tree', 'roof edge' and 'roof ridge' using the ground mask, the NDVI and the entropy image (from the grey-scale orthoimage). Stilla and Jurkiewicz (1999) reconstruct sloped roofs in laser altimeter data analysing the histogram of heights and prismatic models.

This shows again that height data can be a very informative cue to discriminate between object classes, like buildings, streets or vegetation, to reconstruct roof structures and discriminate the edge of roof boundaries. The success of building extraction therefore depends significantly on the details of the height data.

- *Roof material*: Although roof material is not required for this building typology, it could be included in the future as an additional parameter because it can reflect how a building is protected against rough weather and it provides information about the lifestyle. On one hand, the classification of roof materials is challenging due to the wide range of potential materials as well as the variability of the spectral properties of target surfaces influenced by environmental factors like wind, sunlight, moisture, pollutants, biological growth (Berdahl et al., 2008) or corroded materials. On the other hand, roofs are composed of diverse materials, like carton, fabric, thatch, brush, plastic, glass, wood, mud, grass, clay, asbestos, brick, gravel, tar/oil, dark asphalt, rocky components, composite shingle, concrete, tin, steel, metal, solar roof panels or a combination of them. Those materials present a high variability and similarity of reflectance which can be hard to distinguish (Herold and Roberts, 2010; Schöpfer et al., 2010).

  Herold et al. (2003) suggest the use of hyperspectral data as a way to deal with the spectral complexities and mixture of urban environments. Urban spectral libraries reflect these properties in characteristic spectral signatures and related absorption features. Zhu et al. (2011) developed a program for identifying building surface material by using hyperspectral images, showing a good efficiency and accuracy. However, hyperspectral data and resources for the realisation of these experiments are not available in many regions.

vi. Grade of automation is another aspect of building extraction. The term 'automatic' suggests that the whole process is performed without any manual intervention. The automation process depends on the level of expected results and accuracy. Up to now, an automatic line production for building extraction is not easy to reach with 100 % reliability, as the process requires initial parameters defined manually, such as thresholds of height, and the automation involves further challenges in dense and complex urban areas due to the misclassification between roads, shadows and impervious surfaces. The automation of building extraction in an urban environment also varies in terms of boundary accuracy of the mixed objects and the quality of the data explained above.

Nevertheless, these methods analytically and empirically improve algorithms, and they are therefore used more often nowadays. Some methods help to increment the productivity with promising results. And the aim is to automate most steps of the whole process: The grade of automation for building extraction could be classified as follows: *automatic* (buildings could likewise be classified with a high accuracy through threshold and segmentation methods), *semi-automatic* (further fuzzy rules must be developed to distinguish different classes, segmentations, filters and the reshaping and cleaning of building polygons) or *manual* (low grade of automation using visual interpretation and digitalisation methods).

vii. Accuracy, Song and Haithcoat (2005) present a sequence of indices for a comprehensive evaluation of the results from automated building extraction. The indices include detection rate, correctness, matched overlay, area omission error, area commission error, root mean square error, corner difference, area difference, perimeter difference and shape similarity. The most-used indices for accuracy calculation are completeness and correctness. Completeness is the percentage of reference data which is explained by the extracted data, while correctness represents the percentage of correctly extracted data (Heipke et al., 1997).

An interesting benchmark preformatted by ISPRS (Rottensteiner et al., 2012) encouraged researchers to submit results of urban object detection and 3D building reconstruction of two urban areas. The results of the methods for building detection show an area-based completeness between 85 % and 93 % and a correctness between 90 % and 98 %. For buildings larger than 50 m^2, the results are satisfactory. The benchmark clearly shows the importance of the selected method for successful building extraction. Further analyses of the building extraction accuracy might be carried out with a sensitivity analysis in order to investigate the performance of the building extraction under the condition of changing input data and methods (Saltelli et al., 1993). Figure 6 reveals that the accuracy decreases with methods which do not include elevation data; e.g. (Shackelford et al., 2004) extract building footprints from Ikonos images with a correctness of 89.1 % and a completeness of 64.7 %; Vu and Ban (2010) gather shapes and sizes from QuickBird images with a correctness of 85.1 % and a completeness of 85.9 %; or low resolution elevation models, like Sohn and Dowman (2007), which get polyhedral building shapes form Ikonos pan-sharpened and LiDAR data of 3.3 m with a quality of 80.5 %.

The accuracy rises considerably when high resolution elevation models are included (see Figure 6), like Haithcoat et al. (2001), who extract building footprints with a completeness of 93.7 % and a correctness of 97.4 %. Kim and Habib (2009) extract complex polyhedral buildings from multispectral photogrammetric and LiDAR data with a correctness of 89 % and a completeness of 95 %. Rutzinger et al. (2009) extract building footprints from airborne laser scanning with a completeness of 96 % and a correctness of 99.1 %. Cheng et al. (2011) extract building footprints from multi-view aerial imagery and LiDAR data with a 91 % completeness.

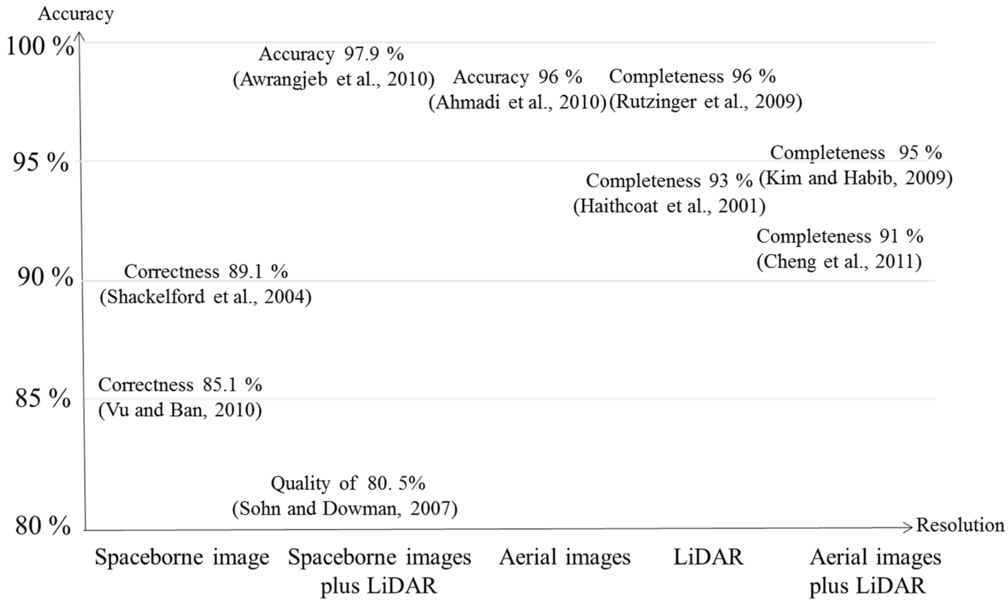

Figure 6: Examples of building extraction accuracy based on literature review

An index which calculates the percentage of correctly detected buildings and the total number of detected buildings is not enough for this implementation; what is rather required are more indices, which ensure that the quality of the building outline, building height and building surface extraction generates coherent results for the typology.

To conclude, building extraction cannot be done with just one method or following a unique algorithm, and its results depend on data source, quality of data, methods and level of results as well as expected accuracy. Many properties of buildings can be extracted and more different levels of products be differentiated depending on the spatial resolution of the digital surface model.

3.1.1.2 Semi-automatic building features extraction − generic workflow

This section presents a generic workflow for the extraction of building features from high resolution data to assemble the relevant methods and to guide activities into a structured process. The generic workflow for a semi-automatic building feature extraction comprises five steps depicted in Figure 7, which bears upon the approach of Brenner (2010). It consists of (i) the preparation of the data sources, (ii) the recognition of cues for a semantic definition of the building, (iii) the conversion of the cues to algorithms, preserving the "relevant" pixels, (iv) the calculation of the building's geometric characteristics and (v) the extraction accuracy evaluation.

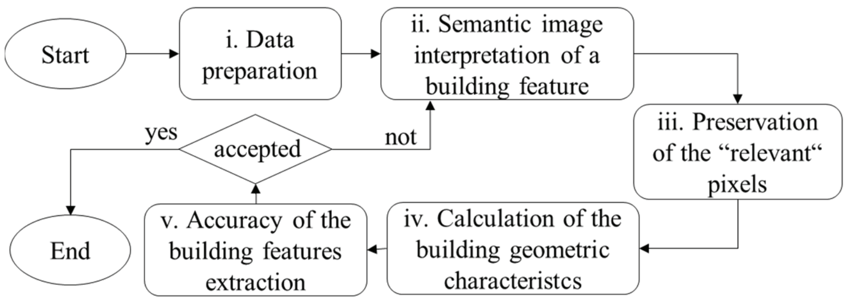

Figure 7: Workflow for a building outline extraction (Blanco-Vogt et al., 2014, p. 2)

i. Data preparation

Data preparation contains principally two activities: (i) acquiring data with a very high resolution and (ii) pre-processing the data seeking for the precision required for the scale; aerial photos must be aero-triangulated, satellite images must have geometric and atmospheric corrections, metadata must be available and supplementary data correctly structured. Experts should evaluate the data in terms of positional accuracy, data quality (Veregin, 1998), data processing levels (Panel et al., 1986), thematic reliability and completeness.

ii. Semantic image interpretation of a building feature

The second step refers to the process of recognising cues of building feature characteristics on the images in order to define the pixels making up this building feature. Semantic image interpretation means determining which pixels constitute a feature, its extents and locations (Bückner et al., 2002; Kluckner, 2011; Rutzinger et al., 2009). The semantic interpretation is carried out by developing questions about the attributes of the feature in the images for a settlement with homogenous characteristics. The answers to these questions are shaping the cues for defining the algorithms for the extraction of the feature from the VHR data.

The problem arises of how to detect the border between buildings in the case of row buildings or a block. If these buildings have different heights, the elevation information can be used to determine the border; otherwise, the building borders must be manually edited.

The process can start with the extraction of *building regions*; it is not a prerequisite for the extraction of a building outline. The following steps may be considered for the semantic definition of building regions: (i) recognising cues based on spectral information, elevation information and characteristics of the urban area, and then (ii) separating water, vegetation and land. An example for the semantic definition of building regions based on spectral and elevation information is depicted in Figure 8, which contains the next cues: (i) buildings have other spectral characteristics than vegetation; (ii) a building has a homogeneous roof texture; (iii) floodplains are quite flat because the height variation is very low and (iv) buildings are elevated.

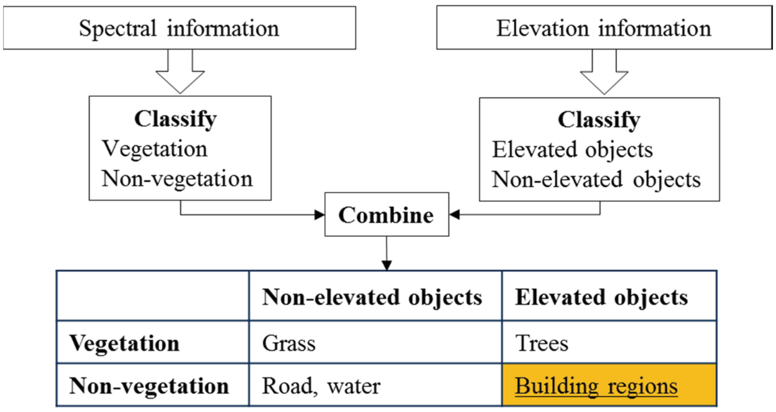

Figure 8: A semantic definition for building regions extraction

Water bodies have a low brightness and are relatively easy to extract automatically because they present spectral dissimilarities to their immediate background. Vegetation can be removed by a simple mask threshold of the vegetation indices and elevation values. Green roofs should be taken into account; they must be reviewed using the NDVI and the DSM. The ground can be separated by using the lowest height values from a DEM or a coarse segmentation for separating water, land and vegetation in order to reduce the confusion for the extraction of buildings and simplify the generation of an image.

The *semantic definition of building outlines* wants to find out which pixels are the candidates to be a building outline and which are not. It is also associated to the detection of pixels that make up the outline and the formation of one polygon. A semantic definition of building outlines in a pilot site may take into account the following *cues* as a reference based on spectral and elevation information for example: What is the building's predominant shape? Are the sides of the buildings parallel or rectangular? How is the urban structure in terms of density of buildings and open space? Are buildings sparse in the area? Are the buildings separated from the garages? What is the size of the garages in relation to the buildings? Are the buildings elongated or are they square? Which of these cues can be distinguished from spectral and elevation information?

iii. Preserve only the "relevant" pixels

The answers to the previous questions help to find the suitable algorithms for filtering certain group of buildings with specific characteristics. What are the best methods to remove the pixels that not fit with the cues? For example the use of masks thresholds, vegetation indices or coarse segmentation for removing vegetation and water bodies can be implemented.

Depending on the complexity of the building distribution in the area and the contrast between the built-up and the open space, morphological filters may be used (e.g.: erode, dilate, fill, detect lines using the Hough Transform, connect pixels, reshape, refine methods like geometric filters, rectangular fit or shape indices). A fine segmentation can be added as an additional level of information to separate impervious buildings, shadows and road objects. These objects possess a certain shape, size and context information that can be used for a finer segmentation. Further characteristics, such as a certain shape, size and context information, can be used for a finer segmentation.

iv. Calculation of the building geometric characteristic

Once the selected pixels fit the semantic definition, they can be converted to a polygon in vector format. The building geometric characteristics are associated with the building's position, its relationship to another object, its size, edge, shape, delta Z value from the ground to the top of the roof, the gradient of the Z value of the roof and the roof material. The calculation implies the reduction of points in the polygon so that only the "relevant" edges and the regularity in term of parallelism and rectangularity are preserved (Zhang et al., 2006; Brenner, 2010).

The followings task should then be carried out: reducing the number of points of the vertices (Douglas and Peucker, 1973), identifying dominant lines in the outline polygon with e.g. RANSAC (Fischler and Bolles, 1981), analysing the orthogonal and topological relation of the polygon in itself and to other objects and using filters like line remove, line snap, probability filter, rough skeleton, smooth, spline, template match or polygon change.

This post-process task should not be applied to all polygons at the same time as this would drastically influence the quality of the building polygon shape, because generalisation values and smoother filters may change the accuracy of the object's extraction in relation to the its real dimension. The values must be adjusted taking into account the form, size and expected orthogonality of a group of polygons.

v. Accuracy of the building feature extraction

Regarding the fifth and last step, Rutzinger et al. (2009) stress out that the quality of building detection results depends on the application of the extracted building data and suggest that several methods must be used for the evaluation. The most common indices for an accuracy calculation are completeness and correctness (Heipke et al., 1997). But these two indices do not ensure the quality required for the implementation in the context of a building typology. The set of indices presented by Song and Haithcoat (2005) allows a comprehensive evaluation of the results from automated *horizontal building outline extraction*. Reference data is assumed to be correct for the calculation of the following indices: area difference, perimeter difference, vertices difference and the root-mean-square error index (RMSE) of the vertices.

Congalton and Green (2008) analyse how and when the reference data should be collected and how the objectivity and consistence for assessing the accuracy could be ensured if the data present a binomial or multinomial distribution.

The RMSE index uses building corners as checkpoints by measuring the average horizontal distance between detected and corresponding “true” building corners, a measure of positional accuracy. This index calculates the distance of each vertex of the extracted polygon to the closest corresponding point in the reference polygon using the following formula.

$$RMSE\ index = \frac{\sum_{i=1}^{n} \min \sqrt{(X_{DBi} - X_{Ri})^2 + (Y_{DBi} - Y_{Ri})^2}}{N_E} \qquad (1)$$

Where X_{Dbi} and Y_{Dbi} are the coordinates of each vertex of the extracted polygon, X_{Ri} and Y_{Ri} are the coordinates of each vertex of the closest reference polygons and N_E is the amount of vertices of the extracted polygon.

Figure 9 gives an example of the differences between a reference polygon and the extracted polygon; a. the original image, b. the aspects which can influence the extraction of the building outline, c. the reference polygon digitalised manually and d. the extracted polygon.

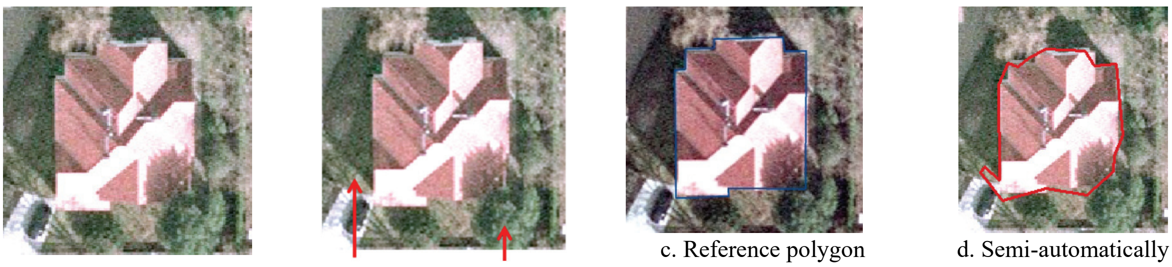

a. Original image

b. Boundary influenced by sunshine | Occlusion due the tree

c. Reference polygon (blue border)

d. Semi-automatically extracted polygon (red border)

Figure 9: Consideration for a building horizontal accuracy

The reference polygon has an area of 316.32 m², a perimeter of 74.96 m and 14 corners. The extracted polygon has an area of 326.11 m², a perimeter of 76.8 m and 18 corners. This results in an area difference of 9.79 m², a perimeter difference of 1.84 m, a corner difference 4 and an RMSE index 2.3. This example shows that the building extraction process must be improved with better filters in order to obtain a higher accuracy.

Height extraction accuracy depends basically on the accuracy of elevation data, which is typically calculated by comparing the heights of the DSM with a finite sample of checkpoint coordinates from an independent source of higher accuracy, assuming a normal distribution of the derived height differences or errors (Aguilar and Mills, 2008). For the assessment of height extraction, it must be considered that the date of acquisition of the DEM and the date of the survey are not too distant as the constructions are constantly changing with new storeys, new buildings and new settlements. The study of Sarabandi and Kiremidjian (2007, p. 52) for the height extraction accuracy assessment may be taken into account, where the height of randomly selected buildings is compared to their height in survey data, based on:

$$\varepsilon = \frac{|H_s - H_E|}{H_s} * 100 \qquad (2)$$

Here H_S is the independent height gathered from survey data and H_E the height extracted from the DSM. Flood (2004) developed guidance for the ASPRS for assessing a vertical accuracy at 95 % confidence level for open terrain, where the error distribution is thought to be close to a normal distribution:

$$RMSE_{(Z)} = \sqrt{\frac{\sum (Z_{data(i)} - Z_{check(i)})^2}{n}} \qquad (3)$$

Compute Accuracy$_{(z)}$ = 1.9600 *RMSE $_{(z)}$ =Vertical Accuracy at 95 percentage confidence level.

Aguilar and Mills (2008) proposed a method for reproducing the statistical behaviour of vertical errors of LiDAR data by using a favourable number of checkpoints, even in the case of datasets with non-normally distributed residuals. This method may be useful here because the heights of buildings in urban areas are not necessarily expected to be normally distributed. They construct a confidence interval to estimate the uncertainty of the RMSE to evaluate LiDAR-derived DEM vertical accuracy, assuming a non-normal error distribution. They also recommend that the number of checkpoints required for computing RMSE bounds at the 95 % confidence level should be 160, whilst it would be only 110 for an 80 % confidence level.

The equation from the paper by Aguilar and Mills (2008) for height accuracy assessments should be applied, taking into account that the number of checkpoints required for computing RMSE bounds at the 95 % confidence level would be 160. Otherwise, the method suggested by Flood (2004) can be implemented if the building heights have a normal distribution behaviour.

The *building surface accuracy* depends on the method selected for the extraction: either the majority value of the slope or the slope classes as explained in the previous section. The higher the spatial resolution data from the surface models, the more accurately the roof details can be improved.

In general, the map scale is directly related to the raster resolution and the detectable size of the objects. In cartography, it is known that the map scale is the result of a multiplication of the raster resolution (in metres) by 2000. If the DSM has a resolution of 2 m for example, the map scale is 1:4,000. Accordingly, Rossiter (2004) defines Minimum Legible Area (MLA) as the minimum ground area that is legible on the map with the formula: MLA, ha = (Scale Number / 1 000)^2 / 250. Applying the formula to the scale of this example: MLA, ha = (2000/1000)^2/250. The MLA for this scale is 0.016 ha (equivalent to 160 m^2). This shows that building roof surfaces with sizes lower than 160 m^2 extracted from a DSM with a resolution of 2 m will not be correctly represented. A recommendation for measuring the quality of the extracted polygons is calculating the four indices for the building outline extraction and the error of the building height and comparing the reference-building height with the extracted one.

3.1.2 Derivation of building parameters for setting up a building taxonomy

The analysis of the parameters required for a building typology is developed through the induction method. This analysis is described in this section. As already mentioned, a building typology is needed for the built classification in large areas. The term “building taxonomy” is taken from the proposal of the Earthquake Engineering Research Institute EERI (Brzev et al. 2011) and defined as: “building taxonomy describes characteristics of an individual building or a class of buildings with similar characteristics (building typology)”. A general definition of taxonomy is a classification that has a name and a rank defined by nomenclature codes.

Pilot sites show that a building is composed of planes, angles, curves, figures and shapes, which define some relevant characteristics of the building and depending on the position of the building in the neighbourhood, it earns some other characteristics. The observed parameters are building properties that every building should have. The selected parameters, which have been observed visually, shall describe these relevant features. Then the chosen parameters are classified in (i) parameters describing geometric characteristics: height, footprint size and elongatedness; (ii) parameters describing the surface of the roof: roof form and roof slope; and (iii) parameters describing contextual information of the buildings: compactness and adjacency. The next step is to analyses the description of each parameter and the method for its gathering.

3.1.2.1 Parameters describing geometric characteristics

Building total height is one of the most import variables because it influences structure, design and function of a building. The height of buildings depends on many factors, like planning regulations, soil support capacity, availability of materials used for the structural system, such as reinforced concrete and steel, technology used for the construction and maintenance of elevators, systems of heating, ventilation and air conditioning. Taranath (2010) presents the influence of the height on a building's structure and functionality in terms of foundations, systems for the vertical transportation of fluids, gases and solids, gravity systems, lateral load-resisting systems, resistance to wind pressures, seismic design and required elements such as elevator, stairs etc. A building’s height may also reflect its population density. All these properties show the importance of building height being included into the typology.

The height of the building is measured from the level of terrain to the top part of the building. A method for obtaining a building’s height using remote sensing data is through digital surface models DSM. A first step in building height detection is to remove the underlying elevation by subtracting the digital terrain model (DTM) from the DSM using morphological filters; as a result, the objects above ground are preserved in the normalized DSM (nDSM). One advantage of flood plain areas is that they are rather flat and the elevation of objects can be measured using fixed values. Terrain models in floodplains normally have no abrupt changes in terrain elevation and the building height can be calculated based only on the DSM. These inconsistencies may be overcome by improving the resolution of the DSM using existing terrain models or feature files (DeVenecia et al., 2007).

The steps for calculating the building height are the following: (i) selection of the maximum value of the nDSM within the building polygon as peak of the building; (ii) selection of the mean value of the DTM within the building polygon and (iii) difference between the two values in the centroid of the building (delta Z). For the calculation of the building height, the following aspects should be considered: (i) the centroid point is not always the highest point of the building; (ii) trees near the building interfere with the height calculation. Filters for trees must therefore be carried out.

Building size determines the relation between the building and its neighbourhood and the contribution to the external space (Sidney, 1996). Building size may infer in the internal architecture, and it may influence ventilation as well as heat and energy consumption (Perez Fernandez, 2008). For instance, the size defines a building's suitability for specific uses such as wineries, garden homes, storage sheds, garages, warehouses or public uses. From remote sensing data, a roof footprint can be detected to define the building size. However, the building footprint determines the tangible building size, which is the outline of the surrounded exterior walls excluding courtyards.

The size dimensions of residential buildings have changed during the times. Buildings in Latin-American before the colonisation were small and had round forms; during the European colonisation, other building techniques were implemented and heights and sizes were expanded. After the independence, many American cities have grown and small row houses with narrow fronts and deeper lengths emerged; the room forms were standardised and the lot sizes decreased. The footprint size can be calculated directly from the building polygon using any GIS tool.

Elongatedness as the width/length ratio may be a parameter that sets up the internal design and structure, the functionality and flexibility for activities in front of a building. It was observed in the pilot sites that many rectangular buildings correspond to warehouses or nursery garden. An example of the importance of elongatedness as a parameter for defining a building typology is the tube houses in Hanoi (Vietnam), which are very long and narrow – presumably due to the fact that the building façade determined the property taxes (Downs, 2007). The function of the long corridor of this type of house is to connect the rooms with the courtyard. Moreover, Committee and Resources (2006, p. 48) state that “a square design plan will give the maximum robustness to resist horizontal loading and floor plan of the building and its orientation to the direction of flow are factors affecting how it will perform in a flood”. Buildings with long walls are more fragile and if the direction of flow intercepts a long wall, floodwater loading and the vulnerability to debris loading are maximised (Ibid).

Elongatedness can be calculated as the ratio between the length and width from the convex hull (Jarvis, 1973). The ratio expresses how relatively square a polygon appears when viewed from the top. For this relation, a minimum bounding rectangle oriented to the x- and y-axes and enveloping the polygon is constructed. Figure 10 presents two categories of elongatedness: squares with a length/width ratio close to 1 and rectangles with a length/width ratio higher than 1.

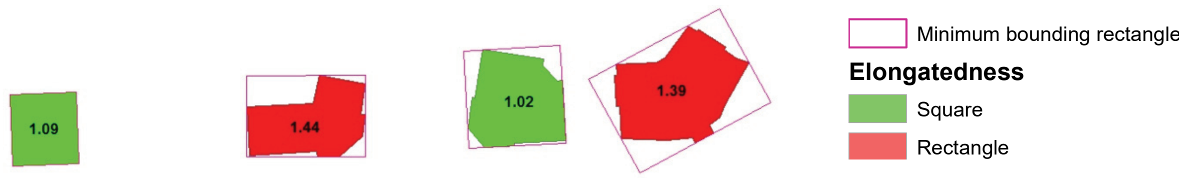

Figure 10: Illustration of polygon elongatedness (Blanco-Vogt et al., 2014)

The steps for the calculation of elongatedness are the following: (i) computation of the bounding box of the polygon, which produces a minimum area bounding rectangle; rotation in the direction of the output shape's long axis and (ii) calculation of the relation between two length and width fields of the bounding box.

3.1.2.2 Parameters describing the surface of the roof

One might think that a building's roof does not have any inference in the assessment of flood impacts. However, building roof characteristics are selected because they define indirectly the building's structure and style in terms of interior volume, drainage, resistance to weather and resistance to water leakage (Blanco-Vogt et al., 2013). The building roof structure can be remotely described by its planimetric roof form and the roof pitch characteristics.

The principal roof function is to protect the habitants from extreme temperatures, rain, snow, sunlight, wind, hail etc. Emmitt and Gorse (2010) describe the functional requirements of a roof with strength, stability, resistance to weathering, durability and freedom from maintenance, fire safety, resistance to the passage of heat and sound, resistance to air leakage, security and aesthetics. The roof can have additional functions such as rainwater harvesting from rooftop catchments. Its designs and materials vary from place to place, determining the building's character, appearance and structure.

The variety of roof styles is huge, including gable roofs, hipped roofs, barn hip roofs, dormer roofs, gambrel roofs, mansard roofs, salt box roofs, a-frame roofs, flat roofs, mono-pitch roofs, lean-to roofs or polyhedral building models for complex structures with horizontal and tilted rooftops, which are bounded by straight lines. Each roof combines figures, forms, angles, materials and slopes.

Planimetric roof form or the shape of the building plan allows us to identify the form complexity of the building: whether the form is square, rectangle, in U, L, T, O, E, H, S, X, Y, with stairs or a combination of several forms. Hence, the amount of vertices may be a parameter in order to detect such a complexity of roof forms.

For example, a simple square, triangle, rectangle or L form contains not more than six vertices; between six and twelve vertices infer that the roof has more rectangular, triangular or curved forms; and more than twelve vertices suppose that the building has a complex structure. Buildings with a dome roof or circular forms usually have a cultural or religious significance. The calculation of the planimetric roof form can be based on many different methods.

Method of counting the vertices: A simple method consists in counting the nodes of the polygons. Nodes that do not define the shape of the building footprint must be eliminated through cleaning and simplifying the polygon with orthogonal and rectangular filters

Figure 11 shows that buildings with a higher amount of vertices are more prominent and imposing than buildings with fewer vertices.

Figure 11: Example of building vertices

Method of the standard distance deviation (sdd): The amount of vertices may vary depending on the interpretation method and the precision for capturing the building polygon. In order to identify the planimetric roof shape, the standard distance of each vertex to the centroid of the polygon is used. The standard distance deviation sdd is a good single measure for the dispersion of the points around the polygon's centroid. The sdd is the two-dimensional equivalent of a standard deviation for a single variable where Xc and Yc are the coordinates of the centroid and Xi and Yi of each vertex. This gives:

$$sdd = \sqrt{\frac{\sum_{i=1}^{n}(X_i - X_c)^2 + \sum_{i=1}^{n}(Y_i - Y_c)^2}{N}} \qquad (4)$$

The centroid point is located at the average x and y coordinates of all the vertices of the polygons. Figure 12 depicts three polygons with their sdd. Square form polygons tend to have a sdd close to 0, while polygons with complex forms have a larger sdd.

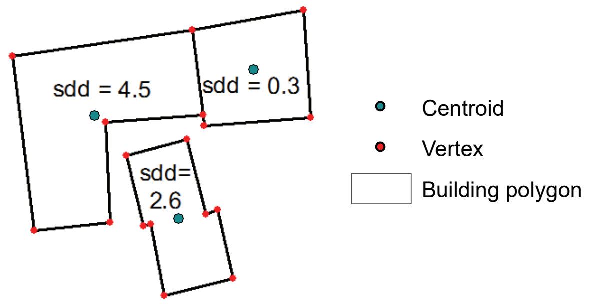

Figure 12: Example of the standard distance deviation of polygons

Methods of form indices: Sarabandi and Kiremidjian (2007) derived three indices for calculating the topological shape attribute of the plan view of a building: the slenderness index, the convexity index and the irregularity index. The slenderness index is the ratio of the perimeter of an object and its area. The convexity index is calculated as the ratio of the area within the circumscribed convex polygon of an object and the area of the object itself. In addition, the irregularity index is calculated based on the normalised equivalent convexity index with similar slenderness.

Roof slope or roof pitch has an effect on a building's interior volume, drainage, style and the material used for covering. The style is affected too because the framing of the roof changes the slope (Emmitt and Gorse, 2010). The roof slope reflects the adaptation to climatic conditions; Carryduff Designs (2011) states for example that flat roofs have historically been used where the climate is arid and the drainage of water off the roof is of secondary importance. Flat roofs came into widespread use in Europe and the Americas in the 19th century when new waterproof roofing materials and the use of structural steel and concrete made them more practical. They became the most commonly used roof type to cover warehouses, office buildings and other commercial buildings as well as many residential structures in the USA.

The slope of a roof, often referred to as the "pitch", is considered as the primary factor in roof design. The slope, or pitch, of a roof is determined by the vertical rise in inches for every horizontal twelve-inch (12") length (called the "run"). Sloping roofs come in many different varieties and angles. The simplest is the lean-to, or shed, which has only one slope. A roof with two slopes forming an "A" or triangle is called a gable or pitched roof. Roofs may have different architectural features such as penthouses, additional floors or courtyard openings. Roofs may contain many attributes.

Method of the majority slope value: The majority value of the slope can be calculated from the digital surface model. Figure 13 depicts an example of roof slopes in degree, and the value shows the majority of the roof slope.

Figure 13: Calculation of the roof slope

The steps proposed for roof pitch calculation are: (i) clipping the digital surface model in the form of the building polygons; (ii) calculating the slope in degrees and (iii) selecting the majority values of the slope for each polygon.

Method of the slope classes: This method classifies the slope in three principal categories and the class with the largest area is selected as the roof slope. Carson Dunlop & Associates (2010) summarise the range of roof pitches or slopes for flat, low-slope or conventional or "steep slope" roofing (see Figure 14).

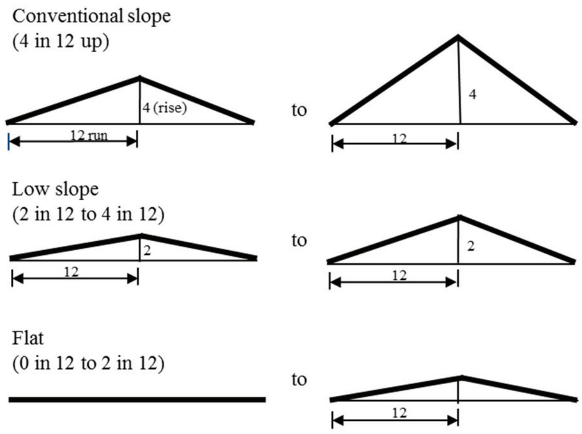

Figure 14: Roof slopes types. Source: Carson Dunlop & Associates

Figure 15 depicts the results of the roof slopes as calculated with the two methods. If the roof has many inclination angles and complex forms (building a), the method of the majority value will generate inconsistence results. When the roof has a simpler roof form, the method of slope classes may not give the correct description of the slope. The method selected for gathering the roof slope description depends on how complex the roof inclination of the majority of the buildings in the case study is.

Straight skeleton method: Aichholzer et al. (1995) developed a method of representing a polygon through a straight skeleton, which can be used as the set of ridge lines of a building's roof, based on walls in the form of the initial polygon. Each point within the input polygon can be lifted into the three-dimensional space by using the time at which the shrinking process reaches that point as its z-coordinate. This method is commonly used for building reconstructions in 3D. For this application, however, a method for a general description of the roof slope is required; therefore the roof pitch is selected here.

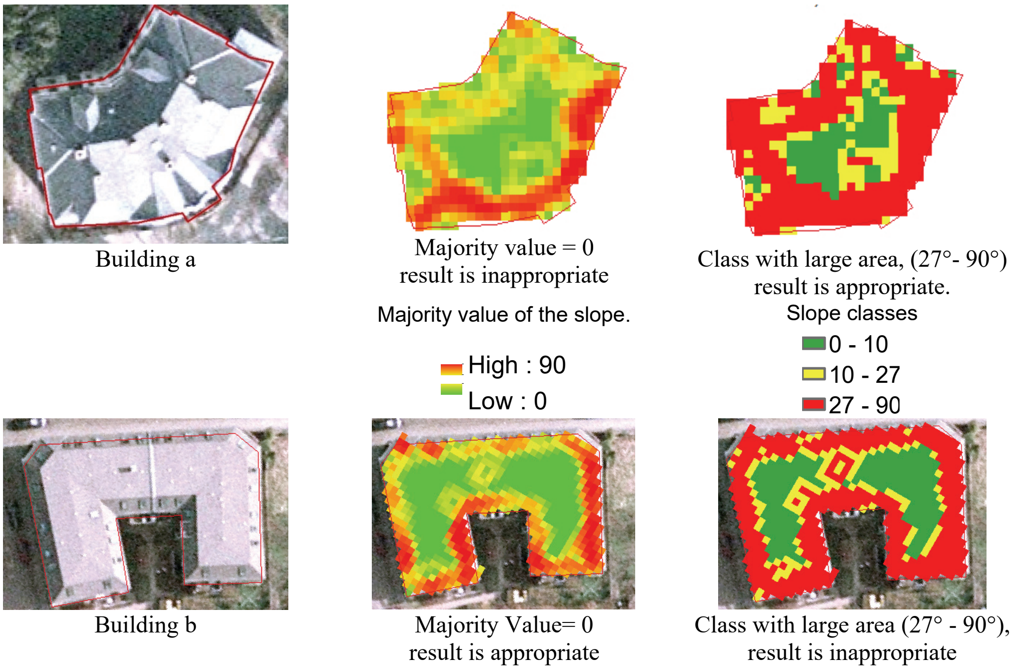

Figure 15: Methods for roof slope calculation (Blanco-Vogt et al., 2014, p. 7)

3.1.2.3 Parameters describing the contextual information of the building

These parameters attempt to describe the spatial attributes and properties of the contextual information of the building. Galster et al. (2001) state that the contextual information can set up the size, shape and arrangement of land parcels or lots and the building form

Compactness of buildings in urban areas: In this context, compactness is understood as a method of classifying the connectivity between the building and the open space, taking as reference (Stilla and Jurkiewicz, 1999), who examined compactness as the circumference/area for the analysis of roofs as well as Girling and Kellett (2005), who consider compactness for the analysis of density, the ecological footprint per household, the fragmentation of natural resources and the relation to impervious surfaces.

Here, compactness is defined as the relation of a building's size to its open space. Compactness helps to determine the agglomeration of buildings, contact with the open space, sunlight or daylight availability, self-shading, flexibility to activities, ventilation as well as privacy, and it may allow to identify if the building follows a pattern of space regulation. The higher the density between the buildings, the higher their values of compactness; or the more space there is between buildings, the higher the values of the inverse compactness.

Moreover, further works may use a compactness index for impact analyses on the buildings based additional water forces. For instance, Committee and Resources (2006) model the water velocity changes between houses and within roadways of a simple rectangular grid layout of houses, demonstrating that the closer the houses are spaced, the higher the flow velocity of the water is. The flood water finds a path to come through and its velocity may be modified by barriers. A radial method is used for the calculation of the index of inverse compactness, which consists in determining the percentage of open space around buildings (5). Open space is defined as green areas or street elements. Figure 16 gives the elements for the index of the inverse compactness of a building.

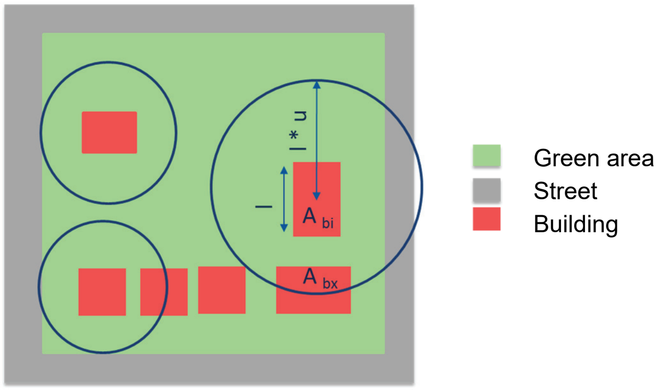

Figure 16: Example of the radial method for obtaining the index of the building compactness

$$Inverse\ \ Compactness = \frac{Ao}{Av} \qquad (5)$$

The index inverse compactness of a building is the relation of the area of open space within the vicinity ring (Ao) and the area of the vicinity ring (Av).

$$Av = \pi * (l * u)^2 - A_{bi} \qquad (6)$$

l: Longest side of the building;
u: Vicinity factor that multiplies the longest side of the building which is used as the radius of the vicinity ring
A_{bi}: Area of the building;

$$Ao = Av - \sum A_{bx} \qquad (7)$$

A_{bx}: Area of the other buildings that intersect the vicinity circle

Steps for the calculation of the index of inverse compactness of a building with a GIS tool: (i) calculating the centroid of the polygon; (ii) calculating the maximum length of the polygon, (iii) generating a circle of which the centre is the polygon's centroid and the radius the maximum length of the building polygon; (iv) extracting the area of the building polygons from the circle; a ring is generated as a result; (v) calculating the area of the open space ring and (vi) joining the area of the ring to the table of the building polygon.

The vicinity factor can be taken from regulation or guidance plans of cities which include a minimum distance between buildings, if it exists. Here, the values of the vicinity factors 1 and 1.5 are compared. The Figure 17 shows that the radial method with a vicinity factor of 1 extends the rank of values and allows us to discretise the building with less open space. The buildings in the middle of the terraced houses have less direct contact with open space than the buildings located at the ends.

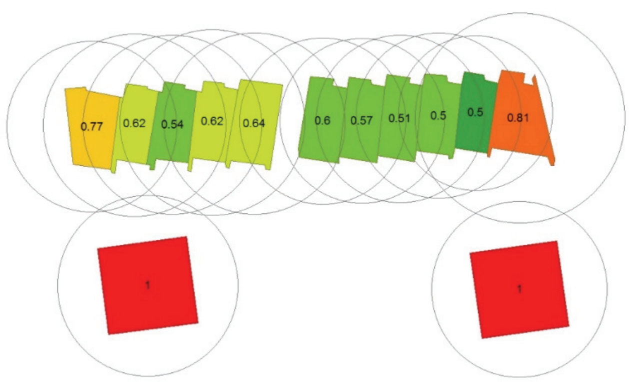

$u = 1$

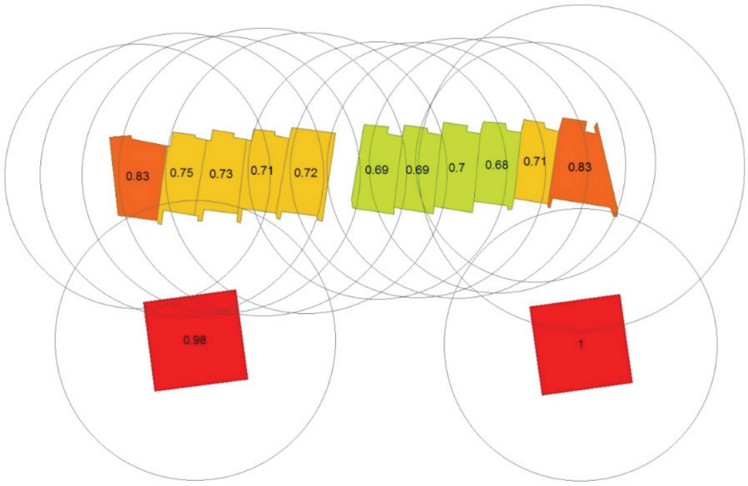

Figure 17: Example of a compactness calculation with different vicinity factors

Adjacency between buildings allows to identify (i) the position of a building with relation to its neighbours and (ii) its fenestration defined as the amount of facades exposed to open space.

The position of a building with relation to its neighbours: The amount of sides that are designed for fenestration may be associated with the position of the building towards its neighbours, whose function is to enclose and protect the contents against hazards. It can be calculated from the amount of a neighbour's building polygons in first and second order. The first order calculates the buildings sharing a wall, while the second order calculates the neighbours of the first neighbours. The number of adjacency and neighbours of every polygon can be calculated through a topological spatial analysis.

The steps for the calculation of adjacency are based on the GIS tool by Maene (2011): (i) "select the neighbours for each building polygon (1st order); (ii) store the ID of the selected neighbours in a list; (iii) join the ID of the 1st order neighbours to the corresponding polygon; (iv) select polygons touching the current selections/1st order neighbours; (v) store the IDs in a list only if neighbouring polygons are found (2nd order)"; (vi) join the ID of the 2nd order neighbours to the corresponding polygon; (vii) count the list of IDs for the 1st and 2nd attributes and (viii) categorise the amount of the IDs for 1st and 2nd neighbours according to Table 2. Figure 18 shows a schematic example of the categories proposed for adjacency.

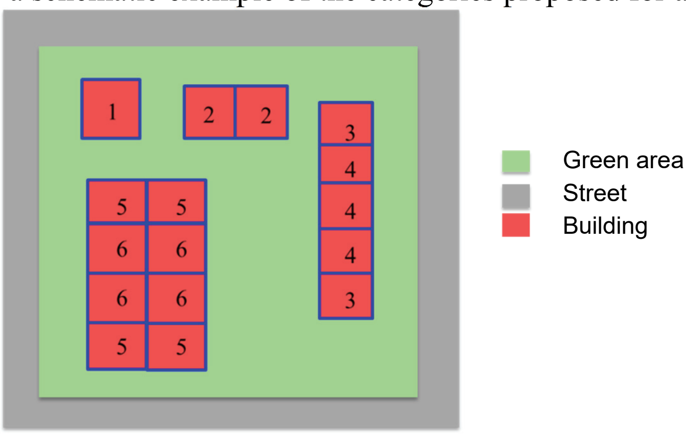

Figure 18: Example of categories of building adjacency

Table 2 presents a classification of the number of adjacency and neighbours based on the proposal by Hussain et al. (2006). There are six groups distinguishable from the grouping of buildings.

Table 2: Categories of adjacency and neighbourhood of building types

Code	Description categories of adjacency	Neighbours first order	Neighbours second order
1	A single or detached building does not have adjacency units or neighbours and normally has windows or entrances for each side of the construction. Within this class, there are either single units for one household or multi-units for many households.	0	0
2	Double or semi-detached buildings are a couple of buildings which share a wall within the construction.	1	0
3	The building in a corner within a line of buildings or terraced houses or row houses.	1	≥1
4	Building within a line of buildings, but not at the corner. These buildings are part of an arrangement of buildings sharing two sides. Normally, this type is used for department buildings, which share some services.	2	≥0
5	The building in the corner of a block. Buildings within a block unit share two or more sides and have one or at most two sides with driveways and air and light inlets.	3	>0
6	The building is located in a block, but not at the corner.	>3	>0

The building fenestration can be derived from the calculation of adjacency. Here, building fenestration is related to the amount of sides that are designed and placed for windows, doors and facades directly to open space. The function of the facades is to enclose and protect the contents of the building, daylight potential, electric light requirements, safety, security, ventilation, accessibility as well as other factors, such as energy-efficient building design in terms of temperature, shadow, irradiance and wind (Cocina, 2011). Figure 19 presents four categories of building fenestration for buildings with four sides. Each value of the categories shows the number of facades exposed to open spaces.

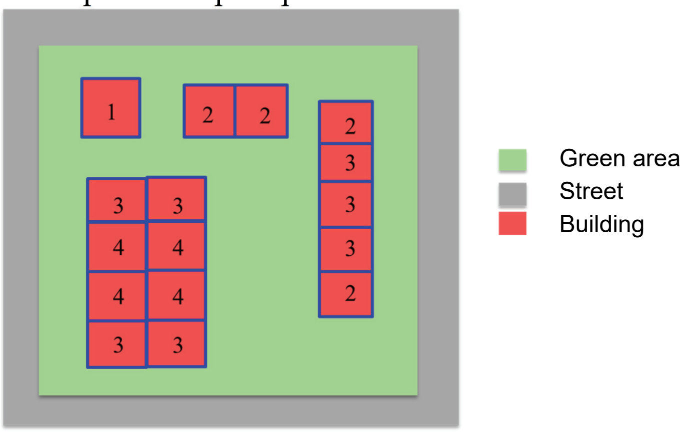

Figure 19: Example of facades exposed to open space

The description of the categories for fenestration is revealed in the next table. The adjacency values can be recoded for finding the fenestration categories. According to the adjacency categories, the adjacency codes 2 and 3 belong to the building fenestration code 3, and adjacency codes 4 and 5 to code 2.

Table 3: Categories for the sides of facades

Code	Categories of building fenestration
1	All sides exposed to open space
2	At least three sides exposed to open space
3	Two sides exposed to open space
4	One side exposed to open space

3.1.2.4 Linking building features with the building parameters

The seven parameters can be collected from non-invasive methods, but they demand expensive field works, interviews, questionnaires or invasive analyses. For this version of the building typology approach, only building outline, building height and building roof surface are taken into account. According to the literature, a very high resolution (spectral and/or elevation data) allows for the extraction of these building features (see section 3.1.1.1). The following scheme (Figure 20) depicts the features required for the calculation of the parameters.

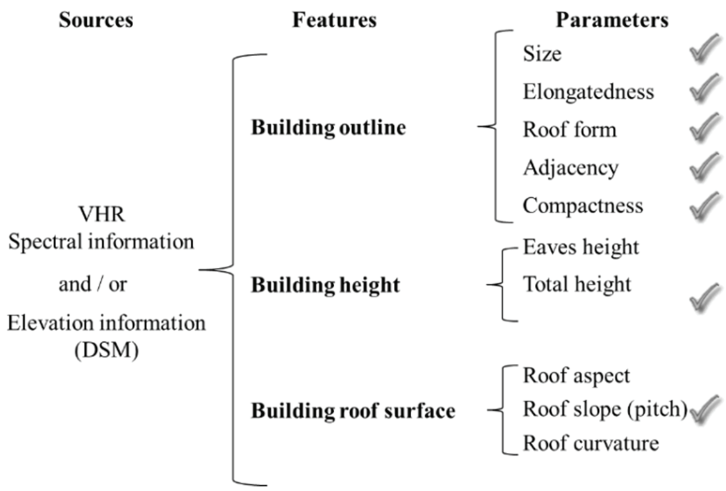

Figure 20: Features which need to be extracted for the calculation of the parameters

The method of the semantic image interpretation helps to identify the characteristics of the building features. Further parameters such as building roof aspect, building roof curvature or building roof slope can be derived from the feature “building surface”. The gathering and analysis of the building roof aspect and building roof curvature can be useful for other types of applications such as rainwater harvesting or solar panels. However, the parameter which is most relevant for the definition of the typology is the building roof slope as demonstrated in the previous section. The quality of the extraction of building outline, building height and building surface can be validated using a combination of the horizontal and vertical accuracy indices (see section 3.1.1.2.v).

3.1.2.5 Setting up the building taxonomy

The parameters above described may be involved in arranging a building typology. These parameters are determined through continuous measurements (size, height, elongatedness and roof slope), discrete variables (adjacency and roof form) and interval scale variables as the values are ranked (compactness). If the roof material had been included as well, it would have been sorted by its reflectance or other properties and their values could be codified as a nominal variable. The distribution, correlations and redundancies between the data could be analysed for each parameter. It is important to note that infrastructure and building attributes are not always distributed according to a bell curve and the patterns of their parameters are not predictable.

An approach for finding patterns and classes between the building's characteristics is coding the data (Adriaans and Zantinge, 1996). Coding information allows to systematically identify variables and values and to ensure their validation. The data codification for each parameter corresponds to a category describing the building characteristics. Although the categorisation of continuous data presents statistical disadvantages in terms of loss of information, power and efficiency (Montgomery, 1991), the classes can describe a building's physical and functional properties and they can also verified directly in the field. Converting themes into codes creates a link between qualitative and quantitative methods (Boyatzis, 1998; Srnka and Koeszegi, 2007). The building taxonomic code associates the quantitative data provided by the digital surface models and GIS calculation with the qualitative data from categorisations carried out by experts.

However, the determination of categories raises the following questions: How many categories are needed to reflect the representativeness of the continuous data? Where is the inflection point for defining a new category? Which method is suitable for assigning a new segment – whether statistic or empiric? What are the exact validation criteria if those categories show the whole universe? Are the categories reliable? How general or detailed should the grouping of the building characteristics be? These questions can be answered by using trial and error testing and the risks of subjectivity can be reduced since the selected parameters capture systemic key differences between the characteristics of the buildings, and they can be related to a building functionality.

The coding starts with induction. Each parameter is codified on the basis of the building's initial description; those categories are then improved in function of the emerging theoretical questions and the results from the empirical application. A preliminary hypothesis is presented with initial values of the categories for each parameter. These values are corroborated with data from different regions. Inevitably, the findings of the categories require the assumptions and experiences of experts in order to make decisions about what are more important in the data and what less.

The delimitation of the category ranges should be carried out with the consensus of experts (civil engineers or architects), who discuss the consistency among the range of the classes for each parameter. The reliability in the judgments for defining these categories can be measured with the percentage of agreement proposed by Boyatzis (1998). The values of the classes can be verified directly on field surveys. For example, if a building's height is less than four metres; its maximum amount of storeys must be one. Four vertices in a building's roof mean that it has a rectangular or trapezoidal form. If the ratio of a building's length and width is 1, this means that the building footprint occupies a square form in the terrain.

Hence, the categories have the advantage that they are related to a description of the attributes. For each category, or class, a code is assigned to show all the values. The code number is a "label" used to facility the handling of the information. The category ranges of every parameter and their code can be developed following the next steps: (i) visual interpretation of the buildings, (ii) corroborating with the knowledge of the experts, (iii) testing if the ranges can be extended or collapsed and (iv) connecting the codes and identifying the patterns. The borders of the classes are adjusted through training and statistical analyses of the values for each class. The categories for each parameter are the result of a verification of the values compared with the building's characteristics.

Miller (1956) confirms that humans can typically maintain seven, plus or minus two, variables covarying in their conscious mind at the same time. The building taxonomic code composed by seven parameters (height, size, elongatedness, roof form, roof slope, compactness and adjacency) can assist experts in identifying the principal structural characteristics of a building; it should be appropriate for any region of the world and can serve as a vehicle for transferring behaviours or patterns of variables to urban areas.

The representation of the parameters in maps and colours, histograms, scaling values, scatter diagrams and correlating variables can help to find empirical patterns, to relate characteristics and a possible hierarchy, to test the ranges of categories in many areas and to attempt to find rules in similar urban areas. In fact, "the inductive approach reflects frequently reported patterns used in qualitative data analysis" (Thomas, 2003). A preliminary classification with initial values of the categories for each parameter is presented in Table 4.

Table 4: Initial codes and description of the parameters

Group of variables	Variable	Code	Values
Criteria that describe the contextual information of the building	Index inverse compactness	1. 2. 3. 4. 5.	> 80 % – 100 % > 60 % – 80 % > 40 % – 60 % > 20 % – 40 % 0 % – 20 %
	Adjacency	1. 2. 3. 4. 5. 6.	Single building (Neighbour 1° = 0 and Neighbour 2° = 0) Pair building or single building with annex (Neighbour 1° = 1 and Neighbour 2° = 0) Corner building within a line of buildings (Neighbour 1° = 1 and Neighbour 2° ≥ 1) Building within a line of buildings (Neighbour 1° = 2 and Neighbour 2° ≥ 0 Building within a block (Neighbour 1° = 2 and Neighbour 2° ≥ 0) Corner building within a block (Neighbour 1° = 3 and Neighbour 2° ≥ 0)
Criteria that describe geometric characteristics	Building footprint - Size	1. 2. 3. 4. 5. 6. 7. 8.	0 - 50 m² > 50 – 100 m² > 100 – 200 m² > 200 – 400 m² > 400 – 800 m² > 800 – 1000 m² > 1000 – 2000 m² > 2000 m²
	Building height	1. 2. 3. 4. 5. 6. 7. 8. 9.	0 – 5 m > 5 – 10 m > 10 – 20 m > 20 – 30 m > 30 – 50 m > 50 – 100 m > 100 – 200 m > 20 – 400 m > 400 m
	Elongatedness	1. 2.	Square: 0.7 – 1.3 Elongated rectangle: > 0.7 and < 1.3
Criteria that describe the surface of the roof	Roof form (footprint)	1. 2. 3. 4. 5. 6.	≤ 6 vertices > 6 – 12 vertices > 12 – 24 vertices > 24 - 48 vertices > 48 – 76 vertices > 76 vertices
	Roof slope (roof pitch)	1. 2. 3.	≤ 10 degrees > 10 – 27 degrees > 27 degrees

The concatenation of the values of each variable gives the building taxonomic code:

$$Building\ \ Taxonomy\ \ Code = P_{ij}\ \&\ P_{nj} \qquad (8)$$

P_i to P_n is the amount of parameters and $_j$ represents the code for the category of the parameter. The amount of taxonomic codes depends of the amount of categories for each parameter. In the previous example, the combination of codes should be 5 x 6 x 8 x 9 x 2 x 6 x 3 = 77 760 building types. Obviously, it is unfeasible for a person to keep in mind the amount of codes. Therefore, this calculation must be carried out by a computer.

The code reveals the principal characteristic of a building and can be translated into a description. For instance, the code '*1111111*' describes a single building (1st digit: adjacency), open space around the building larger than 80 % (2nd digit: compactness), size less than 50 m² (3rd digit: size), one-storey building (4th digit: height), square form in the space (5th digit: elongatedness), very simple form (6th digit: roof form) and flat roof (7th digit: roof pitch). Table 5 gives examples of how to join the values for the generation of the taxonomic code.

Table 5: Taxonomic building code example for a building typology

Compactness	**Adjacency**	**Height**	**Size**	**Elongated.**	**Roof form**	**Roof slope**	**Taxonomic Code**
1	2	2	4	1	2	4	*'1224124'*
4	1	3	2	2	3	3	*'4132233'*

3.1.3 Selection of representative buildings for a building susceptibility assessment

The assessment of potential flood impacts on buildings does not need to be carried out one by one as this would be very expensive, time-consuming and would demand significant technical resources. The selection of representative buildings is therefore required to transfer the knowledge from the assessment of in-depth investigations of individual buildings to other buildings with similar characteristics.

In this section, the definition of representative and non-representative buildings, the strategies for selecting representative buildings and the clustering of the non-representative with the representative buildings is explained. At the end of the section, an example of the process is given.

3.1.3.1 Definition of representative buildings

Representative buildings stand for "typical", "prototype", "archetypal" or "common" buildings within a pilot site. The representativeness can be measured by counting how many times a building shares similar characteristics with other buildings in a settlement. Here, the connotation of *representative* is used for a building belonging to a group of the same building taxonomic code with a higher frequency in a particular area or settlement.

The advantage of the selection of representative buildings is that they stand for a large percentage of buildings in study areas. Table 6 shows three building types: building type '*1224124*' with 150 buildings, building type '*41232233*' with 125 and building type '*2223224*' with only seven buildings. If samples of the building types'*1224124*' and '*41232233*' are selected, the majority of the population is covered statistically. The analyst should choose a threshold of representativeness for separating typical from non-typical buildings by using a histogram with the amount of buildings per taxonomic code.

Table 6: Example of the selection of representatives

Row	**Compact.**	**Adjacency**	**Size**	**Height**	**Elongat.**	**Roof form**	**Roof slope**	**Frequency**	**Represent-tive**
1	*1*	*2*	*2*	*4*	*1*	*2*	*4*	150 (typical)	Yes
2	*4*	*1*	*3*	*2*	*2*	*3*	*3*	125 (typical)	Yes
3	*2*	*2*	*2*	*3*	*2*	*2*	*4*	7 (atypical)	No

3.1.3.2 Clustering of the non-representative with the representative buildings

The expert can collapse the typologies by merging the codes of the relevant parameters based on the frequency diagramm and finding the best way for matching the codes with higher similarity. An approach to find similarities is grouping the data by means of *cluster analysis* (MacQueen, 1967), which allows to identify groups of objects with a similar pattern but which differ from individuals in other groups. (Kaufman and Rousseeuw, 1990) exemplify the different cluster treatments to discover patterns in different types of data through statistical methods.

Here, the method for clustering buildings to representative buildings is based on the *fuzzy clustering*. Coppi et al. (2006, p. 6) explain the method as:

> "[…] to determine *K* clusters, *say* $C_1, \ldots, C_k, \ldots, C_K$, in R^p, capable to single out a "typology" of the units expressed by the "prototypes" characterizing each of the clusters. Usually, the prototype of C_k $(k = 1, \ldots, K)$ is a vector, c_k, in R^p. Traditional "crisp" clustering aims at estimating, for each cluster, a classical characteristic function u_{ik} taking values in {0, 1}, allowing us to assign (u_{ik} = 1) or not assign (u_{ik} = 0) unit *I* to cluster *k* and, at the same time, it aims at providing us with estimates of the prototypes c_k (most often given by the "centroids" of the clusters).
>
> This clustering model is suitably generalized by the fuzzy approach, in that the typology searched for is thought of as a "fuzzy typology", stressing the imprecision/vagueness generally associated, in real-life investigations, with any classification procedure. This is simply achieved by allowing the u_{ik}'s becoming membership functions of the corresponding fuzzy clusters $\hat{C}_k$ $(k=1, \ldots, K)$, defined on the set of *n* units. One of the most popular methods, in this framework, is the Fuzzy K-Means. This is a non-hierarchical technique based on the minimization of the following objective function."

$$F(U,C \mid X,m,K) = \sum_{i=1}^{n}\sum_{k=1}^{K} u_{ik}^{m} d^2(x_i, c_k), \quad (9)$$

The selected representative buildings are the *K* clusters which contain *p* quantitative parameters. The similarities between non-representative buildings and representative buildings are compared, taking values between {0, 1}, the "crisp" values belonging to a membership function. A membership function provides a measure of the degree of similarity of an element with a fuzzy set and helps to identify the borders between the typologies, where they are inherently vague.

The sum of the assigned values gives the percentage of matching with a representative building. Then, the non-representative is grouped to the building type with the largest values of membership. Inductive reasoning, iterative process and trial and error help to generate the membership functions and the rules for selecting the value of the sum for the matching in order to minimise the entropy for every case study. The user can set the ratio of knowledge to data in order to enhance or contrast the parameters giving more restriction to the building type membership. The number of columns depends on how many parameters the taxonomic code has, and the number of rows on the values of the function of membership. The following two examples present the crisp values for a membership function for the seven parameters (e.g. Figure 21).

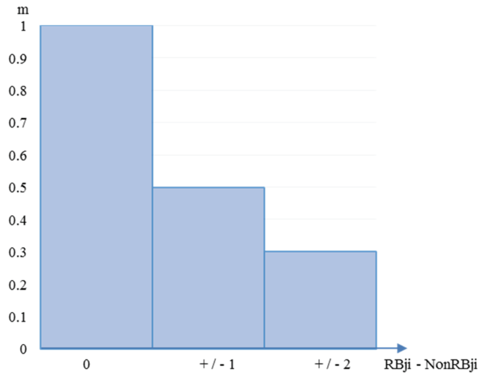

$$U_{R-nonR} = \begin{bmatrix} 1 & 1 & 1 & 1 & 1 & 1 & 1 \\ 0.5 & 0.5 & 0.5 & 0.5 & 0.5 & 0.5 & 0.5 \\ 0.3 & 0.3 & 0.3 & 0.3 & 0.3 & 0.3 & 0.3 \\ 0 & 0 & 0 & 0 & 0 & 0 & 0 \end{bmatrix} \quad \text{Type 1} \quad (10)$$

Figure 21: A membership function for clustering building typologies

The membership function is defined as:

- If RBji – NonRBji = 0, THEN similarity coefficient is = 1,
- If RBji – NonRBji = +/-1 THEN similarity coefficient is = 0.5,
- If RBji – NonRBji = +/-2 THEN similarity coefficient is = 0.3
- If RBji – NonRBji >2 THEN similarity coefficient is = 0

RB_{ij} are the representative buildings for the parameter $_j$ with the category $_i$ and $NonRB_{ij}$ the non-representative buildings for the parameter $_j$ with the category $_i$.

Further membership functions can be developed in order to find more restrictions in the clustering. Example 2 of a membership function:

- Compactness may be clustered in maximal 1 category.
- Adjacency: The values 1 and 2 are fix, but 3 and 4 as well as 5 and 6 may belong to the same group and can be grouped for the building fenestration.
- Size cannot be clustered between other categories.
- Height cannot be clustered between other categories.
- Elongatedness is not a decisive parameter.
- Roof form can vary between two categories.
- Roof pitch can vary between two categories.

$$U_{R-nonR} = \begin{bmatrix} 1 & 1 & 1 & 1 & 1 & 1 & 1 \\ 0.3 & 0.8 & 0 & 0 & 0.8 & 0.8 & 0.4 \\ 0 & 0.5 & 0 & 0 & 0 & 0.5 & 0.2 \\ 0 & 0.1 & 0 & 0 & 0 & 0 & 0 \end{bmatrix} \quad \text{Type 2} \quad (11)$$

Experts will define the frequency of a taxonomic code which is required to be considered as representative. Table 7 depicts the assignation of values of the non-representative buildings to the representative buildings according to the membership function of the equation (10)

Table 7: Selection of representative buildings

Comparison	Compact.	Adjacency	Size	Height	Elongat.	Roof form	Roof slope	Sum	similarity coefficient	Selected
1-3	0.5	1	1	0.5	0.5	1	1	5.5	5.5 / 7 = 0.79	Largestm atching
2-3	0	0.5	0.5	0.5	1	0.5	0.5	3.5	3.5 / 7= 0.5	Lower similarity

The non-representative (row-3) ‘*2223224’* has more similar characteristic with (row-1) with 79 % than ‘*1224124’* with (row-2) ‘*4132233’* with only 50 %. If the similarity coefficient is very low for the two comparisons, this means that the buildings are atypical in the area.

3.1.3.3 Strategies for selected representative buildings

The next step consists in selecting representative building samples or “sample archetypes” for detailed analyses of the physical flood impact based on the building materials and components. Neyman (1934) states that there are two different aspects of the representative method: method of random sampling and the method of purposive selection. Random sampling means that single elements of the population with equal chances for each element are included in the sample. In purposive selection, the unit is an aggregate of things, such as a whole settlement. A random sample by groups is then a combination of the two methods and called *stratified sampling*, which ensures that the results are proportional and representative for the whole population of buildings, which are categorised in building types.

The Sampling Design Tool for ArcGIS designed by NOAA (2012) can be of benefit here for a *stratified selection of samples* for each building type with known size. The tool allows us to define strategies for the selection of representative buildings samples, such as random sampling, grids, along lines called transects or stratified sampling.

A sampling strategy for selecting representative buildings takes into account the following criteria: (i) the linear distance between the selected sample of buildings should be minimal in order to minimise time and costs of the surveys and (ii) it must be ensured that at least one sample of representative buildings with the same code will be analysed.

▪

Table 8 summaries the process for the selection of representative buildings with the help of a schematic example. The following definitions are considered:

- *Building type*, BT: Group of buildings with the same taxonomic code.
- *Representative buildings*, RB: Buildings that are typical or have a higher frequency within the pilot site according to their taxonomic code.
- *Non-representative buildings*, NRB: Buildings that are not typical in the pilot site.
- *Similarity coefficient* between taxonomic codes: The non-representative buildings are grouped to the representative buildings depending on the matching similarity coefficient according to a membership function.
- *Samples of representative buildings*, SRB: Buildings that are selected from the representative building type for the analysis of the physical flood vulnerability.
- *Threshold of representativeness*, TR: Value that separates the amount of typical and non-typical buildings for each settlement using the histogram of building taxonomic codes.

- *Threshold value for clustering*, TVC: It will decide with this value whether a non-representative building can be grouped or not to a representative building, based on the percentage of matching similarities. This threshold value isolates the atypical buildings.

Table 8: Example for the selection of representative building types

Step	Graphic results	Report
1.Calculating of the building typology for each building	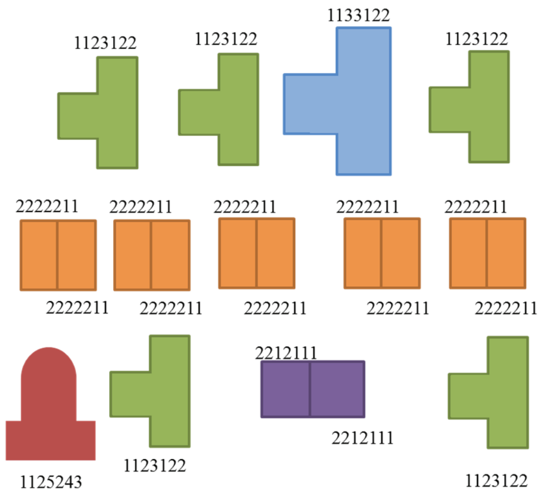	*The sign » means the enter of the user and the sign « means the outcome of the process* »The user enter the polygons outline in vector format and the nDSM « The calculation gives: 19 buildings and 5 building types with its taxonomic code calculated automatically BT *'1123122'* has 5 buildings BT '*2222211'* has 10 buildings BT '*1133122'* has 1 building BT '*2212111'* has 2 buildings BT '*1125243'* has 1 building
2. Definition of the building types with major amounts of buildings	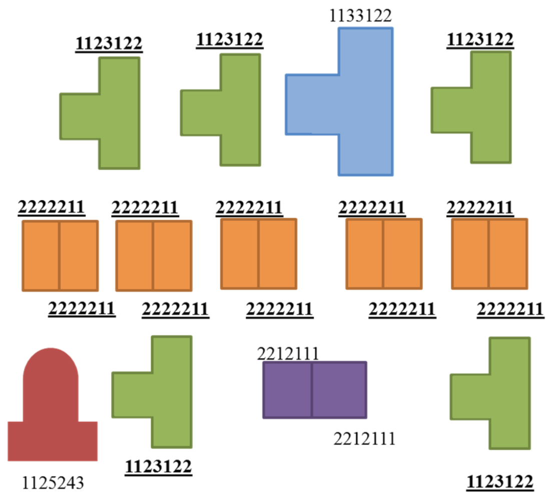	»The user selects the BT with at least 5 buildings as representative building types. «BT '*1123122'* and BT '*2222211'* are the building types with the highest frequency. «BT '*1133122'*, BT '*2212111'* and BT '*1125243'* have a lower frequency than they are the **NRB.**
3. Computation of similarities between non-representative and representative buildings	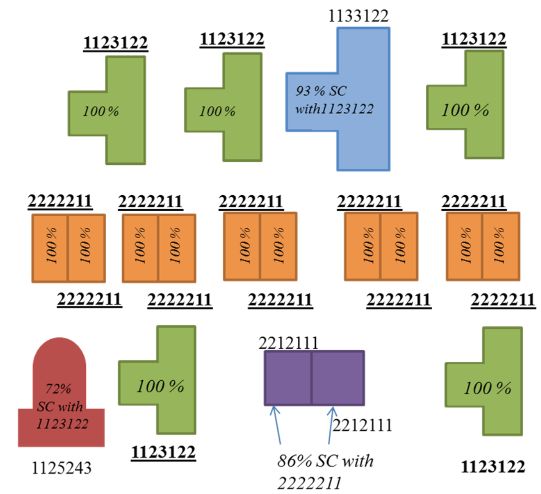	»The user selects the threshold of representiveness **TR** as 5 and the values of the membership function e.g. Formula (10) «The **RBs** receive the highest similarity coefficient (100 %). They act as K centroids of the groups. «For the **NRB,** the similarity coefficient is calculated on the basis of the condition of the membership function.

4.1 Comparing similarities between RB and NRB.

4.2 Taking samples

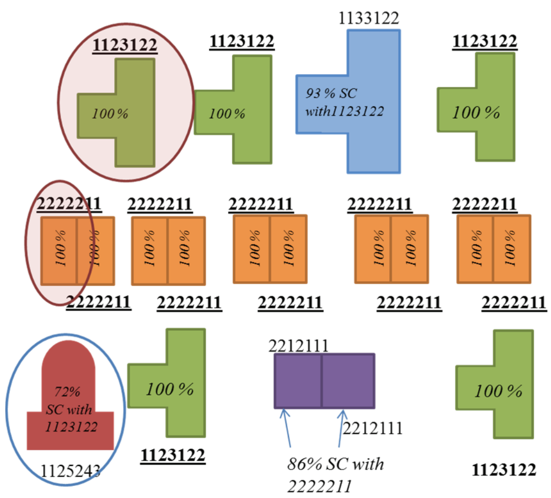

»Threshold value for clustering, **TVC** of 80%

«The **NRB** types are compared to the **RB** with the highest similarity.

The buildings under the threshold value for clustering TVC must be as well be analysed. In this example, the building with the blue circle is an **atypical (AT)** because its similarity threshold is lower than 80%. It must be included in the samples for evaluation.

5. Clustering of non-representative buildings to representative buildings with maximum similarity

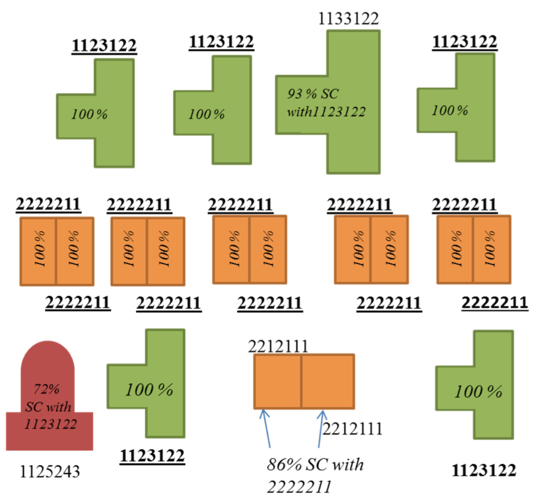

»The user selects the amount of **SRB.**

Example: The user selects at least one buildings of each group of buildings so that the distance between them is minimal in order to minimise transportation costs.

Here, there are three groups of buildings of which the physical flood vulnerability is analysed: RBT *'1123122'*, *'2222211'* and the **AT** *'1125243'*.

3.2 Module 2: Physical susceptibility of representative buildings

Once the representative buildings within a pilot site are selected, the analysis of their physical flood susceptibility is carried out. Figure 22 illustrates the workflow for the assessment of the physical impacts of floods on buildings. For this purpose, the potential flood impacts for representative buildings are analysed according to the process described below.

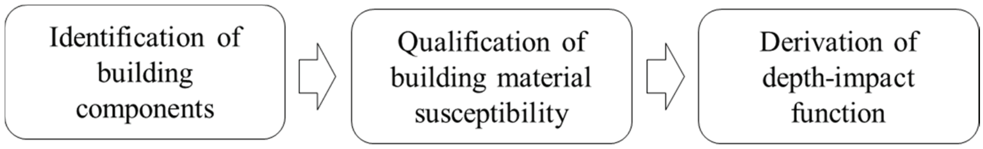

Figure 22: Components of Module 2: "Physical susceptibility of buildings"

3.2.1 Identification of building components

The identification of building components consists in (i) recognising the relevant building components, (ii) their upper and lower height above the ground, (iii) their relevant dimensions and volume calculation and (iv) relevant materials.

3.2.1.1 Relevant building components

Building components can be categorised in structural components, shell components, non-structural components, connectors, inventory and finish components.

Non-invasive methods can be carried out for analysing the presence of structure and shell components of buildings, such as the presence of basements, external windows, external doors, façades, external walls, some roof characteristics, balconies, columns, beams or slabs. At least these components must be distinguished and inventoried for a building susceptibility analysis.

Foundation is the lowest and supporting layer of a structure. It is the part of a structure that transmits the weight of the structure onto the natural ground. Terzaghi and Peck (1967) state that foundations have to deal with groundwater and hydrostatic pressure and the minimum depth of a building foundation requires that the base of every part should be located below the depth where the soil is subject to seasonal volume changes caused by alternate wetting and drying. Methods for designing structures and modelling loads are constantly being refined; important changes have occurred in the design of wood, steel and reinforced concrete structures (Ochshorn, 2010). "Most damages are caused by the wetting of contents and the building structure in the cellar and the ground floor than effects due to flow velocity" (Büchele et al., 2006).

Columns are "vertical elements subjected to compressive stress" (Ochshorn, 2010). They transmit, through compression, the weight of the structure above to other structural elements below. A column that carries the load down to a foundation must have a means to transfer the load without overstressing the foundation material (Concise Encyclopedia, 2013).

Beams are structural elements used for load-bearing applications. "Beams are both stressed and subject to deformation when loaded. Both of these considerations must be accounted for in the design of beams" (Ochshorn, 2010).

Slabs and plates "are flat pieces of concrete, put on the walls or columns of a structure. They serve as a walking surface, but may also serve as a load-bearing member, as in slab homes. The function of the slabs is to provide a flat surface, to support load, sound, heat and fire insulator, act as a divider (privacy) for the occupants, upper slab became the ceiling for the storey below" (EnggPedia, 2013).

External walls are surfaces on the outside of a building; they usually have windows and doors, but not all the time. The exterior walls of a house have several functions. Not only do they define the shape of a house, they also support the floors, walls and roof. "Equally important is their role in separating the house's interior from the outdoors, and to do this effectively they have to block the weather with systems that insulate, shed water, and repel moisture and air infiltration […]" (Green building advisor, 2013).

External windows and doors are features that offer a variety of safety and security options, achieving outstanding weather resistance that can be supplied with a high performance thermal break to improve energy efficiency. They are a movable structure used to open and close off an entrance, typically consisting of a panel that swings on hinges or that slides or rotates inside of a space. They admit ventilation and light control for the physical atmosphere within a space enclosing it, exclude air draft, so that interiors may be more effectively heated or cooled. They act as a barrier to noise, to admit light and air and to give a view to the outside (Thefreedictionary, 2013).

Stairs are "a construction designed to connect a storey to another storey with higher or lower level above the ground". Styles, dimensions and security codes have been established depending on their function, e.g. the stairs code of SMA (2009).

The roof function was described in the section 3.1.1.2.

Regarding to non-structural components, Porter (2005) compared ten criteria for eleven taxonomies of non-structural building components and he concluded that NISTIR 6389 published by the NIST Committee (NIST, 1999) offers a manageable level of details for a classification of non-structural building components. Although this classification is designed for a post-earthquake reconnaissance, it may be reviewed for its applicability in further flood impact analyses and its implementation not only in the USA.

Non-structural components are elements such as architectural features like exterior cladding and glazing, ornamentation, chimneys, ceilings, interior partitions, interior walls and stairs; mechanical components and systems including air conditioning equipment, ducts, elevators, escalators, pumps emergency generators and sprinkler piping; electrical components including transformers, switch gear, motor control centres, lighting and raceways; fire protection systems including piping and tanks; plumbing systems and components including piping, fixtures (FEMA, 2010); other elements such as furniture, household appliances; finish elements such as carpets, veneer, stucco, plastics, adhesives, caulks, putties or glues etc.

A long list of inventory components can be described, which fulfil additional building functions, such as lifts, stairs, sanitary, electrical and gas installations. For a detailed scale, furniture can also be included, based on footprints, invasive methods or complementary information such as census and socio-economic strata. Moreover, reference information on the tenure of certain social groups could help here. Another group of building elements are the connectors, which "constitute an intermediate condition between elements and system, and are not part of the elements themselves" (Ochshorn, 2010).

The above mentioned components highlighted in italic style are selected for this study for the analysis of a flood impact assessment, due to the fact that their characteristic can be collected through non-invasive methods.

3.2.1.2 Component's position above the ground

The components can be arranged according to their position above the ground and related with water levels that could cover them. An example of the list of principal components that can be exposed to water is depicted in Figure 23.

Figure 23: Principal components of the building covered by a floodwater level

The following methods can be used to obtain the position of the components above the ground and their principal dimensions:

Mobile mapping is a technology for collecting geospatial data and detailed landscape models. A mobile vehicle such as an unmanned aerial vehicle (UAVs) or a manned vehicle with synchronised navigation sensors and different types of sensors, such as photographic cameras, radar, laser or omnidirectional images, produces georeferenced images and videos, and is able to generate GIS data, digital maps, 3D models of large scenes and even 3D reconstructions of indoor surfaces (e.g. (Zhu et al., 2007)). This data can be downloaded to GIS desktops or device mobiles, like smartphones. The accuracy is strongly influenced by the control data from the navigation sensors and the quality of the mapping sensor. The costs for the system depend on the accuracy of the Inertial Navigation System (INS) (Li, 2011). An example of mobile mapping is the products of Google Street, which provides panoramic views from positions along many streets in the world, based on different generation of camaras. Zamir and Shah (2010) propose a localization method for measuring the confidence localization accuracy of image localization based on Google Maps Street View.

Terrestrial photogrammetry and terrestrial laser scanning: The integration of close-range photogrammetry and terrestrial laser scanning techniques has improved the geometry and the visual quality of collected 3D models. Stereometric cameras, independent metric cameras, semi-metric cameras and CCD (charge couple devices) "cameras can be equipped with terrestial laser scanning generating point clouds from 3D coordinates" (Lemmens, 2011).

Laser instruments measure height differences, object heights and inclination angles with an accuracy of 3-5 cm. The higher the precision, the higher the prices for the instrument.

Apps measure an object's distance and height with a smartphone by means of the device camera and the use of trigonometry formulae. The accuracy of the distance measurement is about 10-30 cm.

Metre sticks have an uncertainty of half of the smallest division. So if they have centimetre marks, the uncertainty would be 5 mm. They have a high precision, but their use is exhausting and time-consuming.

Known standard dimensions: There is a relation between the height of the components within buildings and anthropometry standards. The heights of objects for interior spaces in residential and office areas have known standard dimensions. Hereby, Diffrient et al. (1974); Panero and Zelnik (1979) present the anthropometric dimension and the relation to the objects located in the houses. Many body functions controlled by the sight movement take place within the range of the eye movement (865-1,905 cm). The position of utensils, devices and equipment, such as emergency signals, doorknobs, shower valves or kitchen counters, are therefore located within this range. The maximum distance to reach elements should be 1,770 to 2,185 cm and the minimum ceiling height 2,030 cm. Furniture should be located at particular heights in order to be accessible.

Information provided by the manufacturer: Many properties and dimensions of components can be extracted from the information provided by the manufacturer, such as catalogues.

Besides the instruments used for gathering the component's dimension, the most important is the accuracy for measuring the lower and higher position of the component above the ground with a precision of 10 +/- cm as well as the principal dimensions of the components, since the flood depth can be estimated at a precision of cm.

3.2.1.3 Relevant dimensions and volume calculation

The following dimensions of a building are calculated from the parameters of the taxonomic code and GIS calculations: A= Area, P= Perimeter, H= Height from nDSM, α = Roof slope, W= Width and L= Length. Appendix B provides the required parameters for the calculation of a component's volume, which can be measured with the methods mentioned above: mobile mapping, omnidirectional imaging, terrestrial photogrammetry, laser instruments, Apps, metre sticks, information provided by the manufacturer or known standard dimension.

There are some applications available for free in the internet which assist the calculation of the material's volume for components such as Home 4 India (2010) and Zhitov (2013). An example of the dimensions which need to be collected in the field and the chosen method or instrument for the calculation of volume is shown in Table 9. A description about the abbreviation of parameters for every component can be seen in Appendix B.

Table 9: Example of methods for measuring building component dimensions

Component	Parameters	Lowest and highest height
Roof cover	*Ts* is extracted from the information of the manufacturer. *La* is measured with the app.	Lowest value from the DSM within the building outline. Highest value from DSM within the building outline.
Roof rafter	*Wr*,*Tr* and *Dr* may be measured with a metre stick or the app.	It may be measured with the app and verified with a metre stick.
Beams	*Wb* and *Tb* may be measured with the app. *Lb* is derived from *W* and *L*	It may be estimated based on questions to the tenant.
External windows	*Hw, Ww, Wt* and *Wb* are measured with the app.	It may be measured with the app.
External walls	*Wb* and *Hw* may be measured with a metre stick.	It may be measured with the app.
External doors	*Hd, Wd* and *Td* may be measured with a metre stick.	It may be measured with the app or a metre stick.
Floor	*Bf* may be extracted from the information of the manufacturer.	It may be measured with a metre stick.
Columns	*D E, Hc, Hd, F* and *G* may be estimated based on questions to the tenant and information of reference from the constructive process.	It may be estimated based on questions to the tenant and on the experience of the surveyor.
Foundations	*Wf* and *Hf* may be estimated based on questions to the tenant.	It may be estimated based on the experience of the surveyor.

3.2.1.4 Identification of relevant component materials

The variety of materials available in cities and many industrialized regions has increased dramatically, "the range commonly available today, even under those general classifications, is far broader than before" (Ward-Harvey, 2009). Materials with less variety and derived from primary sources, such as mud bricks, rammed earth, straw bale, stones, timber, mortar, plaster, terra cotta or slate without any special treatment, are frequently used in regions with low incomes.

The identification of the material of constructive elements requires expert knowledge from civil engineers or architects through *visual inspection* methods. The surveys allow the experts to identify construction processes and the materials used for building types as well as to identify the designation used for the particular material in this region as material designations can vary from region to region.

Friedmann (2005) states that visual inspection involves conscious "attention" by the expert for collecting the information and also explains the limits of a normally sighted human in the visual interpretation. "Seeing" involves a conscious mental effort and focus, a task from which observers can be distracted or which can fail due to "inattentional blindness". To overcome this fact, the expert must train their ability to recognize building components, materials and dimensions, supported by photos or videos as evidence of the data collection in order to maximize the quality of the record data. At this point, the identification of material does not require a qualitative assessment.

Initially finish materials were not taken into account for this approach because of their diversity and the difficulty to identify their characteristics. Table 10 shows an example of the components selected for the above-mentioned building components with their principal material.

Table 10: Identification of the material (example)

Component	Relevant material
Roof cover	Eternit tiles
Roof rafter	Wood
Beams	Concrete
Ceiling	Solid wood, standard, finish/trim
External windows	Wood frames and metal bars
External walls	Block and brick grid types
External doors	Wood
Floor	Cement
Columns	Concrete and metal rods
Foundations	Concrete, brick and stone

3.2.2 Qualification of building material susceptibility

Susceptibility means that the material may be harmed, worn or degraded when facing the flood; whereas resilience as the contrary of susceptibility is often viewed as a positive property: It means a receptor's ability to withstand an impact without significantly changing (Naumann et al., 2010). The degree of experienced harm (susceptibility) uses a susceptibility degree as the inverse value of resistance (Blanco-Vogt and Schanze, 2014). Here it is assumed that 'material susceptibility is the opposite of its resistance'.

In this subchapter, the relation between material resistance and susceptibility is analysed. The building material's resistance is analysed according to international studies whose values are transformed to susceptibility values based on the judgment and the verification of experts.

3.2.2.1 Building material resistance

The resistance of building material is described by Aglan et al. (2004), who developed a guidance for collecting representative, measured and reproducible data on how variously residential materials and systems respond to flooding conditions. Additionally, Aglan et al. (2004) test materials and systems that were commonly found in residential envelopes throughout the U.S. as well as materials that were projected to be more resistant to flood damage. The tests focused on identifying the resistance to physical degradation that results from the wetting and drying cycle associated with flooding.

The experiments by Aglan et al. (2004) provide possible degradation factors in terms of mechanical and physical properties. The tests dealt with neither structural impacts nor bacteriological or toxic analyses, but established the following 13 degradation factors: strength characteristics, dimensional stability, hygroscopic properties, natural drying rate, biological characteristics, ability to be cleaned and restored after floodwater exposure, general appearance, colour, texture, cracking, flaking, efflorescence and odours.

The technical bulletin FEMA (2008) presents five classes of building materials classified according to their ability to resist flood damage. Classes 5 and 4 represent flood-resistant materials; classes 3, 2 and 1 are judged as not flood-resistant. The list contains structural materials and finish materials commonly used for the construction of floors, walls and ceilings. The classification of materials is based on the best available information such as the experiments provided by Aglan et al. (2004)

Flood-resistant materials are capable of withstanding direct and prolonged contact with floodwaters without sustaining significant damage; direct and prolonged contact means at least 72 hours; significant damage means any damage requiring more than low-cost cosmetic repair, such as repainting (FEMA, 2008). This approach only considers materials resistant to plain floods, direct and prolonged contact with floodwater, characterised by a low flow velocity (less than 1 m/s). Table 11 presents the classes of material resistance by FEMA, (2008).

Table 11: Impact susceptibility for plain floods based on FEMA (2008)

Resistance class	Description of resistant class – FEMA
5	Highly resistant to floodwater *damage*, including damage caused by moving water.
4	Resistant to floodwater *damage* from wetting and drying but less durable when exposed to moving water.
3	Can survive wetting and drying but may not be able to be successfully cleaned after floods and rendered free of most harmful pollutants.
2	Not resistant to clean water *damage*. Materials in this class are used in predominantly dry spaces that may be subject to occasional water vapour and/or slight seepage. These materials cannot survive the wetting and drying associated with floods.
1	Not resistant to clean water *damage* or moisture damage. Materials in this class are used in spaces with complete dryness. These materials cannot survive the wetting and drying associated with floods.

Escarameia et al. (2006) provide baseline experimental information on the performance of common building materials and construction elements (walls and floors) under simulated flood conditions. The study involved the testing of 13 different building materials commonly used in domestic house construction in UK. It included the analysis of resilience characteristics in terms of water penetration, drying ability, retention of pre-flood dimensions and integrity and classified them into good, medium and poor.

BMVBS (2006) delivers a list of materials arranged according to components used in buildings with the qualification of resistance. The categories are well suitable, moderately suitable and unsuitable. Committee and Resources (2006) offer a list of common construction materials in a two-dimensional matrix according to their absorbency and susceptibility to damage for a 96-hours water immersion. The materials are categorised into four groups: suitable, mild effects, marked effects and severe effects (see Table 12).

Table 12: Qualification of material resistance by Committee and Resources (2006)

Qualification of resistance	Description of resistance Committee and Resources (2006)
Suitable	These materials or products are relatively unaffected by submersion and flood exposure and are the best available for the particular application.
Mild effects	These materials or products suffer only mild effects from flooding and are the next best choice if the most suitable materials or products are too expensive or unavailable.
Marked effects	These materials or products are more liable to damage under flood than the above category.
Severe effects	These materials or products are seriously affected by floodwaters and have to be replaced if inundated.

Different types of degradation factors have been tested for these four institutions; many other factors such as physical, structural, toxic, bacteriological or even molecular characteristics could be analysed in terms of the material's resistance impacted by plain floodwater. Brzev et al. (2011) for example attempt to obtain the building information from analytical methods using mechanical characteristics of materials, the geometry of structural components and reinforcement ratios. Another detailed research by Hoang et al. (2010) deepens the fungal resistance in some green building materials by testing their equilibrium moisture content. Straube (2006) explains how moisture interacts with building materials by relating the relative humidity in percentage with their water content. Garvin et al. (2005, p. 99) conclude that "the materials performance depends not just on the materials properties, but on the duration of flooding, the effectiveness of the recovery process (including drying and decontamination), the nature of the flood water and other factors that may result in impact damage to the building".

Other sophisticated studies measure the moisture migration or moisture diffusivity of building materials by analysing, for instance the relation between the water penetration of the material in terms of the percentage of the wetted area , by using gamma-ray equipment to measure water content profiles or by including different models and variables (De Freitas et al., 1996; Trechsel, 2001). Moisture levels can be important indicators of several potential failure mechanisms in building materials. However, the material's properties tested for the four named institutions which are initially considered for the determination of floodwater resistance are depicted in Table 13.

Table 13: Properties tested on materials for the determination of floodwater resistance

Country	**Institution**	**Properties tested on the materials for the determination of floodwater resistance**
USA	FEMA (2008), based on Aglan et al. (2004)	Strength characteristics, dimensional stability, hygroscopic properties, natural drying rate, biological characteristics, ability to be cleaned and restored after floodwater exposure, general appearance, colour, texture, cracking, flaking, efflorescence and odours.
UK	HR Wallingford (Escarameia et al., 2006)	Water penetration, drying ability, retention of pre-flood dimensions and integrity
AUS, New South Wales	(Committee and Resources, 2006)	Absorbency
Germany	(BMVBS, 2006)	Unspecified

Experts state that if the water level is higher than the attic, this should lead to a total loss of the building. This is why the roof construction and its materials are not considered by BMVBS (2006). Each institution takes into account different types of components (see Table 14).

Kelman (2002) and Zevenbergen et al. (2008) claim that most walls are strong enough to resist floodwater up to a depth of 0.9 m above ground level; carrying out water resistant measures above this height may cause collapse damage to the structure during a deeper flooding. If this statement is true, only the components lower than 0.9 m should be analysed and roof structure and ceiling should be skipped.

Table 14: Components analysed for their resistance material of the four institutions

Component	FEMA (2008)	Escarameia et al. (2006)	Committee and Resources (2006)	BMVBS (2006)
Floor	X		X	X
Walls	X	X	X	X
Doors			X	X
Windows			X	X
Stairs				X
Building material		X		X
Ceiling	X		X	
Roof structure			X	

Beyond this analysis, Escarameia et al. (2012) demonstrated that the classification systems of resilient building materials lack in approved testing protocols, and they suggest the inclusion of future developments in building regulation, guidance and norms at the European level for overcoming technical barriers. Much effort should be made in developing countries, where the vulnerability is much higher and the knowledge on the material's susceptibility lower.

At this point of the research, the qualification of the building material's resistance does not follow a deterministic calculation and its qualification combines the testing of material properties with expert knowledge. The list of materials by the four institutions are compared in order to find some similarities, such as the qualification of resistance in brick face, brick common, standard plywood (see Table 15).

Table 15: Similarities of qualification of material resistance

Material	Qualification of resistance	Component	Institution
Brick Face or Glazed	5	Walls and ceilings	USA – FEMA Structural Materials
Face brick or blockwork	Suitable	Walls and ceilings	AUS – Committee and Resources
Engineering bricks	Good	Walls	UK – (Escarameia et al., 2006)
Brick Common (clay)	4	Walls and ceilings	USA – FEMA Structural Materials
Common bricks	Mild effects	Walls and ceilings	AUS – Committee and Resources
Plywood All other types	1	Walls, ceilings and floors	USA – FEMA Structural Materials
Standard plywood	Severe effects	Walls and ceilings	AUS – Committee and Resources

There are also some differences in the quality of material resistance, depending on the component. Wood, for example, can have different values of resistance, depending on whether it is used in walls, floors, windows or as building material (Table 16).

Table 16: Differences of wood qualification resistance

Material	Qualification of resistance	Component	Institution
Wood Solid, standard, structural (2x4s)	4	Walls and ceilings	USA – FEMA Structural Materials
Solid wood	Unsuitable	Floors	GER – Hochwasserschutzfibel
Wood (depending on the type)	Well-suited - Moderately suitable	Building material	GER – Hochwasserschutzfibel
Wood (depending on the type)	Moderately suitable - Unsuitable	Windows	GER – Hochwasserschutzfibel

As an approximation for the qualification of the material, a value between 1 to 5 is assigned in order to compare the linguistic terms of the four institutions (BMVBS, 2006; Committee and Resources, 2006; Escarameia et al., 2006; FEMA, 2008). A complete list of the materials analyses from the four institutions for each component with its value of resistance is displayed in Appendix C. The list seems a plausible method for having a list of materials with a qualification of resistance. Based on this list, the experts may develop rules for the assignation of material resistance, depending on experimental testing and knowledge on the behaviour of the material during a flood event.

3.2.2.2 Transformation of a material's resistance to its susceptibility

The aim is to convert the ordinal values of resistance to a cardinal qualification of susceptibility, i.e. qualitative variables to numeric ones, and to identify the relation between resistance and susceptibility. What should be the expected value of susceptibility for each resistance qualification?

Some approaches deal with an opposite scale of resistance, such as Blong (2003), who created a Generic Damage Index Scale for buildings with five classes of natural hazards: light, moderate, heavy, severe and collapse. He also provides a range and a central damage value for each class. Grünthal (1998) elaborated a macro-seismic scale with five classes: negligible to slight damage, moderate damage, substantial to heavy damage, very heavy damage and destruction. This scale could also be used for flood susceptibility. Hollenstein (2005) qualifies vulnerability transforming semi-quantitative descriptions into quantitative ones by using characteristic values for the individual classes. Fedeski and Gwilliam (2007) divide building vulnerability for flood and geological hazards in five classes: very resilient, resilient, average, susceptible, very susceptible; and they estimated a vulnerability index. (Reese and Ramsay, 2010) assume a damage ratio for different types of buildings affected by flood: insignificant, light, moderate, severe and collapse. These classifications of physical damage can be conceptually assimilated as a range of physical susceptibility (see Table 17).

Table 17: Comparison of damage ratio

Damage class (Blong, 2003)	Range	Central damage value	Damage classes (Fedeski and Gwilliam, 2007)	Vulnerability index	Description of damage state (Reese and Ramsay, 2010)	Damage ratio
Light	0.001 - 0.005	0.02	Very resilient	0.1	Insignificant	0 - 0.02
Moderate	0.005 - 0.20	0.10	Resilient	0.3	Light – Non-structural damage or minor non-structural damage	0.02 - 0.1
Heavy	0.20 - 0.60	0.40	Average	0.5	Moderate – Reparable structural damage	0.1 - 0.5
Severe	0.60 - 0.90	0.75	Susceptible	0.7	Severe – Irreparable structural damage	0.5 - 0.95
Collapse	0.90 - 1.00	1	Very susceptible	0.9	Collapse – Structural integrity fails	> 0.95

The approaches of Blong (2003), Fedeski and Gwilliam (2007), Reese and Ramsay (2010) are related to the qualitative values of resistance into ranges of susceptibility in order to derive new insights and further statistical analyses. The transformation is shown Figure 24, Figure 25 and Figure 26.The graphics depict the upper and lower ranges in red colour and the median in green.

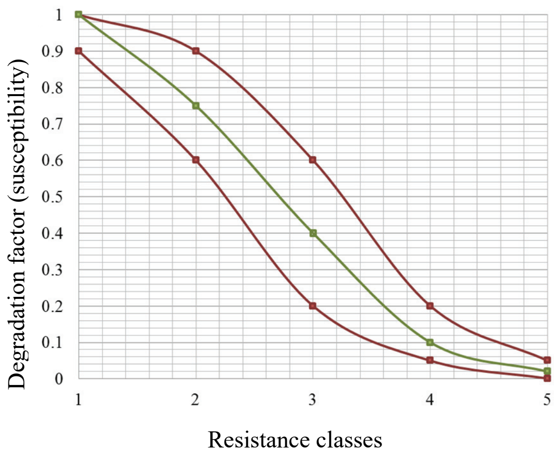

Figure 24: Susceptibility values based on Blong (2003) and resistance classes

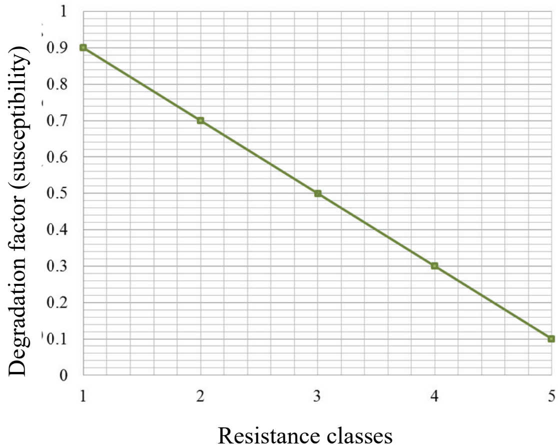

Figure 25: Susceptibility values based on Fedeski and Gwilliam (2007) and resistance classes

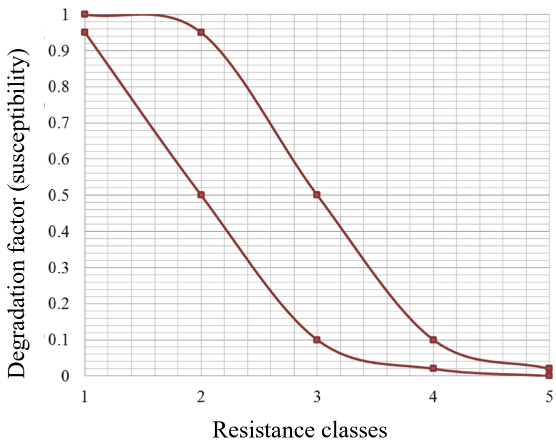

Figure 26: Susceptibility values based on Reese and Ramsay (2010) and resistance classes

But this transformation contains many uncertainties because the approaches take into account other hazard types or assume values without any experimental support. At this point, the relation between susceptibility and material resistance is very ambiguous or diffuse.

The *expert knowledge method* is an initial approximation for determining a material susceptibility value for floodwater, taking into account the qualification of resistance from the four institutions. The experts (surveyors, architects or engineers) may assign a value of susceptibility depending on the use of the material and the characteristics of the floodwater.

Heuristic expert knowledge will describe the relationship between material characteristics and its susceptibility to floodwater. Fuzzy set theory, fuzzy logic and fuzzy random variables might be implemented for measuring the expert judgment values of the material's susceptibility, dealing explicitly with the uncertainty of the knowledge framed in the vagueness of the qualitative terms. The method requires a period of training or learning, the compilation of data stores or knowledge bases from previously established understanding by a variety of experts in order to produce useful results.

There are many approaches for the estimation of the expected values, like the one proposed by Liu and Liu (2003), which presents a hybrid intelligent algorithm incorporating simulation, neural network and genetic algorithm in order to solve general fuzzy random expected value models. Hong and Lee (1996) propose a general learning method as a framework for automatically deriving membership functions and fuzzy if-then rules from a set of given training examples in order to rapidly build a prototype fuzzy expert system.

Kwakernaak (1978) introduced the term fuzzy random as random variables whose values are not real but fuzzy numbers and subsequently redefined as a particular kind of fuzzy set. The values of material susceptibility can yield a pair of envelopes or ranges for the cumulative probability at a given value of resistance on the horizontal axis.

$$d_H(A,B) = \max\left\{ \sup_{a\in A} \inf_{b\in B} |a-b|, \sup_{b\in B} \inf_{a\in A} |a-b| \right\} \qquad (12)$$

The first step consists in converting the vagueness values of susceptibility into random variables. The random variables enable us to deal with more general sources of uncertainty in empirical approaches (Shapiro, 2002).

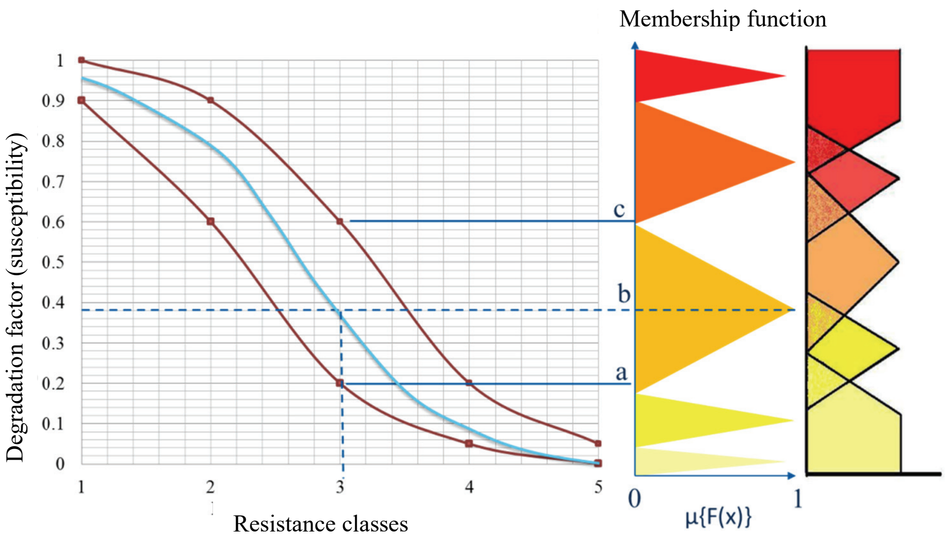

Figure 27: Fuzzy random variable for susceptible values (modified from Sapiro, 2002)

Here, the formulas proposed by Hong and Lee (1996) are considered for determining the membership function. The steps are the following:

- Sort the output values of the training instances in an ascending order.
- Find the value of similarity between adjacent data.

$$s_i = \begin{cases} 1 - \dfrac{diff_i}{C * \sigma_s} \; for \; diff_i \le C * \sigma_s \;, or \; 0 \; otherwise \end{cases} \qquad (13)$$

where s_i represents the similarity between y'_I and y'_{i+1}, $diff_i$ is the distance between y'_I and y'_I and y'_{i+}, σ_s is the standard derivation of $diff_i$'s and C is a control parameter determining the shape of the membership functions of similarity. A larger C causes a greater similarity.

- Find the central-vertex-point bj. In a triangular fuzzy membership function, the value of bj is equivalent to the intrinsic susceptibility factor with the highest membership. If y'I, y'i+1,…y'k belongs to the jth group, then the central-vertex-point b j in this group is defined as:

$$b_j = \frac{y'_i * s_i + y'_{i+1} * \frac{s_i + s_{i+1}}{2} + y'_{i+2} * \frac{s_{i+1} + s_{i+2}}{2} + \cdots + y'_{k-1} * \frac{s_{k-2} + s_{k-1}}{2} + y'_k * s_{k-1}}{s_i + \frac{s_i + s_{i+1}}{2} + \frac{s_{i+1} + s_{i+2}}{2} + \cdots + \frac{s_{k-2} + s_{k-1}}{2} + s_{k-1}} \qquad (14)$$

- The minimum similarity is chosen as the membership value of the two boundary points y'I and y'k.

$$u_j(y'_i) = u_j(y'_k) = \min(s_i, s_{i+1}, \cdots, s_{k-1}) \qquad (15)$$

- Determine the vertex-point a:

$$a = b_j - \frac{b_j - y'_i}{1 - u_j(y'_i)} \qquad (16)$$

- Determine the vertex-point c:

$$c = b_j + \frac{y'_k - b_j}{1 - u_j(y'_k)} \qquad (17)$$

The estimated values can be represented in a range between 0 to 1, where 1 is the most susceptible. Once the values of the membership function (*a, b,* and *c*) of susceptibility are calculated, a median susceptibility value of the fuzzy sets is assigned as the value of the material's susceptibility for the component. Table 18 shows an example of susceptibility values for the component with a confidence limit as a range within which a certain proportion of the susceptibility values fall.

The uncertainty of the susceptibility measurement is expressed as the fuzzy sets 'spectrum' 'intervals', 'ranges' of how much a building material can be harmed by floodwater according to the current state of knowledge on the materials or to previous information on the degrees of resistance analysed by the international agencies. "Fuzzy logic is using pretty much the same tools as probability theory. But it's using them to trying to capture a very different idea, "trying to capture the vagueness". Fuzzy logic is all about degrees of truth - about fuzziness and partial or relative truths" (Chu-Carroll, 2011).

Table 18: Example of the reciprocal value of resistance

Relevant components for RBT_i	Structure material	Resistance class of material (FEMA)	Resistance of the component	Susceptibility
Roof	Clay tile	5	3	0.4 confidence limit = 0.95 interval: 0.2 – 0.6
	Asphalt tile with asphaltic adhesives	3		
Ceiling	Wood solid, preservative-treated, borate	4	4	0.1 confidence limit = 0.95 interval: 0.05 – 0.15
Windows	Metals, non-ferrous (aluminium, copper or zinc)	3	3	0.4 confidence limit = 0.95 interval: 0.3 – 0.5
	Glass, unreinforced	4		
External walls	Brick, common clay	4	4	0.1 confidence limit = 0.95 interval: 0.07 – 0.2
External doors	Metal, hollow	4	4	0.1 confidence limit = 0.95 interval: 0.03 – 0.17
Floor	Concrete, pre-cast or cast-in place	5	5	0.05 confidence limit = 0.95 interval: 0.0 – 0.1
	Polyurethane, formed-in-place	5		
Foundation	Cast stone (in waterproof mortar)	5	5	0. confidence limit = 0.95 interval: 0.0 – 0.1

3.2.2.3 Setting the expert qualification

Detailed information on material properties: Aglan et al. (2004) describe some material properties, which can be observed, inspected and monitored using the human senses of sight, smell and touch. These properties should be documented and recorded photographically. The monitoring of these properties can help to reach a prior susceptibility analysis for other areas (see Table 19).

Moreover, the time duration of water contact of the building materials with floodwater is also a relevant parameter that must be considered for the assessment of building material susceptibility. FEMA (2008) takes as parameter “72 hours” which impacts cause minor damage and the cost reparation is low. Thieken et al. (2010) proposes a inundation duration in four classes 1-3 days, 4-7 days, 8-11 days, >11 days and developed models for the estimation of structural damage and monetary losses in the residential, commercial and agricultural sector. The parameter inundation duration must be set for the experts for the qualification of susceptibility.

Table 19: Additional attributes for the susceptibility qualification

Attribute of the material before and after the flood	Attribute	
Resistant characteristics after flooding	(n)	None
	(sh)	Shearing
	(fl)	Flaking/Scaling
	(be)	Bending
	(cr)	Cracks
	(bu)	Buckling
	(sw)	Swollen

Attribute of the material before and after the flood	Attribute	
General appearance	(d)	Discoloured surfaces
	(i)	Efflorescence due to crystalline deposits of alkaline salts
Biological and chemical reactions characteristics	(m)	Mold growth
	(o)	Spreading odours
	(c)	Corrosion
	(ct)	Contamination due to its intern components
	(ox)	Oxidation
Natural drying speed	Number of days	
Technical standards and specifications in construction	ISO Standards or codes produced by manufacturers' associations. If it exists	
General description of the extraction process and manufacturing of the material	If it exists	

Method for a qualification consensus: A consensus of at least three experts should be reached. A manner of finding this consensus is the *Delphi method*, which is "a structured communication technique, originally developed as a systematic, interactive forecasting method that relies on a panel of experts. Delphi may help to deal with a complex problem as effective process of communication in a group of individual" if there are different interpretations of a material's susceptibility qualification (Linstone and Turoff, 1975).

Based on the information collected in the field and the detailed information on the material properties, the experts are encouraged to revise their earlier qualification in two or more rounds and reply to the other members. A facilitator may provide a summary from the previous rounds as well as the reasons provided for their judgments for supporting the experts' forecasts.

Linstone and Turoff (1975) summarise the design and considerations of the Delphi method. They conclude that the believability and significance for the user of the results of a Delphi inquiry depend as much on the user's perception of the clarity and fit of the reality implied and possibly defined by the results as on the perceived quality of the information.

There is not a deterministic method for a susceptibility building measurement for large scales in flood plain areas yet, but this work proposes the combination of fuzzy set expert analyses and the Delphi method for estimation. These methods may deliver a good assessment of the susceptibility if good information on the materials is available. Nevertheless, all the collected and analysed information should be stored and organised in a robust database in order to be transferred, compared and validated with additional sources of information.

3.2.3 Derivation of a depth-physical impact function

A depth-physical impact function is an approach for the estimation of potential physical alteration, degradation, fragility, loss of structure or loss of volume of building components caused by the water depth of a plain flood (for this study). Other features of flood such as flood duration, flood velocity are not considered.

This function was developed in order to support the assessment of economic damages and/or to overcome the lack of monetary values or refurbishment cost data. Similar to depth-damage functions, depth-physical impact functions are derived as a relationship between the depth of a flood and the susceptibility of the principal material of the volume of the building's components.

Physical impacts on buildings are estimated on the basis of the *potential susceptible material's volume* for components calculated in m³, i.e. degraded material in relation to a maximal susceptibility of 1. The material of the components is continuously impacted when the water level rises.

The example in Table 20 shows how to derive a depth-physical impact function. The left part presents the components arranged according to their lower height, their predominant material, their value of resistance and susceptibility, their total volume and in the last column the susceptible volume in m³ at the highest point, which results of the multiplication of the total volume by the susceptibility value. In addition, the right part associates every volume of the component with a level of water depth. The water levels are depicted in the blue colour row. The potential degradation for every component continually increases from its lower height until the water level overtakes its upper height, as the water depth rises. Up here, the component degradation is considered constant when the flood continues to rise.

In this example, the susceptibility value of the external walls of the basement is 0.02, its lower height 0 m and its upper height 0.6 m above the ground, its susceptible volume is 0.162 m³. If the water level rises by 0.3 m, the potentially degraded material of the external walls may be 0.081 m³. If the water exceeds its upper height, the potential susceptible volume will rise to 0.162 m³.

The values of water depth and cumulative susceptible volume in m³ from Table 20 can be depicted in an x and y chart, which represents the depth-physical impact function. The impact curve for a representative building is shown in Figure 28, where the x-axis depicts the water depth and the y-axis depicts the cumulative susceptible volume in m³ for the components impacted by the floodwater. The curve reflects the deterioration of the building's integrity in m³. Hence, depending on the water depth, an amount of volume in m³ will be degraded according to the value 'b' or 'mean-value' of the fuzzy set of material susceptibility qualification. The values 'a' and 'c' or 'extreme-values' of the fuzzy sets are represented in red for every turning point.

Table 20: Example for the calculation for susceptible material volume

Component	Material	Lower Height	Upper Height	Delta height	Resistance Class	Susceptibility	Volume material m³	Susceptible Vol. in m³ at the highest point														
Roof	Wood structural roof stone cover	7	10.6	3.56	2	0.75	3.2	2.430											0.75	0.844	2.43
Slab - Ceiling 2° to 3° floor	Reinforced concrete d = 20 cm	7	7.2	0.2	5	0.02	38.4	0.768											0.02	0.768	0.768
Slab - Ceiling 1°-2° floor	Reinforced concrete d = 20 cm	3.5	3.7	0.2	5	0.02	38.4	0.768									0.02	0.768	0.768	0.768	0.768	0.768
Stairs	Reinforced, tiled	0.8	5.5	5.5	3	0.4	5.5	2.200								0.4	1.4	1.48	2	2.2	2.2	2.2
Floor	Floating floor carpet tile	0.8	0.9	0.1	1	1	19.2	19.200								19.3	19.3	19.3	19.3	19.3	19.3	19.3
External walls	Sand-lime brick masonry d = 24 cm	0.6	7	6.4	5	0.02	72.1	1.443							0.02	0.045	0.654	0.699	0.992	1.443	1.443	1.443
External fenestration	Plastic windows with thermal insulation glazing	0.6	5	5	5	0.02	1	0.020							0.02	0.02	0.02	0.02	0.02	0.02	0.02	0.02
Slab basement	Reinforced concrete d = 20 cm	0.6	0.8	0.2	5	0.02	38.4	0.768							0.02	0.768	0.768	0.768	0.768	0.768	0.768	0.768
External windows basement	Plastic windows with thermal insulation glazing	0.1	0.3	0.2	5	0.02	0.04	0.001					0.001	0.001	0.001	0.001	0.001	0.001	0.001	0.001	0.001	0.001
External walls basement	Reinforced concrete d = 24 cm	0	0.6	0.6	5	0.02	8.1	0.162				0.02	0.027	0.081	0.162	0.162	0.162	0.162	0.162	0.162	0.162	0.162
Stairs basement	Reinforced concrete and tiles	-2.5	0.6	3.1	3	0.4	3.1	1.240			0.4	1.077	1.105	1.159	1.24	1.24	1.24	1.24	1.24	1.24	1.24	1.24
Floor basement	Topping with protective paint, some floor tiles	-2.6	-2.5	0.1	3	0.4	19.2	7.680		7.68	7.68	7.68	7.68	7.68	7.68	7.68	7.68	7.68	7.68	7.68	7.68	7.68
Foundation	Flat surface reinforced concrete foundation	-3.2	-2.6	0.6	5	0.02	11.9	0.240	0.02	0.24	0.24	0.24	0.24	0.24	0.24	0.24	0.24	0.24	0.24	0.24	0.24	0.24
								Water depth in m	**-3.2**	**-2.6**	**-2.5**	**0**	**0.1**	**0.3**	**0.6**	**0.8**	**3.5**	**3.7**	**5**	**7**	**7.2**	**10.56**
								Cumulative susceptible volume in m³	**0.02**	**7.92**	**8.32**	**9.02**	**9.052**	**9.161**	**9.383**	**29.86**	**31.49**	**32.36**	**33.17**	**34.59**	**35.4**	**37.02**

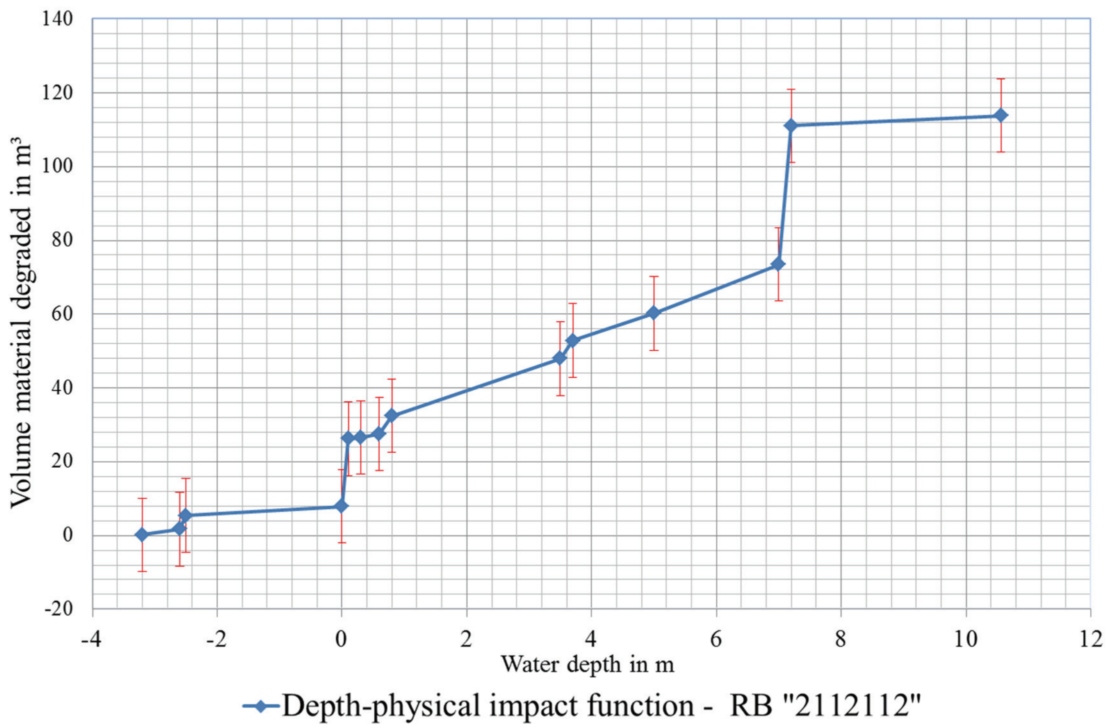

Figure 28: Example of a depth-physical impact function of a representative building.

The next chart exemplifies how much the volume can be degraded for a component in red colour. This chart may serve as support for the calculation of the economic damage as well as for further calculations for refurbishment.

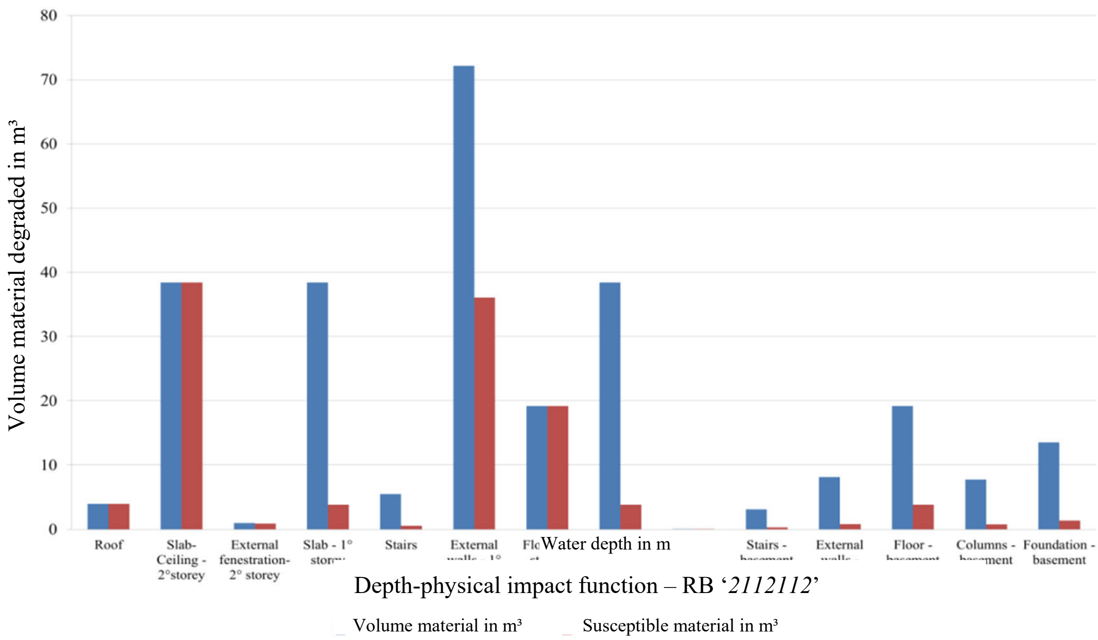

Figure 29: Susceptible volume in m³ by component

3.2.3.1 Median depth-physical impact function

The empirical process shows that the information on materials, components and their heights for the derivation of the depth-physical impact function must be gathered from a number of representative buildings in order to find a behaviour or patterns of the impacts for building types. Therefore, the different depth-physical impact functions must be statistically analysed in order to define the archetype of the potential functions of the buildings of this group.

A *median depth-physical impact function* can condense the information of the volume degradation of the representative buildings belonging to the same building type. One method for condensing the curves is a multiple regression, but multiple regressions will distort the inflection points of the depth-physical impact functions to a lineal or exponential function, showing the results inappropriately. However, assuming that the curve has a normal distribution, probabilistic methods can be used. According to (Kosko, 1994), "probability is a subtheory of fuzzy logic, as probability only handles one kind of uncertainty". Then, a median value and a standard deviation as "unpredictable uncertainty about a mean value" for the value of impact at every water depth can be calculated. The *synthetic* or *median depth-physical impact function* for a building taxonomic code is obtained as follows:

1. Plot the functions of the buildings with the same taxonomic code, with the x values representing the water depth in metre and the y values the impact (see example in Figure 30).
2. Arrange the x values of all functions upward and create a matrix filling it with the y values. The row values of the matrix are the values of the impact.
3. Fill the empty values of the matrix by means of a linear interpolation using (18). A tool for the calculation of the interpolation in excel can be used according to (Mehta, 2012).

$$y_2 = y_1 + \frac{(x_2 - x_1)(y_3 - y_1)}{(x_3 - x_1)} \qquad (18)$$

4. Calculate the median, the standard deviation and box diagrams between the values of the functions (see Figure 31).

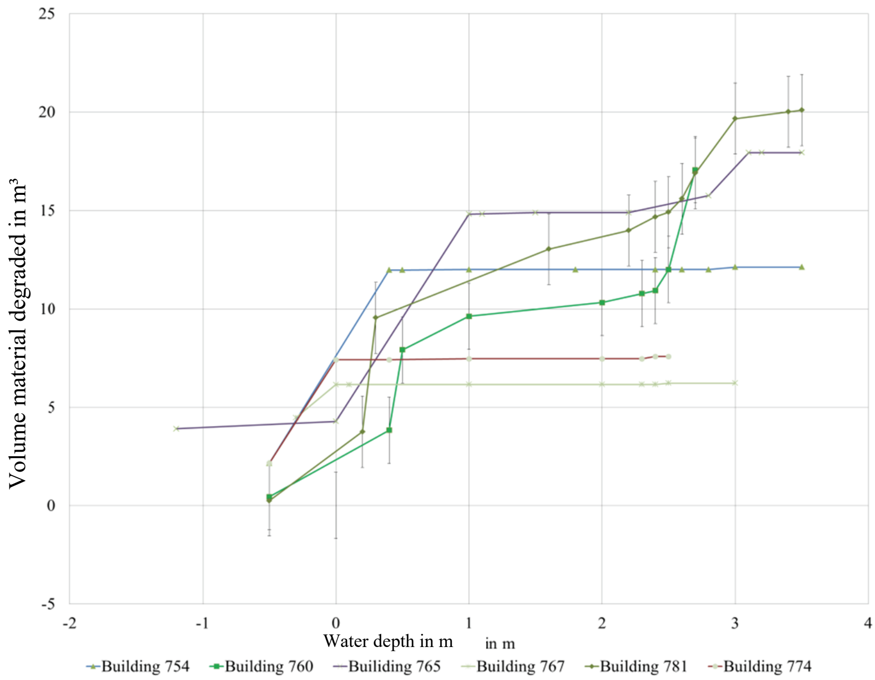

Figure 30: Depth-physical impact functions representative buildings *'1111111'*

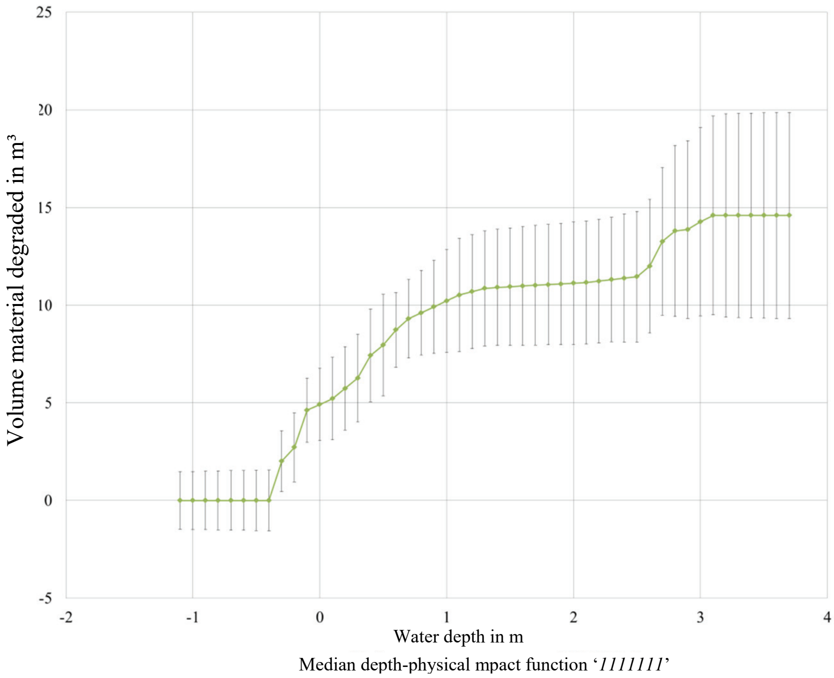

Figure 31: Median of depth-physical impact functions and its standard deviation

Box diagrams with volume components and the susceptible volume of a taxonomic code can be also derived (see Figure 32). The box diagram can help to identify the more susceptible components.

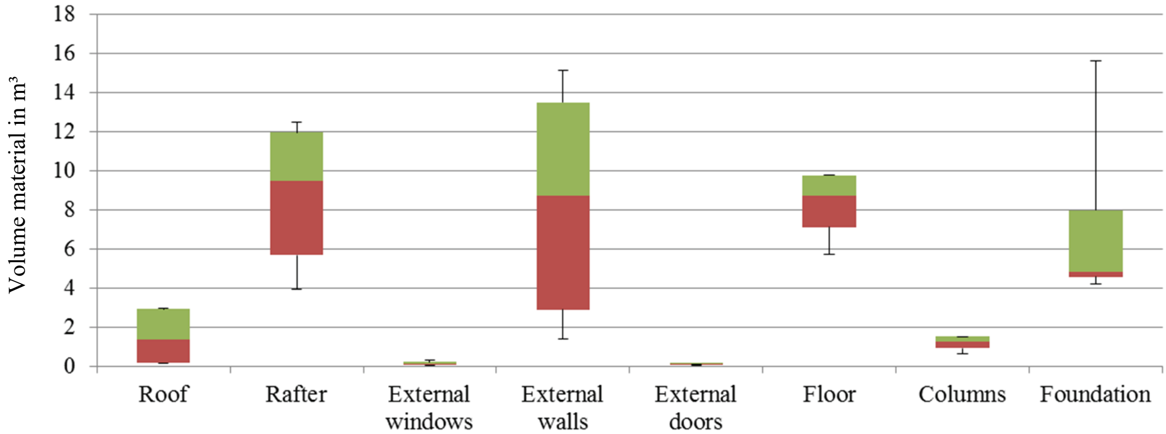

Figure 32: Box diagram for material volume degradation – taxonomic code '*1111111* '

The above outcomes may help to assess the damages based on statistical analyses, allowing us to find general rules or behaviours of a group of buildings with their propensity to experience harms caused by plain floods. The potential impacted volume indicates the process of damage generation.

3.3 Module 3: Technological integration

The objective of this subchapter is to integrate the components of the two previous modules, namely: building taxonomic code and depth-physical impact approaches, using computer-based tools. These tools can be incorporated in further works into a Decision Support System (DSS) according to the proposal of McGahey et al. (2009). The technological tools facilitate and automate the systematic identification of the characteristics of the building structure of the individual buildings located in the floodplain, as well as methods for the assessment of potential impacts on the building components. The system architecture and related software/hardware as well as the users and their requirements are described in the following.

3.3.1 Combination of the depth-physical impact function with the building taxonomic code

The flood susceptibility analysis can be better interpreted combining the values of the depth-physical impact physical functions with artificial inundation scenarios or water depth data (cf. (Winsemius et al., 2013). This interpretation may also vary depending on how the values of the impact are categorised or represented in the maps. To assist this operation, a tool in Python has been developed (see Appendix D).

The depth-physical impact function for a taxonomic code contains information on its maximum and minimum value of degraded volume, the standard deviation by water depth and the volume material of the building. The taxonomic code may be transferred to buildings with similar features by using the matching percentage. Additionally, the qualification of susceptibility can also be applied to other buildings with the same characteristics. For instance, a representative building type in a small city in a flood plain, which contains the description and qualification for potential physical flood impacts, can be transferred to a building with similar characteristics located in another sector of the flood plain. Please note that the success of the results depends on the quality of the input data and the user's experience.

The combination of the physical susceptibility with a 100-year flood model requires the understanding of (i) the map scale and (ii) the statistical analysis that is carried out behind their derivation. The impact for every building can be displayed with the colours green to red, with red standing for the highest impact.

The combination of the values of susceptibility can be represented in different ways. The first consists in displaying the maximum value of the susceptible volume by a taxonomic code. The second option consists in including the water depth scenario for every affected building and assigning the respective susceptible volume, and the third option includes the calculation of a percentage of the susceptible volume in relation to the building volume calculated for the selected representative building. A clear description of the significance of the concepts displayed in the maps should be included in the metadata. The building flood susceptibility for a taxonomic code can then be displayed in three ways:

- Representation of the physical susceptibility "option one" displays the *maximum value of susceptible volume by taxonomic codes*. It reveals how much the material's volume can be degraded if the floodwater covers the whole building. This maximum value must be associated to the taxonomic code.

- Representation of the physical susceptibility “option two” represents the *susceptible material volume* by water depth. Since the water depth varies for every building depending on its altitude on the prone area, this susceptibility value fluctuates for every house. After that, the values should be ranked by equal intervals in order to identify buildings with the similar amount of degraded material.
- Representation of the physical susceptibility “option three” consists in calculating a *percentage of the susceptible volume in relation to its total building material volume*, which may be degraded by a water depth. These percentage values should be ranked every ten points in order to determine how much the percentage of its integrity can be degraded by a water depth.
- A further display of the results can be based on the *standard deviation of the depth-physical impact functions* at a water depth. The standard deviation shows the ranges of variability of the material’s susceptibility by the samples of buildings selected with the same taxonomic codes.

3.3.2 Tools supporting the physical susceptibility analysis

Due to the need to automate and systematise the process for the huge amount of buildings located in floodplains, computer tools are required. These tools can be integrated into a robust architecture that allows the concatenation of the subsequent analysis; thereunder a brief review of some tools used for supporting the flood impact assessment.

Choosing the best tool in terms of data reliability, applicability and interoperability for the use in other areas is not an easy task, as each approach considers particular variables for specific circumstances, which cannot be directly transferred under different conditions. Moreover, the suitability of each approach to different scenarios needs to be thoroughly assessed through experience.

Architecture in open source technologies is developed for collecting, transferring, storing and sharing the components of the physical flood vulnerability analysis for each of the representative buildings. The system architecture is designed to be a multilevel architecture; in this case, it was defined as four-level architecture.

The first level is defined by the data storage, where Postgresql is used as the relational database management system (RDMS). Postgresql was chosen because it is one of the best RDMS on the market and requires no licence. Its high performance and scaling capacity are some of the features that make Postgresql the right tool for this project and its particular needs.

The second level is specified by the Java application, in which all the business logic is determined. Java is one of the most potent programming languages and the Java Enterprise Edition (JEE) provides a full framework to develop web/mobile based applications. It offers a core application which allows to store all the data in the database for this application. This core application is just the point of access to the data; it runs in the Jboss open source application server.

The third level is determined by the clients of the core, the mobile and the web application. The Mobil App is an Android application developed in Java, which reads and writes data to the server through an internet connection. The web application is a web-based application running on the server, which reads data from the database to present the information to the user.

The fourth level is not an open source technology; it integrates building taxonomy and depth-physical impact functions located on the floodplain areas through automatic processing and the creation of a database. For this purpose, tools in an ESRI® ArcGIS™10 environment using Phyton as scripting language have been developed to support the processing that can be visualized and analysed by interdisciplinary stakeholders or later integrated into a DSS. These vulnerability maps can be further used for the derivation of risk maps if water levels of flood zones or hazard maps are included.

3.3.3 The users and their requirements

As the methodology is designed for a pre-flood event, all the methods should be carried out before an event. Figure 33 depicts the workflow for managing, preparing, collecting, analysing and sharing the information as well as the five user groups who interact for the assessment of the building susceptibility for representative buildings.

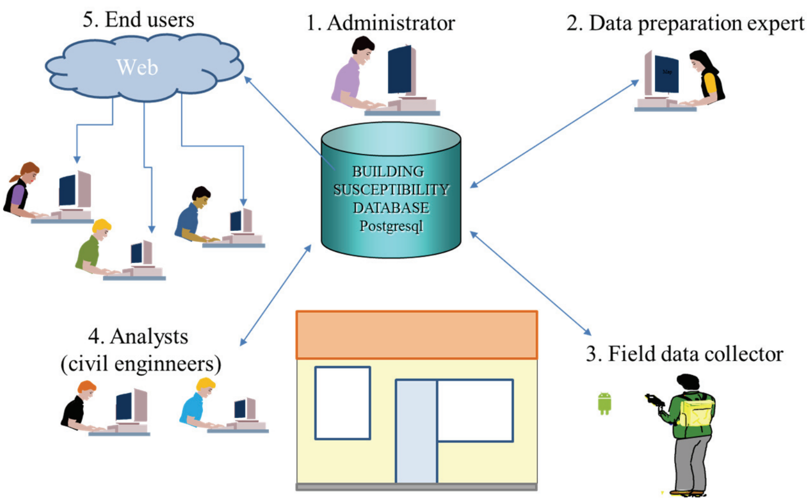

Figure 33: Scheme of the users and their tasks

3.3.3.1 Administrator

The administrator's task is to manage the data quality, user permissions, connections and interfaces. For these activities, a database model was developed in Postgresql in order to store the information of the representative buildings, their components, material, relevant dimensions, resistance value, susceptibility and volume.

The entity relation diagram presented in Figure 34 shows the information that should be stored. The entity "building" shall be prepared in the office based on remote sensing data and GIS calculation. The attributes for the entities "component", "structural material" and "component's dimensions" shall be collected in-situ for the selected representative buildings. The entity "depth-physical impact function" derives from the information of "component" and "structural material". The configuration and installation of the database is depicted in Appendix D1.

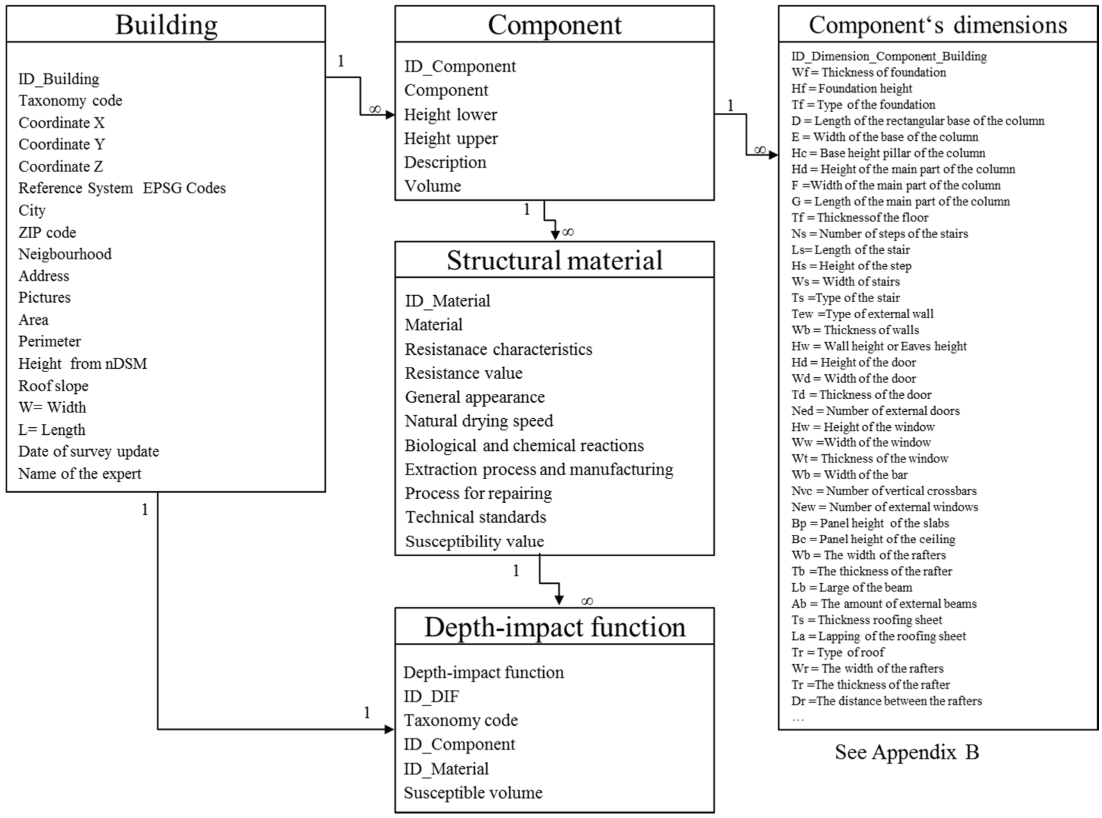

Figure 34: Entity relation diagram

3.3.3.2 Data preparation expert

The expert is responsible for the preparation of spectral and elevation data, the features of extraction algorithm performances, the derivation of the building taxonomic code and the uploading of the information from the selected representative buildings to the database. The explanation for the use of all these tools is depicted in Appendix D2.

For this purpose, an interface was developed in Matlab for the determination of the terrain and vegetation threshold (see Appendix D2.1). Tools for the calculation of the RMSE index was produced in Python for ArcGIS 10 (see Appendix D2.2), another for the derivation of the taxonomic code (see Appendix D2.3), for a selection of representative buildings (see Appendix D2.4) as well as the Sampling Design Tool for ArcGIS designed by NOAA (2012) (see Appendix D2.5). The scripts of the tools are stored on the digital appendix.

3.3.3.3 Field data collector

The surveys of the components, their relevant materials and additional information that can support the analysis of building susceptibility are usually collected in field campaigns. An Android app for smartphones or tablets was developed for this purpose with the following functions:

- Reception of the taxonomy codes and coordinates for the representative buildings within a pilot site
- Selection of components and assignation of their lower and upper height
- Selection of the material's components and assessment of their resistance
- Comments on the material characteristics

- Collection of GPS coordinates for every point
- Capturing of pictures for every building and its components
- Transfer of the collected information to a database using an internet WiFi connection

The explanation for the functions of the app is given in Appendix D3.

3.3.3.4 Analysts

Once the data of building components, heights, relevant materials, their characteristics and pictures has been collected and stored in the database, the analysts (e.g. civil engineers or architectures) can compare, update, synthesise and derive the depth-physical impact functions for the building types. The analysts have to estimate the material's susceptibility value on the basis of information on the material properties. Excel tables can be used for the calculation of the average depth-physical impact function and its standard deviation. A script for assisting the interpolation in Excel is displayed in Appendix D4.

3.3.3.5 End users

The depth-physical impact function values for the building taxonomic code can be shared online with specific users or an interested community. Whether the information is shared or not depends on the determined privacy policies. The functionalities for transferring the information are shown in Figure 35.

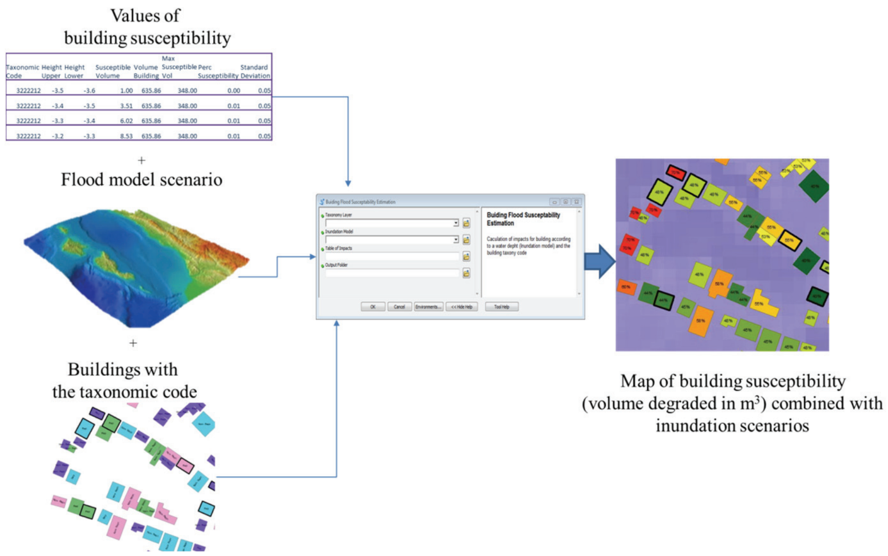

Figure 35: Process for querying and sharing the information

Appendix D5 shows the represented tool for the integration of the inputs for the estimation of impacts in the buildings by a water depth.

- The user connects to a website, where the information is displayed.
- The user makes a query for a city and neighbourhood or ZIP code, or the user sends a list of codes.
- The system lists all the building types belonging to this query by taxonomy code.
- The system gives the option to download the file with the susceptibility values by selecting a taxonomic code.
- The user can combine the file with a flood model scenario and the buildings for analysing the physical flood vulnerability.

4 Results of the methodology testing

The methodology may be implemented in any part of the world where elevation and spectral data are available in high resolution. Before its implementation, it should be tested in different pilot sites in order to find the weak points of the methods. The delimitation of every pilot site can take into account the name of the settlement, even the postal code. Although the postal code was created to deliver mail more efficiently, it has also become a frequent means to identify the geographic position of an area and one can suppose that the sector is a homogeneous area in terms of year of construction, building material and construction techniques.

Three contrasting sectors were selected here: Kleinzschachwitz, a settlement of Dresden in Germany, and two settlements in Colombia, called “Barrio Sur” in Magangué and a small settlement called “La Peña” in the municipality of Cicuco, located in the flood plain of the Magdalena River in Colombia. The three areas have different socio-economic needs. According to Maslow's hierarchy of needs, the population of Kleinzschachwitz is in a stage of self-actualisation, while the population in “La Peña” and “Barrio Sur” is attempting to solve the needs of safety, employment, resources, property and social organisation. The gross domestic product in 2012 (GDP) was $39.7 in Germany, while it was $11.0 in Colombia. 100 % of the people in Germany have access to sanitation facilities, while this rate is about 63 % in rural areas in Colombia and about 82 % in urban areas (CIA, 2013). “La Peña” has no sewer system and “Barrio Sur” a piped sewer system but the sewage is directly deposited into the river.

In the following, a general description of the pilot sites is given, followed by a description of the data collected and the testing of every method of the taxonomic code; a selection of representative buildings, an analysis of the material’s susceptibility, a derivation of the depth-physical impact functions as well as the combination of the depth-physical impact function with the taxonomic codes for a scenario of food are carried out afterwards. The chapter provides a summary of the testing results and the guidance of the methodology.

4.1 Pilot site “Kleinzschachwitz” – Dresden, Germany – Elbe River

The settlement of Kleinzschachwitz in Dresden, Germany, is situated in the Southeast of Dresden, extended along the south bank of the Elbe to the settlement of Pillnitz at 51° 0′ N, 13° 51′ E, around 115 metres above mean sea level in the local exchange area of Leuben. Figure 36 shows the catchment of the Elbe River (148,268 square kilometres) and the location of the pilot site. The tributary stream Lockwitzbach crosses Kleinzschachwitz and flows into the Elbe River. Dresden is located in the temperate zone within the transitional-continental climate area and has a humid continental climate (Dfb), with hotter summers and colder winters than the German average. The average temperature in February is -1.7 °C (28.94 °F) and in July 18.1 °C (64.6 °F). The inner city temperature is 10.2 °C (50.4 °F) averaged over the year. The driest months are February and March, with precipitations of 40 mm (1.6 in). The wettest months are July and August, with 61 mm (2.4 in) of precipitation per month (Deutscher Wetterdienst, 2012).

The city of Dresden has drawn up a flood prevention plan, which contains different activities for preventing future damages caused by floods, such as a progressive modification of the sewer system, water retention, citywide monitoring and an alarm system for groundwater. These activities are framed into the overall aim of the German development policy to break the cycle of poverty and vulnerability.

The purpose of the actions by the federal government on the local level are reconstruction, poverty reduction and disaster risk management (BMZ, 2010). The Environmental Agency of Dresden was responsible for maintenance order II watercourses and establishing flood protection concepts; the State Reservoir Administration of Saxony (part of the Saxon State Ministry for Environment and Agriculture) is responsible for maintenance order I watercourses (rivers and streams) and establishing flood protection concepts.

The colours indicate the relief

Figure 36: Geographic location of the pilot site in catchment area of Elbe River. Source: ESRI

The settlement is one of the best residential areas of the city with single and multi-family houses and villas. Residential buildings are predominant as a result of the major development phase between 1870 and 1914. In addition, new residential buildings have been built since 1990 (Naumann, 2013). The settlement area covers about 154.68 ha.

The heavy flood from 2002, which became known in Germany as the „Jahrhundertflut", caused significant damage at several cultural institutions, like the Kraszewski Museum, the Laubegast Library, parts of the relocated city archives, the Putjatinhaus, the Old Fire Station in Loschwitz and Riesa efau in Frederick city (van Stipriaan, 2002). In 2002, the Elbe surrounded Kleinzschachwitz. The flood was caused by heavy rainfall, which was exceptional in terms of intensity, duration (over a week) and areal distribution (IKSE, 2004). The flood in June 2013 affected the settlement again. Many people had to be evacuated, the transport system was shut down and many houses were damaged.

4.1.1 Module 1: Building taxonomy – "Kleinzschachwitz"

4.1.1.1 Building extraction – "Kleinzschachwitz"

The steps for developing the building outline extraction for this building taxonomy as given in section 3.1.2.2 are tested.

Data and preparation:
The geographic data was re-projected to WGS 1984 UTM Zone 33N corresponding to the parameters of translation and rotation of the ellipsoid. The input data are depicted in Figure 37.

- DSM v. 15.11.2002 (Digit. Surface Model in dm ü. HN), 1m-Grid. Source: Stadtvermessung Dresden. (TopScan, 2002).
- DTM v. 15.11.2002 (Digit. Terrain Model in dm ü. HN), 1m-Grid. Source: Stadtvermessung Dresden. Basel 1841, Transversal Mercator.
- Orthophoto f4_4949sw3 v. 6.9.2005 Spatial Resolution 0.2 m. Bands: 3. Erlaubnis-Nr. 2058/06. Source: (Geobasisinformation und Vermessung, 2005).
- As reference data*:* Polygons of the building information of topographic maps with a scale of 1:10,000 (TK10) (AdV, 2008), generated in the framework from the project MULTI SURE from ATKIS data, captured in 2009 from aerial photographs and updated by the IÖR with the attributes of building types, embedded depths, water levels and damage to buildings.

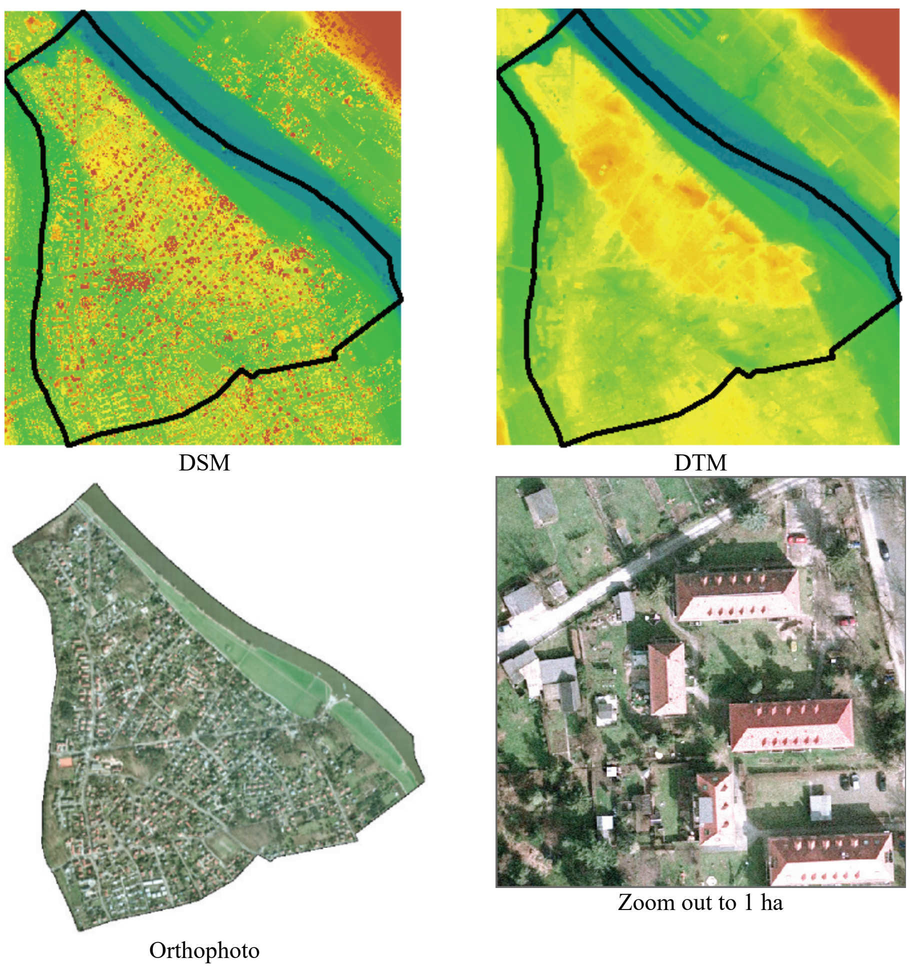

Figure 37: Input data "Kleinzschachwitz"

Semantic definition for building outlines extraction:

The area is principally residential with detached houses and many surrounding trees and a low density of buildings. The images' high contrast helps to distinguish buildings, and the occlusion of buildings due to shadows from trees is very low. The area shows favourable conditions for an automated object extraction. At the beginning of the process, building regions were extracted on the basis of the semantic definition; namely: (i) buildings have different spectral characteristics from vegetation, (ii) floodplains are quite flat, (iii) buildings are elevated and (iv) the building has a homogeneous roof texture or a defined pattern. This process is depicted in Figure 38, which was run using the tool developed in Matlab (see description of the tool in the Appendix D3.1).

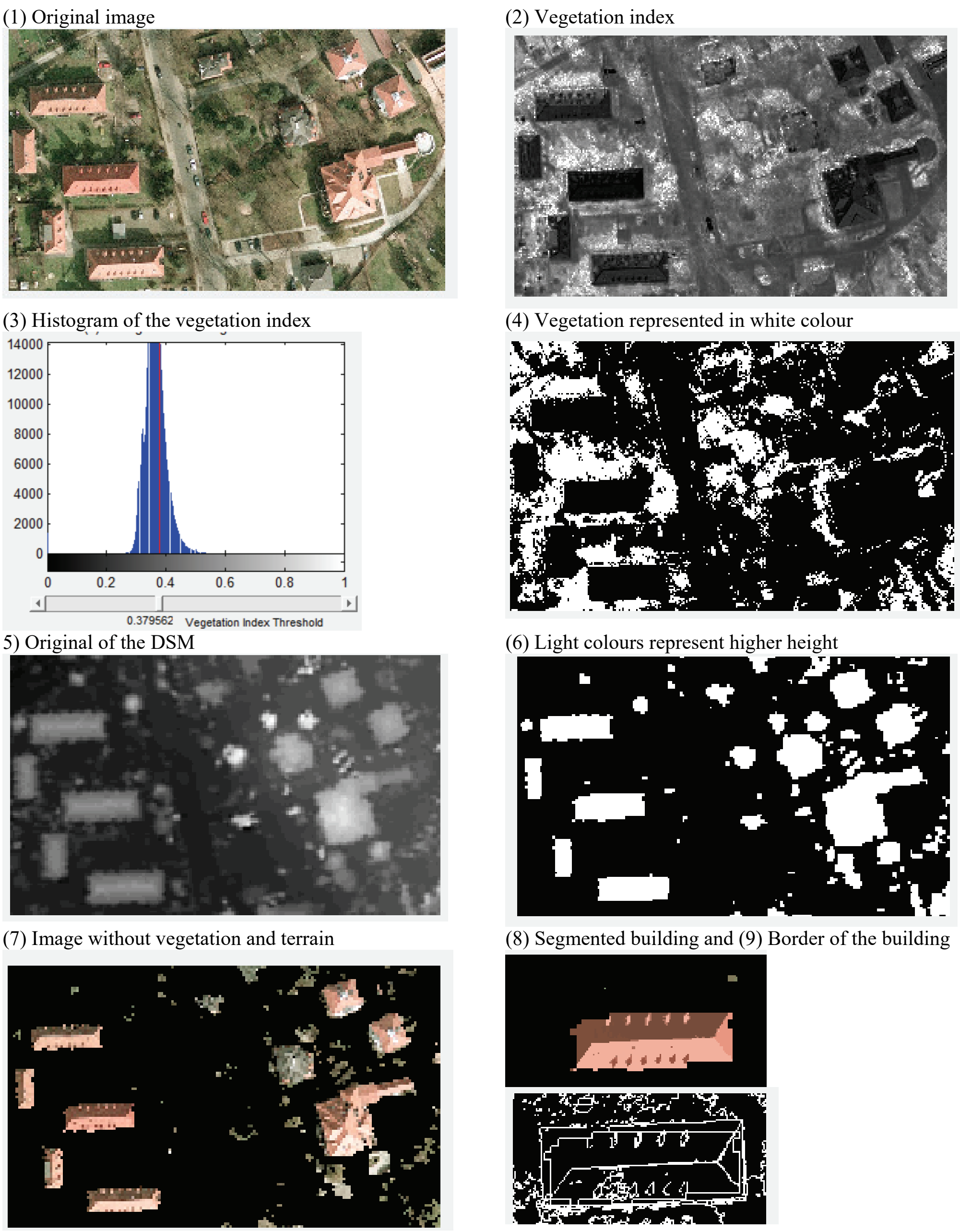

Figure 38: Test for detecting building regions "Kleinzschachwitz"

The building regions in this area are easily distinguishable and extracted with the established thresholds. The NDVI facilitates the separation of trees and the GSD of the DSM allows for a separation of the terrain from elevated objects. However, the extraction of building outlines requires advanced editions. Therefore, the semantic cues for building outlines should be better defined (see Table 21). Later, these criteria are implemented using specialised algorithms of e-cognition in order to separate the buildings and reduce points in the polygon (see Figure 39).

Table 21: Recognising cues of buildings "Kleinzschachwitz"

Cues	Kleinzschachwitz
Are buildings three-dimensional manmade objects and are they elevated?	Yes
What are the predominant shapes of the building?	Square, rectangle, multi-form
Do buildings in the area normally have orthogonal sides?	Building with complex shapes
Are the building roofs overlapped by vegetation?	No
Do the buildings have a higher elevation than their surrounding trees?	Yes
Is there some open space which separates the buildings?	Yes
How is the image contrast?	Good
Does the image present occlusion of the buildings due to shadows?	Yes

a. Original Image

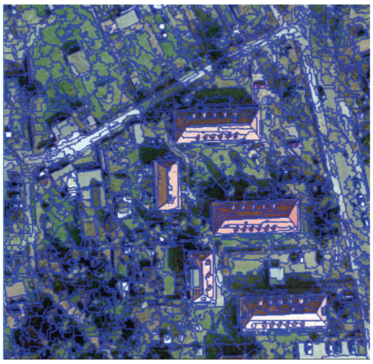

b. Creating objects using the multiresolution segmentation: Algorithm: multiresolution segmentation, scale parameter 25; shape 0.1; compactness 0.5

c. Classifying buildings based on elevation: Algorithm: assign class; class filter: none; threshold condition: Mean DSM >= 118.9 m; class: building

d. Separating buildings from trees using the DSM: Algorithm: assign class; class filter: building; threshold condition: SD DSM >= 20; use class: unclassified

e. Separating buildings from trees using the surrounding neighbour object: Algorithm: assign class; class filter: unclassified; threshold condition; border to building >= 0.31

f. Refining based on the size: Algorithm: merge; algorithm: assign class; class filter: building; threshold condition; area < 3000 pxl; use class: unclassified

Figure 39: Building extraction using algorithms of e-cognition

Some algorithms of the Objective of Erdas 10 module were tested in order to prove the definition of parameters for segmentation and filters. An example of the segmentation process is depicted in Figure 40.

a. Original image

b. Building segmented after extraction of vegetation and terrain

c. Merged segments in vector format. The building outlines are stair-stepped due to the native raster model

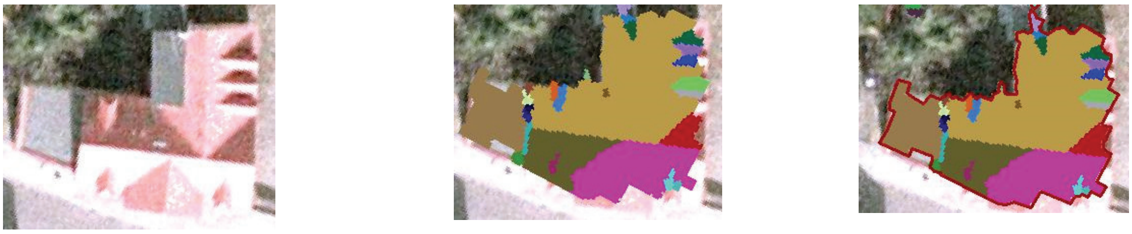

Figure 40:Building extraction using the algorithm of ERDAS-Objetive

e-cognition is robust and with the highest amount of algorithms, while Objective Image was easier to use and had the advantage of an intuitive workflow.

Preserve the "relevant „ pixels and building geometric characteristics:

Different algorithms were tested, such as erode, dilate, fill, detect lines, connect pixels, reshape and filter e.g. (orthogonally and rectangular fit), attempting to preserve the relevant pixels of the buildings (see Figure 41).

Figure 41: Example of preserving the relevant pixels of the building outline.

The process was very time-consuming and strenuous, because the appropriated algorithm for the extraction of some building outlines were not appropriate for other outlines. Therefore, the process cannot be considered as automatic due to the necessity to constantly revise and pan the image and verify the adequate results.

Accuracy evaluation:

As a reference polygon, the building information of topographic map scale 1:10000 (TK10) (AdV, 2008) was considered. Iterative processes are carried out until a better adjustment of the polygons is found, e.g. Figure 42.

Horizontal extraction accuracy assessment: The indices selected for the verification of accuracy of the extraction of building outlines were: RMSE vertices, area difference, perimeter difference and vertices difference (Song and Haithcoat, 2005). The results of the index allow us to improve the identification of cues and to detect the polygons, which require additional reshaping or simplification.

a. Polygon simplified (211 m2)

b. Reference polygon provided by digital topographic maps (219,8 m2)

c. Comparison of the two polygons.

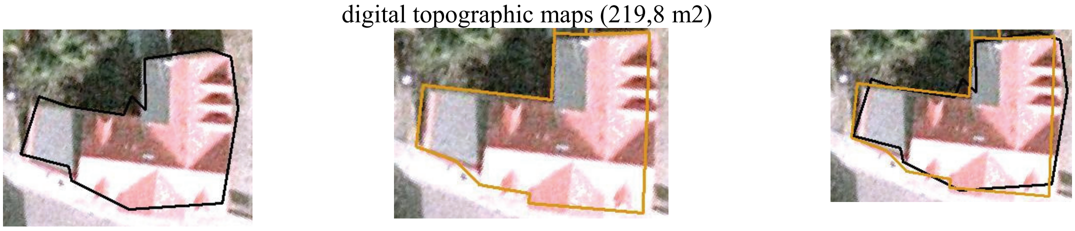

Figure 42: Improving the geometric characteristics of a building

The accuracy calculation helped to detect the difference between the reference polygons of the TK10, which fulfils the precision of the Geobasisinformation und Vermessung Sachsen. Though the building outline method, here proposed, will not exactly match the reference polygon, its result can be accepted for the application of building typology.

The chosen "reliable" polygons are those within the value to 75th percentile for the RMSE vertices, area difference, perimeter difference and vertices difference. In terms of accuracy, the detection rate is 79.5 %, i.e. 928 buildings detected from the 1167 reference polygons. From the 928 detected polygons only 794 fulfil the 75th percentile, giving as result that **68.03 %** of the buildings from the extracted process can be used as input for the next step of the methodology (see Table 22).

Table 22: Accuracy evaluation of the building outline extraction –"Kleinzschachwitz"

	RMSE vertices	**Area difference**	**Perimeter difference**	**Vertices difference**
Minimal	1.65E-05	5.07E-11	2.01E-11	0
25th percentile	0.84	0.095	0.12	1
Media	2.55	1.25	0.98	9
75th percentile	3.86	1.334	1.25	*19*
Maximal	68.54	104.75	250.14	34

Height extraction accuracy assessment: The method of Flood (2004) is chosen for the assessment of the height accuracy. As a result, **1.25 metres** is the vertical accuracy at the 95-percentage confidence level using RMSE (z) x 1.9600.

4.1.1.2 Building taxonomic code – "Kleinzschachwitz"

The next process, as depicted in Figure 43, was carried out several times in order (i) to find inconsistencies for the calculation of the parameters and (ii) to develop the scripts in python.

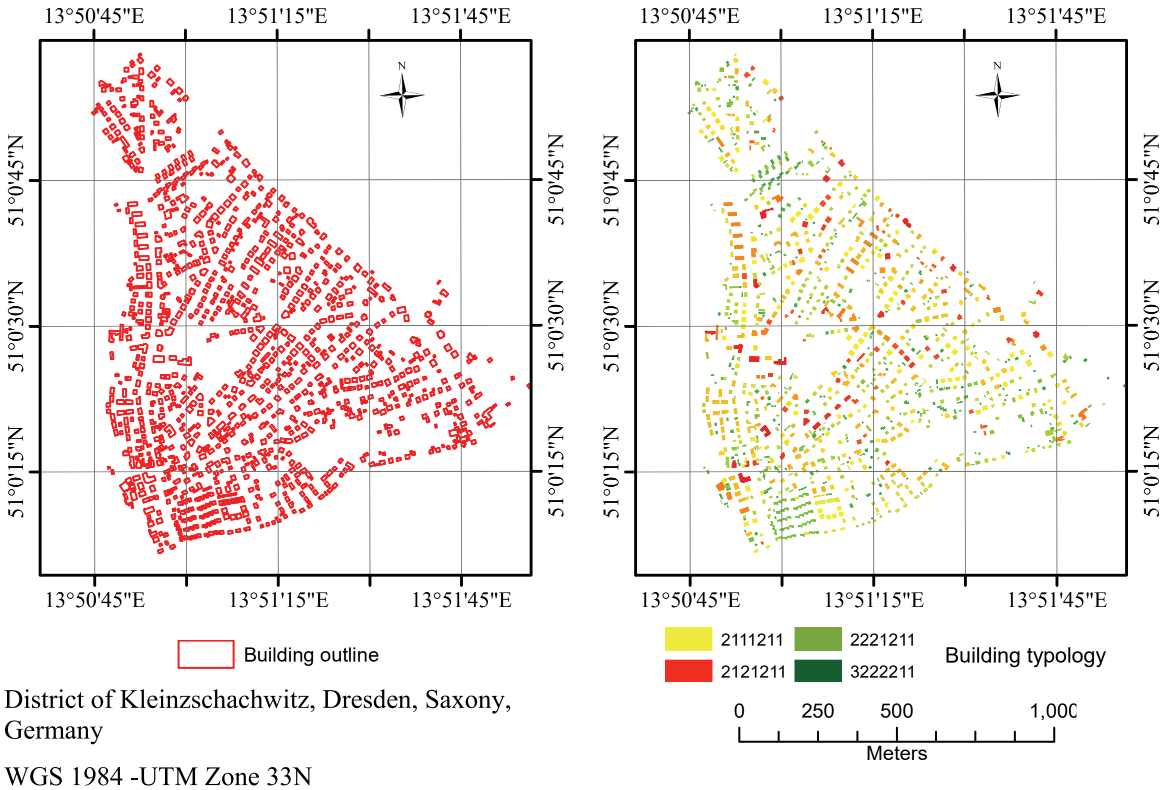

Figure 43: Test 1- Building taxonomic process for the selection of representative buildings

The previous process was carried out based on the initial classification proposed in Table 4 in section 3.1.2.5. This test gives the following inconsistencies:

- Too many building types.
- The representation of the building types does not clearly show the pattern of buildings
- There is redundancy among the categories.

An exploratory data analysis using the scatter diagram and the correlation matrix was done in order to find trends in the relation between the parameters.

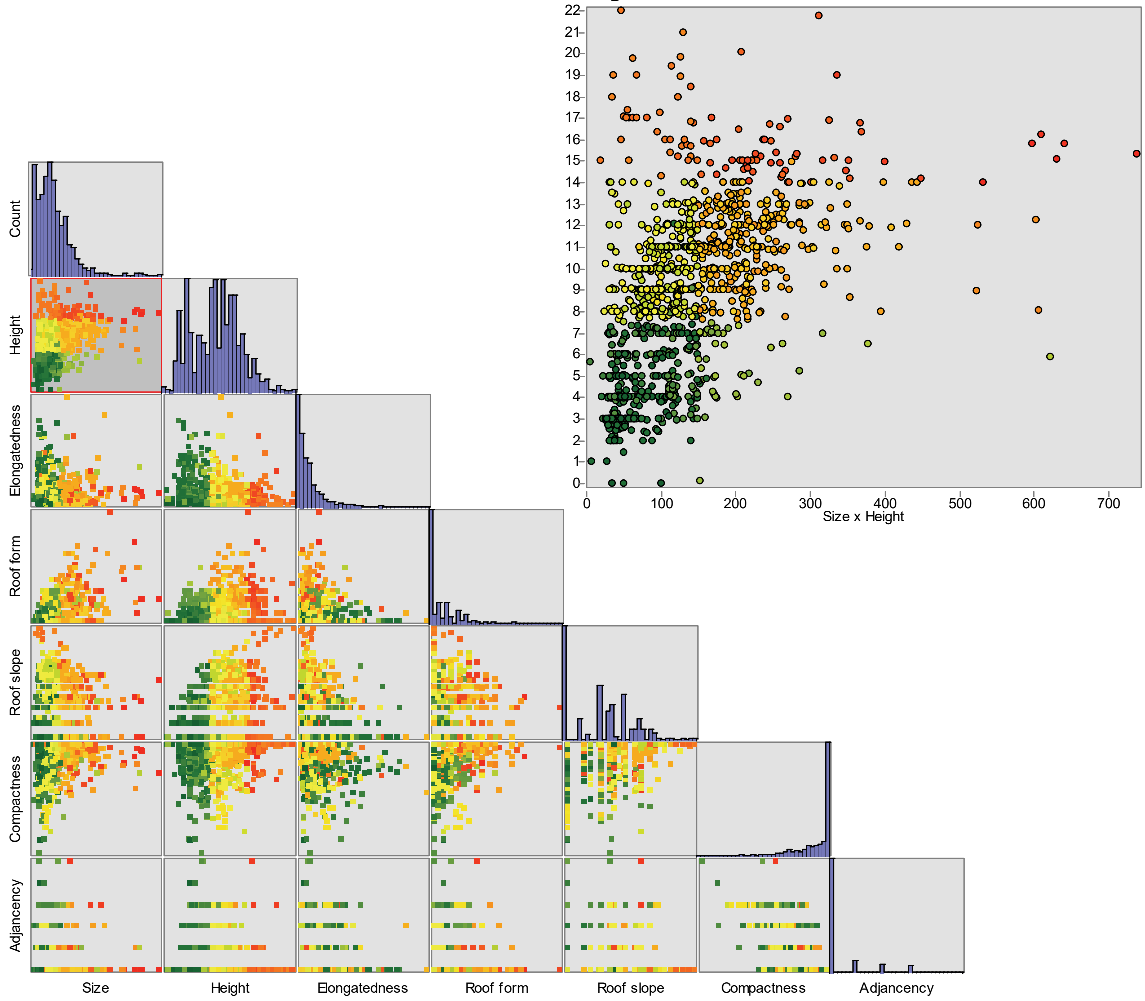

Figure 44: Scatter diagram of value parameters from "Kleinzschachwitz"

The scatter diagram visually displays that height and size present a normal distribution and the other parameters non-normal distributions. The values are dispersed and a defined pattern from a linear transformation cannot be easily identified. This confirms that buildings do not follow a normal distribution and therefore their behaviour cannot be predicted.

The correlation matrix (see Table 23) shows a rather direct relation between size and height, size and roof form, height and roof form as well as height and roof slope. That means the higher the building, the bigger and more complex its roof shape. In this settlement, tall buildings have a larger size and a more complex form than small buildings.

Table 23: Correlation matrix of the parameters of “Kleinzschachwitz”

	Adjacency	*Elongatedness*	*Compactness*	*Size*	*Height*	*Roof form*	*Roof Slope*
Adjacency	1.000						
Elongatedness	0.046	1.000					
Compactness	0.493	0.443	1.000				
Size	0.006	0.142	0.139	1.000			
Height	0.012	-0.255	-0.158	0.387	1.000		
Roof Form	-0.013	0.046	0.112	0.493	0.222	1.000	
Roof Slope	0.013	-0.261	-0.200	-0.015	0.442	-0.071	1.000

If the buildings are located within a block (adjacency value 5 or 6), there is less open space around the building. Then, there is an obvious direct relation between compactness and adjacency. The more compacted, the higher the value of compactness. Buildings located in a block tend to be more compacted and elongated, have narrow facades and use the interspace of the block.

However, these statements apply only to the buildings in this settlement with low-rise buildings (few stories) and large areas or inversely; or its low buildings and flat or steep roof slopes. Nevertheless, the analysis helps to include some adjustment in the definition of the fuzzy set “categories”, such as:

- Reduce the amount of categories of the parameters: The range between the height categories was extended in order to include the height of the basement. The calculation of the height of buildings which are very close to trees presented some inconsistencies. Therefore, those inconsistencies can be reduced if the categories are extended.
- Three categories for compactness better represent the open space in this settlement.
- Change the order of the concatenation of the parameters for a better representation and identification of patterns. It does not imply a hierarchy of the variables. The combination of the parameters height & size & roof form & roof slope & elongatedness & compactness & adjacency visually displays the identification of patterns for a building typology.

Verify visually the differences of the buildings in the same building type and the other building types. This step consists in exporting the polygons to KML format and display them in Street View of Google Earth, and then group them and try to find the best combination. After many tests with a change of the ranges in the categories or position of the parameters, the Table 24 is accepted as the basis for the building typology of Kleinzschachwitz. Figure 45 displays the 123 buildings classes according to the defined parameters of Table 24.

Table 24: Range of categories for parameters (Type 1) – “Kleinzschachwitz”

Parameter	**Code**	**Description**
Height	1	<= 7.5 m
	2	> 7.5 – 13 m
	3	>13 – 30 m
Footprint - Size	1	0 – 50 m²
	2	>150 – 500 m²
	3	>500 – 800 m²
	4	>800 – 1000 m²
Elongatedness (length/width ratio)	1	Square: 0.8 – 1.2
	2	Elongated rectangle:> 0.8 and < 1.2
Roof form	1	< = 12 vertices

Parameter	Code	Description
	2	>12 vertices
Roof slope (Roof pitch)	1	<= 10 degrees
	2	>10 degrees
Index inversely compactness	1	> 66 %
	2	>33 % – 66 %
	3	<= 33 %
Adjacency	1	Single building
	2	Pair building or single building with annex building
	3	The corner building within a line of buildings
	4	Building within a line of buildings
	5	A building within a block
	6	The corner building within a block

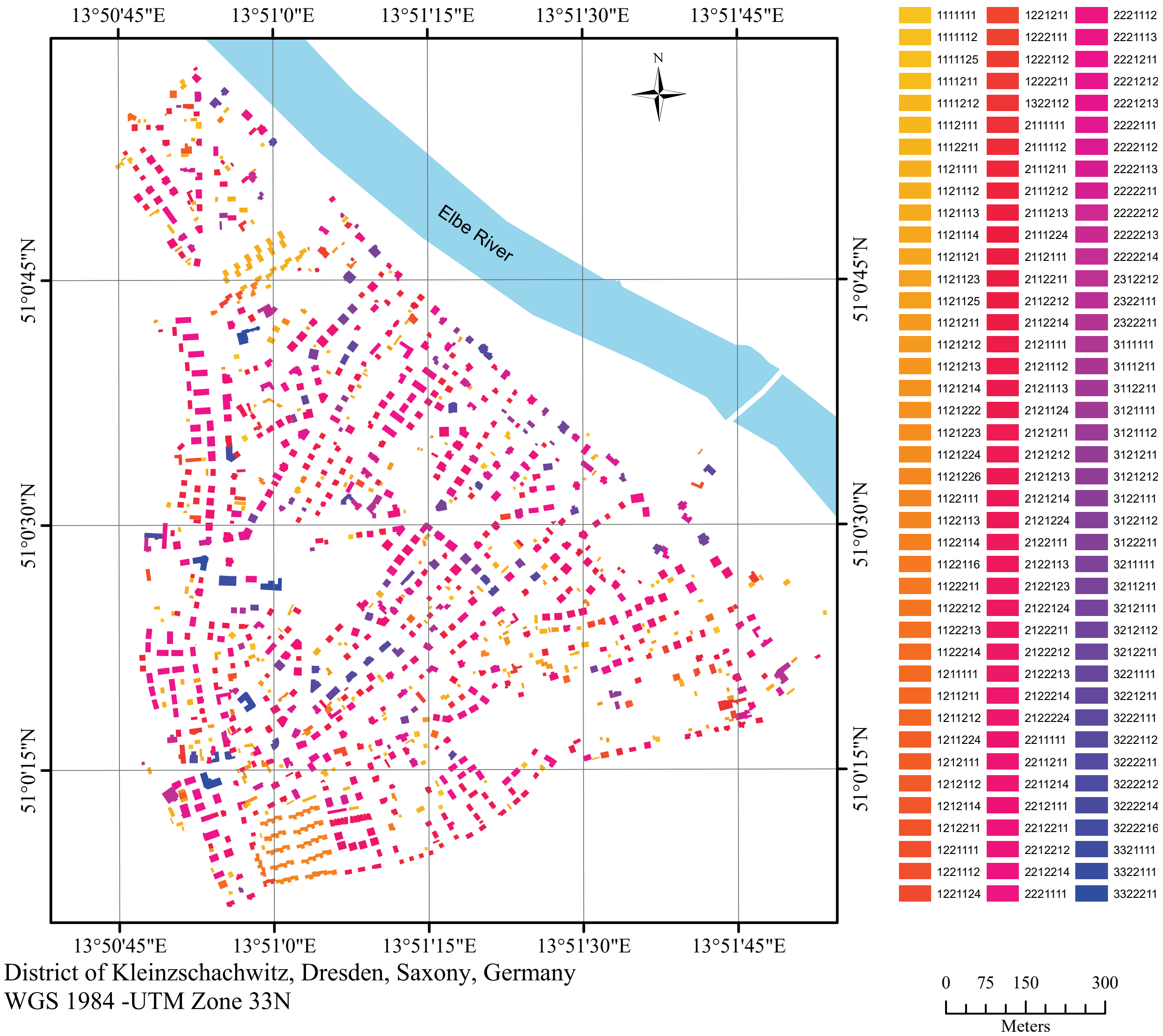

Figure 45: Adjusted building typology – "Kleinzschachwitz"

4.1.1.3 Selection of representative buildings – "Kleinzschachwitz"

A variety of thresholds and different combinations of membership functions were proofed for separating representative buildings from non-representative. For example, the following test was preformatted:

- In the correlation matrix, Table 23 a slightly direct relation between height and size and roof characteristics can be observed. In order to mark a larger variability between these variables, higher weight values for height and lower weight values for size are assigned in the matching matrix. In the same way, compactness will have higher weight values than elongatedness, seeking for the highest variance possible.
- For this pilot site, the parameters building footprint size and roof will have less weight in the membership matrix, and height with higher weight, in order to extend the difference for the grouping. Then the membership function can be defined as (19):

$$U_{R-nonR} = \begin{bmatrix} 1 & 0.8 & 0.8 & 0.8 & 1 & 1 & 1 \\ 1 & 0.3 & 0.5 & 0.3 & 0.5 & 0 & 0.5 \\ 0.5 & 0 & 0 & 0.1 & 0.3 & 0 & 0.3 \\ 0 & 0 & 0 & 0 & 0 & 0 & 0 \end{bmatrix} \qquad (19)$$

As result of this test, 705 buildings are selected as representatitive buildings (black border). Figure 46 shows these buildings and the calculation of similarity of non-representative buildings to representative buildings using matching %.

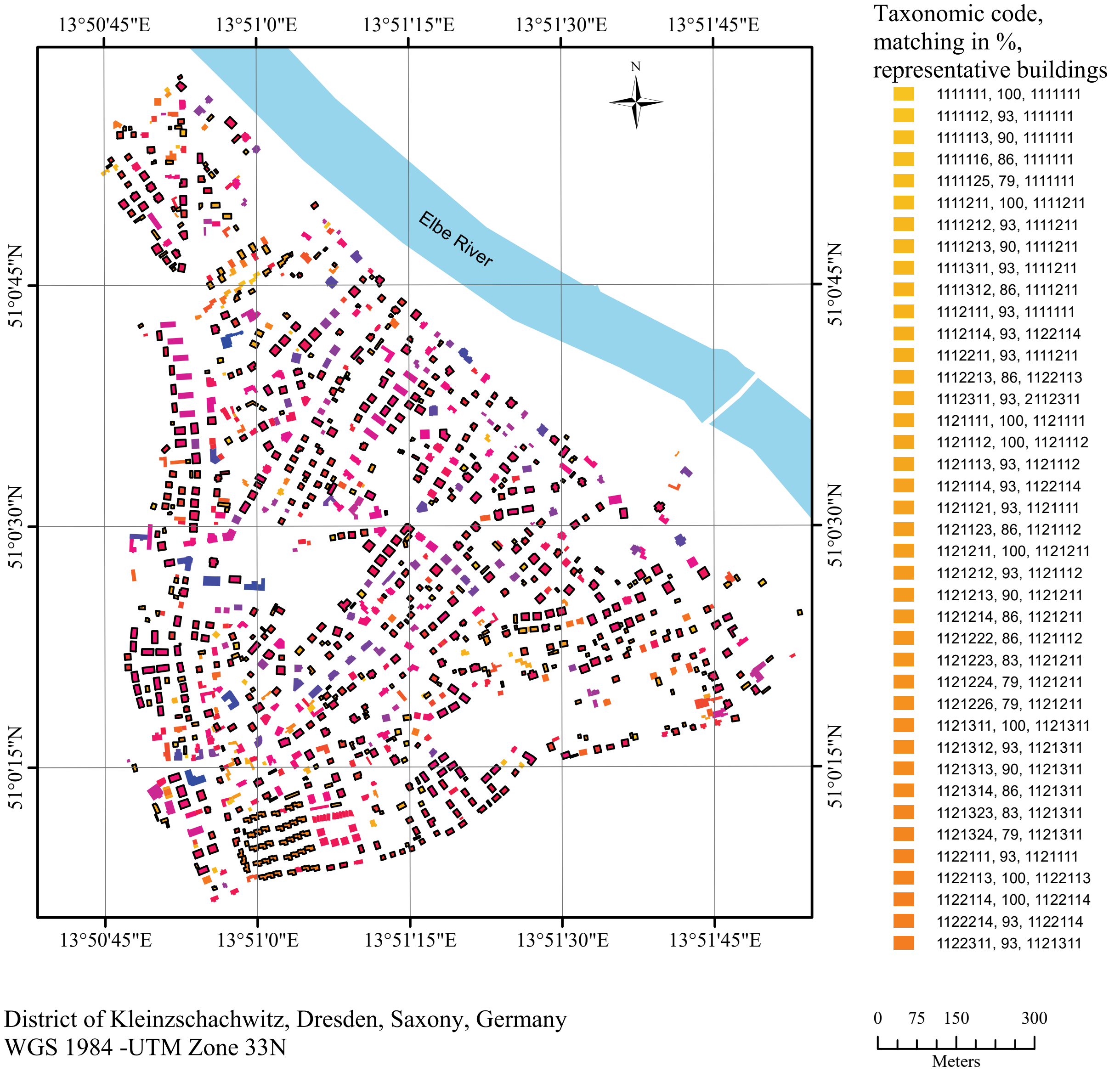

Figure 46: Example of the selection of representative buildings and computing of the similarity of the non-representative buildings (6th test)

Tests of clustering were checked by using the pictures of Google Street View. The pictures of the facades of five buildings are depicted in the next figure to show that the buildings are very similar but not equal. They present slight differences regarding the height point of the house, the size and the form of the roof.

Taxonomic code: '*3211211*'

Representative building type: '*3211211*'

% Matching: 100 %

Taxonomic code: '*2211211*'

Representative building type: '*2211211*'

% Matching: 100 %

a. Typology with three ranges of height

Taxonomic code: '*2211211*'

Representative building type: '*2211211*'

% Matching: 100 %

Taxonomic code: '*2211111*'

Representative building type: '*2211111*'

% Matching: 100 %

Taxonomic code: '*2221211*'

Representative building type: '*2221211*'

% Matching: 100 %

b. Typology with two ranges of height

Figure 47: Example of clustering the buildings

The taxonomic code in the upper Figure 47 a. shows height (first digit from left to right) and has more ranges than the classification in Figure 47 b. This change suffices to vary the grouping of the buildings. That reflects how sensible the classification of the buildings can be if the range of a parameter is changed, and with this the clustering can vary as well.

Similarities of building features within the same building taxonomic code and differences or similarities to the other codes are corroborated on the basis of a visual supervision of the building features. Trial and error is the method here. However in some trials, the processes of classification and clustering give that some representative buildings are not typical in the area, due to some errors in the roof slope categories, and additional vertices derive from a roof form misclassification. Then the ranges of the categories of these parameters must be adjusted again.

14 buildings were chosen as a threshold for the selection of representative buildings. The building types with less than 14 buildings are clustered to the representatives using the

membership function (20). Figure 48 shows the frequency of buildings by taxonomic code and related to the percentage of matching.

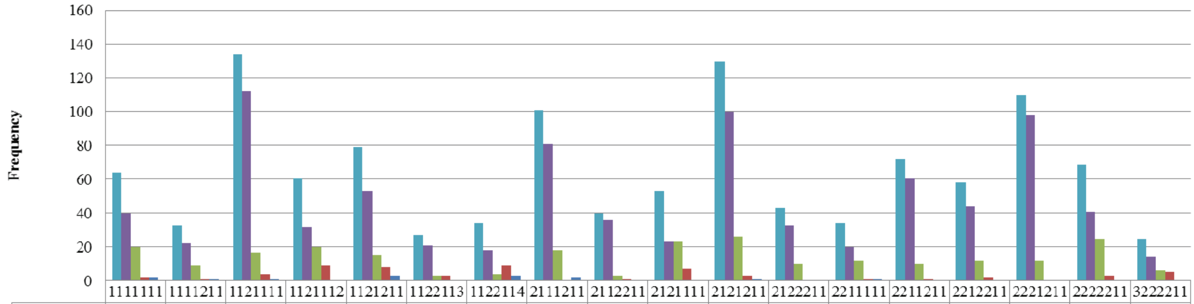

	1111111	1111211	1121111	1121112	1121211	1122113	1122114	2111211	2112211	2121111	2121211	2122211	2211111	2211211	2212211	2221211	2222211	3222211
Total	64	33	134	61	79	27	34	101	40	53	130	43	34	72	58	110	69	25
100 %	40	22	112	32	53	21	18	81	36	23	100	33	20	61	44	98	41	14
90 - 99.9 %	20	9	17	20	15	3	4	18	3	23	26	10	12	10	12	12	25	6
80 - 89.9 %	2	1	4	9	8	3	9		1	7	3		1	1	2		3	5
70 - 79.9 %	2	1	1		3		3	2			1		1					

Figure 48: Frequency of buildings by taxonomic code and percentage of matching

The next membership function for clustering non-representative to representative buildings shows, through visual verification, that the matching of the buildings according to their features was more consistent.

$$U_{R-nonR} = \begin{bmatrix} 1 & 1 & 1 & 1 & 1 & 1 & 1 \\ 0.5 & 0.5 & 0.5 & 0.5 & 0.5 & 0.5 & 0.5 \\ 0.3 & 0.3 & 0.3 & 0.3 & 0.3 & 0.3 & 0.3 \\ 0 & 0 & 0 & 0 & 0 & 0 & 0 \end{bmatrix} \quad (20)$$

849 buildings (72.75 %) are representative buildings, i.e. they are a 100 % match. 245 buildings (20.99 %) are clustered to the representative buildings with a matching range between 90-99 %, 59 buildings (5.05 % with a matching range between 80-89 % and 14 buildings (1.2 %) with a matching range between 70-79 %. These 14 buildings are what is called atypical buildings, according to the seven parameters defined for the taxonomic code. They may differ in their characteristics from the selected representatives.

Figure 49 illustrates one example of the selection of a representative building in the case of the settlement of Dresden. The most right and the most left buildings have the taxonomic code '*3211211*' and possess two attics; the two buildings in the middle have the taxonomic code '*2211211*'. The difference between the two building types is the first digit that represents the height. The buildings in the middle are selected as representative buildings because they have a higher frequency in the settlement, while the other two buildings are non-representative buildings. The non-representative buildings are then clustered to the representative buildings with a matching percentage of 92.9 %. The taxonomic approach was contrasted with the urban building structure implemented by Neubert et al. (2014) in this area and many building types present consistencies and similarities (see Appendix E).

Figure 49: Representative buildings for the taxonomic code '*2211211*' in "Kleinzschachwitz"

Additional pictures of representative buildings for a taxonomic code with the percentage of matching are displayed in Appendix F. These pictures were extracted by means of Street View. The next map (Figure 50) gives the result of the representative buildings and the final building typology for the pilot site of Kleinzschachwitz.

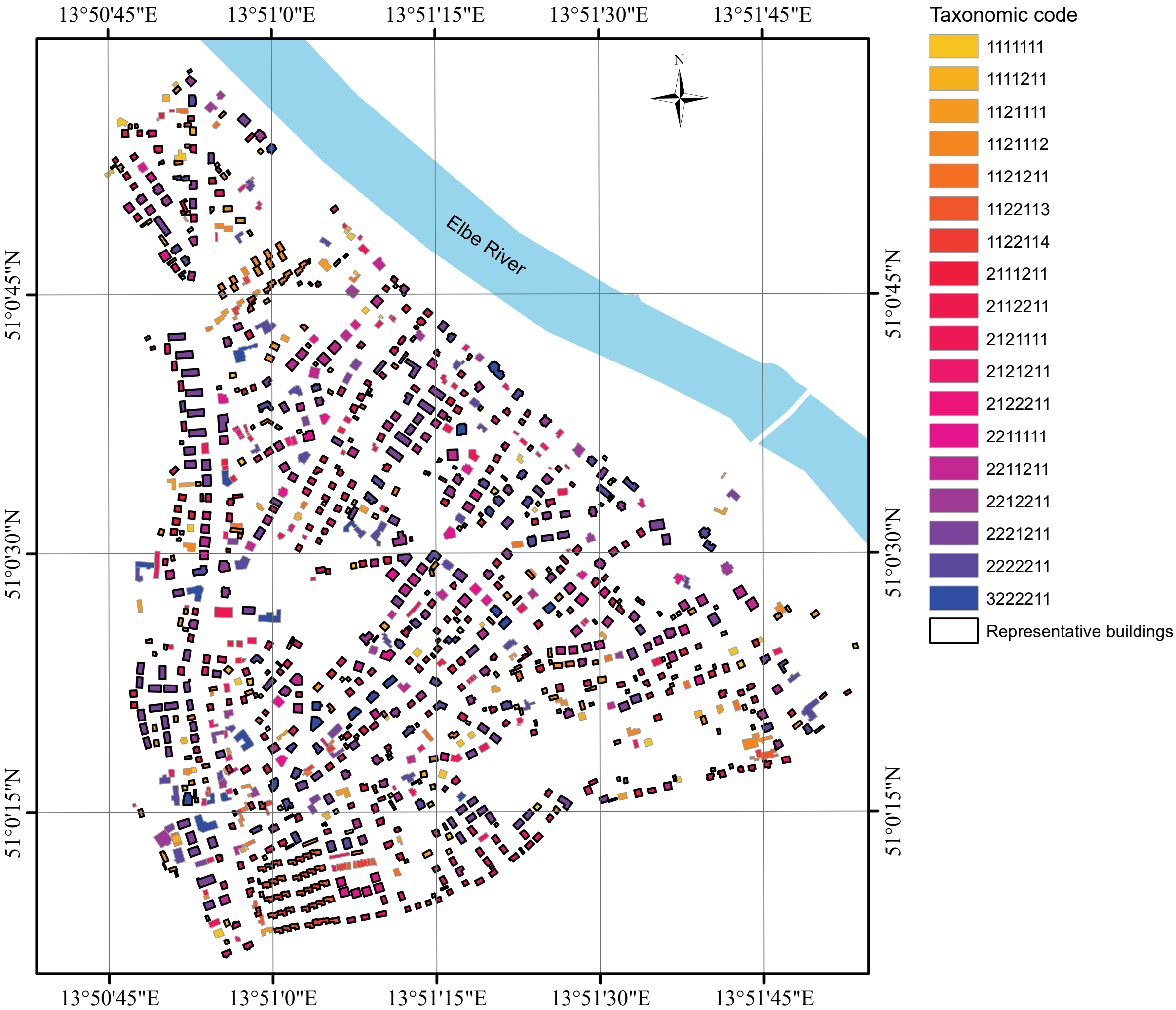

Figure 50: Clustering of representative buildings – "Kleinzschachwitz"

District of Kleinzschachwitz, Dresden, Saxony, Germany
WGS 1984 -UTM Zone 33N

0 75 150 300
Meters

4.1.2 Module 2: Physical susceptibility of representative buildings – "Kleinzschachwitz"

The Regklam project yields methods and indisputable results of impacts on buildings caused by possible climate changes in the model region of Dresden, considering six major hazard types due to summer heat, flooding, heavy rain, hail, wind and snow (Weller et al., 2012). In the context of this project, civil engineers have collected information on the year of construction, occupancy of the building, type of roof, geometry in terms of length, width and area of the storeys, number of storeys and building components for representative buildings. This includes pictures of the facades, blueprints for every storey and basement and a description of the building characteristics.

The components and materials, information provided by the Regklam project, are arranged according to their position referring to the ground. Then the material's resistance values are assigned according to the analysis of BMVBS (2006). After that, based on the expertise by the IOER experts in damage assessment in buildings and the knowledge on the material's characteristics, a range of values for the qualification of the material's susceptibility is considered (with 0 being the lowest value of susceptibility and 5 the highest). The complete calculation of the fuzzy sets is displayed in Appendix G. The qualification is depicted in Table 25.

Table 25: Material susceptibility qualification - "Kleinzschachwitz"

Component	Materials	BMVBS (2006)	Susceptibility value 0-5
Gründung	Streifenfundamente aus Natur- /Bruchstein (Sandstein / Granit)		2-3
Gründung	Streifenfundamente aus Beton, Stampfbeton		1-2
Gründung	Flächengründung aus Stahlbeton (Bodenplatte)		0-1
Fenster	Holzfenster / Holzsprossenfenster	3-1	4-5
Fenster	Kunststofffenster	5-3	4-5
Fenster	Metallfenster		2-3
Außenwände	Bruchsteinmauerwerk (Granit / Sandstein)		1-4
Außenwände	Stahlbeton (Weiße Wanne)		0-1
Außenwände	Mauerwerk Sandstein	5	2-4
Außenwände	Mauerwerk Kalksandstein	5	2-3
Außenwände	Ziegelmauerwerk	5	2-3
Kellerdecke	Preußische Kappendecke		2-3
Kellerdecke	Stahlbetondecke		0-1
Kellerdecke	Lagerhölzer und Schüttung		5
Kellerdecke	Füllkörperdecke (FB-Decke)		1-2
Kellerdecke	Stahlbetonhohldielendecke		2
Kellertreppe	Stahlbeton Bodenfliesen		1-2
Kellertreppe	Betonstufen	5	1
Kellertreppe,	Sandstein - Geschosstreppe	1	2
Fußboden	Vollziegel		2-3
Fußboden	Verbundestrich mit Schutzanstrich	5-3	1

Component	Materials	BMVBS (2006)	Susceptibility value 0-5
Fußboden	Bodenfliesen	5-3	-
Fußboden	Schwimmender Estrich auf Schüttung	5-3	4
Fußboden	Dielung auf Holzbalkendecke Fliesen- oder Holzbelag	1	5
Fußboden	Teppichbodenbelag	1	5
Fußboden	Laminat	1	5
Geschossdecke	Holzbalkendecke als Einschubdecke	3	4
Geschossdecke	Stahlbeton		0-1
Geschossdecke	Holzbalkendecke mit Dämmung und Dielung	3	4

The qualified ranges of the material's susceptibility are converted in fuzzy sets with their crisp values using the formulas by Hong and Lee (1996) as described in section 3.2.2.2 (see Table 26).

Table 26: Fuzzy sets of building material susceptibility – "Kleinzschachwitz"

Component	Material	a	b	c
Foundation	Strip foundations of natural/quarry stone (sandstone/granite)	0.44	0.5	0.56
Foundation	Strip foundations of concrete, stamped concrete	0.24	0.3	0.36
Foundation	Surface foundation of reinforced concrete (bottom panel)	0.04	0.1	0.16
Windows	Wooden windows/timber framed windows	0.84	0.9	0.96
Windows	Plastic windows	0.84	0.9	0.96
Windows	Metal windows	0.44	0.5	0.56
External walls	Masonry (granite/sandstone)	0.33	0.5	0.67
External walls	Reinforced concrete (white tank)	0.04	0.1	0.16
External walls	Masonry sandstone	0.48	0.6	0.72
External walls	Sand-lime brick masonry	0.44	0.5	0.56
External walls	Brickwork	0.44	0.5	0.56
Basement ceiling	Prussian cap ceiling	0.44	0.5	0.56
Basement ceiling	Reinforced concrete slab	0.04	0.1	0.16
Basement ceiling	Storage timber and bulk	1	1	1
Basement ceiling	Filling body blanket (FB ceiling)	0.24	0.3	0.36
Basement ceiling	Reinforced concrete hollow core ceiling	0.4	0.4	0.4
Cellar stairs	Reinforced concrete floor tiles	0.24	0.3	0.36
Cellar stairs	Concrete steps	0.2	0.2	0.2
Basement stairs	Sandstone	0.4	0.4	0.4
Floor	Solid brick	0.44	0.5	0.56
Floor	Topping with protective coating	0.2	0.2	0.2
Floor	Floating screed on bed	0.8	0.8	0.8
Floor	Floorboards on wood beamed ceiling tiles or wood flooring	1	1	1
Floor	Carpet flooring	1	1	1
Floor	Laminate	1	1	1
Floor ceiling	Beamed ceiling as false ceiling	0.8	0.8	0.8
Floor ceiling	Reinforced concrete	0.04	0.1	0.16
Floor ceiling	Beamed ceiling with insulation and floorboards	0.8	0.8	0.8

As experts state “if the water level is higher than the attic, this should lead to a total loss of the building”, the roof construction and materials are not considered for “Kleinzschachwitz”. The assessment of the attributes exposed in Table 19 must be fed in order to find a consensus among the experts about the ranges. However, it is justified that a second qualification is not required due to the validity and expertise of the experts in the first qualification.

Identification of building components:

A building’s structure and shell components such as roof, external fenestration, external walls, floor first storey, slab basement and external windows can be surveyed through non-invasive methods; stairs, columns, slab ceiling and foundation may be inferred from the information collected in the Regklam project.

Derivation of depth-physical impact function:

An example for the derivation of a depth-physical impact function for a representative building with the taxonomic code *‘2111211’* is presented in Table 27.

Table 27: Example of information for a representative building

	**Component**	**Lower height**	**Upper height**	**Material**	**Susceptibility**	**Volume material in m^3**	**Susceptibility * Volume material in m³**
First storey	Roof	2.8	7.4	Timber structure, collar roof with concrete ring beams, roof tile cover	1	7.741	7.741
	Slab ceiling	7	7.2	Hollow core slabs d = 24 cm (FB ceiling), concrete	1	21.895	21.895
	External fenestration	0.5	7	Wooden windows, heat insulation glazing	0.9	1.300	1.170
	External walls	0.5	7.4	Brickwork d = 36.5 cm	0.5	57.760	28.880
	Floor first storey	0.5	0.7	Floating floor, tiles in wet area and hallway	0.8	21.895	17.516
Basement	Slab basement	0.4	0.5	Hollow core slabs d = 24 cm (FB ceiling), concrete	0.2	10.947	2.189
	External windows	0.1	0.4	Wooden windows, heat insulation glazing	0.9	0.060	0.054
	Stairs	-2.2	0.4	Reinforced concrete	0.1	2.600	0.260
	External walls	0	0.4	Brickwork d = 36.5 cm	0.5	4.018	2.009
	Floor	-2.3	-2.2	Screed on concrete base	0.8	10.947	8.758
	Columns	-3.3	2.8	Strip foundations of concrete	0.3	91.500	27.450
	Foundation	-3.3	-2.3	Strip foundations of concrete	0.3	16.742	5.023

Table 28 relates every volume of the component to a level of water depth. The water levels are depicted in the blue colour row. The potential degradation for every component continually increases from its lower height until the water level overtakes its upper height, as the water depth rises. Up here, the component degradation is assumed constant when the flood continues to rise. The green row gives the sum of the susceptible volume for the impacted components for every water depth.

Table 28: Derivation of the building volume degradation for levels of water depth

								1.000	7.155	7.448	7.741	
									1.000	21.895	21.895	
						0.900	0.908	0.996	1.170	1.170	1.170	
						0.500	1.323	9.960	27.235	28.058	28.880	
						0.800	17.516	17.516	17.516	17.516	17.516	
					0.200	2.189	2.189	2.189	2.189	2.189	2.189	
				0.900	0.054	0.054	0.054	0.054	0.054	0.054	0.054	
		0.100	0.235	0.242	0.260	0.260	0.260	0.260	0.260	0.260	0.260	
			0.500	0.877	2.009	2.009	2.009	2.009	2.009	2.009	2.009	
	0.800	8.758	8.758	8.758	8.758	8.758	8.758	8.758	8.758	8.758	8.758	
0.300	4.751	5.196	14.988	15.433	16.768	17.213	18.103	27.450	27.450	27.450	27.450	
0.300	5.023	5.023	5.023	5.023	5.023	5.023	5.023	5.023	5.023	5.023	5.023	
-3.30	**-2.30**	**-2.20**	**0.00**	**0.10**	**0.40**	**0.50**	**0.70**	**2.80**	**7.00**	**7.20**	**7.40**	**Water depth**
0.60	10.57	19.08	29.50	31.23	33.07	37.71	56.14	74.21	92.66	114.38	115.20	**Sum of vol. deg.**

Figure 51 shows the depth-physical impact functions for the four selected buildings depicted in Figure 52. They reflect the deterioration of the building's integrity in m³. This means that the depicted volume of material in m³ will be degraded depending on the water depth.

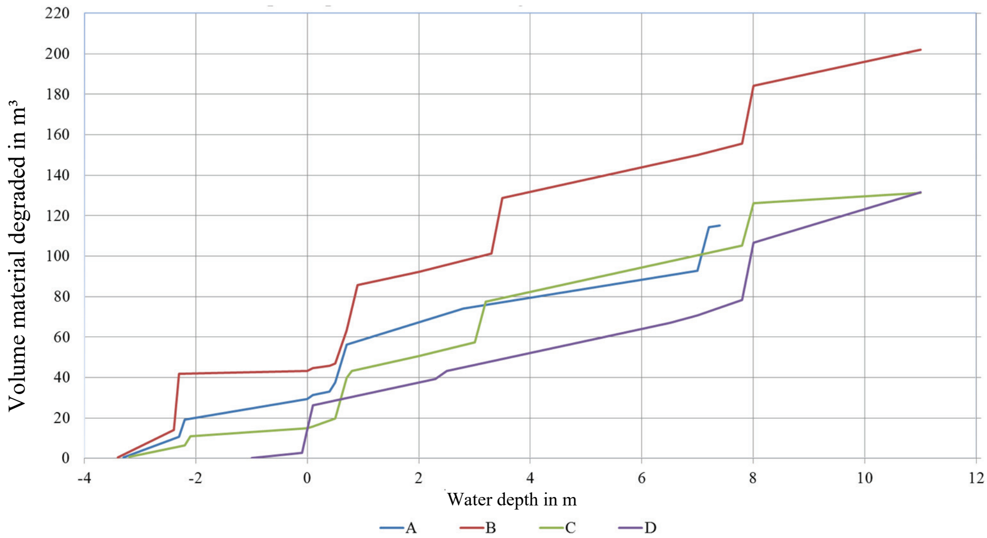

Figure 51: Depth-physical impact functions for representative buildings with tc: *'2111211'*

A B C D

Figure 52: Representative buildings of the taxonomic code *'2111211'*

The synthetic or median depth-physical impact function for buildings with the taxonomic code '2111211' is displayed in Figure 53.

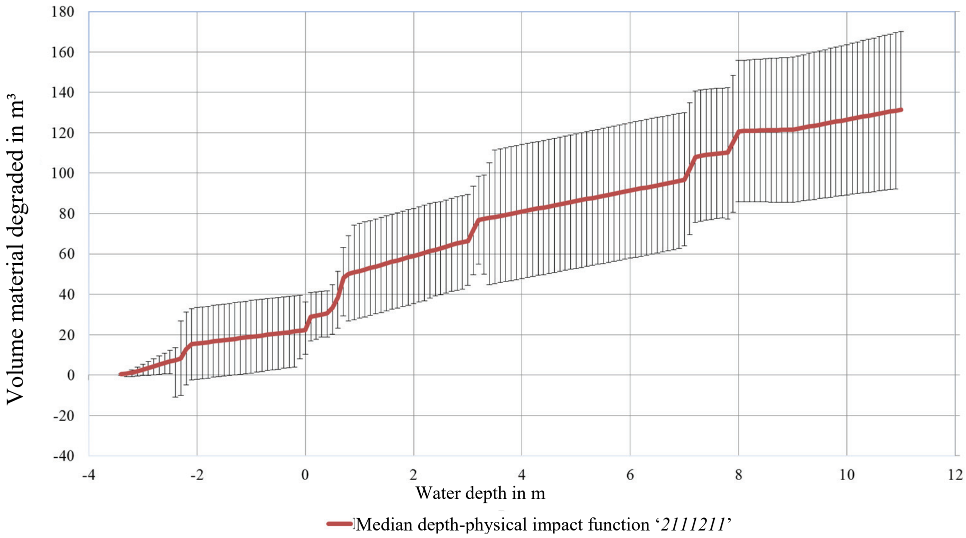

Figure 53: Median depth-physical impact function and range of the standard deviation *'2111211'*

Another test is carried out for comparing the profiles of the calculated depth-physical impact function with the depth-damage function from the Regklam project. Figure 54 shows the following example: The depth-physical impact function has more inflection points than the depth-damage function, which is smoothed. Additionally, the depth-physical impact function reveals the changes of susceptibility for building components.

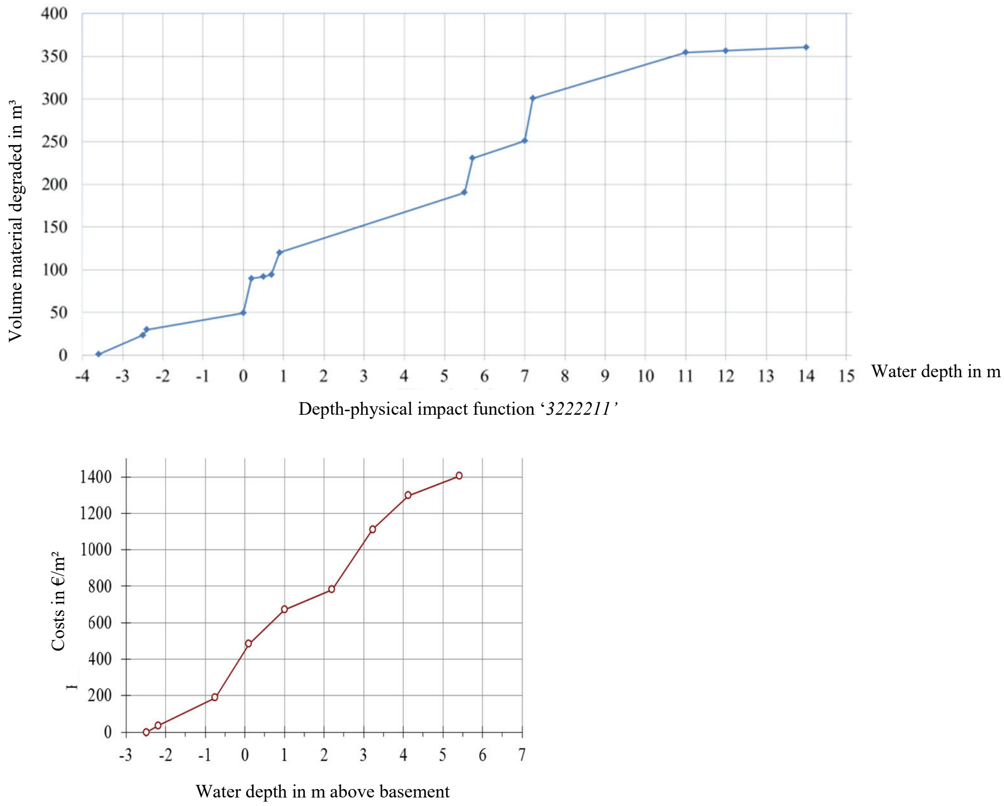

Figure 54: Depth-physical impact functions and depth-damage functions of a representative building

The depth-physical impact function is referenced to the height above the terrain, while the depth-damage function is referenced to the "OKFF EG" (i.e. *Oberkante des fertigen Fußbodens des Erdgeschosses* – top of the finished first floor). The height reference must be homogenised for finding a correlation between the two functions. Once the height is homogenised, a correlation coefficient and a regression can be calculated, which gives a lineal relation between the two functions for a building type.

Table 29: Linear relation between depth-damage function and depth-physical impact function

Building type	**Correlation coefficient**	**Relation**
'3222211' – ME3	0.85	Damage costs in € = 12.6*(degraded volume in m³) - 121.6
'3222212' – MRG 3	0.94	Damage costs in € = 49.9*(degraded volume in m³) - 162.1
'2221211' – M E 7	0.90	Damage costs in € = 45.6*(degraded volume in m³) - 349.5
'2121211' – ME4	0.87	Damage costs in € = 8.9*(degraded volume in m³) - 61.78
'2111211' – EE5	0.93	Damage costs in € = 24.4*(degraded volume in m³) - 168.3

Table 29 reveals any evidence of a mathematical relation or pattern between the two functions. This is due to the fact that depth-damage functions are based on other levels of information, such as construction details, original use, geometry base data, basement quota and present technical performance, which is necessary information for the calculation of refurbishment costs, while the depth-physical impact function includes only the volume degradation of shell and structural materials.

4.1.3 Module 3: Technological integration – “Kleinzschachwitz”

The depth-physical impact functions are converted to flat text and all data is integrated using the tool developed for this aim (see Appendix D). Figure 55 shows the input data for this aim. Figure 55 shows the input data required for the calculation of a physical flood susceptibility map.

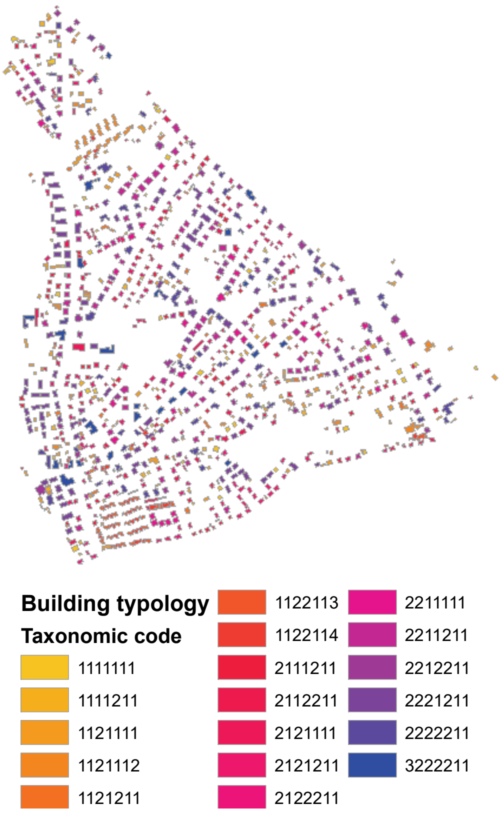

a. Building typology (taxonomic code)

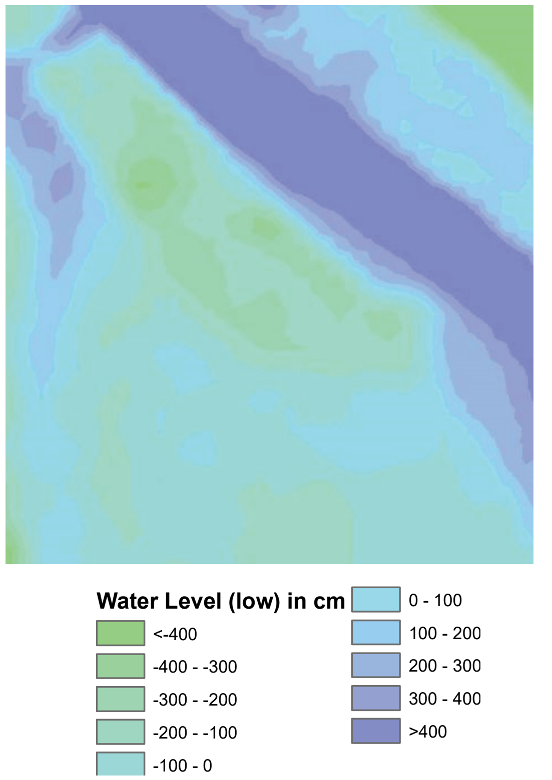

b. Water level in cm for a 100-year flood; MULTISURE project; provided by IOER (2013)

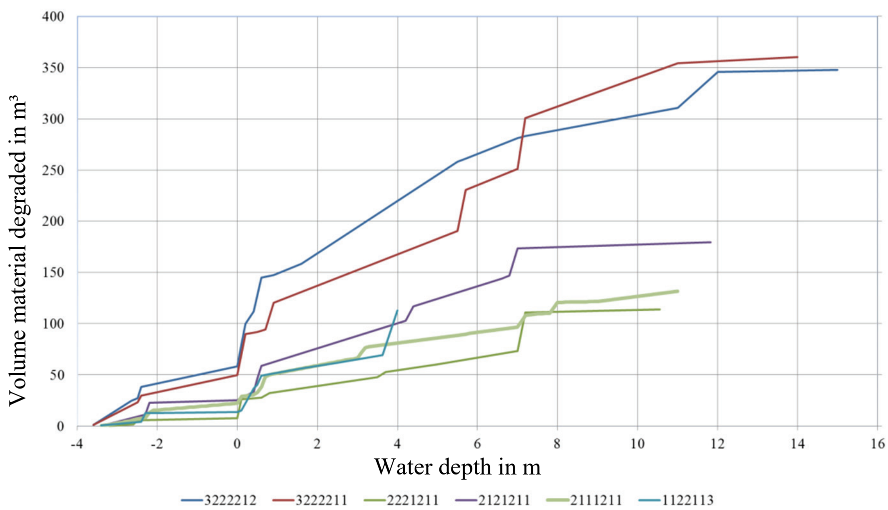

c. Available depth-physical impact functions in “Kleinzschachwitz”

Figure 55: Input data for the calculation of a physical flood susceptibility map – “Kleinzschachwitz”

Figure 55b. shows the groundwater depths (GWFA): Simulated minimum GWFA for the flood event in 2002 based on measured GWFA of Dresden (Grundwasserforschungszentrum, 2012), taking into account the high water level, according to the hydrograph of LfLUG / BfG as well as water levels of the Environmental Agency of the City of Dresden. Representation of the physical susceptibility "option one": The maximum value of susceptibility for the taxonomic code is displayed in the following map (Figure 56).

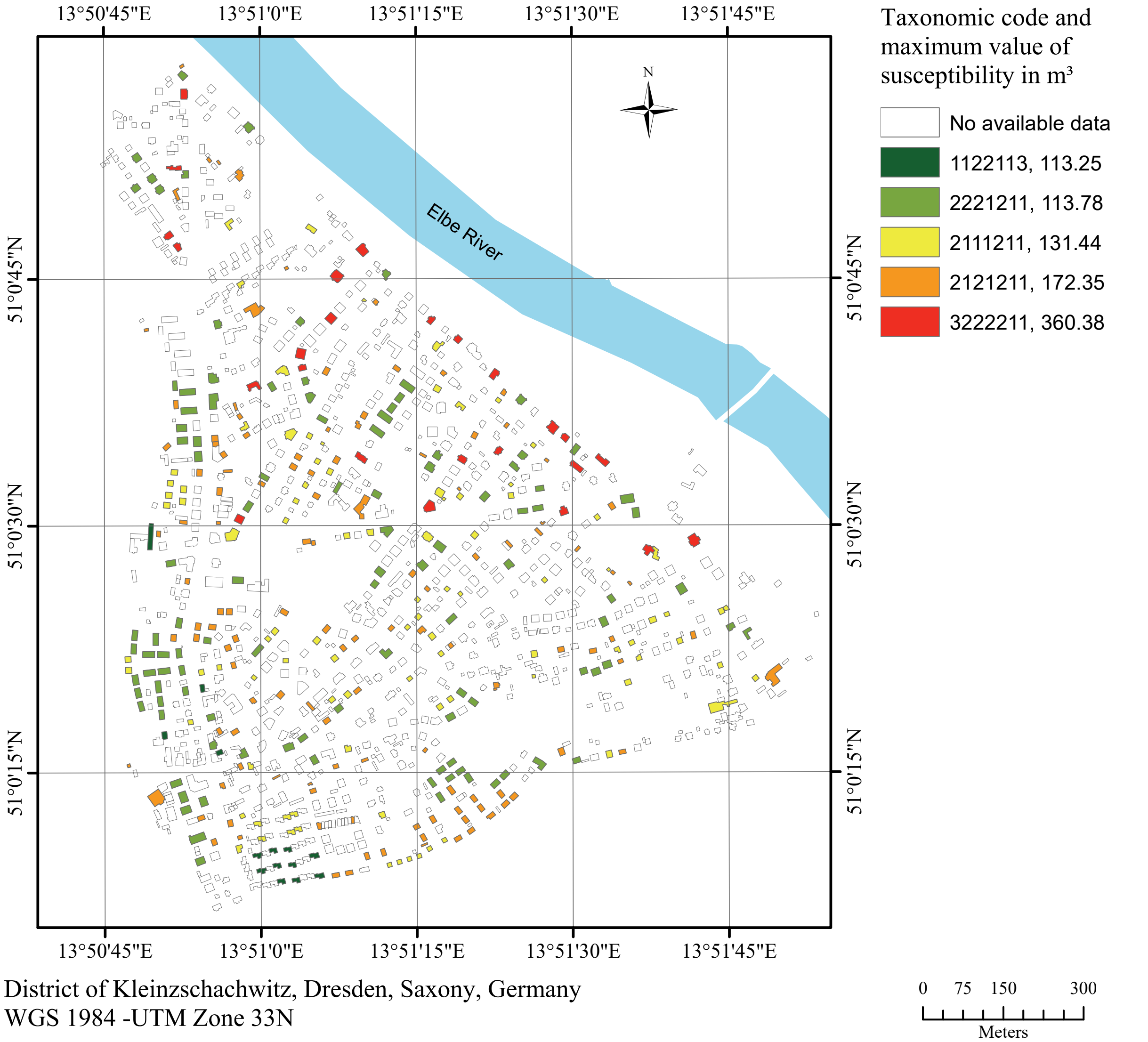

Figure 56: Maximum value of susceptibility for taxonomic code

Representation of the physical susceptibility "option two": The following map displays the susceptible volume in m³ for a water depth scenario.

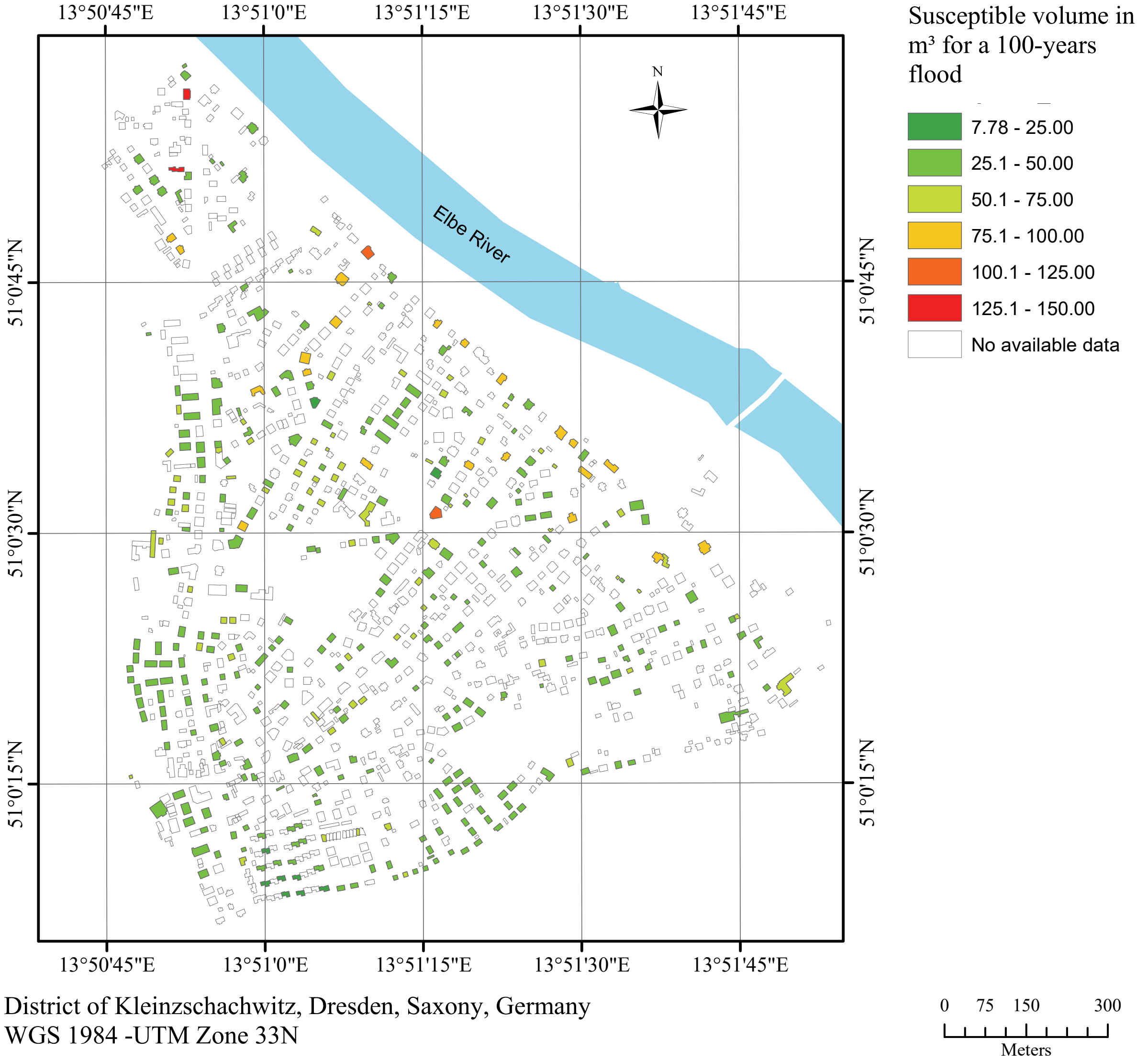

Figure 57: Susceptible volume in m³ for a 100-years flood "Kleinzschachwitz"

Representation of the physical susceptibility “option three”: The susceptible percentage volume by water depth is shown in relation to the building volume that was estimated for the taxonomic code.

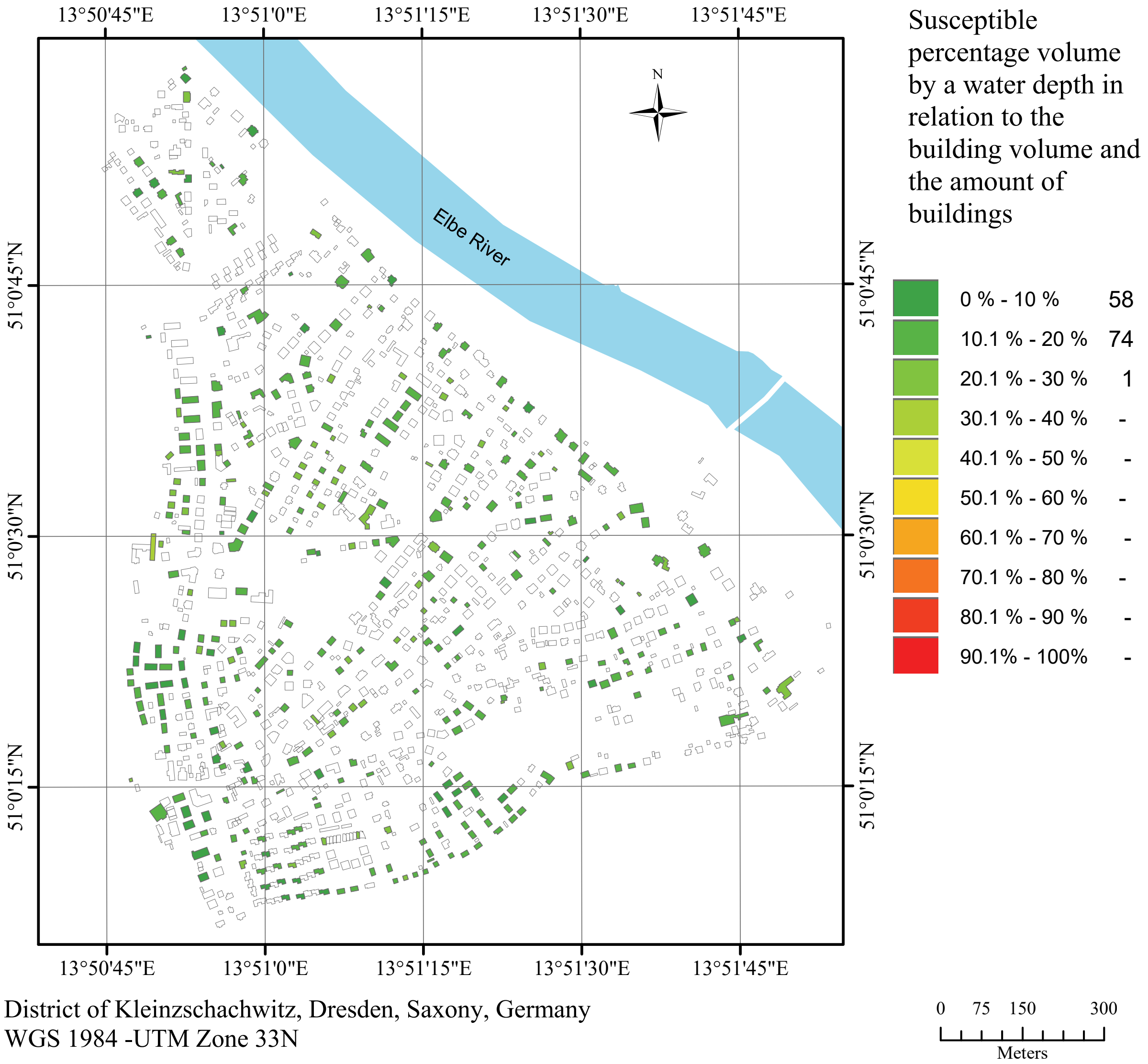

Figure 58: Maximum susceptible material volume in percentages for a 100-year flood for taxonomic code – “Kleinzschachwitz”

4.2 Pilot site "La Peña" – Cicuco, Colombia – Magdalena River

The Magdalena River is the principal river of Colombia with a catchment area of about 277.000 km²; it flows northward on about 1,540 kilometres (see Figure 59) through the western half of the country. Its basin has extensive networks and diverse climatic and biological characteristics. The Magdalena River catchment area corresponds to 22.5 % of the Colombian territory and "has been strongly impacted by population growth, increasing rates of erosion due to deforestation, land use of mining, agriculture, livestock and inputs of sediments and contaminants" (Restrepo, 2005). The United Nations World Water Assessment Program (2003) considers the Magdalena River as the most important Andean river in South America with a high rate of runoff, water yield as well a high population density (Desmond, 2009).

The pilot site covers two sectors located on the floodplain of the Magdalena River in the *Depresión Momposina* **La Peña** in **Cicuco** and **Barrio Sur** in **Magangué**, which are analysed with this methodology. *La Depresión Momposina* includes an important complex of wetlands with a vast quantity of inlets, rivers, swamps and marshes in the lowlands of the Colombian Caribbean. It has become the flooded region of the country due to the periodic flooding of four important rivers: Cauca, Magdalena, San Jorge and Cesar, which merge to form a wide interior delta with an area of more than 40,000 km^2 associated with a network of channels and swamps. The rainy season of the region is typically from April to May and October to November. The climate is very unsteady , as temperatures vary between 18 °C and 46 °C and an annual precipitation of 1207 mm (data collected at Magangué Baracoa Airport; average data collected over a period of 20 years between 1985 and 2005) (IDEAM, 2010a).

Figure 59: Geographic location of the pilot sites and the catchment area of Magdalena River in Colombia; source: Esri & IDEAM

Unfortunately, the region is also affected by a tremendous amount of natural hazards and social problems. It is one of the most threatened regions, facing pressure from agriculture, cattle ranching, urbanization, contamination by residual water and trash, hunting and uncontrolled fishing (Turbay et al., 2000). Most of the waste and sediments of the Andean region converge in the *Depresión Momposina*, from where they are transported to the river mouth into the Caribbean Sea.

The *Depresión Momposina* region is one of the most affected by floods caused by the Niña phenomenon (OCHA, 2010). The majority of people affected by floods during recent years live here and the number of flood events has increased the most. The flood 2010-2011 lasted around 6 months. Poverty is one of the major causes of deaths associated with natural disasters and physical and social vulnerabilities. Figure 60 shows the localisation of the two selected sectors in the country and gives an overview of the distance between the two sectors.

Figure 60: Visualisation of the municipalities selected for Colombia; source: Google Earth

4.2.1 Module 1: Building taxonomy – "La Peña"

4.2.1.1 Building extraction – "La Peña"

This subchapter provides a description of the process of building extraction, i.e. building outline, building height and building surface.

Data preparation "La Peña" – Cicuco:

The available data covers:

- Stereo Images of UltraCAM sensor with GSD 0.15 m with a resolution spectral of 3 bands (blue, green, red). Capture date: November 29^{th} 2007. Data level processing: Level 1A. The aero-photos have the approximate coordinates of the centre of the image (IGAC, 2007). The flight altitude was between 1710 m to 1721 m.a.s.l.
- A mosaic of the images (Figure 61a), a digital surface model (Figure 61b) with a spatial resolution of 2.0 m and a digital terrain model (Figure 61c) were generated using the INPHO software and the extension of MATCH-AT. The aerotriangulation gives a mean standard deviation of rotations of omega 9.6 [deg/1000], phi 9.3 [deg/1000], kappa 14.7 [deg/1000]; mean standard deviations of translations x: 0.167 [metre], y: 0.167 [metre] and z: 0.131 [metre], mean standard deviations of terrain points x: 0.254, y: 0.267 and z: 0.608.

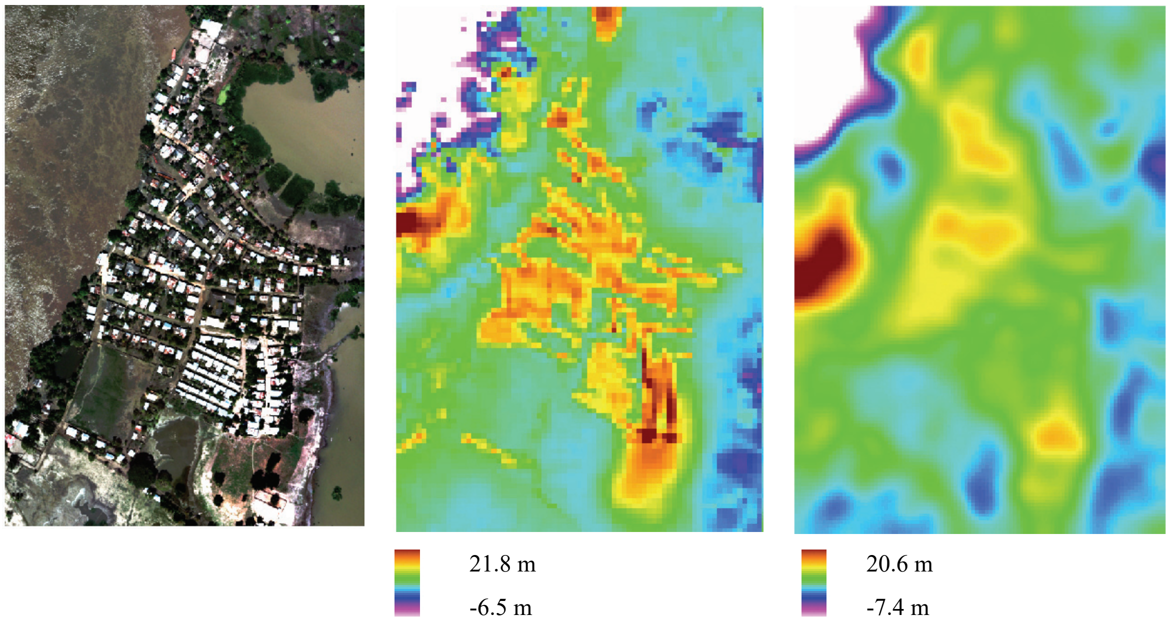

a. Mosaic of images b. Digital Surface Model c. Digital Terrain Model

Figure 61: Input data "La Peña"

Semantic definition for building outlines extraction:

The buildings in "La Peña" are detached residential buildings with two principal roof materials: one roof type with dark colours, which can be confused with the material used for the roads, and a second roof type with a high reflectance and corroded patches. The semantic definition for building regions (see section 3.1.1.2) is implemented using the tool developed in Matlab (Appendix D.3.1). The following figure shows the results of the extraction of the building regions:

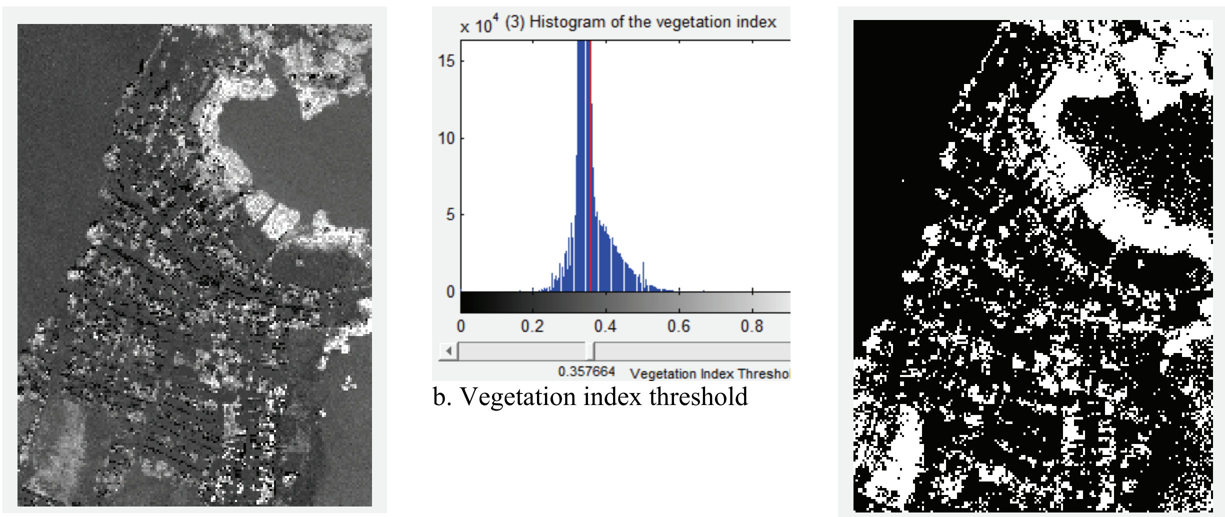

a. Vegetation index b. Vegetation index threshold c. Vegetation mask

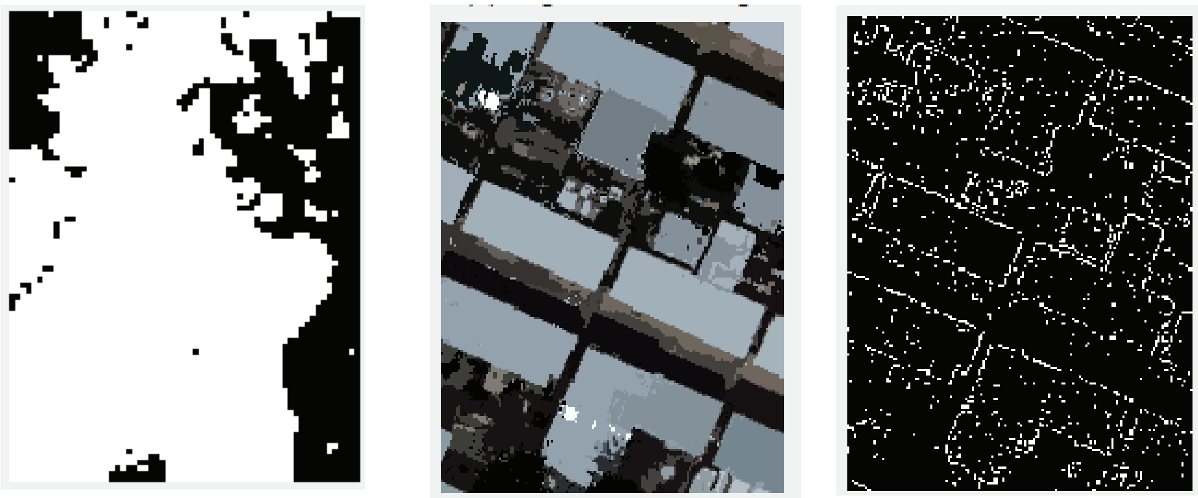

d. Terrain mask

e. Segmented buildings

f. Building borders

Figure 62: Implementation of the semantic definition of building regions for "La Peña" using Matlab

The building borders can be identified in Figure 62f, but there is too much noise and the building outlines are not clearly delimited; so more cues must be identified. Table 30 offers the description for recognising building cues in orthophotos for a better identification of the building characteristics in this sector.

Table 30: Recognising building cues – "La Peña"

Cues	**La Peña**
What are the predominant shapes of the building?	Square
Do buildings in the area normally have orthogonal sides?	Yes
Does the cover of the building normally consist of homogeneous roof material?	Rusty and corroded materials
Are the roofs covered or overlapped by vegetation?	Many buildings
Are the buildings higher than the surrounding trees?	No
Do the buildings have different spectral characteristics than the trees?	Some buildings can have spectral similarities with trees
Is there some open space that separates the buildings?	No pattern in the building distribution
How is the image contrast?	Medium
Does the image present occlusion of the buildings due to shadows?	Some buildings

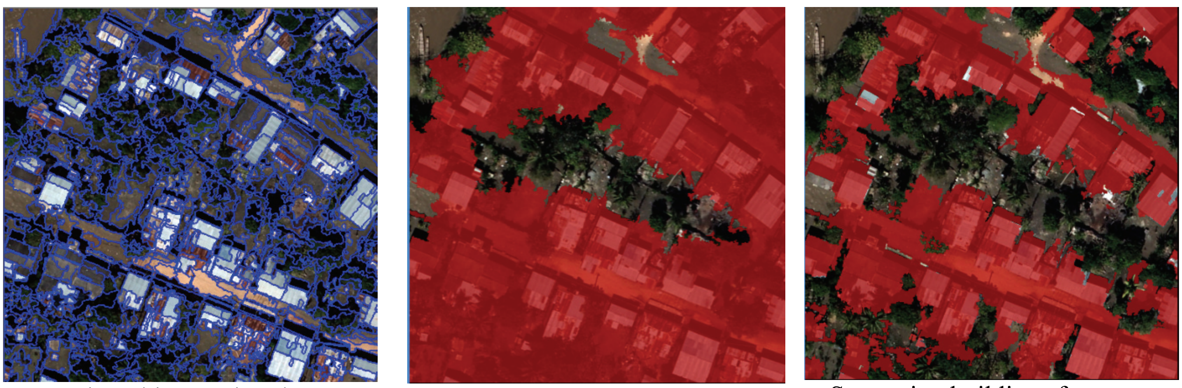

a. Creating objects using the multiresolution segmentation
Algorithm: multiresolution segmentation; scale parameter 25; shape 0.1; compactness 0.5

b. Classifying buildings based on elevation
Algorithm: assign class; class filter: none; threshold condition: mean DSM >= 15.6 m; class: building

c. Separating buildings from trees using the green index: (Green/Red+Green+Blue)
Algorithm: assign class; class filter: building; threshold condition: green index: >=0.3402

d. Separating buildings from trees using the green layer
Algorithm: assign class;
class filter: building;
threshold condition:
green layer: < 39;
use class: unclassified

e. Separating buildings from trees using the surrounding neighbour objects
Algorithm: assign class;
class filter: unclassified;
threshold condition:
border to building >= 0.47;
use class: building

f. Refining based on the size
Algorithm: merge and assign class;
class filter: building;
threshold condition:
area < 350 pxl;
use class: unclassified

Figure 63: Algorithm used for building extraction – "La Peña"

The sequence of algorithms of Figure 63 shown above helps to define some building regions, but not building outlines. Therefore, the process requires supplementary manual edition including the threshold conditions locating the process as semi-automatic.

Preserve the "relevant" pixels:

Since the above result does not meet the expected quality, additional cues are implemented using specialised algorithms of e-cognition in order to separate the buildings and preserve the relevant pixels of the buildings.

Building geometric characteristics:

The buildings detected through the previous step are converted in vectors and analysed in detail to identify their potential improvements, using algorithms such as simplification or merge calculation for the extraction of the building outline. Nevertheless, some inconsistencies could be detected and can be observed in Figure 64 a. – d.:

- The result should not be admitted because of the occlusion of the roof by tree shadows and the irregularity of the roof material; there is not an automatic algorithm for this detection.
- Although they are detected according to the algorithm, these polygons require a manual addition.
- Even if the process detects the outlines, there is a problem regarding the spectral and form characteristics of the roof and the surrounding.
- This building could be extracted using another level of segmentation, but the result clearly does not satisfy the requirements for a building typology.

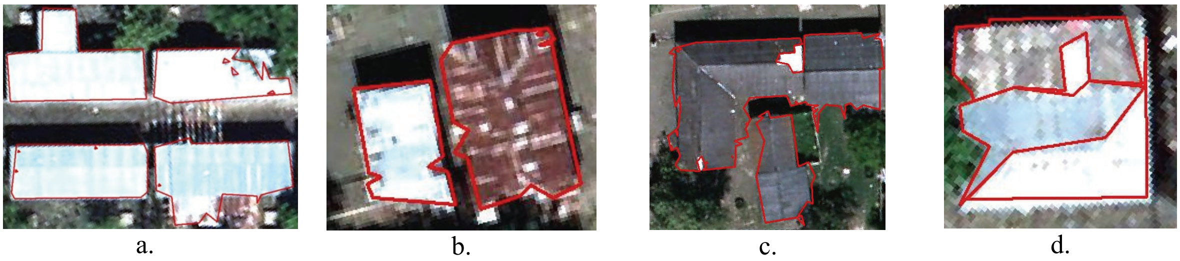

Figure 64: Examples of simplifying polygons using the Douglas-Peucker (1973) algorithm

Horizontal accuracy assessment (RMSE index):

The accuracy of the building outline extraction was calculated on the basis of reference polygons, which were manually delineated, and using the equations of RMSE vertices, area difference, perimeter difference and vertices difference (Song and Haithcoat, 2005). However, there are many inconsistencies and difficulties to get better results due to the low spatial resolution of DSM for this area with small buildings, the heterogeneity of the building materials and the occlusion of the buildings from trees and shadows. The statistics of the four criteria for measuring the accuracy are listed in Table 31.

Table 31: Accuracy evaluation of the building outline extraction – "La Peña"

	RMSE vertices	Area difference	Perimeter difference	Vertices difference
Minimal	1.65E-05	6.07E-11	3.02E-11	0
25^{th} percentile	0.932	0.075	0.074	1
Media	1.799	0.773	0.532	7
75^{th} percentile	*2.670*	*0.999*	*0.955*	*21*
Maximal	32.205	57.709	52.143	863

The polygons determined as "reliable" are those within the lower value to 75th percentile for the RMSE vertices, area difference, perimeter difference and vertices difference. From the 283 initially extracted polygons, only 124 fulfil the 75th percentile, which gives as result that **44 %** of the buildings from the extraction process can be used as input for the next step of the methodology.

Height extraction accuracy assessment:

The method by Flood (2004) was chosen for the assessment of height accuracy, assuming that the building heights in "La Peña" have a normal distribution because most of the buildings possess one storey. The number of checkpoints here does not reach 160 for the RMSE bounds at the 95 % confidence level required for computing the method by Aguilar Mills (2008). As a result, **2.05 metres** is the vertical accuracy at the 95 % confidence level using RMSE (z) x 1.9600. A further method for testing the accuracy of the height of the buildings was to measure the horizontal parallax compared to the height of reference buildings. The form for measuring the horizontal parallax is h = d * H' / r; where: h = building height, H' = flying height, d = length of the object from base to top and r = distance from the principal point of the image to the top of the object. As a result, this test gives an accuracy of 2.15 metres. These results indicate that the accuracy is far too low for building height extraction. However, as all of the buildings of "La Peña" have one storey, it will estimate that the height of the buildings does not exceed 3 metres.

4.2.1.2 Building taxonomic code – "La Peña"

Once the building outline is delineated from the orthophotos and the resolution of the DSM is accepted for the height extraction, the seven parameters are calculated using the tool

(Appendix D, part 3) for the calculation of a building taxonomic code. Initially, the categories for every parameter were taken into account according to the fuzzy sets of Table 4, but the preliminary result presented too many building types and shall be collapsed.

Then an exploratory statistical data analysis (histogram diagram, scatter diagram and the correlation matrix) was carried out in order to find trends and relations among the parameters. The histogram diagrams (blue columns in Figure 65) allow us to identify the minimum and maximum value for each parameter, and they help to define the inflection points for the range of categories. They also show that the parameters for this pilot site do not follow a normal distribution. The scatter diagram plots two parameters with points on a horizontal and a vertical axis and it attempts to show how much one variable can be affected by another.

The diagram of Figure 65 shows that the relation of the parameters is much sprawled. This means that all parameters are independent and have no correlation with other parameters. For instance, here the buildings are short with large and small sizes. In "Kleinzschachwitz" however, the buildings are tall and have large sizes.

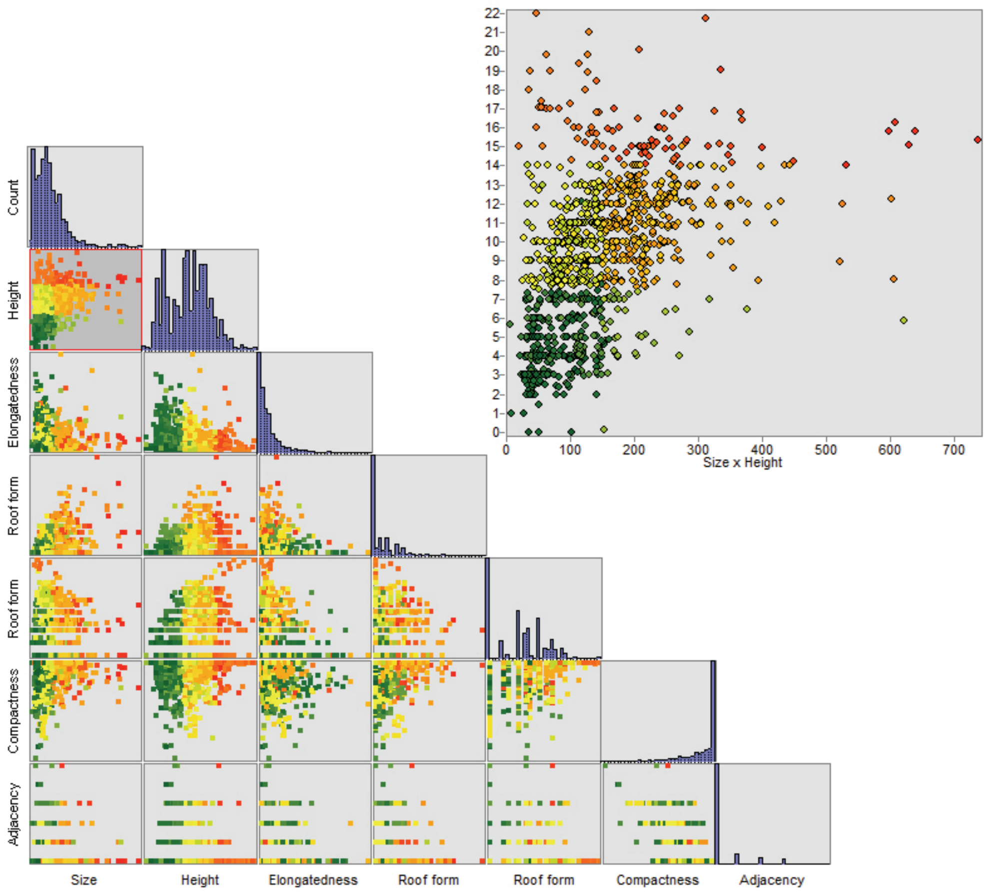

Figure 65: Scatter diagram for building parameters – "La Peña"

The correlation matrix (see Table 32) shows the numerical relation between the parameters. A moderate direct relation between size and height as well as adjacency and compactness is found. A relation between the other parameters is almost imperceptible. This means that all parameters are required for describing the principal relevant characteristics of a building. The correlation between two variables is high; one variable may be eliminated because it has already been explained by the other.

Table 32: Correlation matrix of the parameters of "La Peña"

	Adjacency	*Elongatedness*	*Compactness*	*Size*	*Height*	*Roof form*	*Roof slope*
Adjacency	1.000						
Elongatedness	0.142	1.000					
Compactness	0.519	0.334	1.000				
Size	-0.179	-0.021	-0.006	1.000			
Height	-0.166	0.075	0.071	0.430	1.000		
Roof form	0.061	-0.029	0.166	0.313	0.154	1.000	
Roof slope	0.029	0.125	0.087	0.194	0.204	0.120	1.000

On the basis of the exploratory data analysis and the guide described in section 3.1.2.5, the categories for the seven parameters are then arranged and reclassified as indicated in Table 33.

Table 33: Range of categories for parameters (Type 1) – "La Peña"

Parameter	**Code**	**Description**
Height	1	<= 7.5 m
	2	> 7.5 – 13 m
	3	>13 – 30 m
Footprint - Size	1	0 – 50 m²
	2	>150 – 500 m²
	3	>500 – 800 m²
	4	>800 – 1000 m²
Elongatedness (length/width ratio)	1	Square: 0.8 – 1.2
	2	Elongated rectangle:> 0.8 and < 1.2
Roof form	1	< = 12 vertices
	2	>12 vertices
Roof slope (Roof pitch)	1	<= 10 degrees
	2	>10 degrees
Index inversely compactness	1	> 66 %
	2	>33 % – 66 %
	3	<= 33 %
Adjacency	1	Single building
	2	Pair building or single building with annex building
	3	The corner building within a line of buildings
	4	Building within a line of buildings
	5	A building within a block
	6	The corner building within a block

4.2.1.3 Selection of representative buildings – "La Peña"

The next steps consist in identifying representative buildings on the basis of the frequency of the building types. Figure 65 shows the histogram for the building types and two possible thresholds for separating RB and NRB. The building types *'1111111'*, *'1111112'*, *'1121111'*, *'1121112'* and *'1121122'* have a higher frequency and can be selected as representative for the pilot site. The other building types have a very low frequency, which means that they are not 'typical'.

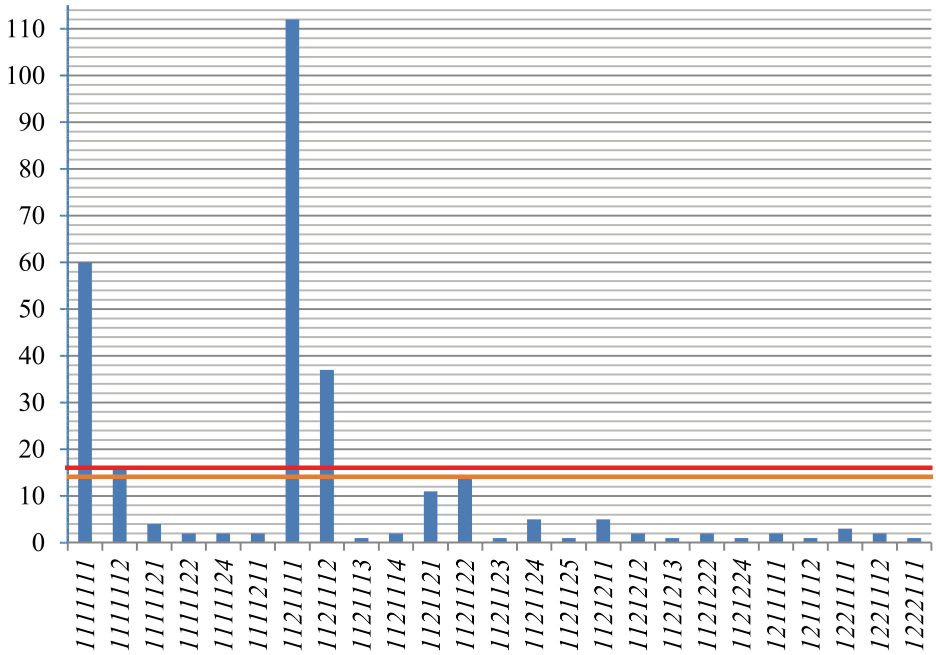

Figure 65: Histogram of the building types and thresholds for the selection of RB

Two tests are attempted here. One test consists in including the building type '*1121122'* as representative with a threshold of representativeness of 14 (orange line), and the other consists in excluding this building type selecting a threshold of representativeness of 16 (red line). Then, the non-representative buildings are clustered with the representative using the matrix of membership (21).

$$U_{R-nonR} = \begin{bmatrix} 1 & 1 & 1 & 1 & 1 & 1 & 1 \\ 0.5 & 0.5 & 0.5 & 0.5 & 0.5 & 0.5 & 0.5 \\ 0.3 & 0.3 & 0.3 & 0.3 & 0.3 & 0.3 & 0.3 \\ 0 & 0 & 0 & 0 & 0 & 0 & 0 \end{bmatrix} \quad (21)$$

Table 34 shows the results of the first test: 82 % (239/290) of the buildings are representative, 51 buildings are not representative, but grouped to the representative buildings, 45 buildings of them with a matching of 90 - 99.9 % and six with a matching of 80 - 89.9 %.

Table 34: Clustering of buildings – Option 1

Representative buildings	**100 %**	**90 – 99.9 %**	**80 – 89.9 %**	**Sum**
'1111111'	60	8		68
'1111112'	16	3	2	21
'1121111'	112	19	1	132
'1121112'	37	7	1	45
'1121122'	14	8	2	24
Sum	239	45	6	**290**

Figure 66 shows the histogram of representative buildings (blue columns) and the matching of the non-representative building.

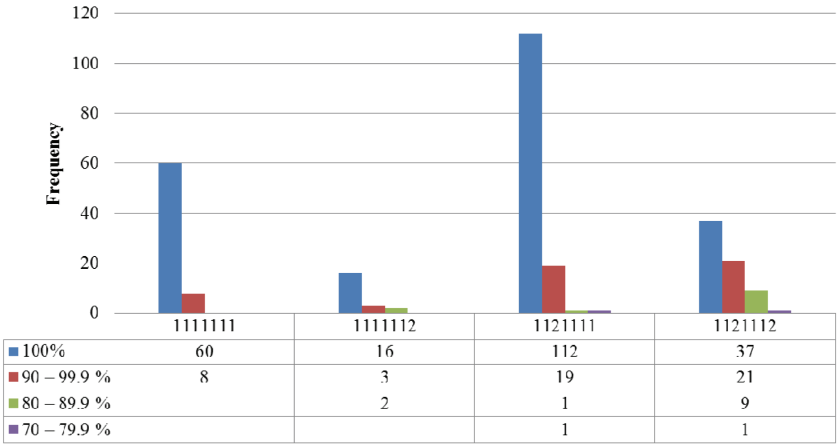

Figure 66: Histogram of clustering buildings – Option 1

Test 2 was carried out in order to exclude the building type *'1121122'* as the buildings of this type could be clustered to a building type with a higher frequency, since the 6th digit '2' describes the compactness and does not reflect any relevant pattern in the area. The result of this test gives four building types, which include 225 representative buildings. 65 non-representative buildings are clustered to the representatives (Table 35).

Table 35: Clustering of buildings – Option 2

Representative buildings	**100 %**	**90 – 99.9 %**	**80 – 89.9 %**	**70 – 79.9 %**	**Sum**
'1111111'	60	8			68
'1111112'	16	3	2		21
'1121111'	112	19	1	1	133
'1121112'	37	21	9	1	68
Sum	225	51	12	2	**290**

The buildings with the taxonomic code *'1121122'* are grouped to those with the taxonomic code *'1121112'* with a matching of 92.8 %. This shows that they are very similar. As a result, 290 buildings are classified in 25 building types, which in turn are clustered to four representative buildings. Figure 67 depicts the histogram of the non-representative buildings clustered to the representative buildings. There are two buildings with a matching lower than 80 %. These buildings are atypical and should be not grouped but assessed without clustering.

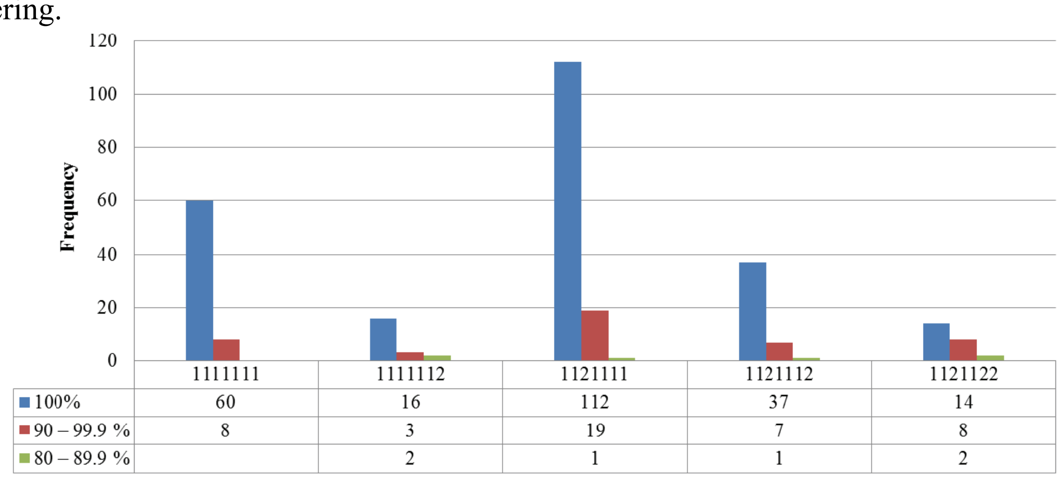

Figure 67: Histogram of clustering buildings – Option 2

25 taxonomic codes were generated as a result of the classification; the polygons with black edges may be regarded as representative buildings (see Figure 69).

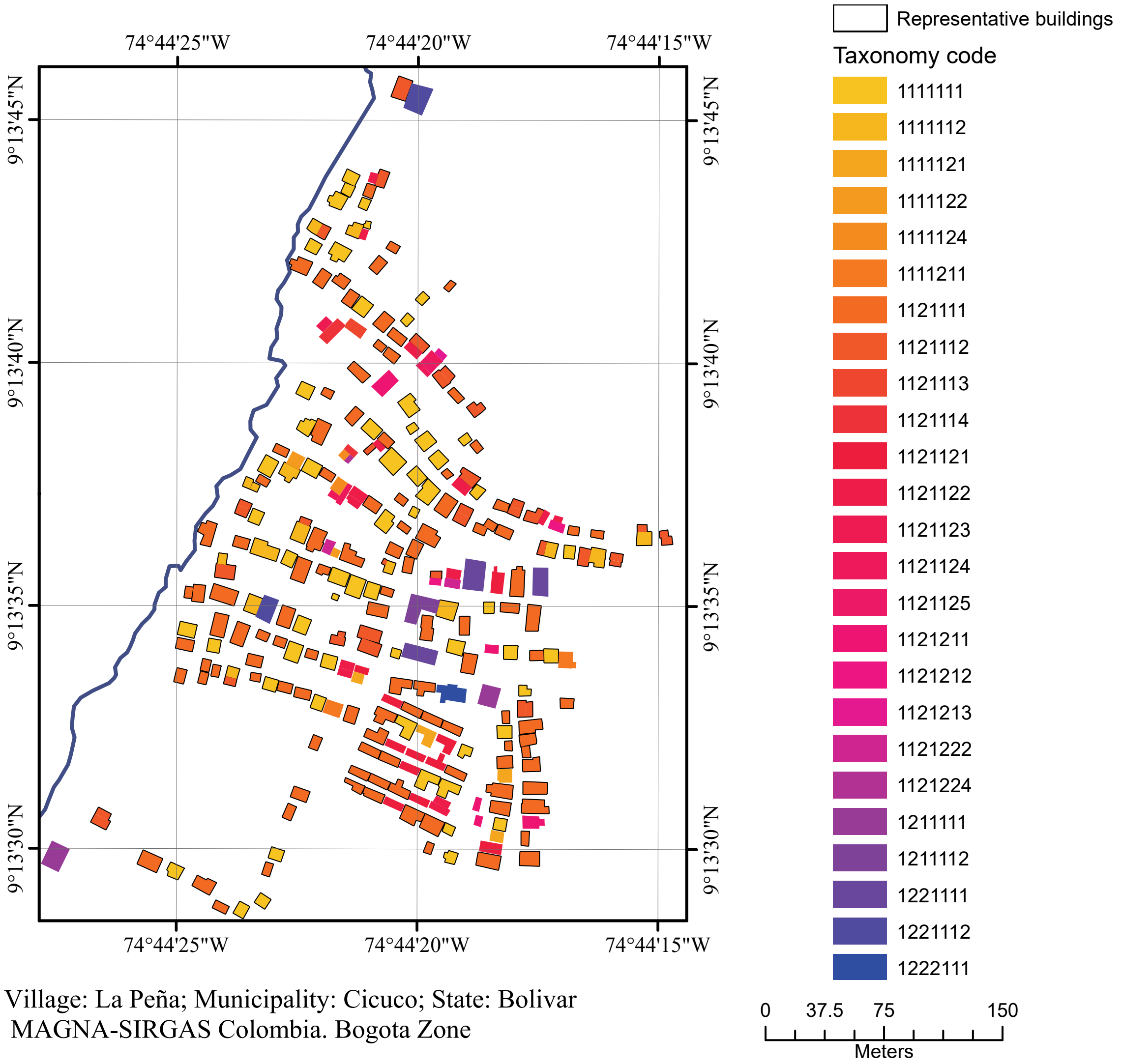

Figure 68: Building typology and representative buildings – "La Peña"

The following map shows the clustered building types and the buildings selected as samples using the stratified sampling method. This map is the basis for the survey and for the next step of the building susceptibility analysis.

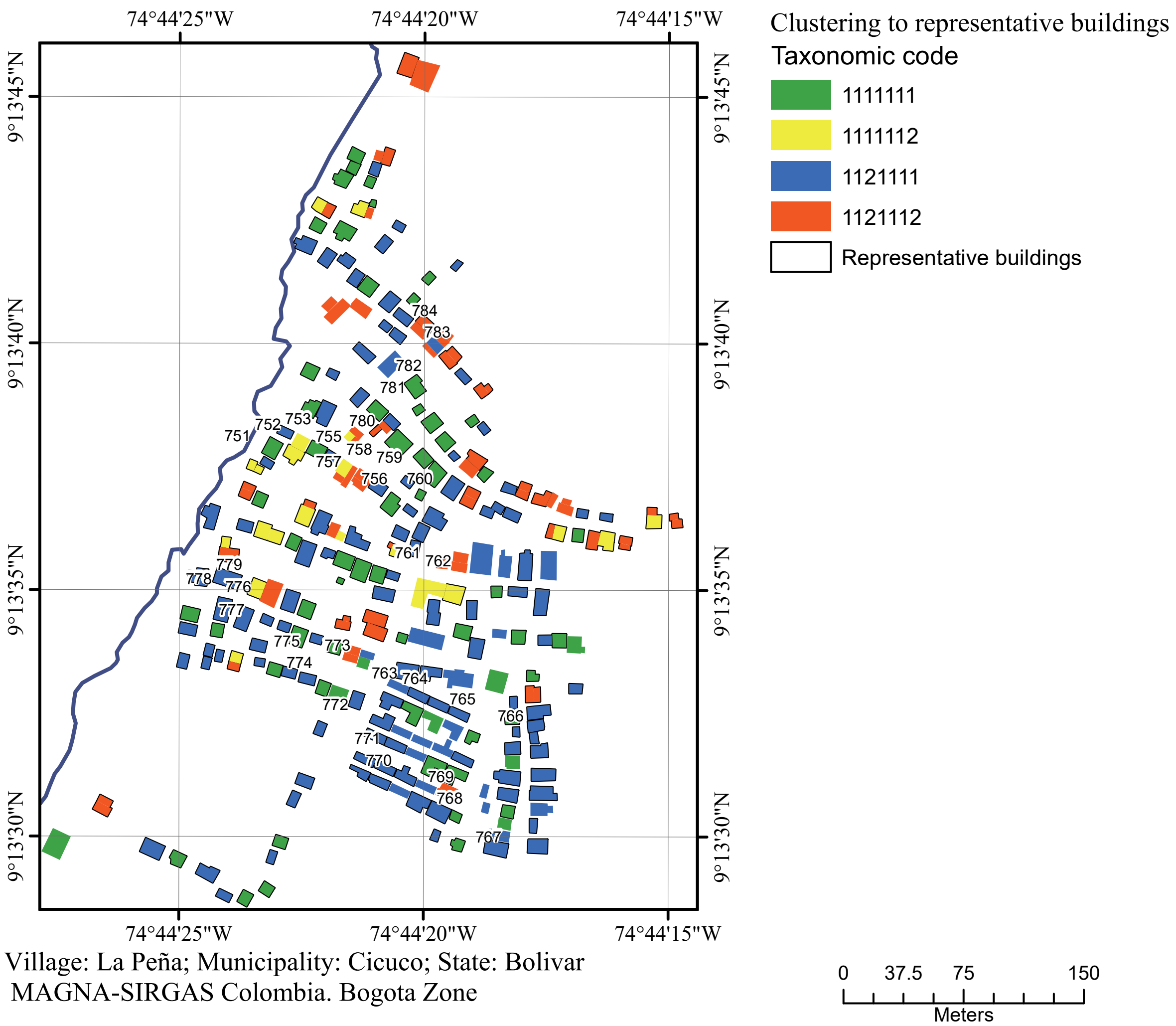

Figure 69: Clustering of buildings to the representative buildings for “La Peña”

Pictures of the selection of representative and non-representative buildings for the four taxonomic building types are displayed in the Figure 70.

'1111111' One storey, footprint size lower than 150 m², square form in the terrain, simple form, flat roof slope, open space area larger than 66 %, single building

Representative building: 754

Representative building: 760

Representative building: 774

Representative building: 781

Representative building: 777

Representative building: 773

'1111112' One storey, footprint size lower than 150 m², square form in the terrain, simple form, flat roof slope, open space area larger than 66 %, double buildings

Representative building: 753

Representative building: 756

Non-Representative building: 762
Matching 92%

Non-Representative building: 780
Matching 92%

'1121111' One storey, footprint size lower than 150 m², rectangle form in the terrain, roof form with less than 8 vertices, flat roof slope, open space area larger than 66 %, single buildings

Representative building: 755

Representative building: 761

Non-Representative building: 763
Matching 92%

Representative building: 776

Representative building: 775

Representative building: 779

'1121112' One storey, footprint size lower than 150 m², rectangle form in the terrain, roof form with less than 8 vertices, flat roof, open space area larger than 66 %, double buildings

Representative building: 759

Representative building: 783

Figure 70: Pictures of representative and non-representative buildings in "La Peña"

According to the seven parameters, the buildings differ in their elongatedness and their adjacency in one category. We have seen that adjacency does not play an important role in this pilot site because most buildings have one façade. Additionally, it can be observed that some buildings within the same group look very similar, while others are built with different materials. That is why the building taxonomy considers only parameters captured from the top and does not take into account the vertical view with its facades for the taxonomic code.

4.2.2 Module 2: Physical susceptibility of representative buildings – "La Peña"

According to section 3.2, the building susceptibility analysis consists in the collection of information about the building components, their material, their dimensions and the calculation of their material volume for the derivation of the depth-physical impact function.

Non-invasive methods have been carried out for assessing the structure and shell components of buildings, such as the presence of basements, external windows, external doors, façades, external walls, some roof characteristics, balconies, columns, beams and slabs. The components can be arranged according to their position above the ground and put in relation with water levels that could cover them. The digital appendix reports on the information collected for selected representative buildings.

Since there is no information on the material´s resistance available in Colombia, which could be used as reference for the susceptibility qualification, four experts were consulted and asked for information on resistance characteristics after flooding, general appearance, biological and chemical reaction characteristics and the natural drying speed of shell and structure components, which they collected while studying the damages of the 2010/2011 flood in the area.

The material's properties selected for the qualification are: *resistance characteristics after flooding* (e.g. shearing, flaking/scaling, bending, cracks, buckling, swollen, none), *general appearance* (discoloured surfaces, efflorescence due to crystalline deposits of alkaline salts, none), *biological and chemical reaction characteristics* (mould growth, spreading odours, contamination due to intern components, oxidation, none) and *natural drying speed* (in number of days); if available, technical standards and construction specifications based on ISO standards or codes from manufacturers' associations were included. Some typical building materials are depicted in Figure 71.


Walls: block of cement


Walls: cooked brick of clay (handmade)


External door: zinc sheets


Walls: fibreboard


Roof: eternit tiles


Floors: ground earth

Figure 71: Selection of typical building materials in "La Peña"

The first discussion by the experts on the susceptibility properties for the building materials in this settlement revealed different descriptions of the material´s alteration after the flood.

Therefore, after a second discussion, they found a consensus concerning the value for each attribute. The columns a, b and c show the qualification of the materials which has been computed for obtaining the fuzzy sets of susceptibility. Figure 73 shows the process for deriving the depth-physical impact function with the fuzzy set values calculated in the Table 36.

Table 36: Expert qualification of material properties in “La Peña”

Content	Material	Resistant characteristics after flooding	General appearance	Biological and chemical reaction characteristics	Natural drying speed	Y1	Y2	Y3	Y4	Y5	a	b	c
Foundation	Cyclopean foundation	None	Efflorescence due to crystalline deposits of alkaline salts	Mould growth	5	0.1	0.3	0.3	0.4	0.5	0.09	0.38	0.52
Background and columns	Pile foundation (tree trunk)	Buckling and flaking/scaling	Efflorescence due to crystalline deposits of alkaline salts	Mould growth	10	0.2	0.3	0.7	0.7	0.8	0.17	0.6	0.87
Floors	Ground (earth)	Cracks	Efflorescence due to crystalline deposits of alkaline salts	Spreading odours	11	0.5	0.7	0.7	0.8	0.8	0.42	0.79	0.81
Floors	Ceramic tablet	None	Discoloured surfaces	Mould growth	1	0.2	0.3	0.3	0.3	0.3	0.19	0.33	0.3
Walls	Zinc sheets	Bending	Discoloured surfaces	Contamination due to its intern components	1	0.5	0.7	0.7	0.7	0.8	0.44	0.75	0.82
Walls	Burned clay brick	Cracks	Efflorescence due to crystalline deposits of alkaline salts	Mould growth	4	0.2	0.2	0.2	0.3	0.3	0.19	0.26	0.31
Walls	Concrete block	Cracks	Efflorescence due to crystalline deposits of alkaline salts	Mould growth	4	0.2	0.4	0.2	0.2	0.3	0.19	0.28	0.3
Walls	Concrete block (air dried) 123	None	Efflorescence due to crystalline deposits of alkaline salts	Mould growth	4	0.6	0.7	0.7	0.8	0.8	0.51	0.79	0.81
Walls	Bahareque (bamboo and earth)	Flaking/scaling and cracks	Efflorescence due to crystalline deposits of alkaline salts	Mould growth and spreading odours	8	0.7	0.9	0.9	1	1	0.57	0.98	1
Walls	Limestone	Flaking/scaling	Discoloured surfaces	Mould growth	4	0.4	0.4	0.4	0.5	0.5	0.39	0.47	0.51
Walls	Limestone and brick type grille	Flaking/scaling	Discoloured surfaces	Mould growth	2	0.5	0.7	0.7	0.8	0.8	0.42	0.79	0.81
Walls	Wood	Buckling and bending	Efflorescence due to crystalline deposits of alkaline salts	Mould growth	5	0.8	0.9	0.9	1	1	0.66	0.99	1
Walls	Plaster	Cracks and flaking/scaling	Efflorescence due to crystalline deposits of alkaline salts	Mould growth	3	0.4	0.4	0.5	0.5	0.6	0.38	0.47	0.65
Doors	Aluminium frame with stainless steel or brass rollers	None	Discoloured surfaces	Contamination due to its intern components	1	0.4	0.4	0.4	0.5	0.5	0.39	0.47	0.51
Doors	Aluminium	None	Discoloured surfaces	Contamination due to its intern components	1	0.2	0.5	0.2	0.3	0.3	0.18	0.29	0.34
Doors	Zinc sheet	Bending and buckling	Discoloured surfaces	Contamination due to its intern components	1	0.7	0.7	0.7	0.8	0.8	0.67	0.76	0.82
Doors	Wood	Buckling	Efflorescence due to crystalline deposits of alkaline	Mould growth	5	0.9	0.9	0.9	1	1	0.87	0.95	1

Content	Material	Resistant characteristics after flooding	General appearance	Biological and chemical reaction characteristics	Natural drying speed	Y1	Y2	Y3	Y4	Y5	a	b	c
			salts										
Windows	Aluminium	None	Discoloured surfaces	Contamination due to its intern components	1	0.2	0.3	0.3	0.3	0.3	0.19	0.3	0.33
Windows	Metal	Bending	Discoloured surfaces	Contamination due to its intern components	1	0.2	0.3	0.3	0.3	0.3	0.19	0.3	0.3
Windows	Wood	Buckling	Efflorescence due to crystalline deposits of alkaline salts	Mould growth and spreading odours	5	0.8	0.9	0.9	1	1	0.66	0.99	1
Windows	Limestone brick type grille	Flaking/scaling	Efflorescence due to crystalline deposits of alkaline salts	Mould growth	2	0.7	0.7	0.7	0.8	0.8	0.67	0.76	0.82
Windows	Wood fretwork panels	Cracks	Efflorescence due to crystalline deposits of alkaline salts	Mould growth	6	0.5	0.5	0.5	0.6	0.7	0.49	0.54	0.79
Windows	Glass	None	Discoloured surfaces	Mould growth	1	0.2	0.2	0.2	0.3	0.3	0.19	0.26	0.31
Roof	Eternit asbestos cement corrugated	Cracks	Efflorescence due to crystalline deposits of alkaline salts	Mould growth	2	0.2	0.2	0.2	0.3	0.3	0.19	0.26	0.31
Roof	Natural fibres - straw	Cracks and shearing	Discoloured surfaces	Mould growth and spreading odours	5	0.7	0.7	0.8	0.8	0.9	0.67	0.75	1
Roof	Zinc sheet	Bending	Discoloured surfaces	Contamination due to its intern components	1	0.3	0.4	0.4	0.5	0.5	0.27	0.49	0.5
Roof trusses and beams	Wood	Buckling	Efflorescence due to crystalline deposits of alkaline salts	Mould growth	6	0.5	0.5	0.5	0.5	0.6	0.5	0.51	0.63
Roof trusses and beams	Aluminium	Bending	Discoloured surfaces	Contamination due to its intern components	1	0.2	0.3	0.3	0.3	0.3	0.19	0.33	0.3

	Lower height	Upper height	Material	Volume m³	Susceptibility a	Susceptible volume a	Susceptibility b	Susceptible volume b	Susceptibility c	Susceptible volume c
Roof	2.5	2.7	Eternit asbestos cement corrugated	2.92	0.19	0.56	0.26	0.76	0.31	0.91
Roof trusses and beams	2.5	2.6	Wood	10.33	0.5	5.17	0.51	5.27	0.63	6.51
Ceiling	2.3	2.4	Not existing		0	0.00	0	0.00	0	0.00
Beam	2.3	2.5	Not existing		0	0.00	0	0.00	0	0.00
External windows	1	2	Metal	0.16	0.19	0.03	0.3	0.05	0.3	0.05
External walls	0.4	2.5	Concrete block	15.12	0.19	2.87	0.28	4.23	0.3	4.54
External doors	0.4	2.4	Aluminium frame with stainless steel or brass rollers	0.05	0.39	0.02	0.47	1.00	0.51	0.02
Floor	0.4	0.5	Tile cement - Terrazo	9.75	0.19	1.85	0.3	2.92	0.55	5.36
Columns	0.4	2.5	Pile foundation (steel)	1.26	0.19	0.24	0.31	0.39	0.55	0.69
Foundation	-0.5	0.4	Cyclopean foundation	5.40	0.09	0.49	0.38	2.05	0.52	2.81
Total volume				45.00		11.22		16.68		20.89

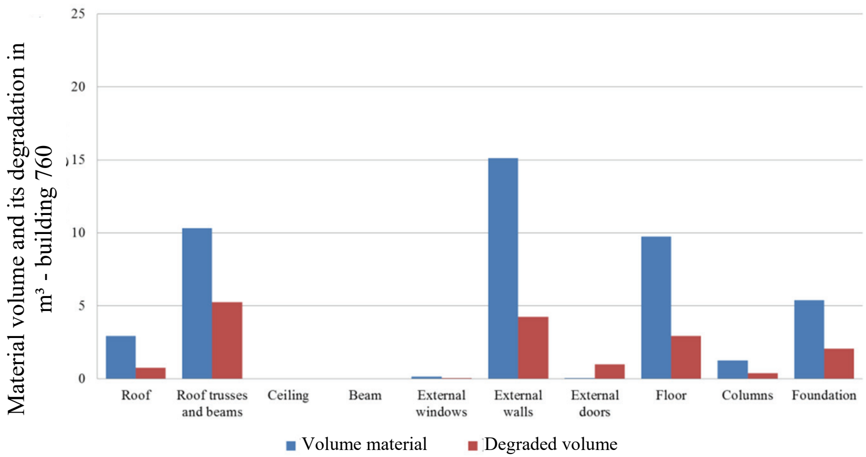

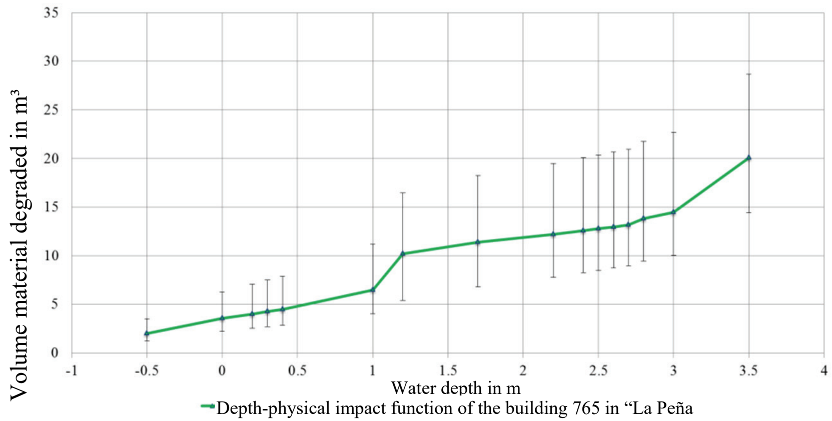

Figure 72: Process for the derivation of the depth-physical impact function

Figure 73 a. displays the depth-physical impact functions and Figure 73 b the median depth-physical impact function for buildings with the taxonomic code '*1111111'*.

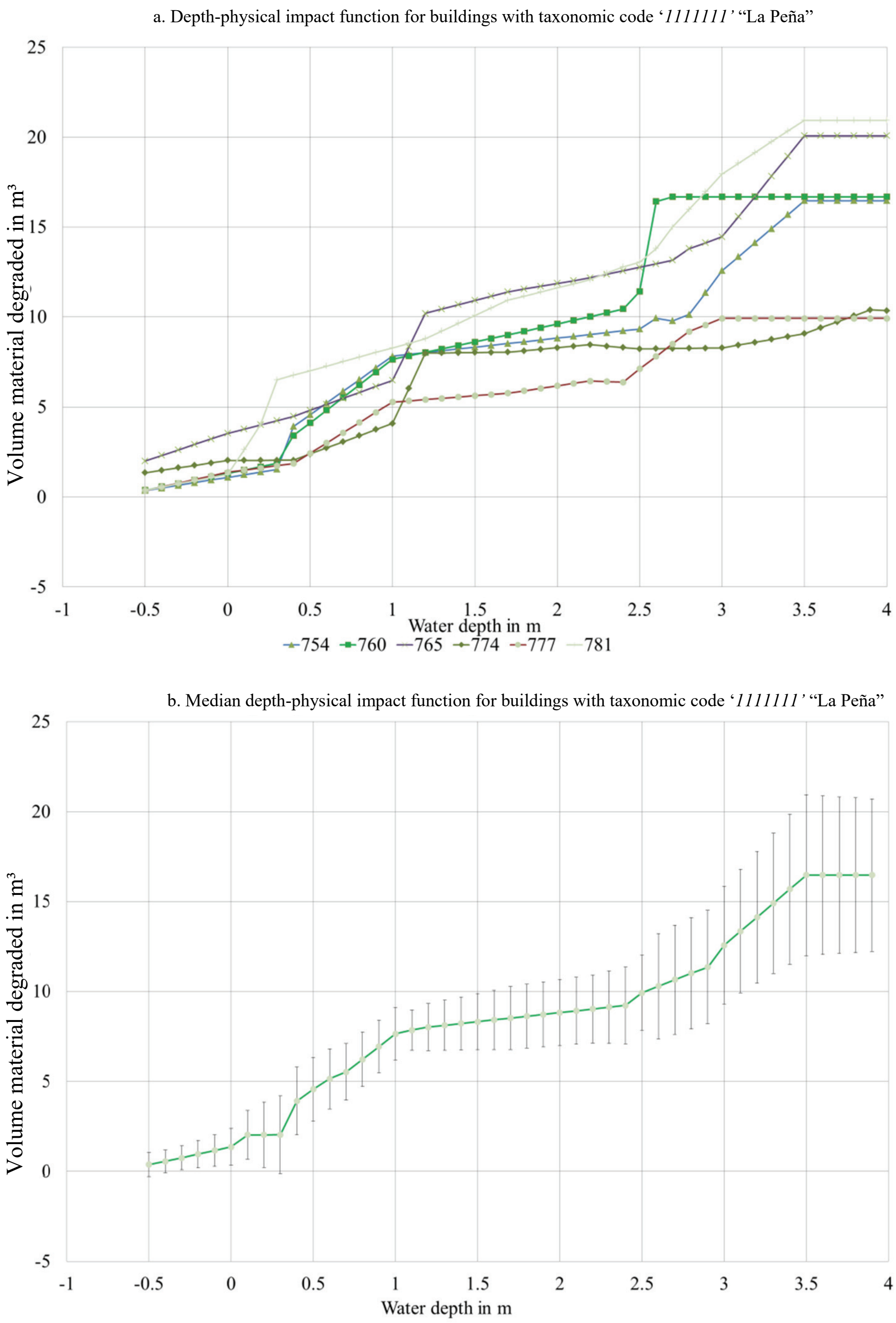

Figure 73: Median depth-physical impact function BT '*1111111*' – "La Peña"

Figure 74 a. shows the depth-physical impact function of buildings with the same taxonomic code. The numeration of the buildings corresponds to building displayed in Figure 70. Figure 74 b shows a broad range of uncertainty of the median depth-physical impact functions. Figure 75 a. displays the same depth-physical impact function except of building 773 (see Figure 70) that shows a different behaviour and increases the deviation standard. Figure 76 b. displays the accepted mean depth-physical impact function for the taxonomic building code '*1121111'*.

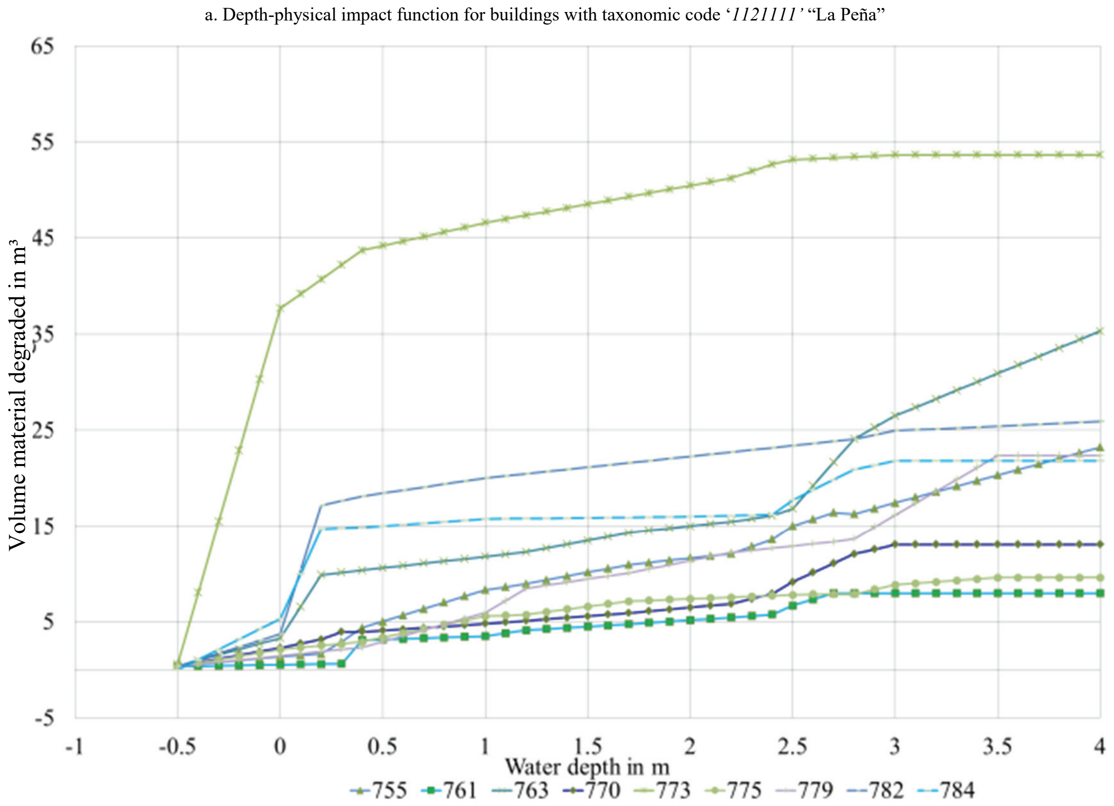

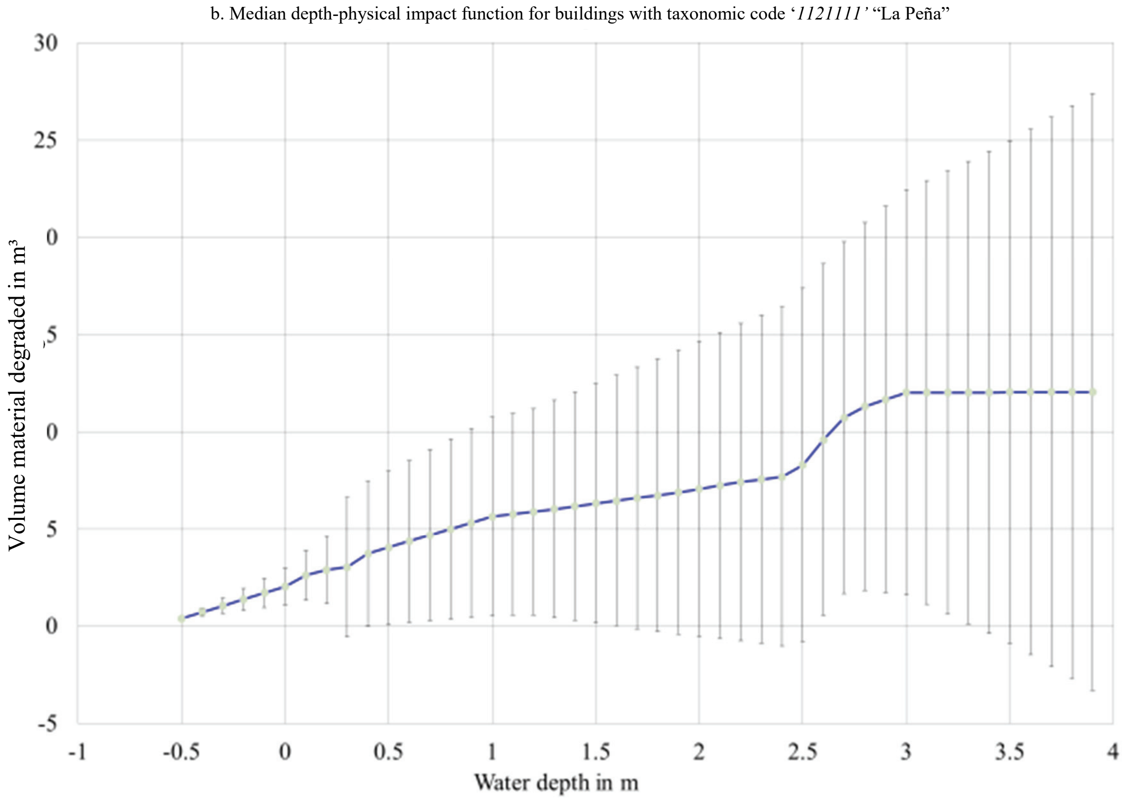

Figure 74: Derivation of the depth-physical impact function *'1111112'* with range of susceptibility

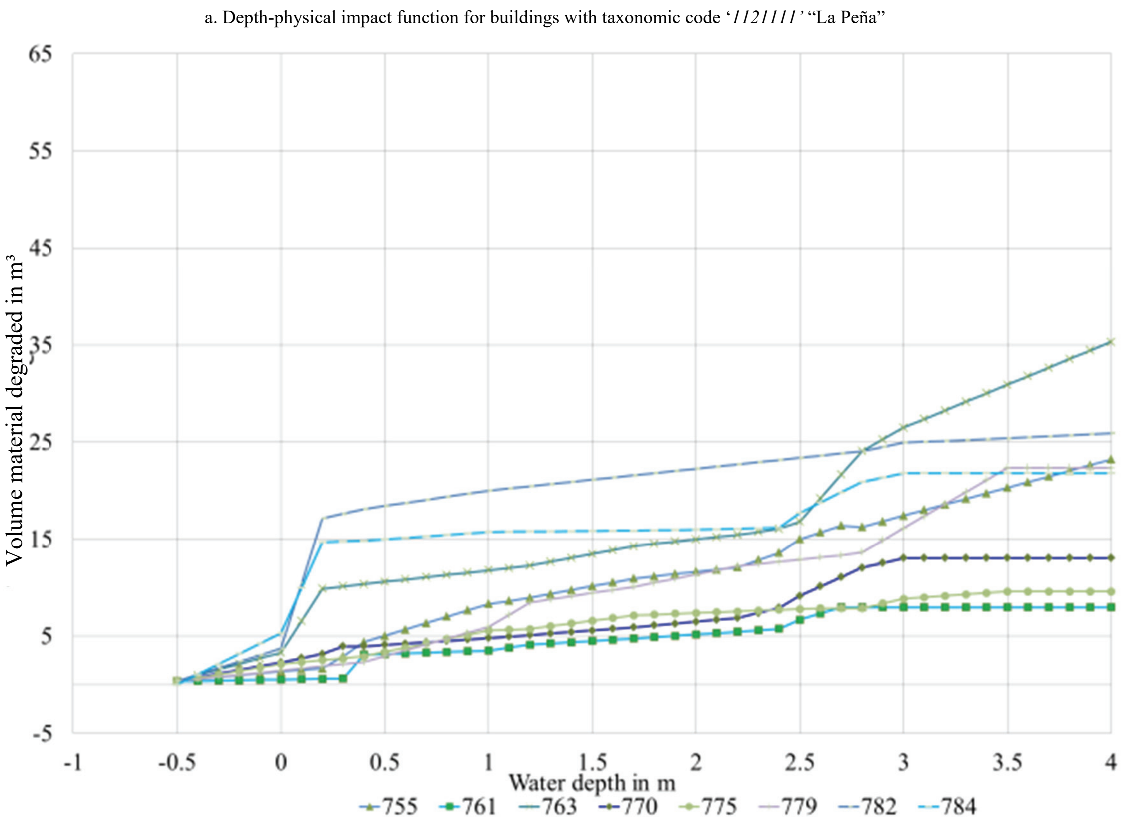

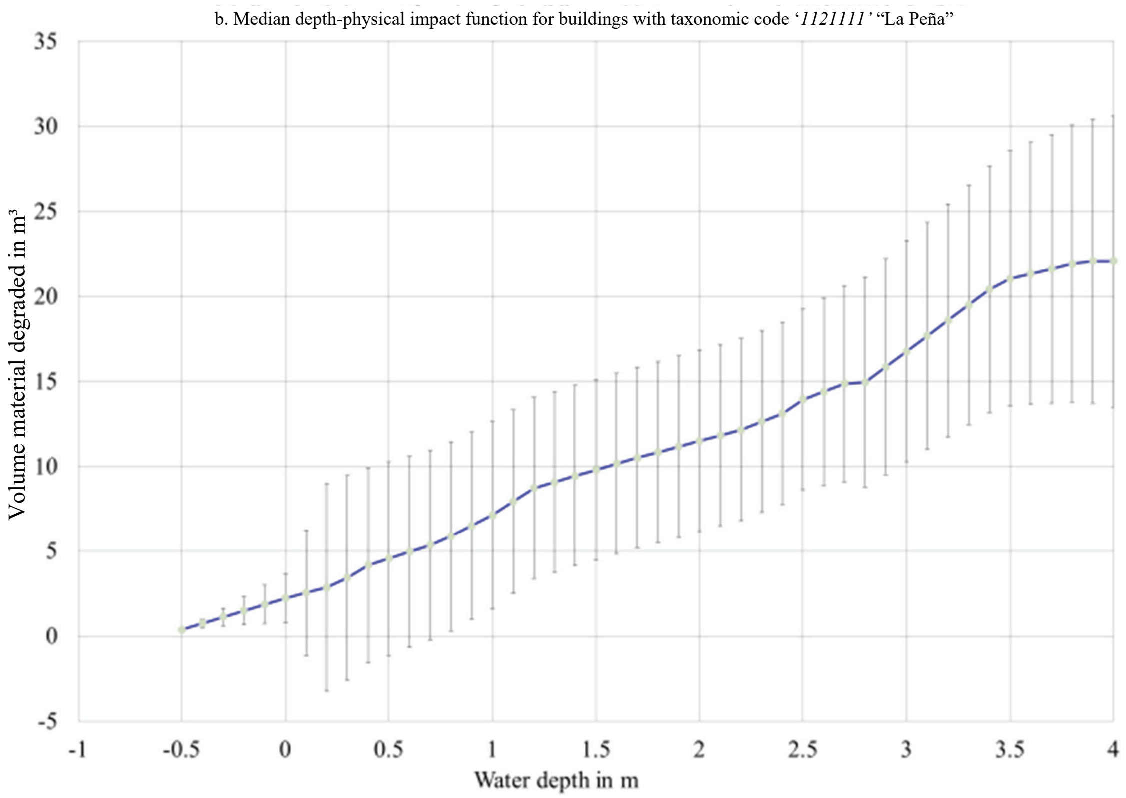

Figure 75: Derivation of the depth-physical impact function '*1121111*' with range of susceptibility

4.2.3 Module 3: Technological integration– "La Peña"

This section shows the process for combining the results of the previous modules. Figure 76 shows the input data required for the calculation of a physical flood susceptibility map.

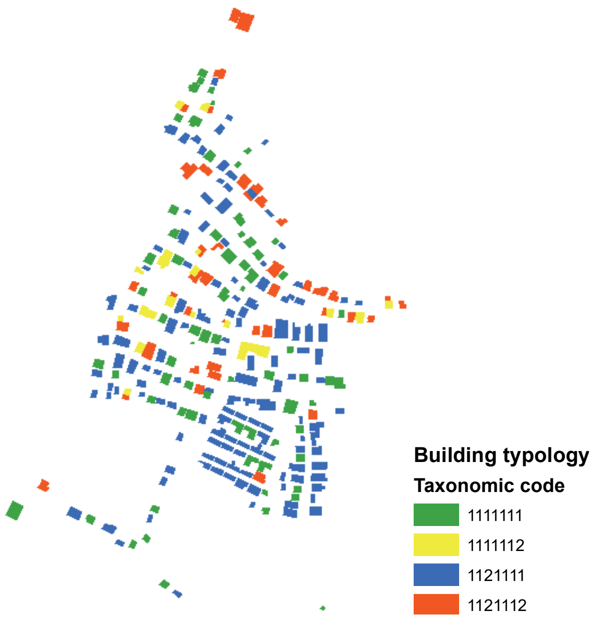

a. Building typology (taxonomic code)

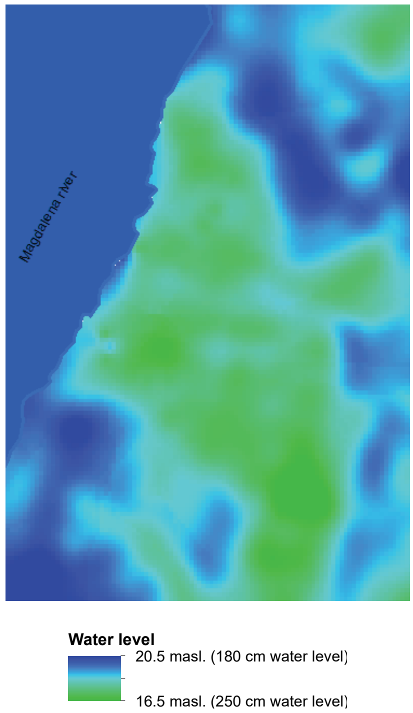

b. Artificial water depth in cm, 100-years flood (see Appendix H)

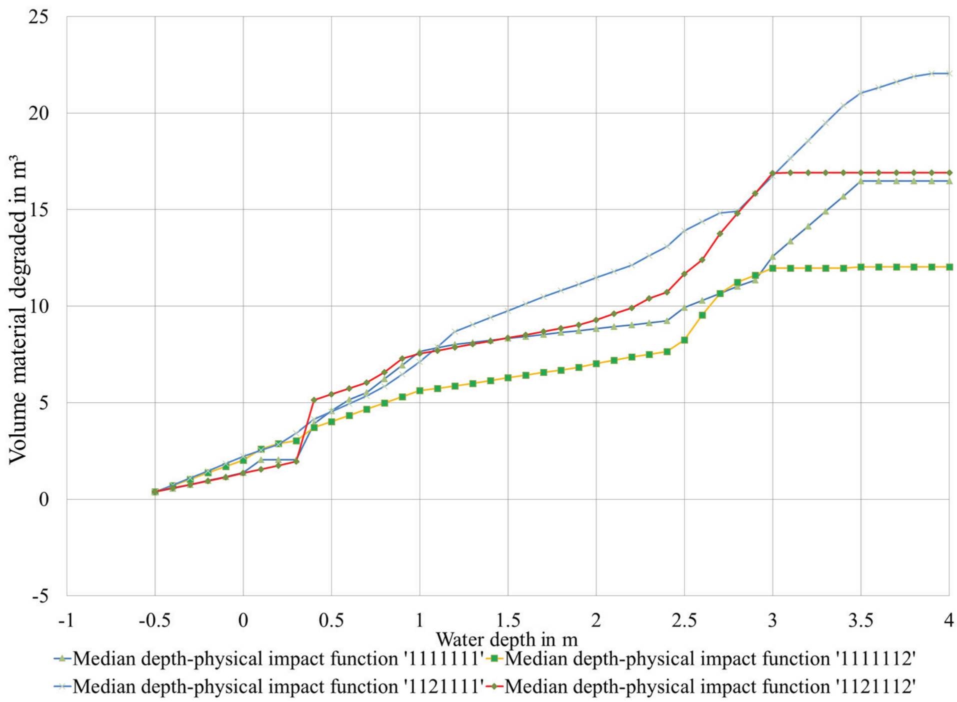

c. Median depth-physical impact functions in "La Peña"

Figure 76: Input data for the calculation of a physical flood susceptibility map – "La Peña"

Representation of the physical susceptibility "option one": The maximum susceptibility value for a taxonomic code is displayed in the following map.

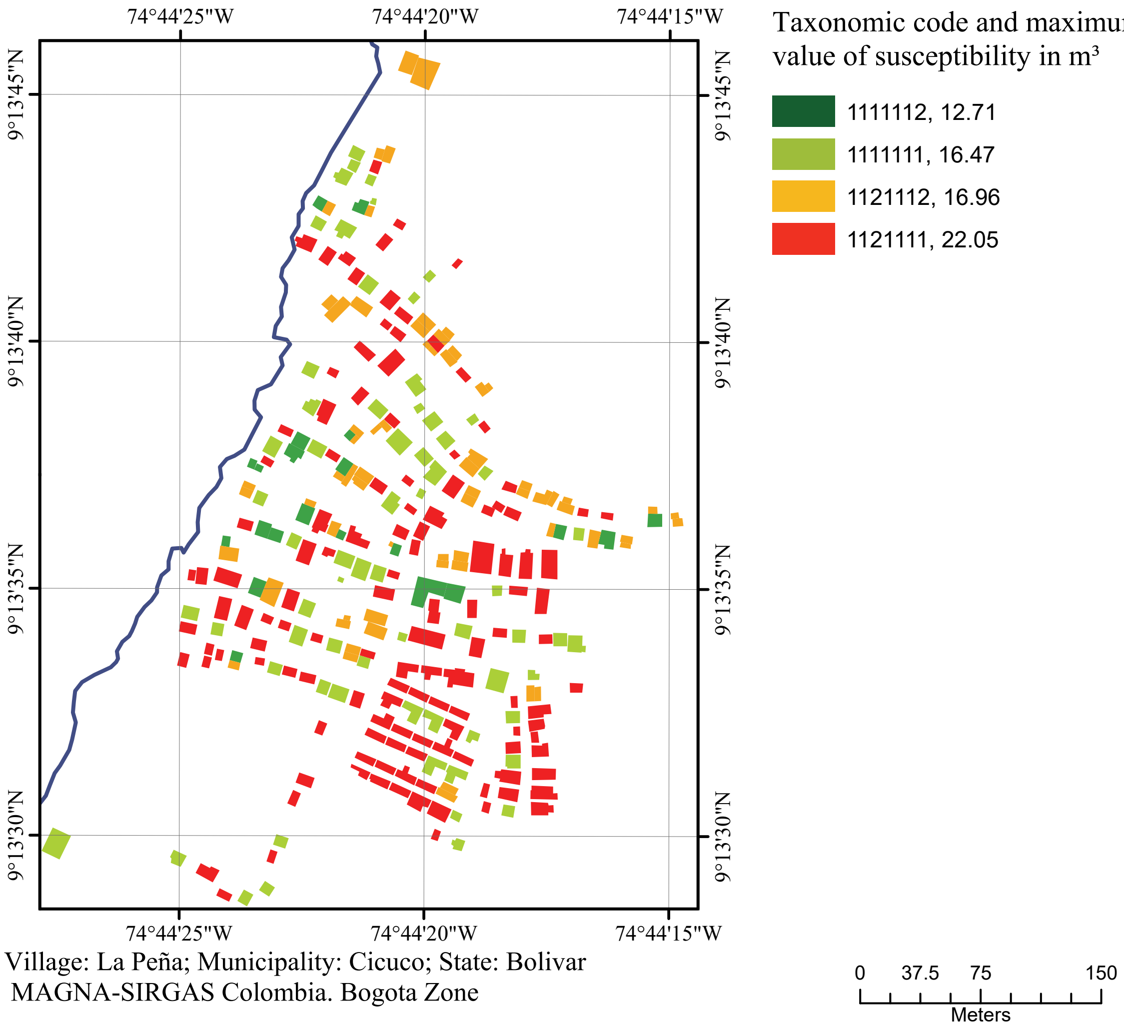

Figure 77: Maximum susceptible material volume in m³ for a taxonomic code – "La Peña"

Representation of the physical susceptibility “option two”: The following map displays the susceptible volume in m³ for a water depth scenario. The inundation model for a100-year flood is estimated using the depicted process in Appendix H.

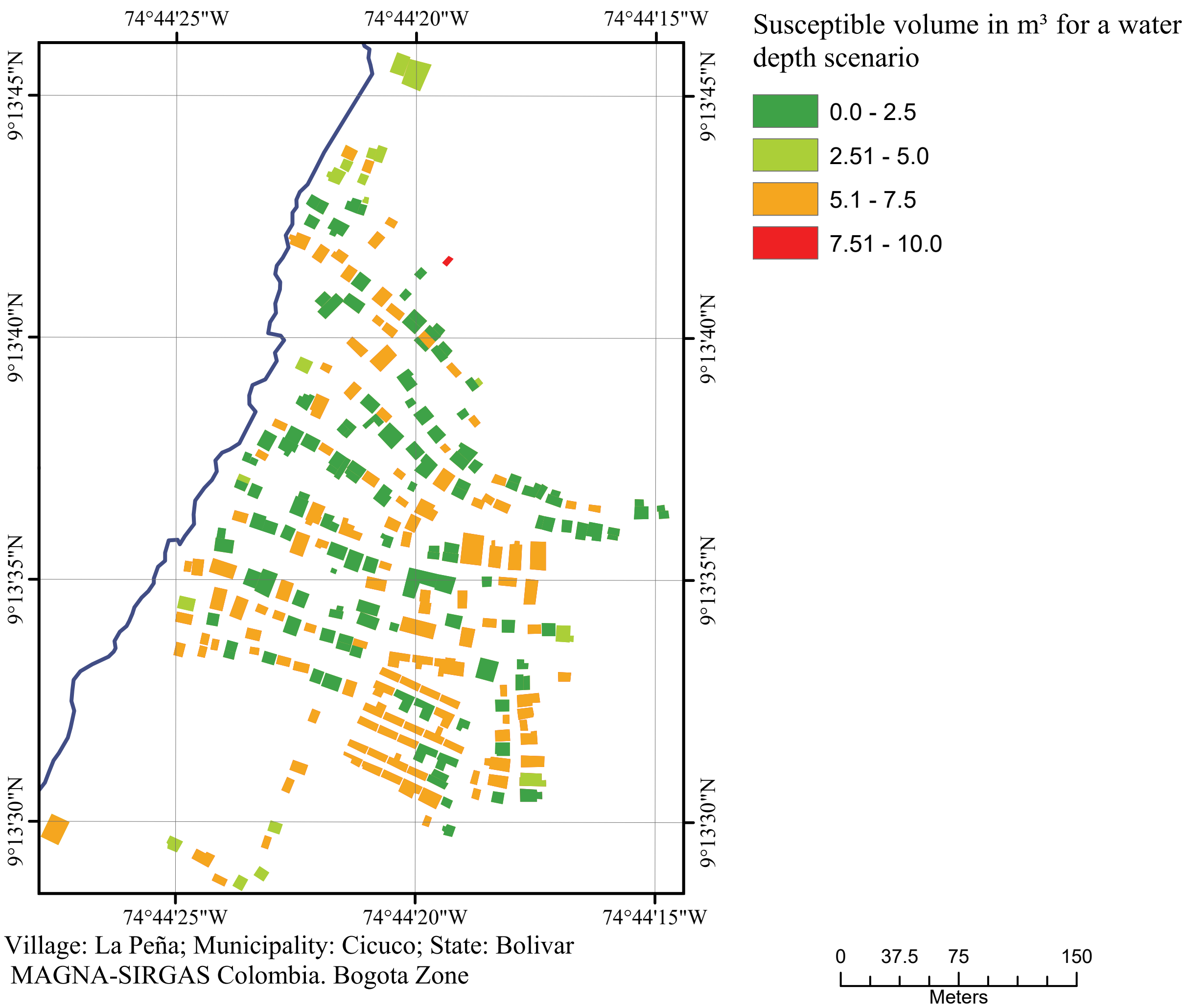

Figure 78: Susceptible volume in m³ for a water depth – “La Peña”

Representation of the physical susceptibility “option three”: The following map shows the susceptible percentage volume by a 100-year flood (see Figure 76 b.) in relation to the building volume that was estimated for a taxonomic code.

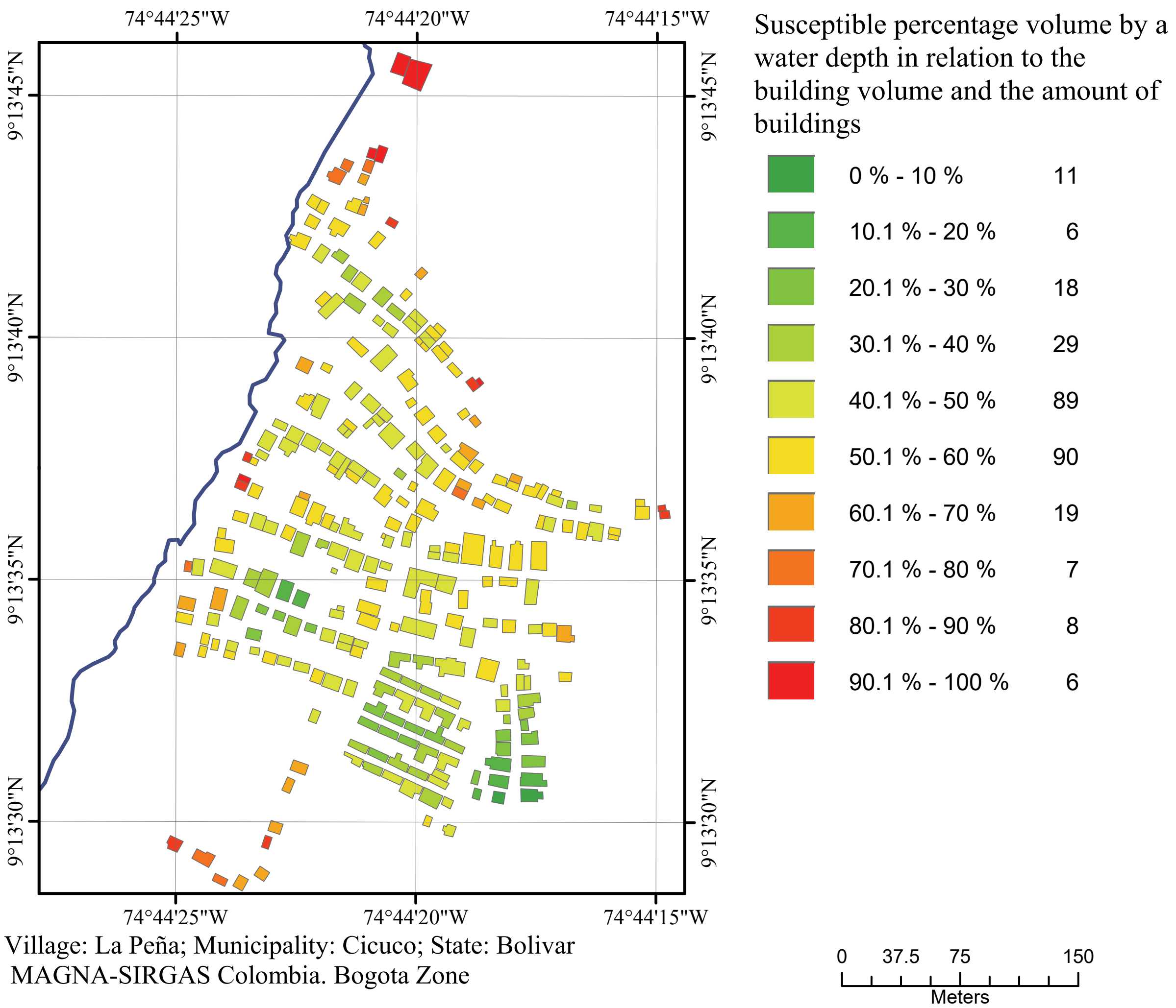

Figure 79: Maximum susceptible material volume in % for a taxonomic code – “La Peña”

4.3 Pilot site "Barrio Sur" – Magangué, Colombia – Magdalena River

Below, the tests of the methods for the three modules with the data of Barrio Sur are presented:

4.3.1 Module 1: Building taxonomy – "Barrio Sur"

The buildings in "Barrio Sur" are buildings with 1, 2 or 3 storeys, mixing residential, commercial and small industry uses.

4.3.1.1 Building extraction – "Barrio Sur"

Data preparation "Barrio Sur":

The available data are:

- UltraCAM photos with 0.15 m of resolution and 3 bands of spectral resolution, donated by IGAC, captured on 29 November 2007 with a flight altitude of 1710.13 m.a.s.l. (See Figure 80) a.)
- Aerial photos sensor RC-30 flight C-2749 captured on 03 February 2005 by IGAC, scanned at 15 Microns.

  The digital surface model was generated from scanned aerial photos (Figure 80 b.), taking as control points the orthoimage of UltraCam, obtaining a resolution of 3 m (Figure 80 c.). The derivation of a better DSM requires the inclusion of height control points, which need reliable and accurate position measurements. As these stereo images were captured in 2005 and since then new buildings or higher storeys at the top of some buildings have been constructed, the enhancement of the DSM requires the survey of a considerable amount of height control points. This survey was not carried out because of lack of security conditions in the area. Therefore, it was decided to verify the amount of storeys of the buildings instead of their height.

a. UltraCam Image b. RC-30 orthophoto c. DSM derived by orthophotos

Figure 80: Input data "Barrio Sur" for the building extraction

The identification of cues for the building outline extraction was carried out for the sector of "Barrio Sur" (Table 37).

Table 37: Cues for the semantic definition of the building extraction for "Barrio Sur"

Cues	Barrio Sur
What are the predominant shapes of the building?	Square and rectangle
Do buildings in the area normally have orthogonal sides?	Yes
Does the cover of the building normally have homogeneous roof materials?	A building may have different roof materials
Are the building roofs covered or overlapped by vegetation?	Some buildings
Are the buildings higher than the surrounding trees?	Some buildings
Do the buildings have different spectral characteristics than the trees?	Yes
Is the floodplain area quite flat?	Yes
Is there some open space that separates the buildings?	Not
How is the image contrast?	Medium
Does the image present occlusion of the buildings due to shadows?	Yes, very occluded

Nevertheless, the segmentation (Figure 81 a.) allows to differentiate fragments of roof materials, helping to delineate the buildings while the terrain mask (Figure 81 b.) infers the process adversely due to the outdated DSM. Moreover, the high density of the buildings, the high reflectance of zinc roofs and the presence of shadows handicap a semi-automatic extraction based on the semantic definitions. Therefore, the process was aborted and the decision taken to delineate building outlines manually.

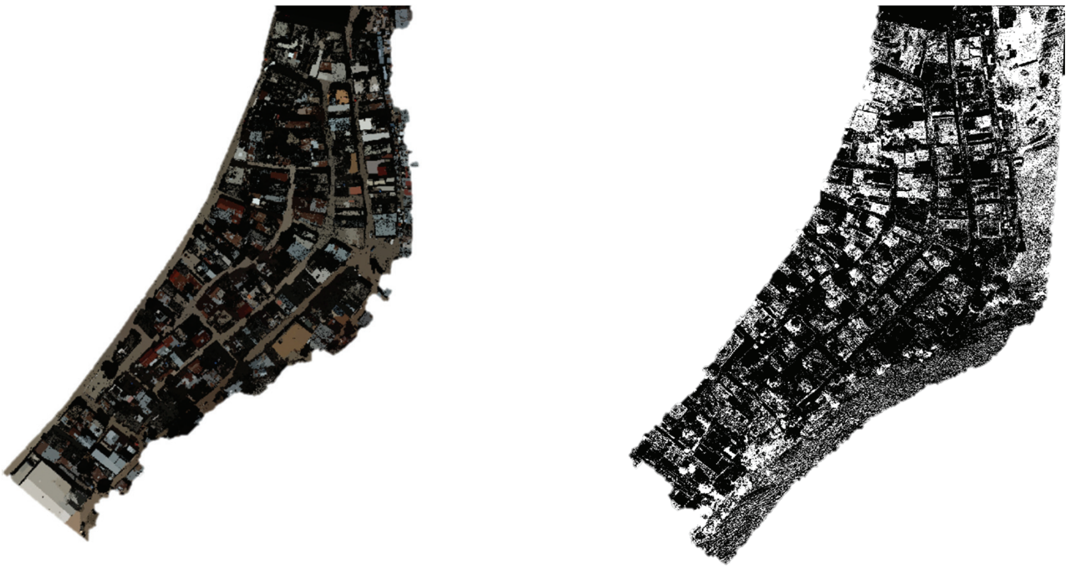

a. Segmentation b. Terrain mask

Figure 81: Implementation of the semantic definition of building regions in "Barrio Sur"

4.3.1.2 Building taxonomic code – "Barrio Sur"

Notwithstanding, the DSM does not have the quality for implementing building outline extraction techniques, but for the extraction of the parameter of building height, the DSM gives approximately values. The seven parameters are then calculated automatically using the Python tool of ArcGIS and the scatter diagram is displayed (see Figure 82) to find the correlation between the variables and to identify signals for the definition of the category ranges.

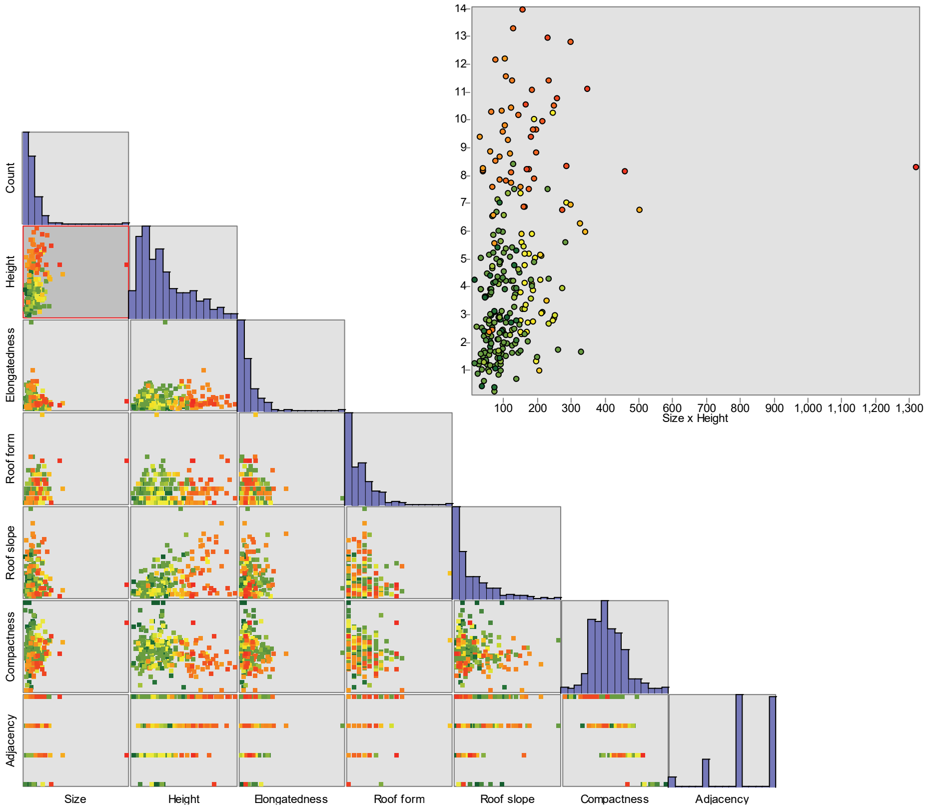

Figure 82: Scatter diagram parameters ‘Barrio Sur’

Table 38 shows the categories defined for this pilot site. Due to the density of the buildings in the area, the categories for the adjacency parameter are established with four classes according to the fenestration classification (see Table 3). The intervals of the other parameters are the same as intervals of the classification of “La Peña”.

Table 38: Range of categories for parameters (Type 2) – “Barrio Sur”

Parameter	Code	Description
Building height	1	<= 7.5 m
	2	> 7.5 – 13 m
	3	>13 – 30 m
Footprint - Size	1	0 – 50 m²
	2	>150 – 500 m²
	3	>500 – 800 m²
	4	>800 – 1000 m²
Elongatedness (length/width ratio)	1	Square: 0.8 – 1.2
	2	Elongated rectangle:> 0.8 and < 1.2
Roof form	1	< = 12 vertices
	2	>12 vertices
Roof slope (Roof pitch)	1	<= 10 degrees
	2	>10 degrees
Index inversely compactness	1	> 66 %
	2	> 33 – 66 %
	3	<= 33 %
Adjacency	1	All sides exposed to open space
	2	At least three sides exposed to open space
	3	Two sides exposed to open space
	4	One side exposed to open space

Figure 83 shows as a result the 260 building that are classified in 77 building types. These are too many building types for a small area, reflecting that the buildings have a variety of building structures and they do not follow a standard or similar pattern and/or they were constructed without any defined regulation.

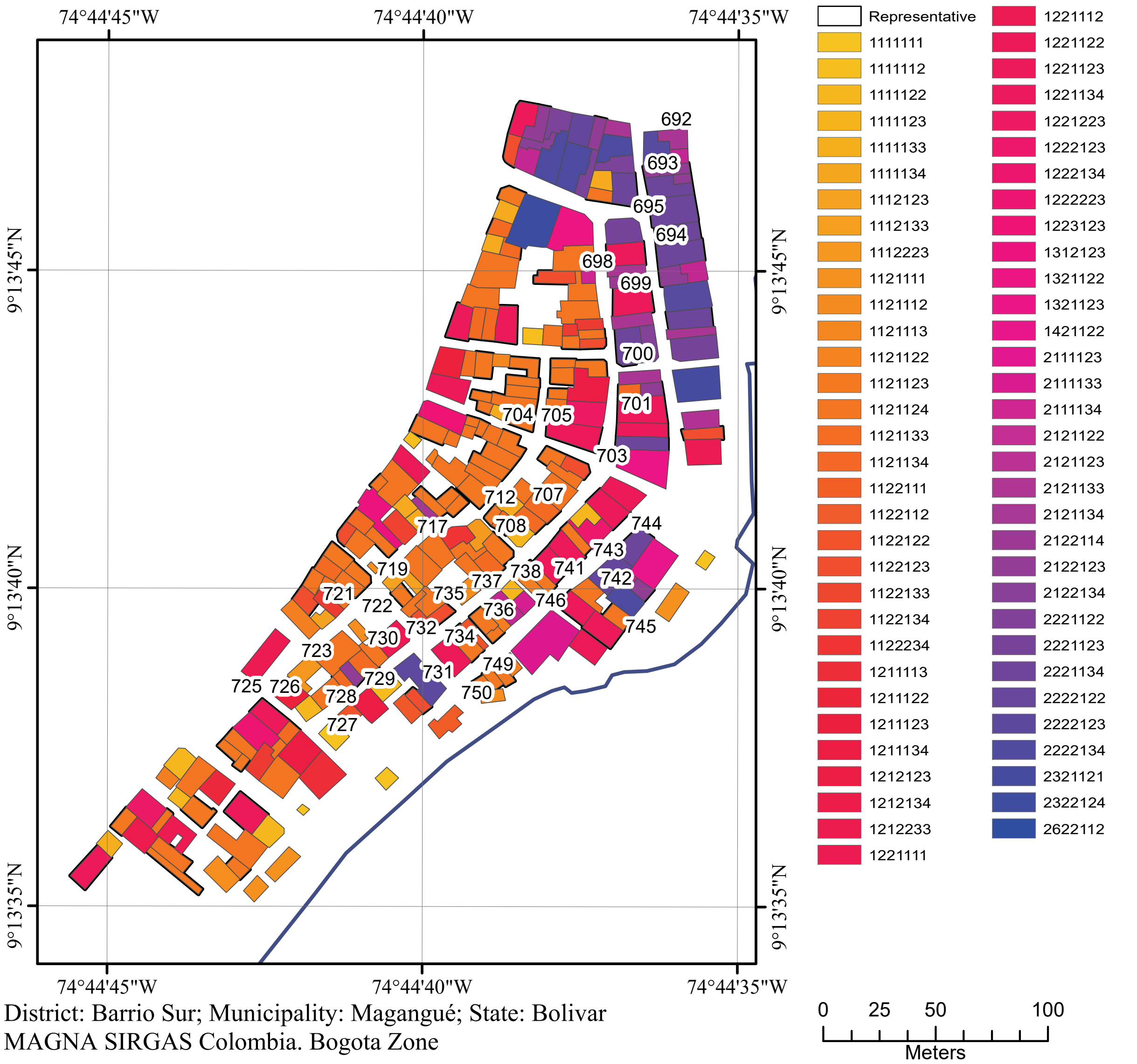

Figure 83: Building typology and representative buildings map – “Barrio Sur”

4.3.1.3 Selection of representative buildings – “Barrio Sur”

Nine buildings are selected as the threshold of a representative building type on the basis of the building type histogram. The non-representative buildings are then clustered with the representatives using the matrix of membership (10) described in section 3.1.3. The clustered buildings and the selected building samples are shown in the following map. The buildings are clustered to the seven building taxonomic codes with the highest frequency, as shown in the Figure 85 and Table 39.

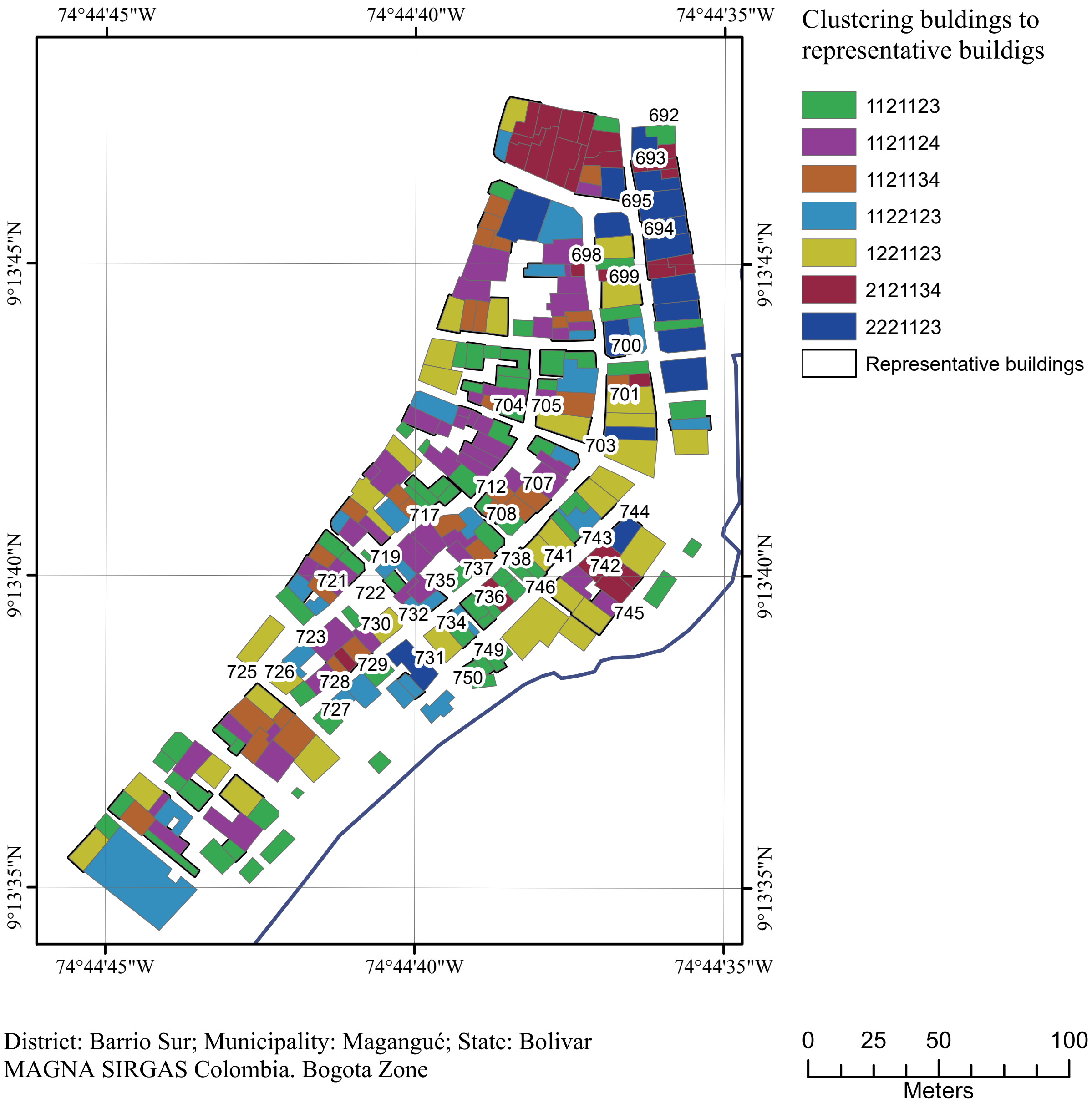

Figure 84: Selected representative and non-representative buildings – “Barrio Sur”

Table 39: Frequency for clustering to representative buildings – “Barrio Sur”

Building taxonomic code	Frequency	Clustering buildings to representative buildings
‘1121123’	36	76
‘1121124’	19	50
‘1121134’	15	31
‘1122123’	9	27
‘1221123’	16	33
‘2121134’	9	27
‘2221123’	9	16

In Figure 85, it can be observed that buildings clustered to representative buildings present similar structures and features. For instance, the buildings with the taxonomic building code *'2121134'* have a balcony, the buildings with the code '*1221123'* similar roof eaves and brick type grille under the eaves. However, the buildings with the code '*1121123'* are located at the corner of the block, but their structure and design are different including wood walls and concrete blocks walls.

'2221123'	Two storeys, footprint size between 150 m² and 500 m², rectangle form in the terrain, roof form with less than 8 vertices, flat roof, open space area between 33 % and 66 %, three or two sides exposed to open space

Representative building: 700

Representative building: 695

Non-representative building:723
2222122 with a matching of 85.7 %
to 2221123

'2121134'	Two storeys, footprint size between 150 m² and 500 m², rectangle form in the terrain, roof form with less than 8 vertices, flat roof, open space area between 33 % and 66 %, one side exposed to open space

Non-representative building: 693
Matching 92.8 %

Non-representative building: 737
Matching 92.8 %

Non-representative building: 747
Matching 92.8 %

'1221123'	One storey, footprint size between 150 m² and 500 m², rectangle form in the terrain, roof form with less than 8 vertices, flat roof, open space area between 33 % and 66 %, two or three sides exposed to open space

Representative building: 701

Representative building: 699

Representative building: 697

Non-representative building: 724
Matching 92.8 %

Non-representative building: 730
Matching 92.8 %

Representative building: 732

'1121123'	One storey, footprint size with an area lower than 150 m², rectangle form in the terrain, roof form with less than 8 vertices, flat roof, open space area between 33 % and 66 %, two sides exposed to open space

Representative building: 719

Representative building: 708

Representative building: 712

Non representative building: 727
Matching 85.7 %

Figure 85: Sample of representative buildings in "Barrio Sur"

Figure 86 shows that the buildings with one storey can have a variety of designs and structures without a defined pattern of construction. The basic similarity corresponds to the first codes 1- one storey and 1- footprint size with an area lower than 150 m².

'1121124'	One storey, footprint size with an area lower than 150 m², rectangle form in the terrain, roof form with less than 8 vertices, flat roof, open space area between 33 % and 66 %, one side exposed to open space

Representative building: GSM 1

Representative building: GSM 2

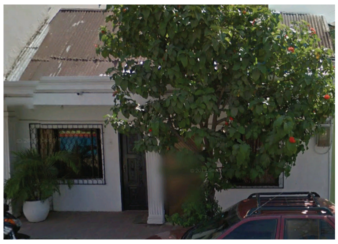

Representative building: GSM 3

GSM (Google Street Map)

'1122123'	One storey, footprint size with an area lower than 150 m², rectangle form in the terrain, roof form with more than 8 vertices, flat roof, open space area between 33 % and 66 %, two side exposed to open space

Representative building: GSM 4

Representative building: GSM 5

Representative building: GSM 6

'1121134'	One storey, footprint size with an area lower than 150 m², rectangle form in the terrain, roof form with less than 8 vertices, flat roof, open space area less than 33 %, one side exposed to open space

Representative building: 720

Representative building: GSM 7

Representative building: GSM 8

Figure 86: Sample of representative buildings in "Barrio Sur"

4.3.2 Module 2: Physical susceptibility of representative buildings – "Barrio Sur"

The process for the physical susceptibility analysis in Barrio Sur was carried out similar to "La Peña", according to the description of the method in section 3.2. The components and materials of the representative buildings were identified using non-invasive methods. Some typical building materials are depicted in Figure 87.

Floor: tiles cement – Terrazo

External walls: clay brick

Roof: eternit with trimble raftler

External doors: metal grille and metal roller door

Internal door: trimble

Roof: lightened plate and waterproofing

External doors: metal

Walls: trimble

External walls and external doors: wood

Figure 87: Some typical building materials

The variety of materials available in Barrio Sur is higher than in "La Peña", due to the fact that the economic development in Barrio Sur is faster because of the presence of commercial uses and small factories. The material found in La Peña (see Table 36) is also present in Barrio Sur. Table 40 contains the assessment of the additional building materials in Barrio Sur. The columns a, b and c show the qualification of the materials.

Table 40: Expert qualification of material's properties in "Barrio Sur"

Content	Material	Resistant characteristics after flooding	General appearance	Biological and chemical reaction characteristics	Natural drying speed	Y1	Y2	Y3	Y4	Y5	a	b	c
Foundation	Pile foundation (steel)	Bending	Efflorescence due to crystalline deposits of alkaline salts	Contamination due to its intern components	2	0.2	0.3	0.3	0.3	0.5	0.19	0.31	0.55
Foundation	Floor slab, concrete	None	Efflorescence due to crystalline deposits of alkaline salts	Mould growth	3	0.2	0.3	0.3	0.4	0.5	0.19	0.35	0.54
Floors	Tile cement - Terrazo	None	Discoloured surfaces	Mould growth	2	0.2	0.2	0.3	0.4	0.5	0.19	0.3	0.55
Floors	Vinyl	Flaking/scaling	Efflorescence due to crystalline deposits of alkaline salts	Mould growth	3	0.6	0.7	1	1	1	0.5	0.94	1
Walls	Common brick clay (air drying)	Cracks and shearing	Efflorescence due to crystalline deposits of alkaline salts	Mould growth	5	0.5	0.7	0.7	0.8	0.8	0.42	0.79	0.81
Doors	Metal grille and metal roller door	None	Discoloured surfaces	Contamination due to its intern components	1	0.3	0.4	0.4	0.5	0.5	0.27	0.49	0.5
Windows	Wire mesh resistant polymer - 'Anjeo'	Bending	Discoloured surfaces	Mould growth	1	0.3	0.3	0.4	0.5	0.5	0.28	0.44	0.52
Roof	Concrete – Slabs plate	Buckling	Efflorescence due to crystalline deposits of alkaline salts	Mould growth	2	0.4	0.4	0.4	0.5	0.6	0.39	0.45	0.67
Roof	Plate lightened with waterproofing	Buckling	Efflorescence due to crystalline deposits of alkaline salts	Mould growth	2	0.3	0.3	0.3	0.3	0.4	0.3	0.31	0.42
Roof	Clay tiles	Cracks	Efflorescence due to crystalline deposits of alkaline salts	Mould growth	3	0.9	0.9	0.9	1	1	0.87	0.95	1

Figure 88 sorts the range of material susceptibility with its median values. It can be observed that the perception of susceptibility for burned clay brick and metal has a lower uncertainty than pile foundation tree trunks or a cyclopean concrete foundation.

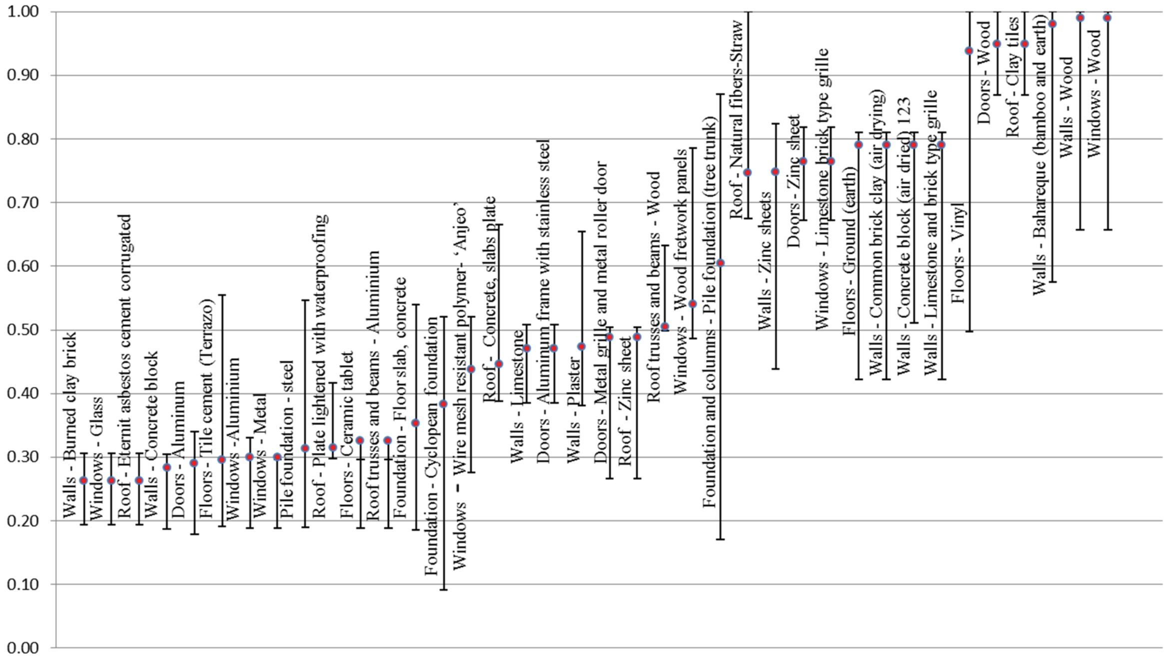

Figure 88: Materials sorted by their susceptibility in "La Peña" and "Barrio Sur"

An example of the susceptible volume calculation is given in Figure 89 for the building clustering to the taxonomic code *'2221123'*.

A B C

Figure 89: Representative buildings of the taxonomic code *'2221123'* in "Barrio Sur"

The calculation of susceptible volume is carried out as shown for all the representative buildings of this pilot site (see Table 41). Then the relation of water depth and susceptible volume is calculated as depicted in Table 42.

Table 41: Example of information collected for the analysis of susceptibility – Building *‘2221123’*

	Component	Lower Height	Upper Height	Material	Susceptibility	Volume material in m^3	Susceptible Volume
Second floor	Roof	6.4	6.6	Plate in concrete, steel and waterproofing	0.31	39.22	12,16
	External fenestration	4.2	5.5	Wood	0.99	4.80	4,75
	External walls	3.4	6.4	Cement block and plaster	0.79	33.08	26,14
	Floor	3.3	3.4	Ceramic tiles	0.28	19.61	5,49
First floor	Slab	3.1	3.3	Concrete and steel plate	0.45	39.22	17,65
	External windows	2.5	3.0	Coated aluminium	0.30	1.00	0,30
	External walls	0.2	3.0	Cement block and plaster	0.79	32.08	25,35
	External doors	0.2	2.5	Metal gate and fence	0.49	1.00	0,49
	Floor	0.0	0.2	Terrazo	0.42	19.61	8,24
	Columns	-1.0	6.6	Concrete and steel rods	0.30	3.08	0,92
	Foundation	-1.0	0.2	Cast stone	0.38	11.82	4,49

Table 42: Derivation of the building susceptible volume for water depth in relation to the material

											0.31	12.16	
								0.99	4.75	4.75	4.75	4.75	
							0.79	8.03	19.80	26.14	26.14	26.14	
						0.28	5.49	5.49	5.49	5.49	5.49	5.49	
					0.45	17.65	17.65	17.65	17.65	17.65	17.65	17.65	
			0.30	0.30	0.30	0.30	0.30	0.30	0.30	0.30	0.30	0.30	
	0.79	1.67	20.96	25.35	25.35	25.35	25.35	25.35	25.35	25.35	25.35	25.35	
	0.49	0.49	0.49	0.49	0.49	0.49	0.49	0.49	0.49	0.49	0.49	0.49	
	0.42	8.24	8.24	8.24	8.24	8.24	8.24	8.24	8.24	8.24	8.24	8.24	
0.30	0.40	0.41	0.59	0.63	0.64	0.65	0.66	0.73	0.83	0.89	0.91	0.92	
0.38	4.49	4.49	4.49	4.49	4.49	4.49	4.49	4.49	4.49	4.49	4.49	4.49	
-1.00	0.20	0.30	2.50	3.00	3.10	3.30	3.40	4.20	5.50	6.20	6.40	6.60	**Water depth**
0.68	6.59	15.29	35.07	39.49	39.95	57.45	63.46	71.75	87.39	93.79	94.11	105.98	**Sum**

The depth-physical impact functions with their media and standard deviation for the selected representative buildings are depicted in Figure 90.

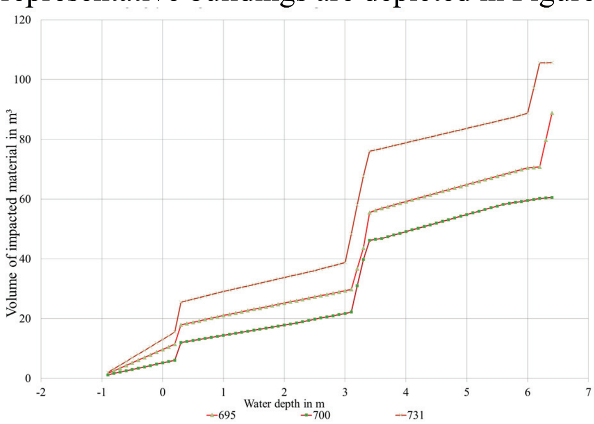

Depth-physical impact function for buildings with taxonomic code: *‘2221123’*

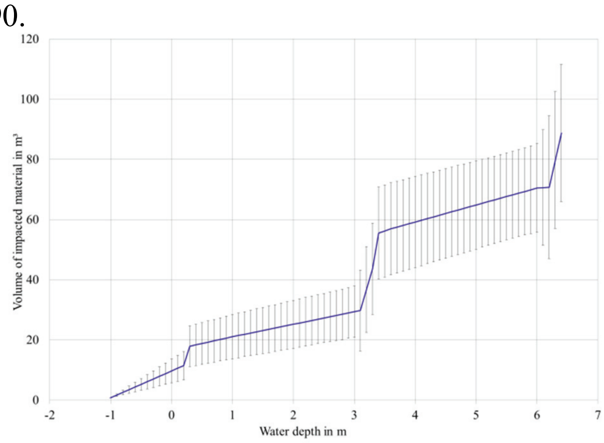

Median depth-physical impact function for buildings with taxonomic code: *‘2221123’*

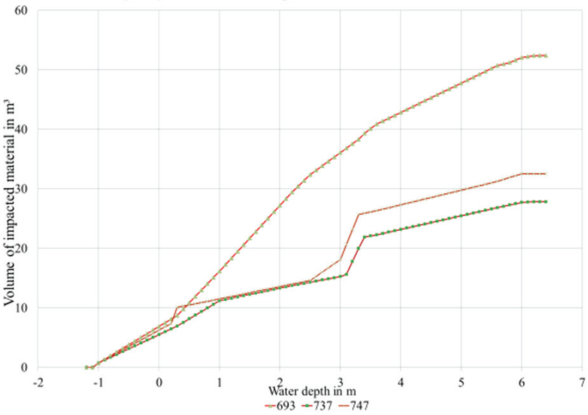

Depth-physical impact function for buildings with taxonomic code: *'2121134'*

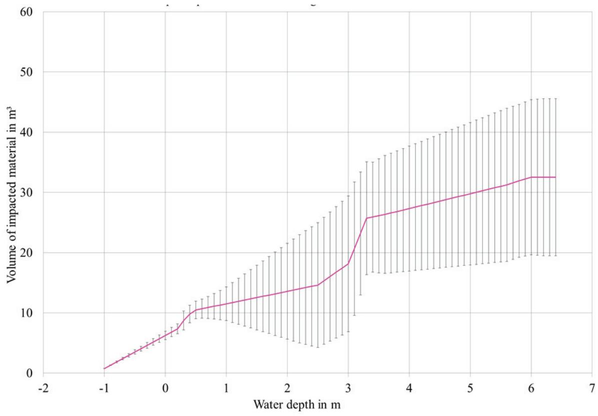

Median depth-physical impact function for buildings with taxonomic code: *'2121134'*

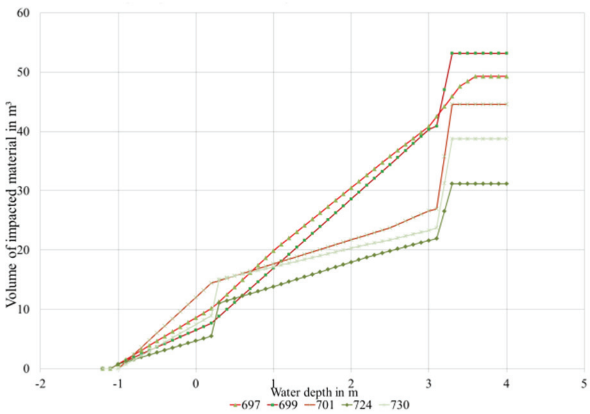

Depth-physical impact function for buildings with taxonomic code: *'1221123'*

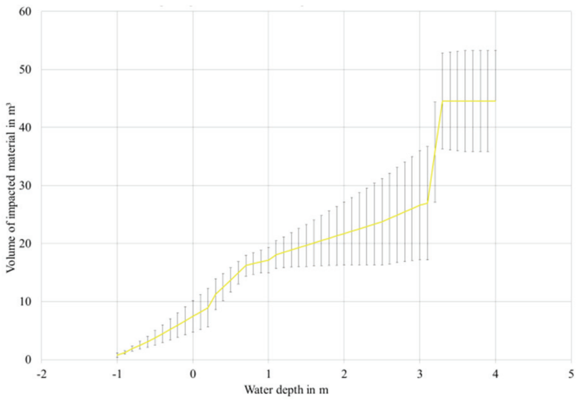

Median depth-physical impact function for buildings with taxonomic code: *'1221123'*

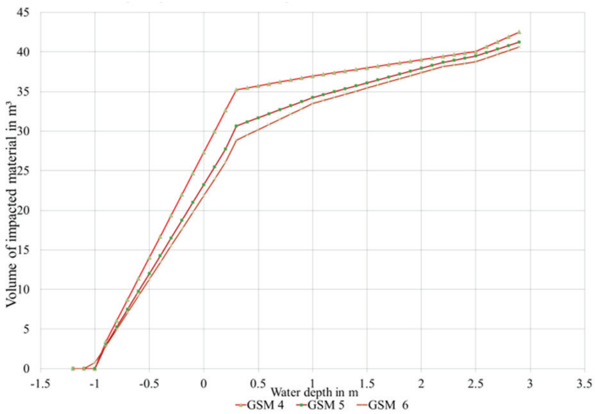

Depth-physical impact function for buildings with taxonomic code: *'1122123'*

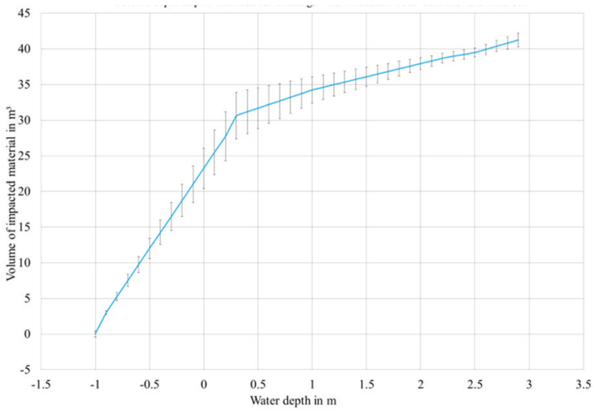

Median depth-physical impact function for buildings with taxonomic code: *'1122123'*

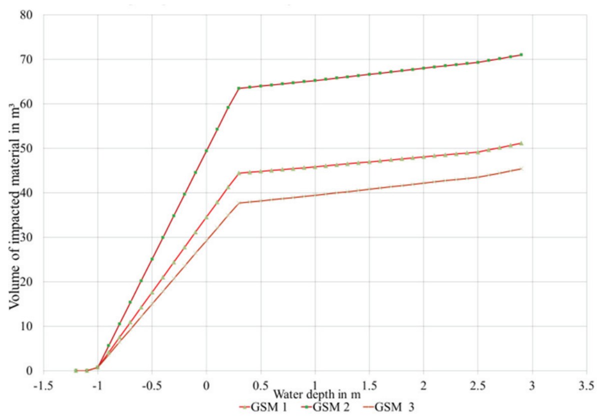

Depth-physical impact function for buildings with taxonomic code: *‘1121134’*

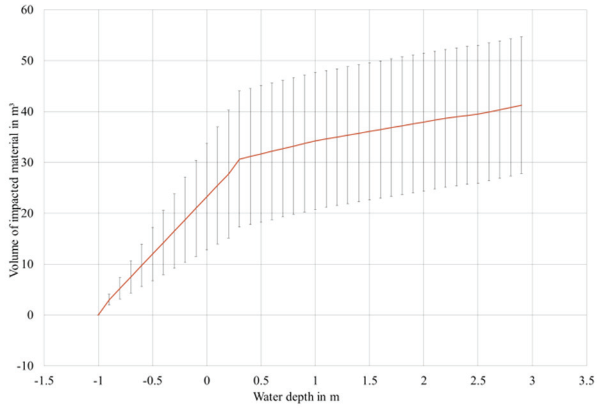

Median depth-physical impact function for buildings with taxonomic code: *‘1121134’*

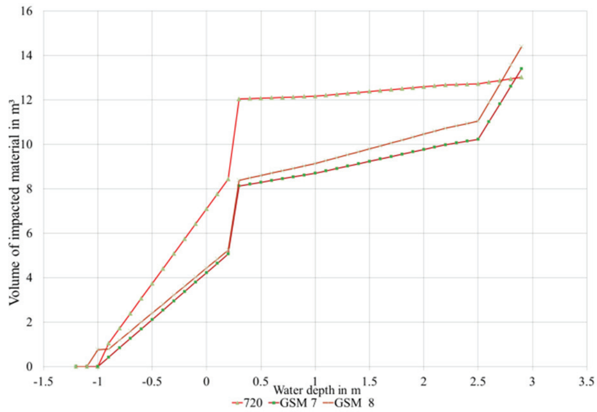

Depth-physical impact function for buildings with taxonomic code: *‘1121124’*

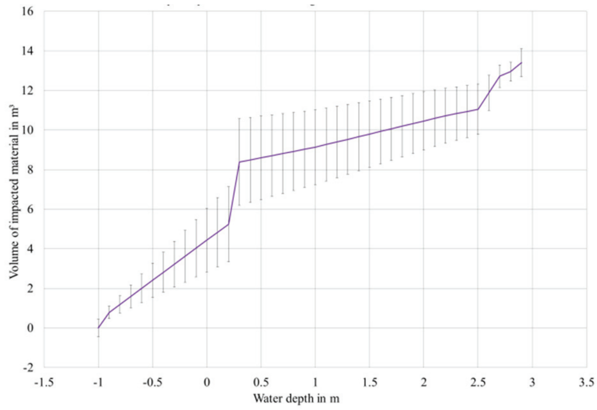

Median depth-physical impact function for buildings with taxonomic code: *‘1121124’*

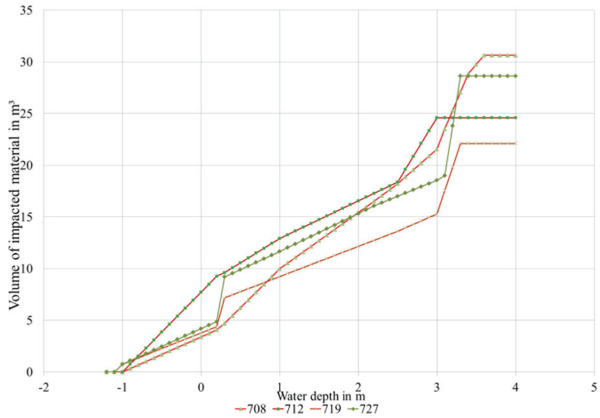

Depth-physical impact function for buildings with taxonomic code: *‘1121123’*

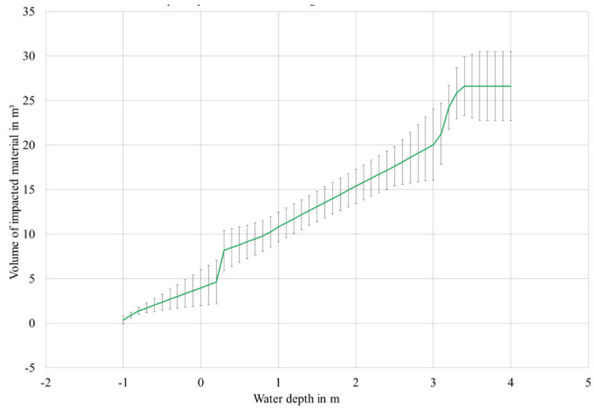

Median depth-physical impact function for buildings with taxonomic code: *‘1121123’*

Figure 90: Depth-physical impact functions of representative buildings – “Barrio Sur”

4.3.3 Module 3: Technological integration – "Barrio Sur"

This section shows the combination of the depth-physical impact functions with the building taxonomic code. Figure 91 shows the input data required for the calculation of the physical flood susceptibility in Barrio Sur. The following three inputs are required: a. building typology, b. water level and c. depth-physical impact functions of the representative buildings.

a. Building typology: building taxonomic code

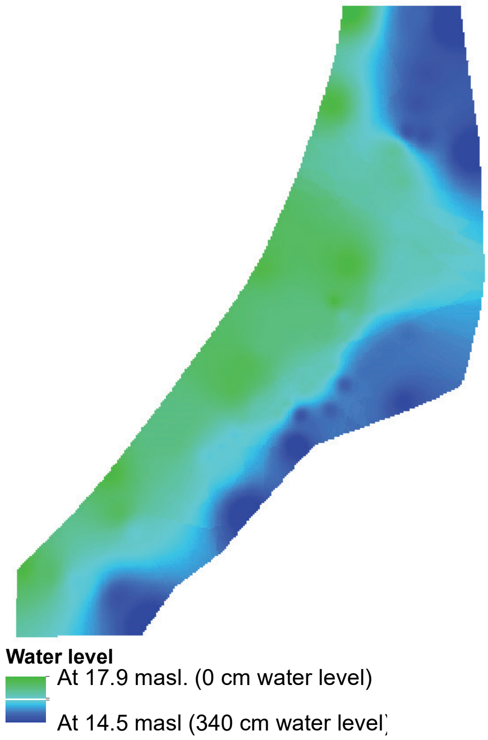

b. Artificial water level in cm, 100-year flood (see Appendix H)

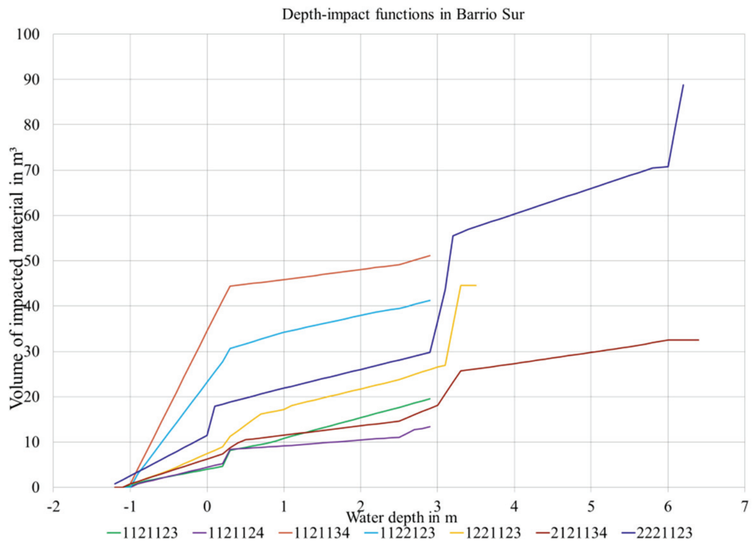

c. Median depth-physical impact functions of the representative building types in "Barrio Sur"

Figure 91: Input data for the calculation of a physical flood susceptibility – "Barrio Sur"

Representation of the physical susceptibility “option one”: The maximum susceptibility value for a taxonomic code is displayed in the following map (see Figure 92).

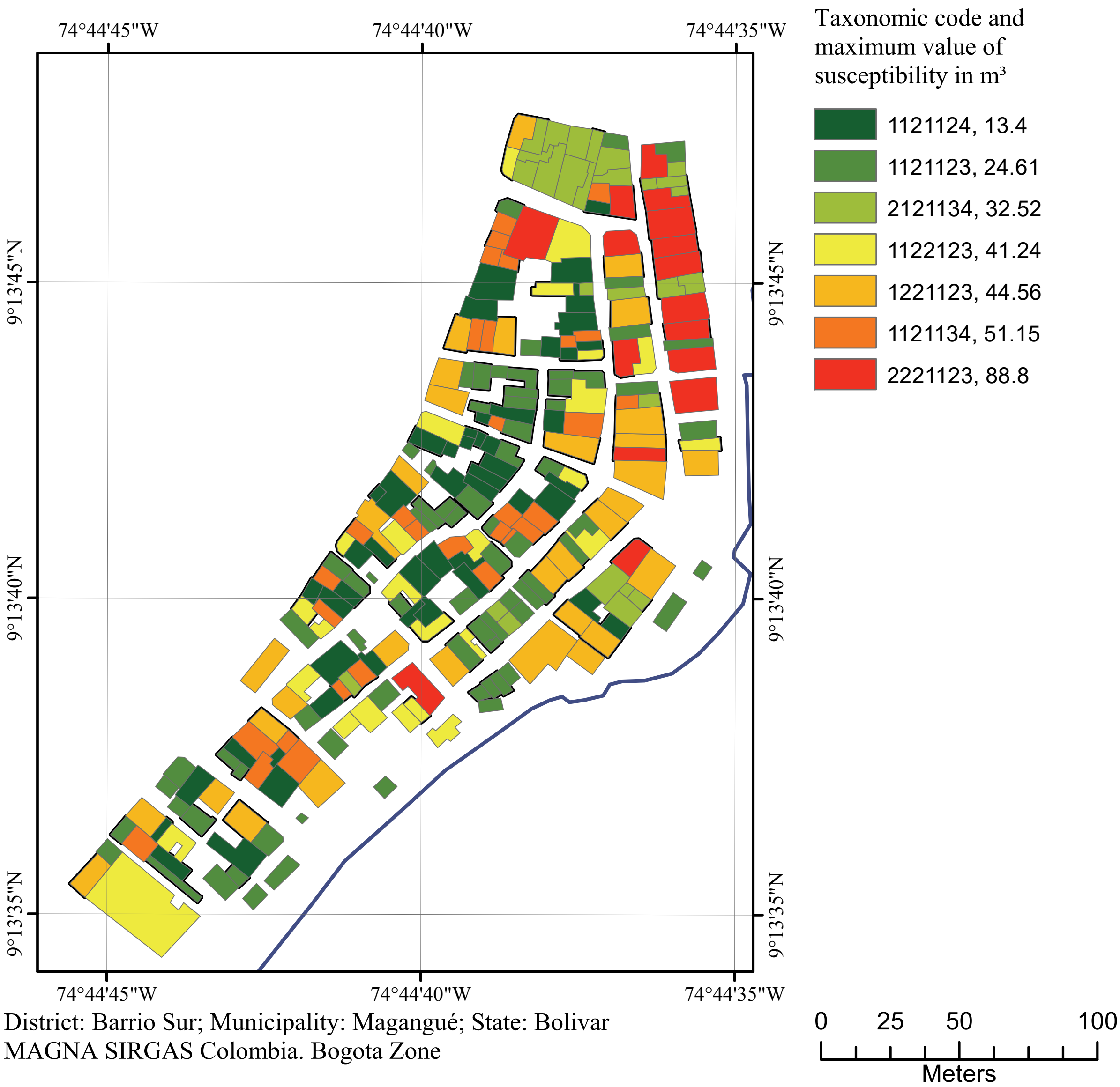

Figure 92: Maximum susceptible volume in m³ – “Barrio Sur”

Representation of the physical susceptibility “option two”: The following map displays the susceptible volume in m³ (inundation model) for a100-year flood.

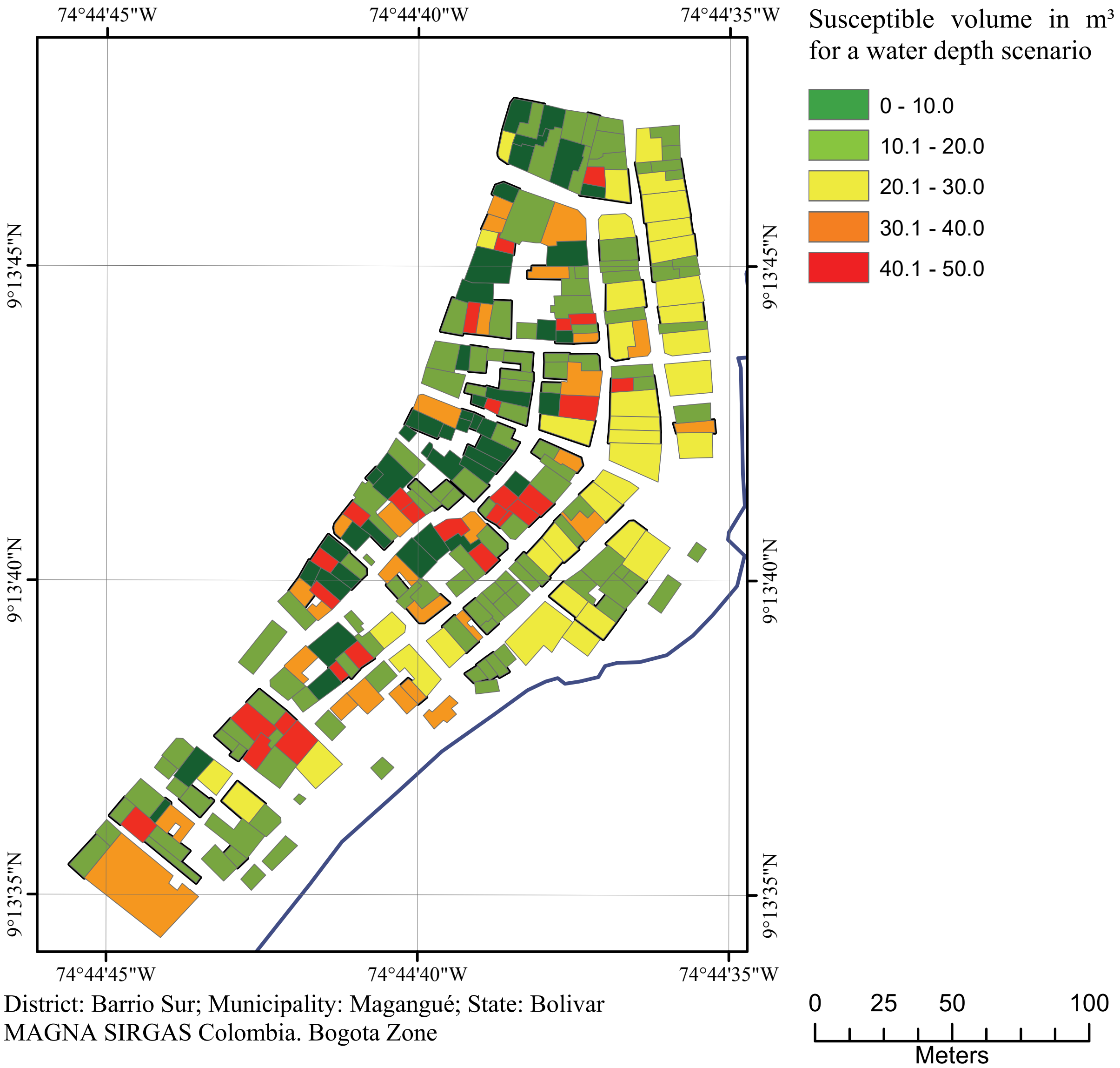

Figure 93: Susceptible volume in m³ for a 100-year flood

Representation of the physical susceptibility “option three”: This map gives the susceptible percentage volume by a 100-year flood (Figure 91.b.) in relation to the building volume that was estimated for taxonomic code.

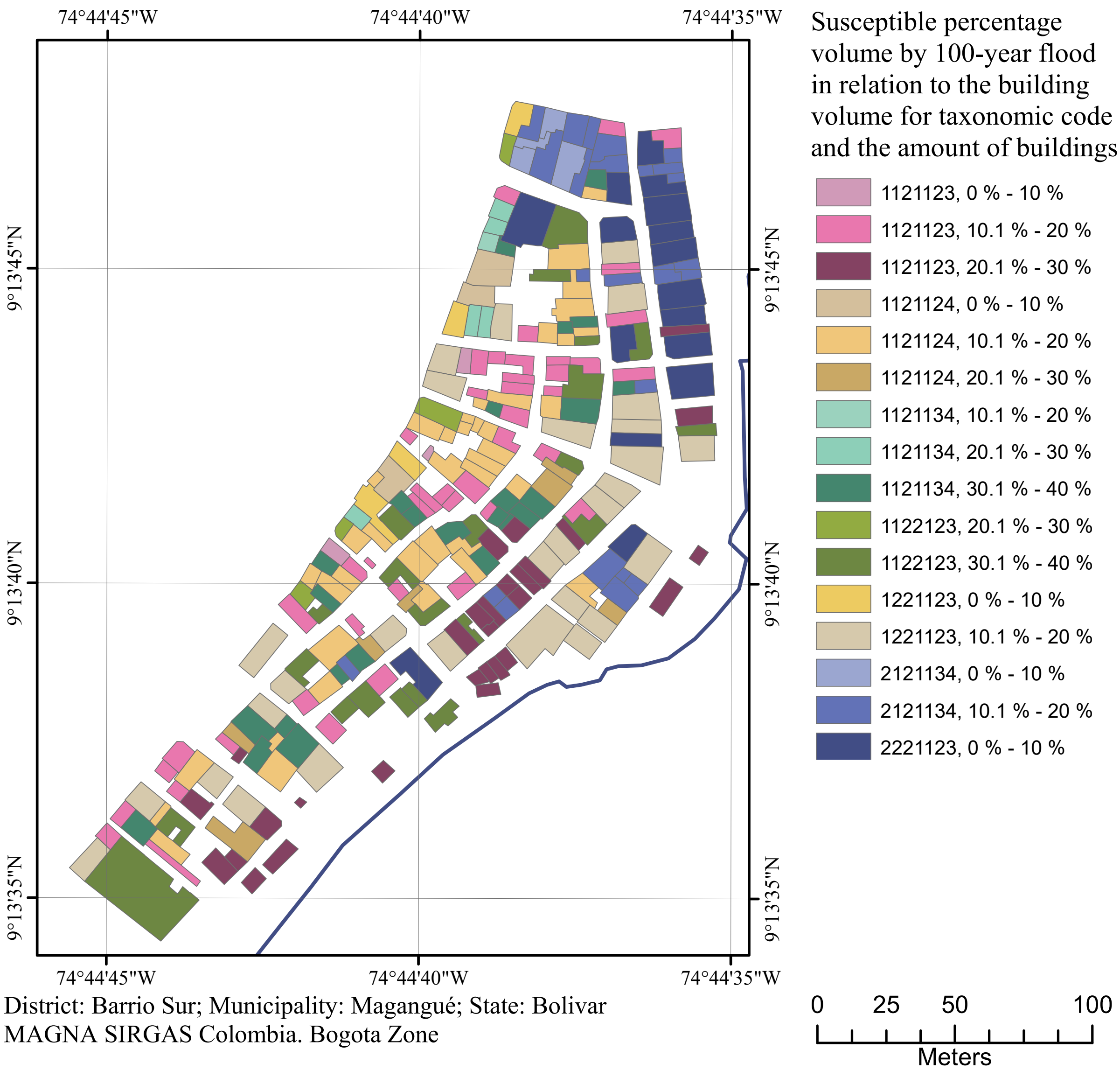

Figure 94: Susceptible percentage volume by building taxonomic code

4.4 Empirical findings

4.4.1 Empirical findings of Module 1

Behind the interpretation of the numeric results of the pilot sites, the aim of this methodology is to assist the collection of building structure data in a systematic, consistent and structured way, supporting the transfer of knowledge on physical flood susceptibility for the calculation of damages in areas where information is lacking. Table 43 shows a compendium of the selected parameters and the obtained results for the three pilot sites by applying the methods of Module 1.

Table 43: Compendium of results and selected parameters for the pilot sites

	Kleinzschachwitz	**La Peña**	**Barrio Sur**
Building extraction			
Input data			
Resolution DSM	1 m	2 m	3 m
GSD spectral data	0.15 m	0.15 m	0.15 m
Amount of spectral bands	3 RGB	3 RGB	3 RGB
Amount of extracted building polygons	1167	283	260
Accuracy of the building feature extraction (see 3.1.1.2 v.)			
Horizontal accuracy assessment (percentage of buildings semi-automatic extracted) (cf. Song and Haitcoat, 2005)	68 %	44 %	0 %
Height accuracy (automatic extraction) Formula (3)	1.25 m	2.05 m	3.3 m
Building taxonomy			
Building types	123	25	77
Selection of representative buildings			
Selected threshold of similarity	14	16	9
Amount of representative buildings	849 buildings classified in 18 taxonomic codes	225 buildings classified in 4 taxonomic codes	113 buildings classified in 7 taxonomic codes
Amount of non-representative buildings	304 buildings classified in 93 taxonomic codes	58 buildings classified in 21 taxonomic codes	138 buildings classified in 65 taxonomic codes
Atypical building types	14 buildings classified in 12 taxonomic codes	0	9 buildings classified in 5 taxonomic codes
Selected ranges of	Type 1	Type 1	Type 2

	Kleinzschachwitz	La Peña	Barrio Sur
categories for parameters	Table 24	Table 33	Table 38
Selected membership function of similarity	Type 1 Function (10)	Type 1 Function (10)	Type 1 Function (10)
Threshold of representativeness	14	0	9
Threshold value for clustering for isolating the atypical	80 %	80 %	80 %
Samples selected for the analysis of representative buildings	9 buildings for 6 taxonomic codes	22 buildings for 4 taxonomic codes	21 buildings for 7 taxonomic codes

Empirical findings of the building extraction

The extraction of building characteristics from high-resolution data seems to outcome in plausible results. Up to now, the process for gathering the building characteristics from very high-resolution data has not been completely automated yet because the user must enter values, such as height thresholds or vegetation masks, and reference data with higher precision. Moreover, visual interpretation must always be taken into account for an accuracy assessment. Additionally, an automatic building extraction process is limited to areas with small and few-stories buildings, a high density, buildings with corrosion patches on the roof, buildings occluded by trees and shadows, as the shape and spatial context of these buildings cannot be extracted automatically but rather require visual interpretation.

A workflow for a building feature extraction from remote sensing data has been defined and described. It is generic and can be implemented for any type of very high-resolution data. It was demonstrated that the method for recognising building cues can be the same for the three sectors (Table 21, Table 30, Table 37). These cues are the basis for a building semantic interpretation, which can be converted into algorithms for the building feature extraction.

The extraction of building features for the proposed building typology requires both high-resolution images and digital surface models. Although the challenge to achieve an acceptable accuracy for the building extraction for the pilot site in Colombia in terms of data resolution is still huge, the importance of a building extraction for the flood impact analysis in areas with a lack of information on the building structure was demonstrated.

The height data is the primordial source for the calculation of the building typology as well as for the generation of the water level scenarios. The digital surface models for the two areas in Colombia present some uncertainties, as they were not adjusted with vertical control points. Therefore, for overcoming this issue, the estimation of the water depth for the buildings in La Peña and Barrio Sur was supported through the photographs taken of the buildings.

As a result, the building extraction process yielded the detection of only 44 % of the buildings in “La Peña” and 0 % of buildings in “Barrio Sur”. The inconsistencies for the buildings’ extraction in this selected area are due to the presence of corrosion in the roof materials, the occlusion of the buildings by trees and shadows and the low resolution of the DSM in combination with numerous small buildings. The latter has been overcome through additional fieldwork. The issue of the DSM’s resolution for this area was compensated through validation in the fieldwork. The testing of the methodology in other cases has proved that the proposed resolution of the DSM with > 1 m significantly improves the accuracy; buildings that did not fit the criteria of accuracy were manually edited.

The building's height, outline and roof structure can be derived through a huge variety of methods and data sources. However, the most important criteria are the spatial resolution of the surface models and the consistency of the indices for measuring the accuracy. Buildings with a homogeneous roof texture were acceptably detected using the available data for the pilot sites; an identification of buildings with a corroded roof, however, was not possible. According to the relevant building extraction aspects of the application of a flood impact assessment, the following minimum requirements are taken into account (see Table 44).

Table 44: Minimum requirements for the building extraction for a flood impact assessment

Aspect	Minimum requirement
Data source	Stereo images, multi-stereo images, omnidirectional images, LiDAR, aerial images, images from space-borne sensors < 1m resolution
Data quality	Zero cloud cover, low occlusion of buildings by shadows, trees or tall buildings
Data processing level	Level 3
Features to be extracted	Building outline Building height Roof slope
Grade of automation	Semi-automatic including threshold of height and threshold of vegetation index
Methods and algorithms	*Building outline:* depending on the data source, selection of the method from section 3.1.1 with the best precision *Building height:* depending on the GSD of the DSM *Roof slope:* depending on the complexity of the roof structure in the case study
Object representation	LoD1 / LoD2
Accuracy	Comparison of reference data and calculation of the following indices: *Building outline*: RMSE vertices, vertex difference, area difference and perimeter difference (Song and Haithcoat, 2005) *Building height:* RMSE (z) (Aguilar and Mills, 2008; Flood, 2004)
Application	Building typology for the analysis of physical flood vulnerability

Under the above-mentioned conditions, the building feature extraction could not produce encouraging results.

Empirical findings of the building taxonomy

A characterisation of buildings for large areas using remote sensing and GIS analysis is proposed here. A building typology called 'building taxonomic code approach' condenses extensive and varied parameters into a brief format, establishing a clear link among the building's geometrical characteristics. The taxonomic code helps to facilitate and simplify the communication between the users who are dealing with building structure surveys in the urban areas.

Seven building parameters describing the relevant distinguishable characteristics of a building are shown and can be gathered through remote methods. These parameters form the building taxonomic code, which can serve as an instrument to transmit further analyses of flood impacts and to support field surveys in large river floodplain regions more efficiently. The taxonomic code approach extracted from spatial data seemed to present a reliable, standard and automatic method, which may be extended, adapted and transferred to other pilot sites. The following conclusions were drawn from observing the characteristics of the buildings within a taxonomic code:

Height is the most important parameter, as the building height defines the structure and the amount of components. Although a span of 2.05 to 3.5 metres is a high error value for a DSM for the implementation of building extraction, this error can still be admitted for the building height estimation since the elevation data for the building typology is ranked. The accuracy of the DSM is the cue for the building feature extraction, i.e. separating buildings from sealed surface and vegetation; however, the information on the amount of stories suffices to calculate the 'height' as a parameter for the derivation of the building taxonomic code, since the height value of the DSM is coded. If the building outline is available, a precision of 1 m of the DSM can be enough for determining the amount of stories.

Size, roof form and elongatedness are important parameters as they define additional constructive functions, such as internal distribution. However, their calculation depends on the building outline delineation as the walls between buildings cannot always be detected from remote sensing data, which can interfere in the inclusion of vertices and affect the calculation of these parameters.

The roof slope defines the style of the building, and its calculation from remote sensing data depends on the GDS of the DSM. It can be very sensitive as it can infer slightly in the misclassification of the building typology. The DSM of "Kleinzschachwitz" with a GSD of 1 m allowed the identification of the roof slope. However, for "La Pena" and "Barrio Sur", the GSD of 2 m did not allow to estimate the roof slope, which therefore had to be assumed in the lowest range of the classification since most of the buildings have flat roofs.

Adjacency is a useful parameter for the building classification in Kleinzschachwitz, identifying single buildings, double buildings and the buildings in a row or a block as well as the relation of the amount of façades exposed to open space. However, due to the simplicity of the buildings in "La Peña", adjacency did not reveal any additional information there. In "Barrio Sur", the adjacency is recoded in the categories of building *fenestration*, as it allows to simplify the amount of building codes due to the density of buildings in urban areas.

Compactness revealed in Kleinzschachwitz that most buildings with more open space were wealthier and equipped with more special design features than buildings with less open space. The code of compactness for the two areas in Colombia showed the degree of consolidation and – in contrast to Kleinzschachwitz – the higher the value of available open space, the lower the quality of the building materials.

Here, the three selected areas do not cover all the different varieties of building types and characteristics. However, the categorisation of the parameters for the three areas was very similar (Table 24, Table 33 and Table 38). The only difference between the categories is the assignation of the code of adjacency for the pilot site "Barrio Sur". It seems that other areas can be classified with those parameter ranges.

The subjectiveness of the category definition was reduced through the visual verification of the relevant building characteristics and through the help of the scatter diagrams and histograms in order to find a correlation between the variables or a normal, linear or exponential behaviour among them. In addition, the automatic generation of the taxonomic code based on remote sensing always requires the verification of geometric and contextual information about the building characteristics in fieldwork.

There is always uncertainty, depending on the quality of the initial data in terms of currentness and resolution and the expected similarity of the building belonging to a type. But on the whole, spatial data seems to be a good means to analyse relevant building parameters for a building typology.

Empirical findings of the selection of representative buildings

New methods based on statistical analyses are proposed for supporting the large-scale identification of building characteristics and the assessment of physical flood susceptibility making the collection more effectively. These methods do not pretend to substitute the traditional assessment of impact/damage approaches. The definition of representative buildings based on the frequency of the building types turns out to be reliable and easily applicable by using statistical methods.

The fuzzy clustering method is a good means for grouping non-representative buildings to representative buildings as the buildings are grouped through the membership function, which generates a value of matching indicating the degree of similarity of a building to a representative building. Low matching values describe the buildings that are atypical for a pilot site. These atypical buildings may have different structural characteristics from the majority of buildings, such as hospitals, schools, churches or factories. The advantage of the fuzzy clustering method is the fact that it is a non-hierarchical technique, seeking to find the best matching within the group of variables. Although the three areas show many differences, the membership functions were the same for all. This confirms the applicability of the method for the clustering of buildings.

A visual verification of the buildings belonging to one building type must follow. The verification can be conducted remotely with the help of Google Street View. However, as Google Street View is not available worldwide, field surveys must be realised.

4.4.2 Empirical findings of Module 2

The identification of building components and the qualification of the building material susceptibility represent pre-processes needed for the derivation of the depth-physical impact functions – an approach that is itself the actual contribution of Module 2.

Table 45 presents a compendium of the median volume material and the susceptible volume in m³ for each taxonomic code. The percentage of degradation relates the susceptible volume material to the total material. For taxonomic codes with more than three samples, the standard deviation of the susceptible volume is calculated.

Table 45: Compendium of physical susceptibility analysis for taxonomic code

	Amount of assessed buildings	**Median vol. material in m³**	**Max. value of susceptible vol. by taxonomic codes in m³**	**% of susceptible vol. in relation to its total building material vol.**	**Max. standard deviation of the susceptible vol.**
Kleinzschachwitz					
‘3222212’	1	635.86	348.00	54.73%	
‘3222211’	1	626.47	360.38	57.53%	
‘2221211’	1	268.72	113.78	42.37%	
‘2121211’	1	274.82	172.35	62.71%	
‘1122113’	1	162.53	113.25	69.68%	
‘2111211’	4	247.17	131.44	53.18%	38.75
La Peña					
‘1111111’	6	25.02	16.47	65.83%	4.24
‘1111112’	3	40.34	12.71	31.51%	0.91
‘1121111’	8	31.58	22.05	69.82%	8.59
‘1121112’	5	27.04	16.96	62.72%	3.53

	Amount of assessed buildings	Median vol. material in m³	Max. value of susceptible vol. by taxonomic codes in m³	% of susceptible vol. in relation to its total building material vol.	Max. standard deviation of the susceptible vol.
Barrio Sur					
‘1121123’	4	72.88	24.61	33.77%	2.7
‘1121124’	3	51.20	13.40	26.18%	0.70
‘1121134’	3	145.87	51.15	35.07%	13.44
‘1122123’	5	104.23	41.24	42.75%	8.70
‘1221123’	3	143.33	44.56	31.09%	12.39
‘2121134’	3	98.97	32.52	32.86%	13.04
‘2221123’	3	282.77	88.8	31.40%	22.79

We can see in Table 45 that the buildings in Kleinzschachwitz possess a large amount of material in comparison to the other two areas, where the percentage of potential degradation due to flooding fluctuates between 42.37 % and 69.68 %. The buildings in La Peña have a low amount of material, which reflects the fragility of a house for residential uses. The maximal percentage of degradation ranges from 31.51 % to 69.82 %. The buildings in Barrio Sur possess a lower percentage of degradation than those of Kleinzschachwitz. The percentages reveal that the experts who qualify the material have a different perception of the material degradation.

The information on building materials in Kleinzschachwitz was collected for IOER during the Regklam project. It was impossible to collect further information on the building material as a permission to visit the settlement in order to collect and identify the external materials of the shell structure could not be obtained. Therefore, just one building for five taxonomic codes has a sample for the analysis.

The derivation of the depth-physical impact function requires a structured and consistent collection of the representative buildings’ relevant components: their principal materials, the material properties for the susceptibility qualification, their related dimensions such as width, length and thickness, as well as the location above the terrain (lower and upper height).

The determination of the material’s susceptibility contains many uncertainties. Two steps for an approximation are recommended here: (i) Information on the available material’s resistance assuming that susceptibility is the opposite of resistance incorporating the resistance values of international approaches, e.g. (BMVBS, 2006; Committee and Resources, 2006; Escarameia et al., 2006; FEMA, 2008); (ii) The conversion of qualitative resilience values into a range of susceptibility requires a further qualification from the experts, which consists in the fuzzy expert knowledge and Delphi methods enabling the integration of local and scientific knowledge, and they can be used to improve the understanding of the material’s susceptibility, including evidence for the material’s properties.

The experts’ qualification is subject to how they interpret the concept of susceptibility as well as to the available information on the materials. The definition of the material´s intrinsic susceptibility includes different interpretations; one that is susceptible for one person has another interpretation for the next. The range of interpretation could be reduced by means of laboratory tests and a better knowledge on the extraction process and the manufacturing of the materials. Since the testing in laboratories is not always feasible for all the materials, the qualification of susceptibility depends on the best information available on the materials and consistent and organized information collected in the field, that supports the empirical expert knowledge.

Trained and experienced personnel should conduct the surveys on the material´s properties. Good results depend on the investigators' experience and their knowledge. This information collected by trained personnel is required for an inventory of the representative buildings, which allows the experts to better understand the qualification of the susceptibility.

Due to the uncertainties in the qualification of susceptibility, we can consider: defining a range of susceptibility for every component including the values *a* and *c* of the fuzzy sets; and calculating a median depth-physical impact function with the standard deviation indicator for a group of buildings with the same taxonomic code. In addition, the maximum value of the susceptible volume for the building type is displayed in the physical vulnerability map. Box diagrams can help to identify the susceptible component if many buildings for a taxonomic code are statistically analysed. As just three or four buildings per taxonomic code were assessed for the pilot sites, the box diagrams were not suitable for the derivation.

It has proved impossible to use one unique deterministic method for the derivation of the social and economic vulnerabilities from the material susceptibility analysis. However, the thesis makes a step in that direction, particularly in assisting a large-scale systematic and standardised data collection for settlements in order to improve the validity of further in-depth investigations and hence enable the simulation of future vulnerabilities and risks.

4.4.3 Empirical findings of Module 3

Taking advantage of the technological advances in data collection, such as GPS in smartphones or apps, and data storing, such as a database in Postgres, as well as data processing, such as python scripts and Matlabs, new tools were developed to simplify and control the whole process and the integration of the methods for a building susceptibility assessment.

However, the app for collecting information in the field requires further testing and improvements to achieve an easier operation. It needs a certain deftness to handle the app for information collection as well as knowledge on how to identify materials and components.

4.4.4 Guidance of the methodology

This guide summarises the required methods and tools for deriving an analysis of building flood vulnerability using spatial data for large river floodplains. This guidance synthesises the methodological framework of chapter 3.

What are the principal components of the analysis of the building flood susceptibility at the scale of river floodplains?

i. Setting up a building typology
ii. Analysing the susceptibility of the relevant materials for representative buildings

What kinds of parameters are required for the building typology?

i. The building features required for the proposed building taxonomic code are: building outline, building height and building surface. This building taxonomic code describes the geometry (building height, building footprint size and elongatedness), contextual information (adjacency and compactness) and roof characteristics (roof form and roof slope). The building's outline, height and surface can be extracted from a huge variety of data sources, methods using a wide range of algorithms and software. However, what is most important is the evaluation of the accuracy of the building outline by means of higher precision reference data and a GSD lower than 1 m of the DSM (see section 3.1.1.2).

ii. Once the building taxonomic code for all the buildings is computed, representative buildings can be selected on the basis of the frequency. Non-representative buildings can be grouped to the representatives through membership functions obtaining a matching value of the taxonomic codes.

iii. The verification of the building typology should be supported by comparing the parameters with reference information on the buildings, such as pictures collected in the field.

Which steps should be taken into account for collecting information for an susceptibility analysis for representative buildings?

The susceptibility analysis for representative buildings takes into account the following steps:

i. The identification of the buildings' structural components

ii. The measurement of the lower and upper height of structural components

iii. The measurement of the principal dimensions of structural components

iv. The identification of the components' relevant materials

v. The calculation of the volume of the components' relevant materials

vi. The estimation of the material's susceptibility; the assignation of a susceptibility value can be realized:
   a. based on researches on the material's resistance from reputed institutions
   b. based on expert knowledge

vii. The calculation of the components' susceptible volume, by multiplying the susceptibility with the volume of the component

viii. The derivation of depth-physical impact functions, relating every component's lower and upper height with the susceptible volume; the lower and upper height represent the point to where the floodwater can rise

The previous steps should be realised for at least five buildings within the same taxonomic code in order to calculate a median depth-physical impact function with its standard deviation. The median depth-physical impact function allows to identify the ranges of the susceptible material volume as an initial input for further monetary calculations.

How can the building flood susceptibility be displayed on a map?

There are four alternatives:

i. Display the maximum value of every building's susceptible volume for its respective taxonomic code.

ii. Combine the building typology and its depth-physical impact functions with water depth information from inundation maps or inundation scenarios. The building vulnerability map displays the buildings' susceptible volume for a water level.

iii. Calculate a percentage of the susceptible volume in relation to its total building volume.

iv. Calculate the standard deviation of the depth-physical impact functions at a water depth.

Can the information on building typology and depth-physical impact functions be transferred to other areas?

The transfer of information can be successful as long as the relevant areas have similar development conditions and are located in the same region, assuming that the areas share similar construction materials. For instance, the median depth-physical impact function for the buildings with the taxonomic code *‘1111111’* located in the north of the lower catchment of the Magdalena River in Colombia may be used for buildings located in the middle catchment. The methods and steps for setting up the building typology can be followed as long as high resolution DSM and building outlines are available.

The steps for the depth-physical impact function approach can be applied to other plain floodplain areas as well. The most important consideration of this approach is that the derivation of the depth-physical impact function requires a structured information collection to ensure a reliable assignation of the material’s susceptibility.

What are the factors which affect the accuracy of a physical flood susceptibility map?

The quality of the results depends on the following aspects:

i. Resolution of the input data, which defines the scale of the maps
ii. Horizontal and vertical accuracies of the extracted building features
iii. Assignation of the u_{ik} values in the membership function for clustering the taxonomic codes
iv. Availability of information on the building material’s properties in terms of resistant characteristics, general appearance, biological and chemical reaction characteristics and natural drying speed
v. Empirical knowledge by the experts on material properties and its susceptibility to floodwater
vi. Consistency in the automation of the whole process.

5 Discussion

The discussion below is separated into conceptual framework and methodological framework while linking the conceptual and empirical findings to the proposed objectives.

5.1 Discussion on the conceptual framework

This thesis narrows down the vast concept of flood vulnerability and the relation between its various dimensions, and it focuses on proving the definition of its components (susceptibility, function/value and coping capacity/resilience). The basic framework of flood risk developed by Schanze (2006) bears the conceptual and methodological framework for the analysis of the flood physical susceptibility of this work; it enables to identify and separate the variables and boundaries of the analysis.

The methodology's structure was designed through the understanding of each vulnerability dimension as well as the separation of its variables and components, as shown in the cells of Table 1. This table synthesised the definitions of all five vulnerability components and their meaning for susceptibility, value/function and coping capacity/resilience. The table also summarises the relevant explanations offered by Neubert et al. (2014), Krapesch et al. (2011), Mesjasz (2011), Naumann et al. (2010), Tapsell (2008), Zevenbergen et al. (2008), Schanze (2006), Samuels et al. (2006) i.a. Once the relevant variables are identified and the differences between existing flood modules understood, modules, methods and variables can be identified and grouped in order to analyse how they can be integrated into the methodology. The scheme depicted in Figure 2 shows one part of the relations between the physical flood vulnerability on one hand and the social and economic vulnerabilities on the other. This scheme can be extended as to include further vulnerability factors and interrelationships, such as described by e.g. Douglas (2005), Green et al. (2011).

The works of Green et al., (2011), Jongman et al. (2012) and Winsemius et al. (2013) allow to define the methodology's focus as an ex-ante, synthetic and empirical approach for large river floodplains based on expert knowledge and the damages data collection from inundation events. Hence, the methodology provides methods and tools for a systematic data collection to reduce the uncertainties in flood damage assessments.

5.2 Discussion on the methodological framework

Two components were relevant for the development of this methodology: (i) the literature that enabled to identify the key trends and gaps in the damage assessment models and (ii) the field works that allowed to observe the relevant features for the derivation of the modules with their methods as wells to recognise the gaps and limits of flood damages assessment. The combination of these components was essential to define the problem and deal with its complexity and to familiarise with the potential approaches for a proposed solution.

The approaches developed here do not pretend to compete with synthetic approaches for assessing the damage prior to a future event, such as e.g. HAZUS (Scawthorn et al., 2006) and HOWAD (Neubert et al., 2014). In fact, the building taxonomy approaches and mean depth-physical impact functions might rather support these models in areas where the characterisation of the built structure and information on building material resistance are lacking.

The modules may also be interchanged for the analysis of other vulnerability factors, which can be classified according to the approach proposed by Füssel (2007). A consideration of the entire physical flood vulnerability would require the operationalisation of both the physical function of construction elements and their coping capacity in terms of physical resilience (see Figure 2). To address these two, further research is needed to reach a particular trade-off between physical validity and resource efforts for the fieldwork.

Uncertainties always exist in the context of damage assessment, which depends on the availability and reliability of information. Hence, the developed methods attempt to systematise and automate the data collection processes and their analysis, allowing experts to assess the impacts in a more accurate way for the generation of the depth-damage or depth-stage functions. The combination of the methods into modules can help to reduce the uncertainties of flood damage assessment identified by Merz et al. (2004) and Jongman et al. (2012).

Combining the three modules appears to be effective for classifying and characterising the building structure and the subsequent susceptibility assessment in any settlement, irrespective of it's eco-climatic or socio-economic condition. The implementation of the methods in two completely different regions in Germany and Colombia confirms this. It was proved that the methodology presents a systematic procedure to reduce efforts compared with extensive ex-post damage surveys, and it can complement ex-ante synthetic damage simulation modelling.

5.2.1 Discussion on Module 1: the building taxonomic approach

Module 1 contains three new approaches to reduce the efforts for the flood susceptibility assessment by narrowing down the amount of buildings with the same taxonomic code to a number of representative buildings, suitable for assessing the building's materials and components. This building classification takes into account the variables which can be derived remotely as a basis for further information collection in surveys.

A comprehensive literature review of the principal concerns for a building extraction from remote sensing was classified in terms of data sources, data quality, data processing level, level of result, object representation, features to be extracted, their methods and algorithms, grade of automation, accuracy and application. This classification synthesises the relevant key factors for building extraction while taking into account the works by Brenner (2010), Schöpfer et al. (2010) and Rutzinger et al. (2009). Moreover, techniques and algorithms have been arranged by sensor type to identify features for the building extraction from remote sensing data.

The methodology does not provide a unique solution but instead advances the understanding of methods that can be applied to the building feature extraction and the assessment of flood impacts. The implementation of the methodology in another region may have as reference the methods provided in Chapter 3.1.1: (i) the relevant factors that intervene in the building feature extraction; (ii) a generic workflow for semi-automatic building feature extraction which are based on existing literature and (iii) the synthesised information described in the empirical findings p. 157f and Table 44.

Inductive reasoning led to the identification of seven parameters and the key features for the development of this building taxonomic approach at a large scale. Although information on building age, building use, building condition, type of occupation and construction techniques are essential variables required for a more precise flood damage assessment (Naumann et al., 2010), the building taxonomic approach can be used as a screening method to identify the relevant building characteristics as an alternative for urban structure types

(Blum and Gruhler, 2011) instead of the general information provided by Corine Land Cover (Bossard et al., 2000). Moreover, the building taxonomic approach with its seven parameters is *generic* as it can be applied under different conditions, if high-resolution spatial data is available, as demonstrated in the Dresden pilot site and the two settlements in Cicuco and Magangué.

The pictures depicted in Figure 71, Figure 86 and Figure 105 show the efficiency of the building taxonomic approach for grouping the buildings on the basis of the seven parameters. Approaches for clustering buildings by urban structure types proves unfeasible in Barrio Sur and Cicuco due to missing information on building age and the complexity of identifying street and open space patterns.

The weaknesses of this approach are related to the data quality on the building outline extraction algorithms as the building outline extraction may mislead the identification of the borders that separate properties. Therefore, the calculation of size, elongatedness, adjacency and compactness parameters is based on the semantic definition described here and not on property borders. The indices calculation presented by Song and Haithcoat (2005) can lead to unsatisfying results if the building outline differs too much from the reference data. Building height and building roof slope depend on DEM reliability and currentness; conditions like building changes, reconstructions and new settlements must be considered as well. Nevertheless, the principal quality analysis criterion is that the data must fit the purpose.

The building extraction process presented here does not allow the direct derivation of additional levels of information (i.e building use, occupancy class, multifamily dwelling), nor the identification of hotspots (i.e schools, hospitals, banks). These levels of information normally require an additional data source and field verification. Therefore, this building taxonomic approach can be used as a forecast for the gathering of further information levels and to support survey verification. Moreover, long-term plans for data acquisition, data preparation, data update, data storage, data improvement, field surveys for data validation, software and hardware maintenance, employment training, increasing knowledge in terms of the development of new collection and extraction methods, development of privacy and transfer policies must be economically and operationally reasonable and designed for proper and accurate building extraction results as well as a further testing of the methodology.

A transferability of the approach to other study regions seems to depend mainly on the accessibility of very high-resolution data. Although there are currently certain limitations in many regions of the world, improvements may be expected from new sensors. There is a rapidly increasing trend towards the availability and accessibility of spatial data and the improvements of their properties in terms of resolution. For instance, unmanned aerial vehicles may support the collection of very high-resolution images and the improved accuracy of the extracted features. Additionally, new free algorithms for feature extraction play a role, such as SpaceEye (ICIS, 2009), which allows to process the global data of Google Earth with simple imagery functions, such as segmentation and edge extraction. These technological advances will contribute in the near future to the collection of a huge amount of data, which can be classified for the analysis of settlements.

The classification of the buildings is adjusted through (i) statistical analyses (histogram diagram, scatter diagram and the correlation matrix) in order to find trends and relations in the parameters and (ii) advice from experts (i.e. civil engineers, architects), who discuss the class relevance for a subsequent susceptibility assessment. An automatic derivation of the building taxonomic code and methods for selecting representative buildings and for clustering the non-representative buildings to the representatives help to reduce the uncertainty of the building classification and to support an efficient data collection in-situ.

The approach attempts to make a step further in the issue defined by Douglas (2007) and Jongman et al. (2012). The validity of this building typology is borne out visually comparing pictures of the buildings with the obtained parameters in the taxonomic code.

The parameters in the building taxonomic code are equally important as they attempt to describe the relevant characteristics of a building. However, the membership function for clustering non-representative to representative buildings can be adjusted for giving more importance to a certain parameter in order to heighten its hierarchy in relation to the other parameters.

5.2.2 Discussion on Module 2: the depth-physical impact function

The second module of the methodology shows how the information can be systematically collected and analysed for the derivation of a depth-physical impact function. This can be used for transferring and broadcasting the data on a potential impact at the scale of the floodplain. It can be considered as a contribution to the issue identified by Merz et al. (2004) about the need to improve the refinement, standardisation and data collection for flood damage estimations.

The process for deriving a depth-physical impact function considers the measuring of two types of uncertainties: (i) the intervals of susceptibility qualification by the experts and (ii) the derivation of a synthetic depth-physical impact function that considers the standard deviation of the volume degradation of the selected representative buildings with the same taxonomic code. These uncertainties allow to understand and improve the intuitive knowledge involved in the interpretation of a flood impact assessment. The uncertainty of the intervals of susceptibility qualification by the experts uses the concept of fuzzy set membership, facilitating the interpretation of material resistance, while the synthetic depth-physical impact function uses the standard deviation and the median as a probability measure of degradation relating to a water depth. The more data is collected, the higher the certainty of an ex-ante assessment.

A median depth-physical impact function (see e.g. Figure 90) can better represent the differences of the volume susceptibility for buildings that belong to the same building taxonomic group rather than a unique synthetic function, as a median depth-physical impact function contains the standard deviation of the susceptible volume for the representative buildings at a different height. It helps to understand the complexity of modelling the buildings' properties and the challenges to cluster these properties.

The following boundaries must be considered when the depth-physical impact function approach is implemented:

(i) The proposed method assesses the potential impacts on the building materials caused by plain floods along large rivers. These floods are characterised by a low flow velocity and are therefore supposed to cause any no collapse of buildings. However, the collapse of the material of building components, which depends on their specific susceptibility, is considered. The highest assessed value shows that the material can generate the collapse of the component. However, further works should consider the knowledge of building material impacts due to hydrodynamic pressure, hydrostatic pressure above one metre, floating debris of the floodwater impact on the buildings, chemical toxic contamination, moisture diffusivity or transmission in the building materials and flood duration.

(ii) The material susceptibility qualification can be determined from the resistance tables of international institutions and local expert's knowledge. The lack of experts possessing the appropriated knowledge can extend the uncertainty of the susceptibility results. The names of the materials and their characteristics should be correctly identified, so that the experts can definitely assess every material property. Otherwise, subsequent calculations could lead to wrong results.

(iii) The building components for the derivation of depth-physical impact functions selected for the analysis in this work are structural and shell components. Non-structural components such as furniture, building equipment, connections, interior accessories or building inventory can be included for detailed studies. The experts can identify the susceptibility based on construction techniques, structural design, construction qualities or the material assembly of component constructions, for a deeper analysis on a detailed scale.

The inundation depth is usually the main parameter from which the fraction of damages is calculated (Messner et al., 2007). The impacts of plain floods with a low velocity and hydrostatic pressures of less than 1 m/s on building elements are taken into account in the depth-physical impact function. Plain floods with these characteristics permit that some building elements can be saved.

The period of inundation in Kleinzschachwitz lasted over a week and in the pilot sites in Colombia more than 6 months. The experts in Colombia did not consider the information about the conditions of the building materials before the flood because it did not exit. They did not know if there were previous impacts in the materials. Therefore the assessment in Colombia has an additional grade of uncertainty. The reasons for the uncertainty of the assessment are variable: (i) a lack of information on material characteristics previous of the flood; (ii) expected standards of life quality; (iii) the constructive techniques of building components; (iv) the perception of building protection (e.g. insulation to improve the thermal efficiency, snow protection); (v) the understanding of the parameters for the qualification and (vi) the understanding of the scale of work.

The modelling of impacts caused by flash floods, urban floods, coastal floods and debris requires further detailed information such as: hydrostatic pressure caused by the weight of water, which increases as the water rises; hydrodynamic forces from moving water, which depends on the flow velocity (Committee and Resources, 2006). Hydrologic and hydraulic factors affect the extent of damage, including inundation depth, flow velocity, the duration of inundation and pollution. These variables are not considered in this work.

6 Conclusions and outlook

This chapter presents the research achievements in terms of the proposed objectives as well as the contribution to science.

6.1 Conclusions

In this dissertation, a methodology for the high-resolution spatial analysis of the physical flood susceptibility of buildings in large river floodplains is developed. The methodology is composed of two main frameworks: a conceptual and a methodological one. The frameworks presented in this paper show a novel approach that has some potential for analysing the physical flood susceptibility on a large scale and can support detailed civil engineering analyses and further social and economic susceptibility analyses. The methods can be transferred to other areas with similar characteristics.

The conceptual framework analyses the vulnerability dimensions and their interrelation by understanding the physical flood susceptibility. It gives a coherent and comprehensive review of flood risk concepts, breaking down the concept and characteristics of physical flood susceptibility and its relation to other types of vulnerabilities based on the most recent literature. Hence, the relation between social and economic vulnerability on the one hand and the physical vulnerability on the other, as well as the need to improve the methods for its determination were confirmed.

The methodological framework consists of three modules which ensure the consistency for the analysis of the physical flood susceptibility and allow to connect the methods. The developed methods in this thesis may provide a first screening of the building stock using a reliable source, such as high-resolution spatial analysis in large river floodplains, before more detailed models can be used.

These modules are engrained with operational tools, including the users' tools and tasks for the assessment of the flood impacts on buildings. The methodology also shows the limitations and relevant considerations for its implementation.

The methodology's applicability and operability are demonstrated by testing the methods in two areas with different social and climatic conditions. Moreover, the methodology constitutes a valuable support for analysing the physical flood susceptibility on a large scale with a high resolution in terms of an efficient use of time, area coverage, data consistency and accessibility for users who cannot investigate huge areas manually.

A method for measuring the uncertainty is set up for each approach: the accuracy of the building extraction can be calculated by combining the horizontal and vertical indices; the validity of clustering the building taxonomic codes can be validated by using the matching percentage; the vagueness of the qualification of the material´s susceptibility can be determined by using a combination of fuzzy set expert analyses and Delphi methods and the derivation of the mean depth-physical impact function includes the standard deviation for the impacted volume of the analysed buildings which share the same taxonomic code.

The implementation of this methodology requires strengthening of institutions at the regional and local level, in order to enable them to effectively fulfil the tasks presented in Figure 33. It implies political plans for: (i) financial investments in preparing human resources to collect and analyse the remote and in-situ data; (ii) financial investments in technological infrastructure for storing data as well as (iii) long-term plans for the maintenance of the resources. Investments in the assessment of the physical susceptibility of buildings are worthwhile because they do not only serve to identify vulnerable settlements, but also allow to define measurements and actions for the mitigation of economic and social losses caused by floodplains.

The developed approaches may be considered as a meaningful contribution to the enhancement and standardisation of data collection for flood impact analyses in buildings located in a floodplain. Still, the potential of the work should be extended when more collected data has been analysed which may support the experts in assessing the flood impacts.

6.2 Outlook

The trend reveals that the lack of data with the desired resolution for building extraction for every site will be overcome in the future thanks to new generations of cameras (e.g. Laser scan, unmanned aerial vehicles), sensors (e.g. near-infrared, shortwave infrared, thermal infrared bands,) and data from e.g. multi-stereo view or omnidirectional imaging, data accessibility, such as Google maps and Google Street View. The enhancement in terms of spectral and spatial resolution of these sources of data will help us to separate buildings from other sealed surfaces, vegetation and heterogeneous multiple-surface layers and for scanning the building geometric characteristics and its components. The combination of this information with the knowledge of experts can support pre-event analysis for the estimation of flood impacts.

The advance of methods and algorithms will allow the users to extract building features and parameters from free sources, such as the application of ICIS (2009). Tools like these will facilitate the implementation of the semantic image interpretation of a building feature. The development in tools and data requires in the near future the definition of a pricing policy for data acquisition as well as the interest of decision makers. That allows the realisation of the extraction of buildings with their precise location in the prone floodplain areas at low expenses. Accordingly, the use of spectral and elevation data provides more advantages for the extraction of building parameters than other sources. Moreover, other analyses can be carried out with these sources: e.g. the calculation of the distance between the building to the water surface or the position of the building in relation to an assistance spot.

The building taxonomic code is a valuable and reliable source of information, which can be used in other urban areas and in other types of applications, such as social researches (e.g. living condition index, demographic studies, service availability), economic researches (e.g. insurance schemes, cadastral appraisals), energy assessment (e.g. TABULA (Loga et al., 2012)) as well as the assessment of social and economic vulnerabilities. Hence, the approaches must also be tested for supporting further works in social and economic vulnerability analyses, using for example the depth-residential impact function and the depth-damage function in order to build a coherent and holistic picture of patterns and trends of the flood risk and its complexity and dynamic in urban areas.

The approaches of the building taxonomic code and the selection of representative buildings can help to reduce costs and the time required for the surveying of information in urban areas, allowing us to synthesise the process and to transfer knowledge on the building structure. Nevertheless, further settlements should be tested on the basis of this classification in order to strengthen it. In addition, experts can expand the taxonomic code by adding more variables or by subdividing them.

The mean depth-physical impact function must also be tested to support the analysis of other vulnerability types, including e.g. the material's susceptibility for hydrostatic and hydrodynamic variables. This approach can provide a first screening of the building stock before more detailed damage models are used, such as e.g. HAZUS, HOWAD, FLEMOps or the Multi-coloured Manual. The results of those analyses should be implemented and tested within spatial planning policy at national, regional and local level in floodplains (Samuels et al., 2010) as an important chain link of the Millennium Development Goals, to which disaster risk reduction is inherently related (UNISDR, 2007).

The material list of the four named institutions with its resistance classes may be extended on the basis of this approach, increasing the knowledge on various building materials in developing countries. This information may support the calculation of the susceptible volume for components in representative buildings contributing to finely grained analyses by civil engineers. The susceptibility of building materials can be included in the databases of the Building Information Model (BIM), which help civil engineers and architects to find the adequate materials for the construction of new buildings in a floodplain.

The understanding of the difference in the assessment of building material susceptibility in the two regions (Colombia and Germany) can be deepened in further studies through the analysis of the building function (see section 2.1). Collection of detailed information of the material properties, methods for bringing closer the opinion for the qualification and studies about the understanding of the living conditions in the two regions should be carried out. For instance, the live conditions in the pilot sites in Colombia are influenced by the weather and the socio-economic situation and it was observed that the constructions in the pilot sites in Colombia neither require protection against cold weather nor need cellars to store food for the inhabitants.

The integration of the approaches requires the constant development of scripts, GIS tools and databases for making the process more efficient and reliable. Therefore, data filters and index measurements are indispensable in order to guarantee coherent results.

The here developed tools for data collection, data storing and data integration are in the initial stage of development and require continuous testing and improving. Additionally, a further level should be developed to assist the final users and to achieve integration into a DSS. The following activities are proposed: (i) definition of policies for the transfer and conditional use of the information, (ii) testing of the tools for every level of the architecture, (iii) creation of constrictions and filters for data storing, (iv) feeding of the database, (v) increase of knowledge and (vi) training of the experts and users in regard to the whole methodology. These multidisciplinary activities should be integrated including the requirements and capabilities of the majority of the users.

This guidance of the methodology can also be transferred and used for the physical-impact assessment of other types of natural hazards, such as flood duration, flash floods, coastal floods, estuarine floods, groundwater floods and fluvial floods. The qualification of the building material susceptibility for these types of hazards must also be investigated in further works.

References

Abbott, G., McDuling, J., Parsons, S. and Schoeman, J.: Building condition assessment: a performance evaluation tool towards sustainable asset management, p. 14. [online] Available from: http://researchspace.csir.co.za/dspace/handle/10204/1233(Accessed 1 November 2013), 2007.

Adedeji, A. and Salami, A.: Environmental hazard: Flooding and Its Effects on Residential Buildings in Ilorin, Nigeria, [online] Available from: http://www.unilorin.edu.ng/publications/adedeji/%2821%29-Environmental%20Hazards.pdf (Accessed 1 November 2012), 2008.

Adriaans, P. and Zantinge, D.: Data Mining, Pearson Education, New Delhi. ISBN: 9788131707173, 1996.

AdV, A. der V. der L. der B. D.: Dokumentation zur Modellierung der Geoinformationen des amtlichen Vermessungswesens, [online] Available from: http://www.landesvermessung.sachsen.de/inhalt/produkte/karten/top/tk10/tk10.html (Accessed 10 October 2013), 2008.

Aglan, H., Wendt, R. and Livengood, S.: Field Testing of Energy-Efficient Flood-Damage Resistant Residential Envelope Systems Summary Report, [online] Available from: http://www.ibsadvisorsllc.com/_library/ORNL_Field_Testing_of_Energy_Efficient_Flood_Damage_Resistant_Residential_Envelope_Systems.pdf(Accessed 15 August 2013), 2004.

Aguilar, F. J. and Mills, J. P.: Accuracy assessment of lidar-derived digital elevation models, The Photogrammetric Record, 23 (122), 148-169, doi:10.1111/j.1477-9730.2008.00476.x, 2008.

Ahmadi, S., Zoej, M. J. V., Ebadi, H., Moghaddam, H. A. and Mohammadzadeh, A.: Automatic urban building boundary extraction from high resolution aerial images using an innovative model of active contours, International Journal of Applied Earth Observation and Geoinformation, 12(3), 150-157, doi:10.1016/j.jag.2010.02.001, 2010.

Aichholzer, O., Aurenhammer, F., Alberts, D. and Gärtner, B.: A Novel Type of Skeleton for Polygons, Journal of Universal Computer Science, 1(12), 752-761, doi:10.1007/978-3-642-80350-5_65, 1995.

APFM, A. P. on F. M.: Urban Flood Risk Management. A tool for Integrated Flood Management, [online] Available from: http://www.apfm.info/publications/tools/Tool_06_Urban_Flood_Risk_Management.pdf (Accessed 1 November 2013), 2008.

Ashley, R., Garvin, S., Boults, E., Vassilopoulos, A. and Zevenbergen, C.: Advances in urban flood management, Taylor & Francis, Leiden, The Netherlands. ISBN: 9780415436625, 2007.

Awrangjeb, M., Ravanbakhsh, M. and Fraser, C. S.: Automatic detection of residential buildings using LIDAR data and multispectral imagery, ISPRS Journal of Photogrammetry and Remote Sensing, 65(5), 457-467, doi:10.1016/j.isprsjprs.2010.06.001, 2010.

Awrangjeb, M., Zhang, C. and Fraser, C. S.: Automatic reconstruction of building roofs through effective integration of lidar and multispectral imagery, Melbourne, Australia. [online] Available from: hhttp://www.isprs-ann-photogramm-remote-sens-spatial-inf-sci.net/I-3/203/2012/isprsannals-I-3-203-2012.pdf (Accessed 15 June 2013), 2012.

Badilla, E.: Flood hazard, vulnerability and risk assessment in the city of Turrialba, Costa Rica, Master thesis, International Institute For Geo-Information Science and Earth Observation, Enschede, The Netherlands, 2002.

Balica, S.: Applying the flood vulnerability index as a knowledge base for flood risk assessment, UNESCO-IHE, Delft, The Netherlands, ISBN 9780415641579, 2012.

Berdahl, P., Akbari, H., Levinson, R. and Miller, W. A.: Weathering of roofing materials – An overview, Construction and Building Materials, 22(4), 423-433, doi:http://dx.doi.org/10.1016/j.conbuildmat.2006.10.015, 2008.

Berks, F., Colding, J. and Folke, C., Eds.: Navigating social-ecological systems: building resilience for complexity and change, Cambridge University Press, New York, ISBN 9780521815925, 2003.

Birkmann, J.: Measuring vulnerability to promote disaster-resilient societies: Conceptual frameworks and definitions, edited by J. Birkmann, Measuring Vulnerability to Natural Hazards: Towards Disaster Resilient Societies Second Edition, 9-54, ISBN-13: 978-92-808-1202-2, 2013.

Blanco-Vogt, A., Haala, N. and Schanze, J.: Building extraction from remote sensing data for parameterising a building typology: a contribution to flood vulnerability assessment, pp. 147-150, Sao Paulo, doi: 10.1109/JURSE.2013.6550687, 2013.

Blanco-Vogt, A. and Schanze, J.: Assessment of the physical flood susceptibility of buildings on a large scale, Natural Hazards and Earth System Science, 14(8), 2105-2117, doi:10.5194/nhess-14-2105-2014, doi:10.5194/nhess-14-2105-2014 ,2014.

Blanco-Vogt, A., Haala, N. and Schanze, J.: Building parameters extraction from remote sensing data and GIS analysis for the derivation of a building taxonomy of settlements – a contribution to flood building's susceptibility assessment. In: International Journal of Image and Data Fusion, 1- 20, DOI:10.1080/19479832.2014.926296, 2014.

Blong, R.: A New Damage Index, Natural Hazards, 30(1), 1-23, doi:10.1023/A:1025018822429, 2003.

Blum, A. and Gruhler, K.: Typologies of the Built Environment and the Example of Urban Vulnerability Assessment, edited by B. Müller, pp. 147-150, Springer Berlin Heidelberg. [online] Available from: http://dx.doi.org/10.1007/978-3-642-12785-4_17 (Accessed 25 January 2011), 2011.

BMVBS: Hochwasserschutzfibel. Bauliche Schutz- und Vorsorgemaßnahmen in hochwassergefährdeten Gebieten, Berlin. [online] Available from: http://www.elementar-versichern.bayern.de/Hochwasserschutzfibel.pdf (Accessed 25 June 2013), 2006.

BMZ, F. M. for E. C. and D. (BMZ), Germany: Disaster risk management: contributions by German Development Cooperation, Bonn. [online] Available from: http://www.preventionweb.net/publications/view/9444 (Accessed 25 September 2013), 2010.

Bossard, M., Feranec, J. and Otahel, J.: CORINE land cover technical guide – Addendum 2000, edited by EeaEditors, European Environment, (40), 105, 2000.

Boults, E. and Sullivan, C.: Illustrated History of Landscape Design, John Wiley & Sons, Hoboken, New Jersey. ISBN: 9780470289334, 2010.

Boyatzis, R. E.: Transforming Qualitative Information: Thematic Analysis and Code Development, SAGE Publications, Thousand Oaks, California, ISBN-13: 978-0761909613, 1998.

Brauch, H. G.: Concepts of security threats, challenges, vulnerabilities and risks, edited by H. G. Brauch, Ú. Oswald Spring, C. Mesjasz, J. Grin, P. Kameri-Mbote, B. Chourou, P. Dunay, and J. Birkmann, Coping with global environmental change disasters and security, 5, 61-106, doi: 10.1007/978-3-642-17776-7_2, 2011.

Brauch, H. G. and Oswald Spring, Ú.: Introduction: Coping with Global Environmental Change in the Anthropocene, in Coping with Global Environmental Change, Disasters and Security, vol. 5, edited by H. G. Brauch, Ú. Oswald Spring, C. Mesjasz, J. Grin, P. Kameri-Mbote, B. Chourou, P. Dunay and J. Birkmann, pp. 31-60, Springer Berlin Heidelberg. [online] Available from: http://dx.doi.org/10.1007/978-3-642-17776-7_1, 2011.

Brenner, C.: Building extraction, in Airborne and Terrestrial Laser Scanning, vol. XXXVI, edited by G. Vosselman and H.-G. Maas, Cap. 5, pp. 169-212, CRC Press, Scotland, ISBN: 978-1904445-87-6, 2010.

Brito, P. L. and Quintanilha, J. A.: Literature review, 2001-2008, of classification methods and inner urban characteristics identified in multispectral remote sensing images, GEOBIA, vol. 4th, pp. 586-591, Rio de Janeiro, 2012.

Brzev, S., Scawthorn, C., Charleson, A. and Langenbach, R.: Proposed GEM Taxonomy: β ver. 0.1, Global Earthquake Model. [online] Available from: http://www.nexus.globalquakemodel.org/gem-building-taxonomy/posts/updated-gem-basic-building-taxonomy-v1.0 (Accessed 25 September 2013), 2011.

Büchele, B., Kreibich, H., Kron, A., Thieken, A., Ihringer, J., Oberle, P., Merz, B. and Nestmann, F.: Flood-risk mapping: contributions towards an enhanced assessment of extreme events and associated risks, Natural Hazards and Earth System Science, 6(4), 485-503, doi:10.5194/nhess-6-485-2006, 2006.

Bückner, J., Müller, S., Pahl, M. and Stahlhut, O.: Semantic interpretation of remote sensing data, in ISPR2002 Working group VII/7, p. 5, Graz, Austria, doi: 10.1.1.221.9937, 2002.

Cançado, V., Brasil, L., Nascimento, N. and Guerra, A.: Flood risk assessment in an urban area: Measuring hazard and vulnerability, Edinburgh, Scotland, UK. [online] Available from: http://web.sbe.hw.ac.uk/staffprofiles/bdgsa/11th_International_Conference_on_Urban_Drainage_CD/ICUD08/pdfs/699.pdf (Accessed 1 November 2013), 2008.

Canny, J.: A Computational Approach to Edge Detection, Pattern Analysis and Machine Intelligence, IEEE Transactions on, PAMI-8(6), 679-698, doi:10.1109/TPAMI.1986.4767851, 1986.

Cardona, O.: Disaster Risk and Vulnerability: Concepts and Measurement of Human and Environmental Insecurity, edited by H. G. Brauch, Ú. Oswald Spring, C. Mesjasz, J. Grin, P. Kameri-Mbote, B. Chourou, P. Dunay and J. Birkmann, Coping with global environmental change disasters and security, 5, 107-121, doi 10.1007/978-3-642-17776-7_3, 2011.

Cardona, O., Yamín, L., Bernal, G. and Ordaz, M.: Indicators of disaster risk and disaster risk management (IDB-IDEA-ERN), Inter-American Development Bank, [online] Available from: http://idbdocs.iadb.org/wsdocs/getdocument.aspx?docnum=35177671, (Accessed 1 November 2013), 2009.

Carley, J., Engineer, S. C., Blacka, M., Engineer, C., Cox, R., Attwater, C., Watson, P., Officer, N. A. and Council, C. C.: Modelling Coastal Processes and Hazards to Assess Sea Level Rise Impacts for Integration into a Planning Scheme, IPWEA, [online] Available from: https://higherlogicdownload.s3.amazonaws.com/IPWEA/68838c32-065d-4d08-9818-2ffb1a96c24b/UploadedImages/PDFS/Impacts%20&%20Risk%20Assessment%20I/Carley_ModellingCoastalProcessesHazardsToAccessSeaLevelRise.pdf, (Accessed 1 November 2013), 2011.

Carryduff Designs: Roof Types, Design Guides [online] Available from: http://www.carryduffdesigns.co.uk/roof/roof-types.html (Accessed 25 June 2013), 2011.

Carson Dunlop & Associates: Summary of Definitions of Roof Slope Types, [online] Available from: http://www.carsondunlop.com/ (Accessed 21 June 2013), 2010.

Chai, D., Förstner, W. and Yang, M.: Combine markov random fields and marked point processes to extract building from remotely sensed images, Melbourne, Australia. [online] Available from: http://www.isprs-ann-photogramm-remote-sens-spatial-inf-sci.net/I-3/365/2012/isprsannals-I-3-365-2012.pdf (Accessed 21 June 2013), 2012.

Cheng, L., Gong, J., Li, M. and Liu, Y.: 3D building model reconstruction from multi-view aerial imagery and lidar data, Photogrammetric Engineering and Remote Sensing, 77(2), 125-139, 099-1112/11/7702–0125, 2011.

Chu-Carroll, M.: Fuzzy Logic vs. Probability, Scientopia [online] Available from: http://scientopia.org/blogs/goodmath/2011/02/02/fuzzy-logic-vs-probability/ (Accessed 14 October 2013), 2011.

CIA, C. I. A.: The world Factbook, [online] Available from: https://www.cia.gov/library/publications/the-world-factbook/fields/2004.html (Accessed 25 January 2014), 2013.

City of Ottawa: Urban Natural Areas Environmental Evaluation Study, [online] Available from: http://www.ottawa.ca/en/env_water/tlg/alw/green_areas/evaluation_study/index.html (Accessed 21 June 2013), 2006.

Cocina, W.: Fenestration studies on building energy using the facade evaluation facility, Master thesis, University of Nevada, Las Vegas. [online] Available from: http://digitalscholarship.unlv.edu/thesesdissertations/1289/ (Accessed 21 June 2013), 2011.

Committee and Resources: Reducing Vulnerability of Buildings to Flood Damage: Guidance on Building in Flood Prone Areas, Hawkesbury-Nepean Floodplain Management Steering Committee, Hawkesbury. [online] Available from: http://www.ses.nsw.gov.au/content/documents/pdf/resources/Building_Guidelines.pdf (Accessed 25 September 2013), 2006.

Concise Encyclopedia: Britannica Digital Learning, [online] Available from: http://www.merriam-webster.com/dictionary (Accessed 21 June 2013), 2013.

Congalton, R. G. and Green, K.: Assessing the Accuracy of Remotely Sensed Data: Principles and Practices, Second Edition, Taylor & Francis. ISBN: 9781420055139, 2008.

Coppi, R., Gil, M. A. and Kiers, H. A. L.: The fuzzy approach to statistical analysis, Computational Statistics & Data Analysis, 51(1), 1-14, doi:10.1016/j.csda.2006.05.012, 2006.

Cormagdalena: Estudio de navegabilidad del río Magdalena, Bogotá, Colombia. [online] Available from: http://fs03eja1.cormagdalena.com.co/nuevaweb/AdmonCon/Documentos/estudio%20de%20navegabilidad%20del%20r%c3%8do%20magdalena.pdf (Accessed 21 June 2013), 2000.

Corzo, H.: Estimación integral del riesgo de inundación en ríos de llanura de un centro urbano, Neuquén, Argentina. [online] Available from: http://www.cadp.org.ar/docs/congresos/2010/07.pdf (Accessed 21 June 2013), 2010.

CRED, Guha-Sapir, D., Vos, F., Below, R. and Posserre, S.: Annual Disaster Statistical Review 2010 The numbers and trends, Centre for Research on the Epidemiology of Disaster, Brussels, Belgium. [online] Available from: http://www.cred.be/sites/default/files/ADSR_2010.pdf (Accessed 21 June 2013), 2010.

Cutter, S. L. and Finch, C.: Temporal and spatial changes in social vulnerability to natural hazards, Proceedings of the National Academy of Sciences of the United States of America, 2301-2306, doi: 10.1073/pnas.0710375105 , 2008.

Dash, J., Steinle, E., Singh, R. and Bähr, H.: Automatic building extraction from laser scanning data: an input tool for disaster management, Advances in Space Research, 33(3), 317-322, doi:10.1016/S0273-1177(03)00482-4, 2004.

Dean, R. G. and Dalrymple, R. A.: Coastal Processes with Engineering Applications, Cambridge University Press. [online] Available from: http://dx.doi.org/10.1017/CBO9780511754500 (Accessed 21 June 2103), 2001.

Desmond, E.: The Impact of Global Change on Erosion and Sediment Transport by Rivers: Current Progress and Future Challenges, The United Nations World Water Assessment Programme, UNESCO-IHP, Paris, France. [online] Available from: http://unesdoc.unesco.org/images/0018/001850/185078E.pdf, 2009.

Deutscher Wetterdienst: Ausgabe der Klimadaten-Mittelwerte bezogen auf den Standort für den Zeitraum 1961-1990. [online] Available from: http://www.dwd.de/bvbw/appmanager/bvbw/dwdwwwDesktop?_nfpb=true&_pageLabel=dwdwww_result_page&gsbSearchDocId=675120 (Accessed 10 October 2013), 2012.

DeVenecia, K., Stewart, W. and Bingcai, Z.: New approaches to generating and processing high resolution elevation data with imagery, edited by D. Fritsch, pp. 297-308, Stuttgart. [online] Available from: http://www.ifp.uni-stuttgart.de/publications/phowo07/330DeVenecia.pdf, 2007.

Diffrient, N., Tilley, A. R. and Bardagjy, J.: Humanscale 1/2/3, Mit Press, Cambridge, Mass. ISBN: 9780262040426, 1974.

Douglas, D. H. and Peucker, T. K.: Algorithms for the reduction of the number of points required to represent a digitized line or its caricature, Cartographica The International Journal for Geographic Information and Geovisualization, 10(2), 112-122, doi: http://dx.doi.org/10.3138/FM57-6770-U75U-7727, 1973.

Douglas, J.: RISK-NAT (Module 4): Methods and tools for risk evaluation, Progress report RP-54041-FR, BRGM, Progress report RP-54041-FR, BRGM, Orleans, France. [online] Available from: http://www.brgm.fr/publication/rechRapportSP. jsp, 2005.

Douglas, J.: Physical vulnerability modelling in natural hazard risk assessment, Natural Hazards and Earth System Science, 7(2), 283-288, doi:10.5194/nhess-7-283-2007, 2007.

Downs, T.: Hanoi & Halong Bay Encounter, Lonely Planet, Hanoi, Vietnam. ISBN: 9781741790924, 2007.

Downton, M. W. and Pielke, R. A.: How Accurate are Disaster Loss Data? The Case of U.S. Flood Damage, Natural Hazards, 35(2), 211-228, doi: 0.1007/s11069-004-4808-4, 2005.

Dutta, D., Herath, S. and Musiake, K.: A mathematical model for flood loss estimation, Journal of Hydrology, 277(1-2), 24–49, doi:10.1016/S0022-1694(03)00084-2, 2003.

Dutta, D. and Tingsanchali, T.: Development of loss functions for urban flood risk analysis in Bangkok. In: International symposium on new technologies for urban safety of mega cities in Asia. International Center for Urban Safety Engineering, University of Tokyo, Japan, 2003.

Egli, T. and Wehner, K.: Non structural flood plain management: measures and their effectiveness, edited by I. C. for the P. of the Rhine, International Commission for the Protection of the Rhine. [online] Available from: http://www.iksr.org/index.php?id=266&L=3&pdfPage=1 (Accessed 21 June 2013), ISBN: 3-935324-47-2, 2002.

Eleutério, J. and Martinez, E. D.: Automating the evaluation of flood damages: methodology and potential gains, Geophysical Research Abstracts, 12(2), 7063-7063, 2010.

Emmitt, S. and Gorse, C.: Barry's Introduction to Construction of Buildings, Wiley-Blackwell, Oxford, UK. ISBN: 1-4051-1055-4. [online] Available from: http://samples.sainsburysebooks.co.uk/9781405146791_sample_378914.pdf (Accessed 21 June 2013), 2010.

Ender, J. H. G. and Brenner, A. R.: PAMIR – A Wideband Phased Array SAR/MTI System, 4th European Conf on Synthetic Aperture Radar, 150(3), 157-162, ISBN: 3-8007-2697-1, 2003.

EnggPedia: The engineering Encyclopedia, [online] Available from: http://www.enggpedia.com (Accessed 21 June 2013), 2013.

Escarameia, M., Karanxda, A. and Tagg, A.: Improving the flood resilience of buildings through improved materials, methods and details, CIRIA, London, UK. [online] Available from: http://www.ciria.org.uk/flooding/pdf/WP5 Lab Testing Report.pdf (Accessed 25 September 2013), 2006.

Escarameia, M., Tagg, A. F., Walliman, N., Zevenbergen, C. and Anvarifar, F.: The role of building materials in improved flood resilience and routes for implementation, Rotterdam, The Netherlands. [online] Available from: http://eprints.hrwallingford.co.uk/572/1/HRPP538_The_role_of_building_materials_in_improved_flood_resilience_and_routes_for_implementation.pdf (Accessed 21 June 2013), 2012.

Van Essen, R.: Maps Get Real: Digital Maps evolving from mathematical line graphs to virtual, pp. 3-18, Springer Berlin Heidelberg, Berlin/Heidelberg. [online] Available from: http://dx.doi.org/10.1007/978-3-540-72135-2_1 (Accessed 21 June 2013), 2008.

Evans, E., Hall, J., Thorne, C., Penning-Rowsell, E., Watkinson, A. and Sayers, P.: Future flood risk management in the UK, Proceedings of the ICE Water Management, 159(1), 53-61, 2006.

EXCIMAP, Exchange circle on flood mapping: Handbook on good practices for flood mapping in Europe, [online] Available from: http://ec.europa.eu/environment/water/flood_risk/flood_atlas/pdf/handbook_goodpractice.pdf, 2007.

Fedeski, M. and Gwilliam, J.: Urban sustainability in the presence of flood and geological hazards: The development of a GIS-based vulnerability and risk assessment methodology, Landscape and Urban Planning, 83 (1), 50-61, ISSN: 0169-2046, 2007.

Fekete, A.: Validation of a social vulnerability index in context to river-floods in Germany, Natural Hazards and Earth System Science, 9(2), 393-403, www.nat-hazards-earth-syst-sci.net/9/393/2009, 2009.

FEMA, E. M. I.: Introduction to Hazard Mitigation, Training FEMA [online] Available from: http://training.fema.gov/EMIWeb/IS/is393alst.asp (Accessed 21 June 2013), 2004.

FEMA, E. M. I.: Flood Damage-Resistant Materials Requirements for Buildings Located in Special Flood Hazard Areas in accordance with the National Flood Insurance Program, [online] Available from: http://www.fema.gov/library/viewRecord.do?id=1580 (Accessed 21 June 2013), 2008.

FEMA, E. M. I.: Earthquake-Resistant Design Concepts. An Introduction to the NEHRP Recommended Seismic Provisions for New Buildings and Other Structures, Federal Emergency Management Agency.The Building Seismic Safety Council (BSSC), established by the National Institute of Building Sciences (NIBS). [online] Available from: http://bssc.nibs.org/client/assets/files/bssc/P749/P-749_Chapter4.pdf (Accessed 21 June 2013), 2010.

Fischler, M. A. and Bolles, R. C.: Random sample consensus: a paradigm for model fitting with applications to image analysis and automated cartography, edited by M. A. Fischler and Oe. Firschein, Communications of the ACM, 24(6), 381-395, ACM 0001-0782/81/0600-0381 1981.

Flood, M.: Vertical Accuracy Reporting for Lidar Data, ASPRS Guidelines, ASPRS, Maryland. [online] Available from: http://www.asprs.org/a/society/committees/lidar/Downloads/Vertical_Accuracy_Reporting_for_Lidar_Data.pdf (Accessed 21 June 2011), 2004.

Forte, F., Strobl, R. O. and Pennetta, L.: A methodology using GIS, aerial photos and remote sensing for loss estimation and flood vulnerability analysis in the Supersano-Ruffano-Nociglia Graben, southern Italy, Environmental Geology, 50(4), 581-594, doi: 10.1007/s00254-006-0234-0, 2006.

Fraser, C. ., Baltsavias, E. and Gruen, A.: Processing of Ikonos imagery for submetre 3D positioning and building extraction, ISPRS Journal of Photogrammetry and Remote Sensing, 56(3), 177-194, doi:10.1016/S0924-2716(02)00045-X, 2002.

De Freitas, V. P., Abrantes, V. and Crausse, P.: Moisture migration in building walls – Analysis of the interface phenomena, Building and Environment, 31(2), 99-108, doi:10.1016/0360-1323(95)00027-5, 1996.

Friedmann, D.: The Nature of Vision – Inspecting Complex Systems, Why We See or Do Not See Things We Are Looking For – Or Should Be Looking For, InspectAPedia [online] Available from: http://inspectapedia.com/vision/vision.htm (Accessed 21 June 2013), 2005.

Fugate, D., Tarnavsky, E. and Stow, D.: A Survey of the Evolution of Remote Sensing Imaging Systems and Urban Remote Sensing Applications, edited by T. Rashed and C. Jürgens, Remote Sensing and Digital Image Processing, 10 (Chapter 7), 119-139, doi: 10.1007/978-1-4020-4385-7, 2010.

Füssel, H.-M.: Vulnerability: A generally applicable conceptual framework for climate change research, edited by J. Banhart, M. F. Ashby and N. Ae. Fleck, Global Environmental Change, 17(2), 155-167, doi:10.1016/j.gloenvcha.2006.05.002, 2007.

Galaz, V., Olsson, P., Hahn, T., Folke, C. and Svedin, U.: The Problem of Fit among Biophysical Systems, Environmental and Resource Regimes, and Broader Governance Systems: Insights and Challenges, in Institutions and Environmental Change Principal Findings Applications and Research Frontiers, edited by O. R. Young, L. A. King, and H. Schroeder, pp. 147-186, MIT Press., Cambridge, USA. doi: 10.7551/mitpress/9780262240574.001.0001, 2008.

Galster, G., Hanson, R., Ratcliffe, M. R., Wolman, H., Coleman, S. and Freihage, J.: Wrestling Sprawl to the Ground: Defining and Measuring an Elusive Concept, Housing Policy Debate, 12(4), 681-717, Preview, doi: 10.1080/10511482.2001.9521426, 2001.

Garvin, S., Reid, J. F. and Scott, M.: Construction Industry Research and Information Association C623, Standards for the repair of buildings following flooding, CIRIA Publication, London, 2005.

GEF: Progress on the implementation of the GEF strategic approach to capacity development, Global Environment Facility, GEF Council, Washington, DC. [online] Available from: http://www.thegef.org/gef/node/557 (Accessed 21 June 2013), 2005.

Geobasisinformation und Vermessung: Landeseinheitliche Parameter für Orthophotos aus Bildflügen mit digitalen Kameras, [online] Available from: http://www.landesvermessung.sachsen.de/inhalt/produkte/luftbild/luftser/paramdop.html (Accessed 23 September 2013), 2005.

Gerke, M., Heipke, C. and Straub, B. M.: Building extraction from aerial imagery using a generic scene model and invariant geometric moments, IEEEISPRS Joint Workshop on Remote Sensing and Data Fusion over Urban Areas Cat No01EX482, 0, 85-89, doi:10.1109/DFUA.2001.985732, 2001.

Girling, C. L. and Kellett, R.: Skinny streets and green neighborhoods: design for environment and community, Island Press, Washington, ISBN: 9781597266277, 2005.

Google maps: The never-ending quest for the perfect map, Google TM Official Blog [online] Available from: http://googleblog.blogspot.de/2012/06/never-ending-quest-for-perfect-map.html (Accessed 21 June 2013), 2012.

Green building advisor: Structure: Exterior Walls, [online] Available from: http://www.greenbuildingadvisor.com/green-basics/structure-exterior-walls (Accessed 25 September 2014), 2013.

Green, C. H., Viavattene, C. and Thompson, P.: Guidance for assessing flood losses, CONHAZ report, Flood Hazard Research Centre, Middlesex. [online] http://www.iwrm-net.eu/node/14965 (Accessed 21 June 2013), 2011.

Grigillo, D., Kosmatin Fras, M. and Petrovič, D.: Automated building extraction from IKONOS images in suburban areas, International Journal of Remote Sensing, 33(16), 5149-5170, doi: 10.1080/01431161.2012.659356, 2012.

Gröger, G., Kolbe, T., Nagel, C. and Häfele, K.-H.: OGC City Geography Markup Language (CityGML) En-coding Standard. [online] Available from: http://www.citygml.org/index.php?id=1522 (Accessed 21 June 2013), 2012.

Gromicko, N. and London, R.: How to Determine the Age of a Building, International association of professional home and commercial property inspectors, Inspecting the word [online] Available from: http://www.nachi.org/determine-building-age.htm (Accessed 21 June 2013), 2011.

Grundwasserforschungszentrum, D.: Gemeinsame Mitteilungen des Dresdner Grundwasserforschungszentrums e.V. und seiner Partner, Hille. ISSN 1611-5627, Dresden, Germany. [online] Available from: http://www.gwz-dresden.de/dgfz-ev/veroeffentlichungen/schriftenreihe-dgfz-ev-partner.html (Accessed 7 August 2013), 2012.

Grünthal, G.: European Macroseismic Scale 1998 EMS-98, European Seismological Commision, Luxembourg. [online] Available from: http://media.gfz-potsdam.de/gfz/sec26/resources/documents/PDF/EMS-98_Original_englisch.pdf, ISBN 2-87977-008-4, 1998.

GTZ, G. A. for T. C., DKKV, G. C. for D. R. and University of Bayreuth: Linking Disaster Risk Reduction and Poverty Reduction, Disasters, 43, 709, [online] Available from: http://www.unisdr.org/files/3293_LinkingDisasterRiskReductionPovertyReduction.pdf, (Accessed 7 August 2013), 2008.

Guillaso, S., D'Hondt, O. and Hellwich, C.: Building Characterization using Polarimetric Tomographic SAR Data, pp. 234-237, Sao Paulo, doi: 10.1109/JURSE.2013.6550708, 2013.

Haala, N. and Kada, M.: An update on automatic 3D building reconstruction, ISPRS Journal of Photogrammetry and Remote Sensing, 65(6), 570-580, doi:10.1016/j.isprsjprs.2010.09.006, 2010.

Haala, N. and Rothermel, M.: Dense Multi-Stereo Matching for high quality digital elevation models, PFG Photogrammetrie, Fernerkundung, Geoinformation – Jahrgang 2012, (Heft 6), 327–340, doi:10.1127/1432-8364/2012/0121, 2012.

Haggag, M. A. and Ayad, H. M.: The urban structural units method: a basis for evaluating environmental prospects for sustainable development, Urban Design International, 7(2), 97-108, doi:10.1057/palgrave.udi.9000071, 2002.

Haithcoat, T., Song, W. and Hipple, J.: Building Extraction – LIDAR R&D Program for NASA/ICREST Studies. [online] Available from: http://www.grc.missouri.edu/icrestprojarchive/NASA/FeatureExtraction-Buildings/REPYear2-build-extraction.pdf (Accessed 25 June 2012), 2001.

Hansson, K., Danielson, M. and Ekenberg, L.: A framework for evaluation of flood management strategies, Journal of Environmental Management, 86(3), 465-480, doi:10.1016/j.jenvman.2006.12.037, 2008.

Heiden, U., Heldens, W., Roessner, S., Segl, K., Esch, T. and Mueller, A.: Urban structure type characterization using hyperspectral remote sensing and height information, Landscape and Urban Planning, 105(4), 361-375, doi:10.1016/j.landurbplan.2012.01.001, 2012.

Heipke, C., Mayer, H., Wiedemann, C. and Jamet, O.: Evaluation of automatic road extraction, pp. 151-160, ISPRS, München. [online] Available from: http://citeseerx.ist.psu.edu/viewdoc/download?doi=10.1.1.30.7686&rep=rep1&type=pdf (Accessed 21 June 2013a), 1997.

Herold, M., Gardner, M. and Roberts, D.: Spectral resolution requirements for mapping urban areas, Institute of Electrical and Electronics Engineers, Inc, 445 Hoes Ln, Piscataway, NJ, 08854-1331, UK,. [online] Available from: http://ieeexplore.ieee.org/lpdocs/epic03/wrapper.htm?arnumber=1232205 (Accessed 21 June 2013), doi: 10.1109/TGRS.2003.815238, 2003.

Herold, M. and Roberts, D.: The Spectral Dimension in Urban Remote Sensing, pp. 47-66, Springer Netherlands, doi:10.1007/978-1-4020-4385-7_4, 2010.

Hoang, C. P., Kinney, K. A., Corsi, R. L. and Szaniszlo, P. J.: Resistance of green building materials to fungal growth, International Biodeterioration & Biodegradation, 64(2), 104-113, doi:10.1016/j.ibiod.2009.11.001, 2010.

Hollenstein, K.: Reconsidering the risk assessment concept: Standardizing the impact description as a building block for vulnerability assessment, Natural Hazards And Earth System Science, 5(3), 301-307, SRef-ID: 1684-9981/nhess/2005-5-30, 2005.

Home 4 India: Material Estimate Calculator, [online] Available from: http://homes4india.com/MaterialEstimator.aspx (Accessed 21 June 2013), 2010.

Hong, T.-P. and Lee, C.-Y.: Induction of fuzzy rules and membership functions from training examples, Fuzzy Sets and Systems, 84(1), 33-47, doi:10.1016/0165-0114(95)00305-3, 1996.

Hussain, M., Davies, C. and Barr, R.: Classifying Buildings Automatically: A Methodology, [online] Available from: http://www.geos.ed.ac.uk/~gisteac/proceedingsonline/GISRUK2007/PDF/6A2.pdf. (Accessed 21 June 2013), 2006.

ICDE: Mapa de emergencia invernal, [online] Available from: http://www.icde.org.co (Accessed 21 June 2013), 2011.

ICE: About structures and buildings. The Institution of Civil Engineering, Structures and buildings, [online] Available from: http://www.ice.org.uk/topics/structuresandbuildings/About (Accessed 7 September 2013), 2010.

ICIS: Simple Google Earth Image Enhancement With SpaceEye, Image Processing and Intelligent Systems Laboratory, School of Electronic Information, Wuhan University, China, 2009.

IDEAM: Informe Hidrológico Diario, Instituto de hidrología, metereología y estudios ambientales, Bogotá, Colombia. [online] Available from: http://www.pronosticosyalertas.gov.co/jsp/loader.jsf?lServicio=Publicaciones&lTipo=publicaciones&lFuncion=loadContenidoPublicacion&id=751 (Accessed 21 June 2013a), 2010 a.

IDEAM: Inventario de información, Instituto de hidrología, metereología y estudios ambientales, Bogotá, Colombia. [online] Available from: http://institucional.ideam.gov.co/jsp/inventario-de-informacion_2190 (Accessed 21 June 2013b), 2010 b.

IDMC: Global estimates 2014: people displaced by disasters, [online] Available from: http://www.internal-displacement.org/publications/2014/global-estimates-2014-people-displaced-by-disasters/ (Accessed 21 June 2015), 2014.

IFRC: India: Monsoon Floods 2014 Emergency Plan of Action (EPoA), DREF Operation MDRIN014. International Federation of Red Cross And Red Crescent Societies. [online] Available from: http://reliefweb.int/report/india/india-monsoon-floods-2014-emergency-plan-action-epoa-dref-operation-mdrin014 (Accessed 03 November 2014), 2014.

IGAC: Características básicas de ortoimages., Banco Nacional de Imagenes. Bogotá-Colombia, [online] Available from: http://mapascolombia.igac.gov.co/wps/portal/mapasdecolombia/c0/04_SB8K8xLLM9MSSzPy8xBz9CP0os3g_0xBjb1MjYwMDMxcTAyPDEEtfDw9HQwN3Y_2CbEdFAFS69wA!, 2007.

IKSE: Dokumentation des Hochwassers vom August 2002 im Einzugsgebiet der Elbe, Magderburg. [online] Available from: http://www.ikse-mkol.org/uploads/media/Text_Tabellen.pdf (Accessed 10 October 2013), 2004.

Interspect Kft: How the world's most detailed aerial image was made, [online] Available from: http://www.interspect.net/index.php/Cegunk-es-eszkozparkunk/aktualitasok.html (Accessed 21 June 2013), 2012.

Jacobsen, K.: DEM generation from satellite data, Remote Sensing in Transition, 513-525, Millpress Rotterdam, ISBN 90 5966 007 2, 2004.

Janssen, M. and Ostrom, E.: Resilience, vulnerability, and adaptation: A cross-cutting theme of the International Human Dimensions Programme on Global Environmental Change, 237-239, doi:10.1016/j.gloenvcha.2006.04.003, 2006.

Jarvis, A.: Integration of Photogrammetric and LiDAR Data for Accurate Reconstruction and Visualization of Urban Environments, UCGE Reports Number 20282. Master Thesis, University of Calgary, Calgary, Alberta. [online] Available from: http://www.ucalgary.ca/engo_webdocs/AH/08.20282.Anna_Jarvis.pdf (Accessed 21 June 2013), 2008.

Jarvis, R. A.: On the identification of the convex hull of a finite set of points in the plane, Information Processing Letters, 2(1), 18-21, doi:10.1016/0020-0190(73)90020-3, 1973.

Jensen, J. R. and Cowen, D. C.: Remote sensing of urban/suburban infrastructure and socio-economic attributes, Photogrammetric Engineering and Remote Sensing, 65(5), 611-622, 0099-1112I99I6505-611, 1999.

Jha, A., Bloch, R. and Lamond, J.: Cities and Flooding A Guide to Integrated Urban Flood Risk Management for the 21st Century, World Bank, GFDRR Global Facility for Disaster Reduction and Recovery, Washington D.C. [online] Available from: https://www.gfdrr.org/node/1068 (Accessed 21 June 2013), 2012.

Jiang, B. and Yao, X.: Geospatial analysis and modeling of urban structure and dynamics: an overview, pp. 3-11, Springer Netherlands. [online] Available from: http://dx.doi.org/10.1007/978-90-481-8572-6_13 (Accessed 21 June 2013), 2010.

Jongman, B., Kreibich, H., Apel, H., Barredo, J. I., Bates, P. D., Feyen, L., Gericke, A., Neal, J., Aerts, J. C. J. H. and Ward, P. J.: Comparative flood damage model assessment: towards a European approach, Natural Hazards and Earth System Science, 12(12), 3733-3752, doi:10.5194/nhess-12-3733-2012, 2012.

Kabolizade, M., Ebadi, H. and Ahmadi, S.: An improved snake model for automatic extraction of buildings from urban aerial images and LiDAR data, Computers, Environment and Urban Systems, 34(5), 435-441, doi:10.1016/j.compenvurbsys.2010.04.006, 2010.

Kailasrao, D. N., Husen, S. and Vikram, S.: A review of techniques to recognise and extract man-made objects from topographic images, International journal of advanced scientific and technical research, 361-375, 0099-1112/04/7012–1383, 2012.

Kang, J., Su, M. and Chang, L.: Loss functions and framework for regional flood damage estimation in residential area, Journal of Marine Science and Technology, 13(3), 193-199, [online] Available from: http://jmst.ntou.edu.tw/marine/13-3/193-199.pdf (Accessed 21 June 2013), 2005.

Kasperson, J. X., Kasperson, R. E. and Turner, B. L.: Regions at Risk: Comparisons of Threatened Environments, edited by J. X. Kasperson, R. E. Kasperson, and B. Le. Turner II, United Nations University Press. [online] Available from: http://www.unu.edu/unupress/unupbooks/uu14re/uu14re00.htm#Contents (Accessed 21 June 2013), ISBN 92-808-0848-6, 1995.

Kaufman, L. and Rousseeuw, P. J.: Finding Groups in Data, edited by L. Kaufman and P. Je. Rousseeuw, Wiley. [online] Available from: http://doi.wiley.com/10.1002/9780470316801, 1990.

Kelman, I.: Physical Flood Vulnerability of Residential Properties in Coastal, Eastern England, Ph.D. thesis, University of Cambridge, U.K. Ph.D. Thesis. [online] Available from: www.ilankelman.org/phd/IlanKelmanPhDDissertation.doc (Accessed 21 June 2013), 2002.

Kim, C. and Habib, A.: Object-Based Integration of Photogrammetric and LiDAR Data for Automated Generation of Complex Polyhedral Building Models, Sensors, Peterboroug, 9(7), 5679-5701, 2009.

Kim, T., Javzandulam, T. and Lee, T.: Semiautomatic reconstruction of building height and footprints from single satellite images, Engineering, 4737-4740, doi:10.3390/s90705679, 2007.

Kluckner, S.: Semantic Interpretation of Digital Aerial Images Utilizing Redundancy, Appearance and 3D Information, Ph.D. Thesis, Graz University of Technology, Graz, February. [online] Available from: http://www.icg.tugraz.at/publications/semantic-interpretation-of-digital-aerial-images-utilizing-redundancy-appearance-and-3d-information (Accessed 21 June 2013), 2011.

Kosko, B.: Fuzzy Thinking: The New Science of Fuzzy Logic, HarperCollins Publishers Limited, ISBN-13: 978-0786880218, 1994.

Krapesch, G., Hauer, C. and Habersack, H.: Scale orientated analysis of river width changes due to extreme flood hazards, Natural Hazards and Earth System Science, 11(8), 2137-2147, doi:10.5194/nhess-11-2137-2011, 2011.

Kreibich, H., Seifert, I., Merz, B. and Thieken, A. H.: Development of FLEMOcs – a new model for the estimation of flood losses in the commercial sector, Hydrological Sciences Journal, 55(8), 1302-1314, ISSN: 0262-6667, 2010.

Kron, A.: Flood Damage Estimation and Flood Risk Mapping, in Advances in Urban Flood Management, pp. 213-235, Taylor & Francis. [online] Available from: http://dx.doi.org/10.1201/9780203945988.ch10, ISBN 0–203–94598–0, 2007.

Krueger, T.: Digitale Geländemodelle im Hochwasserschutz: Detektion, Extraktion und Modellierung von Deichen und vereinfachte GIS-basierte Überflutungssimulationen, Ph.D. Thesis, Technische Universität Dresden. [online] Available from: http://nbn-resolving.de/urn:nbn:de:bsz:14-qucosa-25018 (Accessed 21 June 2013), 2009.

Kruger, F., Meissner, R., Grongroft, A. and Grunewald, K.: Flood induced heavy metal and arsenic contamination of Elbe River floodplain soils, Acta Hydrochimica et Hydrobiologica, 33(5), 455-465, doi: 10.1002/aheh.200400591, 2005.

Kuhlicke, C., Scolobig, A., Tapsell, S., Steinführer, A. and De Marchi, B.: Contextualizing social vulnerability: findings from pilot sites across Europe, Natural Hazards, 58(2), 789-810, doi: http://dx.doi.org/10.1007/s11069-011-9751-6, 2011.

Kundra, H., Panchal, V. K., Arora, S., Karandeep, S. and Kaura, H.: Extraction of Satellite Image using Particle Swarm Optimization, International Journal of Engineering, 4(1) [online] Available from: http://www.cscjournals.org/csc/manuscript/Journals/IJE/volume4/Issue1/IJE-151.pdf (Accessed 21 June 2013), 2010.

Kwakernaak, H.: Fuzzy random variables – I. definitions and theorems, Information Sciences, 15(1), 1-29, doi:10.1016/0020-0255(78)90019-1, 1978.

Lafarge, F., Descombes, X., Zerubia, J. and Pierrot-Deseilligny, M.: Automatic building extraction from DEMs using an object approach and application to the 3D-city modeling, ISPRS Journal of Photogrammetry and Remote Sensing, 63(3), 365-381, doi:10.1016/j.isprsjprs.2007.09.003, 2008.

Lasswell, H. D.: The structure and function of communication in society, in The Communication of Ideas, pp. 37-52, New York-: The Institute for Religious and Social Studies. [online] Available from: http://www.themedfomscu.org/media/elip/The%20structure%20and%20function%20of.pdf, 1948.pdf, 1948.

Leichenko R.M. and O'Brien K.L.: The Dynamics of Rural Vulnerability to Global Change: The Case of southern Africa, 1-18, doi: 10.1023/A:1015860421954, 2002.

Lein, H., Berthling, C., Brun, C., Rod, J. and Vatne, G.: A conceptual model for assessing the geography of social vulnerability, environmental hazards and climate change, in Climate Change: Global Risks, Challenges and Decisions, vol. 6. doi:10.1088/1755-1307/6/4/442007, 2009.

Lemmens, M.: Geo-information: Technologies, Applications and the Environment, Springer. ISBN: 9789400716674, 2011.

Levy, J.: Multiple criteria decision making and decision support systems for flood risk management, Stochastic Environmental Research and Risk Assessment, 19(6), Springer-Verlag, 438-447, doi:10.1007/s00477-005-0009-2, 2005.

Li, R.: Mobile Mapping: An Emerging Technology for Spatial Data Acquisition, in The Map Reader, pp. 170-177, John Wiley & Sons, Ltd. [online] Available from: http://dx.doi.org/10.1002/9780470979587.ch24, 2011.

Linstone, H. A. and Turoff, M.: The Delphi method: techniques and applications, Addison-Wesley Pub. Co., Advanced Book Program. ISBN: 9780201042948, 1975.

Liu, W. and Yamazaki, F.: Building height detection from high-resolution TerraSAR-X imagery and GIS data, pp. 033-036, Sao Paulo. doi:10.1109/JURSE#.2013.6550659, 2013.

Liu, Y.-K. and Liu, B.: A class of fuzzy random optimization: expected value models, Information Sciences, 155(1-2), 89-102, doi:10.1016/S0020-0255(03)00079-3, 2003.

Loga, T., Diefenbach, N., Dascalaki, E. and Balaras, C.: Application of Building Typologies for Modelling the Energy Balance of the Residential Building Stock: TABULA Thematic Report N° 2, edited by N. Diefenbach and T. E. Loga, Institut Wohnen und Umwelt GmbH. [online] Available from: http://www.building-typology.eu/tabula.html (Accessed 25 September 2013), 2012.

López, D. L.: Spatial analysis and modeling to assess and map current vulnerability to extreme weather events in the Grijalva – Usumacinta watershed, México, IOP Conference Series: Earth and Environmental Science, 8, doi: 10.1088/1755-1315/8/1/012021, 2009.

MacQueen, J. Some methods for classification and analysis of multivariate observations. Proceedings of the Fifth Berkeley Symposium on Mathematical Statistics and Probability, Volume 1: Statistics, 281--297, University of California Press, Berkeley, Calif., MR0214227, 1967.

Maene, C.: Find Adjacent & Neighboring Polygons. [online] Available from: http://resources.arcgis.com/de/gallery/file//geoprocessing/details?entryID=50F58FCF-1422-2418-884B-A053393CEF92 (Accessed 25 June 2012, 2011.

Magsino, S. L., Eno, J. P. and Edkin, E. J.: Applications of Social Network Analysis for Building Community Disaster Resilience: Workshop, National Research Council, National Academies Press. [online] Available from: http://www.nap.edu/catalog.php?record_id=12706 (Accessed 21 June 2013), 2009.

Maiwald, H. and Schwarz, J.: Berücksichtigung der Fließgeschwindigkeit bei Hochwasser-Schadensmodellen, Bautechnik, 86(9), 550-565, doi:10.1002/bate.200910056, 2009.

Majlingová, A. and Lubinszká, Z.: An assessment of urban area flood susceptibility, Ostrava. [online] Available from: http://gis.vsb.cz/GIS_Ostrava/GIS_Ova_2011/sbornik/papers/Lubinszka.pdf (Accessed 29 August 2013), 2011.

Manyena, S. B.: The concept of resilience revisited, Research Associate, Disaster and Development Centre, School of Applied Sciences, Northumbria University, UK, 433-450, doi:/10.1111/j.0361-3666.2006.00331.x, 2006.

Marshall, S.: Streets & patterns, Taylor & Francis, Routledge. ISBN: 9780415317504, 2005.

McGahey, C., Mens, M., Sayers, P., Luther, J., Petroska, M. and Schanze, J.: Methodology for a DSS to support long-term flood risk management planning, [online] Available from: http://www.floodsite.net/html/partner_area/search_results3b.asp?docID=874 (Accessed 25 September 2013), 2009.

McGlone, J. C. and Shufelt, J. A.: Projective and Object Space Geometry for Monocular Building Extraction, Image Rochester NY, 54-61, doi: 10.1109/CVPR.1994.323810, 1994.

Mehta, T.: Interpolation using a VBA function, [online] Available from: http://www.tushar-mehta.com/excel/newsgroups/interpolation/#A_VBA_function_, 2012.

Mercer, B.: Combining LIDAR and IfSAR: What can you expect?, Photogrammetric Week, (1999), 227-237. [online] Available from: http://www.ifp.uni-stuttgart.de/publications/phowo01/Mercer.pdf (Accessed 25 September 2013), 2001.

Merz, B., Kreibich, H., Thieken, A. and Schmidtke, R.: Estimation uncertainty of direct monetary flood damage to buildings, Natural Hazards and Earth System Science, 4(1), 153-163, doi:10.5194/nhess-4-153-2004, SRef-ID: 1684-9981/nhess/2004-4-153, 2004.

Mesev, V.: Classification of Urban Areas: Inferring Land Use from the Interpretation of Land Cover, in Remote Sensing of Urban and Suburban Areas, vol. 10, edited by T. Rashed, C. Jürgens and F. D. Meer, pp. 141-164, Springer Netherlands. [online] Available from: http://dx.doi.org/10.1007/978-1-4020-4385-7_8, 2010.

Mesjasz, C.: Economic Vulnerability and Economic Security, edited by H. G. Brauch, Ú. Oswald Spring, J. Grin, P. Kameri-Mbote, B. Chourou, P. Dunay and J. Birkmann, pp. 123-156, Springer Berlin Heidelberg. [online] Available from: http://dx.doi.org/10.1007/978-3-642-17776-7_1, 2011.

Messner, F. and Meyer, V.: Flood Damage, Vulnerability and Risk Perception – Challenges for Flood Damage Research, edited by J. Schanze, E. Zeman, and J. Marsalek, pp. 149-167, Springer Netherlands. [online] Available from: http://www.floodsite.net/html/partner_area/search_results3b.asp?docID=50 (Accessed 25 September 2013), 2006.

Messner, F., Penning-Rowsell, E., Green, C., Tunstall, S., Veen, A. V. D., Tapsell, S., Wilson, T., Krywkow, J., Logtmeijer, C. and Fernández-Bilbao, A.: Evaluating flood damages: guidance and recommendations on principles and methods, FLOODsite Project Deliverable D9.1 Contract No: GOCE-CT-2004-505420. [online] Available from: http://www.floodsite.net/html/partner_area/project_docs/T09_06_01_Flood_damage_guidelines_D9_1_v2_2_p44.pdf (Accessed 21 June 2013), 2007.

Meyer, V. and Messner, F.: National Flood Damage Evaluation Methods. A Review of Applied Methods in England, the Netherlands, the Czech Republic and Germany, [online] Available from: http://www.econstor.eu/bitstream/10419/45193/1/505414783.pdf (Accessed 25 September 2013), 2005.

Michaelsen, E., Arens, M. and Doktorski, L.: Elements of a Gestalt Algebra: Steps towards Understanding Images and Scenes, in Proceedings of IMTA Workshop with VISAPP, pp. 65-73., 2008.

Michelin, J.-C., Mallet, C. and David, N.: Building edge detection using small-footprint airborne full-waveform lidar data, Melbourne, Australia. [online] Available from: http://www.isprs-ann-photogramm-remote-sens-spatial-inf-sci.net/I-3/147/2012/isprsannals-I-3-147-2012.pdf (Accessed 21 June 2013), 2012.

Middelmann-Fernandes, M. H.: Flood damage estimation beyond stage-damage functions: an Australian example, Journal of Flood Risk Management, 3(1), 88-96, doi: 10.1111/j.1753-318X.2009.01058.x, 2010.

Miller, G.: The Magical Number Seven, Plus or Minus Two: Some Limits on Our Capacity for Processing Information, edited by T. Me. Newcomb, Psychological Review, 63(2), 81-97, doi:10.1037/h0043158, PMID 13310704, 1956.

Montgomery, D. C.: Introduction to statistical quality control, Wiley, Arizona State. [online] Available from: http://dl4a.org/uploads/pdf/581SPC.pdf (Accessed 30 September 2013), 978-0-470-16992-6, 1991.

Moon, K., Downes, N., Rujner, H. and Storch, H.: Adaptation of the Urban Structure Type Approach for Vulnerability Assessment of Climate Change Risks in Ho Chi Minh City, edited by IsocarpEditors, Structure, 1-7. [online] Available from: http://www.isocarp.net/Data/case_studies/1596.pdf (Accessed 21 June 2013), 2009.

Mourato, S., Fernandez, P. and Moreira, M.: Flood risk assessment in an urban area: Vila Nova de Gaia, in Comprehensive Flood Risk Management FLOODrisk2012, edited by K. Schweckendiek Editors, pp. 671-679, CRC Press Taylor & Francis Group, Rotterdam, The Netherlands. [online] Available from: http://dspace.uevora.pt/rdpc/handle/10174/6927 (Accessed 29 August 2013), ISBN: 978-0-415-62144-1, 2013.

Müller, B.: German Annual of Spatial Research and Policy 2010, in Urban Regional Resilience: How Do Cities and Regions Deal with Change?, edited by B. Müller, Springer, Berlin / Heidelberg. [online] Available from: http://dx.doi.org/10.1007/978-3-642-12785-4_1, 2011.

Munich Re: Floods dominate natural catastrophe statistics in first half of 2013, Press releases [online] Available from: http://www.munichre.com/en/media_relations/press_releases/2013/2013_07_09_press_release.aspx (Accessed 13 August 2013), 2013.

Naumann, T.: Ergebnisse der Gebäudetypenkartierung, Regklam, Project, Leibniz-Institut für ökologische Raumentwicklung, Dresden, Germany. [online] Available from: http://www.regklam.de/themen/stadt-und-lebensraum/gebaeude/?tx_sbtab_pi1[tab]=52 (Accessed 2 September 2013), 2013.

Naumann, T., Nikolowski, J., Golz, S. and Schinke, R.: Resilience and Resistance of Buildings and Built Structures to Flood Impacts – Approaches to Analysis and Evaluation, edited by B. Müller, pp. 89-100, Springer Berlin Heidelberg. [online] Available from: http://dx.doi.org/10.1007/978-3-642-12785-4_9, 2010.

Naumann, T., Nikolowski, J., Golz, S. and Schinke, R.: Resilience and Resistance of Buildings and Built Structures to Flood Impacts – Approaches to Analysis and Evaluation, in German Annual of Spatial Research and Policy 2010, edited by B. Müller, pp. 89-100, Springer Berlin Heidelberg. [online] Available from: http://dx.doi.org/10.1007/978-3-642-12785-4_9, 2011.

Neubert, M., Naumann, T. and Deilmann, C.: Synthetic water level building damage relationships for GIS-supported flood vulnerability modeling of residential properties, pp. 1717-1724, Boca Raton-: CRC Press, Oxford, UK.doi:10.1201/9780203883020.ch203, 2009.

Neubert, M., Naumann, T., Hennersdorf, J. and Nikolowski, J.: The Geographic Information System-based flood damage simulation model HOWAD, Journal of Flood Risk Management, doi:10.1111/jfr3.12109, 2014.

Neyman, J.: On the Two Different Aspects of the Representative Method: The Method of Stratified Sampling and the Method of Purposive Selection, Journal of the Royal Statistical Society, 97(4), 558-625, doi:10.2307/2342192, 1934.

NIST: UNIFORMAT II Elemental Classification for Building Specification, Cost Estimating, and Cost Analysis, National Institute for Standards and Technology, Washington D.C. [online] Available from: http://fire.nist.gov/bfrlpubs/build99/PDF/b99080.pdf (Accessed 21 June 2013), 1999.

NOAA, B. B.: Sampling Design Tool for ArcGIS, Silver Spring. [online] Availabe from: http://www.arcgis.com/home/item.html?id=ecbe1fc44f35465f9dea42ef9b63e785 (Accessed 21 June 2013), 2012.

OAS, O. of A. S.: Primer on Natural Hazard Management in Integrated Regional Development Planning, http://www.oas.org [online] Available from: http://www.oas.org/usde/publications/unit/oea66e/begin.htm#Contents (Accessed 21 June 2013), 1991.

OCHA, U. N. O. for the coordination of H. A.: Temporada de lluvias 2010 Fenómeno de La Niña Informe de Situación, Colombia. [online] Available from: http://www.unocha.org/ (Accessed 21 June 2013), 2010.

Ochshorn, J.: Structural Elements for Architects and Builders: Design of columns, beams, and tension elements in wood, steel, and reinforced concrete, Elsevier Science, Burlington, MA, USA. ISBN: 978-1-85617-771-9, 2010.

Oxford Dictionaries: The world's most trusted dictionaries, [online] Available from: http://www.oxforddictionaries.com, 2013.

Pan, X.-Z., Zhao, Q.-G., Chen, J., Liang, Y. and Sun, B.: Analyzing the Variation of Building Density Using High Spatial Resolution Satellite Images: the Example of Shanghai City, Sensors (Peterboroug, 8(4), 2541-2550, doi:10.3390/s8042541, 2008.

Panel, E. D., Aeronautics, U. S. N., Administration, S. and Center, G. S. F.: Earth observing system: report of the EOS Data Panel. Data and information system, NASA. ISBN: 9467270048, ASIN: B00B6EAPHW, 1986.

Panero, J. and Zelnik, M.: Human dimension & interior space: a source book of design reference standards, Whitney Library of Design, New York. ISBN: 0851394574, 1979.

Penning-Rowsel, E., Johnson, C., Tunstall, S., Tapsell, S., Morris, J., Chatterton, J. and Green, C.: The Benefits of Flood and Coastal Risk Management: a Manual of Assessment Techniques, p. 238, Middlesex University Press, Middlesex, ISBN 1 904750 51 6 , 2005.

Penning-Rowsell, E.: The Multi-Coloured Manual, [online] Available from: http://www.mdx.ac.uk/research/science_technology/environmental/flood/publications/index.aspx (Accessed 21 June 2013), 2010.

Perez Fernandez, N. P.: The influence of construction materials on life-cycle energy use and carbon dioxide emissions of medium size commercial buildings. Master Thesis. [online] Available from: http://researcharchive.vuw.ac.nz/handle/10063/653 (Accessed 21 June 2013), 2008.

Pistrika, A.: Flood Damage Estimation based on Flood Simulation Scenarios and a GIS Platform, European Water, 30(3), 3-11, [online] Available from: http://www.ewra.net/ew/pdf/EW_2010_30_01.pdf (Accessed 21 June 2013),2010.

Porfírio Dal Poz, A.: Photogrammetric Refinement of Laser-Based Building Roof Contours, pp. 029-032, Sao Paulo. doi:10.1109/JURSE#.2013.6550658, 2013.

Porter, K. A.: A Taxonomy of Building Components for Performance-Based Earthquake Engineering, Department of Civil Engineering and Applied Mechanics California Institute of Technology, University of California, Berkeley. [online] Available from: http://citeseerx.ist.psu.edu/viewdoc/download?doi=10.1.1.90.1198&rep=rep1&type=pdf (Accessed 21 June 2005), 2005.

Prewitt, J.: Object enhancement and extraction, in Picture Processing and Psychopictorics, edited by B. Lipkin and A. Rosenfeld, pp. 75-149, Academics, New York. [online] Available from: http://web.eecs.utk.edu/~qi/ece472-572/reference/edge-Prewitt70.pdf (Accessed 21 June 2013), ISBN:0124515509, 1970.

Qi, H. and Altinakar, M. S.: A GIS-based decision support system for integrated flood management under uncertainty with two dimensional numerical simulations, Environmental Modelling & Software, 26(6), 817-821, doi:10.1016/j.envsoft.2010.11.006, 2011.

Reese, S. and Ramsay, D.: RiskScape: Flood fragility methodology, New Zealand Climate Change Research Institute Victoria University of Wellington. [online] Available from: http://www.victoria.ac.nz/sgees/research-centres/documents/riskscape-flood-fragility-methodology.pdf (Accessed 21 June 2013), 2010.

Restrepo, J.: Los sedimentos del río Magdalena: reflejo de la crisis ambiental, Fondo Editorial Universidad EAFIT. ISBN: 9789588173900, 2005.

Roberts, L. G.: Machine perception of three-dimensional solids, Ph.D. Thesis, Massachusetts Institute of Technology, Massachusetts. [online] Available from: http://dspace.mit.edu/bitstream/handle/1721.1/11589/33959125.pdf?sequence=1 (Accessed 21 June 2013), 1963.

Rossiter, D. G.: Digital soil resource inventories: status and prospects, Soil Use and Management, 20(3), 296-301, doi:10.1111/j.1475-2743.2004.tb00372.x, 2004.

Rottensteiner, F., Sohn, G., Jung, J., Gerke, M., Baillard, C., Benitez, S. and Breitkopf, U.: The ISPRS benchmark on urban object classification and 3d building reconstruction, Melbourne, Australia. [online] Available from: http://www.isprs-ann-photogramm-remote-sens-spatial-inf-sci.net/I-3/293/2012/isprsannals-I-3-293-2012.pdf, 2012.

Rottensteiner, F., Trinder, J., Clode, S. and Kubik, K.: Fusing airborne laser scanner data and aerial imagery for the automatic extraction of buildings in densely built-up areas, RealTime Imaging, 35(B3), 512-517. [online] Available from http://espace.library.uq.edu.au/view/UQ:100820 (Accessed 21 June 2013), 2003.

Rutzinger, M., Rottensteiner, F. and Pfeifer, N.: A comparison of evaluation techniques for building extraction from airborne laser scanning, IEEE Journal of Selected Topics in Quantum Electronics, 2/1, 11-20, doi: 10.1109/JSTARS.2009.2012488, 2009.

Saltelli, A., Andres, T. H. and Homma, T.: Sensitivity analysis of model output: An investigation of new techniques, Computational Statistics & Data Analysis, 15(2), 211-238, doi:10.1016/0167-9473(93)90193-W, 1993.

Samuels, P.: RIBAMOD: River Basin Modelling, Management and Flood Mitigation Final Report, Final Report, HR Wallingford Ltd, London, UK. [online] Available from: http://www.hrwallingford.co.uk/projects/RIBAMOD/sr551.pdf (Accessed 21 June 2013), 1999.

Samuels, P., Gerke, M., Sayers, P., Dominique Creutin, J., Kortenhaus, A., Klijn, F., Mosselman, E., van Os, A. and Schanze, J.: A framework for integrated flood risk management, Edinburgh. [online] Available from: http://web.sbe.hw.ac.uk/staffprofiles/bdgsa/IAHR_2010_European_Congress/Papers%20by%20session%20final/Flood%20Management%20III/FMaIIIa.pdf (Accessed 21 June 2013), 2010.

Samuels, P., Gouldby, B., Klijn, F., Messner, F., van Os, A., Sayers, P., Schanze, J. and Udale-Clarke, H.: Language of Risk – Project Definitions (Second Edition), [online] Available from: http://www.floodsite.net/html/partner_area/search_results3b.asp?docID=747 (Accessed 25 September 2013), 2009.

Samuels, P., Klijn, F. and Dijkman, J.: An analysis of the current practice of policies on river flood risk management in different countries, Irrig. and Drain., 55(S1), pp. 141-150, doi:10.1002/ird.257, 2006.

Santangelo, N., Santo, A., Di Crescenzo, G., Foscari, G., Liuzza, V., Sciarrotta, S. and Scorpio, V.: Flood susceptibility assessment in a highly urbanized alluvial fan: the case study of Sala Consilina (southern Italy), Natural Hazards and Earth System Science, 11(10), 2765-2780, doi:10.5194/nhess-11-2765-2011, 2011.

Sarabandi, P. and Kiremidjian, A.: Development of algorithms for building inventory compilation through remote sensing and statistical inferencing, Ph.D. Thesis, Stanford University, Department of Civil and Environmental Engineering, Stanford. [online] Available from: http://matrix.gpi.kit.edu/downloads/TR164_Sarabandi.pdf (Accessed 21 June 2013), 2007.

Scawthorn, C., Blais, N., Seligson, H., Tate, E., Mifflin, E., Thomas, W., Murphy, J. and Jones, C.: HAZUS-MH Flood Loss Estimation Methodology. I: Overview and Flood Hazard Characterization, Natural Hazards Review, 7(2), 60, doi:10.1061/(ASCE)1527-6988(2006)7:2(60), 2006.

Schanze, J.: Flood Risk Management – A Basic Framework, in Flood Risk Management: Hazards, Vulnerability and Mitigation Measures, vol. 67, edited by J. Schanze, E. Zeman and J. Marsalek, pp. 1-20, Springer Netherlands. [online] Available from: doi:10.1007/978-1-4020-4598-1_1, 2006.

Schöpfer, E., Lang, S. and Strobl, J.: Segmentation and Object-Based Image Analysis, in Remote Sensing of Urban and Suburban Areas, vol. 10, pp. 141-164, Springer Netherlands. [online] Available from: http://dx.doi.org/10.1007/978-1-4020-4385-7_2, 2010.

Schwarz, A.-M., Béné, C., Bennett, G., Boso, D., Hilly, Z., Paul, C., Posala, R., Sibiti, S. and Andrew, N.: Vulnerability and resilience of remote rural communities to shocks and global changes: Empirical analysis from Solomon Islands, Global Environmental Change, 21(3), 1128-1140, doi:10.1016/j.gloenvcha.2011.04.011, 2011.

Shackelford, A. K., Davis, C. H. and Wang, X. W. X.: Automated 2-D building footprint extraction from high-resolution satellite multispectral imagery, Geoscience and Remote Sensing Symposium, 3 (Proceedings. 2004 IEEE International), 1996, 1999, doi:10.1109/IGARSS.2004.1370739, 2004.

Shapiro, A.: A Fuzzy Random Variable Primer, Smeal College of Business, Smeal College of Business, (Penn State University), 14. [online] Available from: https://www.soa.org/library/proceedings/arch/2008/arch-2008-iss1-shapiro.pdf+&cd=1&hl=de&ct=clnk&gl=de, (Accessed 21 June 2013), 2002.

SIAC, IGAC, IDEAM and DANE: Reporte final de áreas afectadas por inundaciones 2010-2011, Sistema de Información Ambiental de Colombia, Instituto Geográfico Agustín Codazzi, Instituto de hidrología, metereología y estudios ambientales, Bogotá, Colombia. [online] Available from: https://www.siac.gov.co/documentos/DOC_Portal/DOC_Agua/20120508_Repor_fin_areas_afec_inun_2010-2011.pdf (Accessed 21 June 2013), 2011.

Sidney, D.: Land Development Handbook, in Land Development Handbook: Planning, Engineering, and Surveying, Third Edition, McGraw Hill Professional, Access Engineering. ISBN-10: 0071494375, 1996.

Singh Ahluwalia, S.: A Framework for Efficient Condition Assessment of the Building Infrastructure, Ph.D. Thesis, University of Waterloo, Waterloo. [online] Available from: http://libdspace.uwaterloo.ca/bitstream/10012/4093/1/Shipra%20SA_PhD%20Thesis.pdf (Accessed 21 June 2013), 2008.

Sirmacek, B., Angelo, P. and De, P. R.: Detecting complex building shapes in panchromatic satellite images for digital elevation model enhancement, ISPRS Istanbul Workshop, Modeling of optical airborne and spaceborne Sensor(XXXVIII). [online] Available from: www.isprs.org/proceedings/XXXVIII/1-W17/13_Sirmacek.pdf (Accessed 21 June 2013), 2010.

Sliuzas, R., Kuffer, M. and Masser, I.: The Spatial and Temporal Nature of Urban Objects, in Remote Sensing of Urban and Suburban Areas, vol. 10, pp. 67-84, Springer Netherlands. [online] Available from: http://dx.doi.org/10.1007/978-1-4020-4385-7_5, 2010.

SMA: Stair Codes – SMA Visual Interpretation of 2009 IRC, Stairway Manufacturers' Association, Fall River, MA. [online] Available from: http://www.stairways.org/SMA-Books/Stair-Code-2009-Visual-Interpretation (Accessed 21 June 2013), 2009.

Smith, D. I.: Flood damage estimation – a review of urban stage-damage curves and loss functions, WaterSA, 20(3), 231-238, ISSN: 0378-4738, 1994.

Sobel, I. and Feldman, G.: A 3x3 Isotropic Gradient Operator for Image Processing, (Never published but presented at a talk at the Stanford Artificial Project), 1968.

Soergel, U., Michaelsen, E., Thiele, A., Cadario, E. and Thoennessen, U.: Stereo analysis of high-resolution SAR images for building height estimation in cases of orthogonal aspect directions, ISPRS Journal of Photogrammetry and Remote Sensing, 64(5), 490-500, doi:10.1016/j.isprsjprs.2008.10.007, 2009.

Sohn, G. and Dowman, I.: Data fusion of high-resolution satellite imagery and LiDAR data for automatic building extraction, ISPRS Journal of Photogrammetry and Remote Sensing, 62(1), 43-63, doi:10.1016/j.isprsjprs.2007.01.001, 2007.

Song, W. S. W. and Haithcoat, T. L.: Development of comprehensive accuracy assessment indexes for building footprint extraction. doi: 10.1109/TGRS.2004.838418, 2005.

Song, Y. and Shan, J.: Building extraction from high resolution color imagery based on edge flow driven active contour and JSEG, Archives, (2003), B3a: 185-190. [online] Available from: http://www.isprs.org/proceedings/XXXVII/congress/3_pdf/28.pdf (Accessed 21 June 2013), 2005.

Srnka, K. J. and Koeszegi, S. T.: From Words to Numbers, How to Transform Qualitative Data Into Meaningful Quantitative Results, 59(1), 29-57, JEL Classification: M19, 2007.

Stilla, U. and Jurkiewicz, K.: Integrated Spatial Databases, vol. 1737, pp. 34-46, Springer Berlin/Heidelberg. [online] Available from: http://dx.doi.org/10.1007/3-540-46621-5_3, 1999.

Van Stipriaan, U.: Nun ist es doch die Elbe: Rekordhochwasser flutet Dresden, Flut 2002 [online] Available from: http://www.stipriaan.de/rekordwasser.html (Accessed 10 October 2013), 2002.

Storch, H.: The Spatial Dimensions of Climate Change at the Mega-urban Scale in South-East-Asia. Urban Environmental Planning Strategies for Ho Chi Minh City´s Response to Climate Change, in 45th ISOCARP Congress 2009, edited by IsocarpEditors, p. 12, The Hague: ISOCARP, Porto, Portugal. [online] Available from: http://www.isocarp.net/Dat%ase_studies/1594.pdf (Accessed 21 June 2013), 2009.

Straube, J.: BSD-138: Moisture and Materials, Building science, Ontario, Canada. [online] Available from: http://www.buildingscience.com/documents/digests/bsd-138-moisture-and-materials (Accessed 21 June 2013), 2006.

Tack, F., Buyuksalih, G. and Goossens, R.: 3D building reconstruction based on given ground plan information and surface models extracted from spaceborne imagery, ISPRS Journal of Photogrammetry and Remote Sensing, 67(0), 52-64, doi:10.1016/j.isprsjprs.2011.10.003, 2012.

Tapsell, S.: Socio-economic and ecological evaluation and modelling methodologies, Project FLOODsite, FLOODsite Consortium. [online] Available from:

http://www.floodsite.net/html/partner_area/project_docs/t10_07_13_methodologies_d10_1_v_1_3_p01.pdf (Accessed 29 August 2013), 2008.

Taranath, B. S.: Reinforced concrete design of tall buildings, CRC Press Taylor & Francis Group, Boca Raton. ISBN: 9781439804803, 2010.

Taubenböck, H., Klotz, M., Wurm, M., Schmieder, J., Wagner, B. and Esch, T.: Delimiting Central Business Districts – A physical approach using remote sensing, pp. 017-020, Sao Paulo. [online] Available from: http://elib.dlr.de/82279/1/Delimiting_Central_Business_Districts.pdf (Accessed 21 June 2013), doi: 10.1109/JURSE.2013.6550655, 2013.

Terzaghi, K. and Peck, R. B.: Soil mechanics in engineering practice, 2nd ed., Wiley, Michigan. ISBN: 9780471852735, 1967.

Thefreedictionary: The Free Dictionary, [online] Available from: http://www.thefreedictionary.com (Accessed 21 June 2013), 2013.

Thieken, A. H., Mariani, S., Longfield, S. and Vanneuville, W.: Preface: Flood resilient communities – managing the consequences of flooding, Nat. Hazards Earth Syst. Sci., 14(1), 33-39, doi:10.5194/nhess-14-33-2014, 2014.

Thieken, A. H., Seifert, I. and Merz, B.: Hochwasserschäden: Erfassung, Abschätzung und Vermeidung, Oekom Verlag GmbH, München. ISBN: 9783865811868, 2010.

Thomas, D. R.: A general inductive approach for qualitative data analysis, Population English Edition, 27(2), 237-246, doi: 10.1177/1098214005283748, 2003.

Thywissen, K.: Components of Risk: A Comparative Glossary, Studies of the University: Research, Counsel, Education, UNU Institute for Environment and Human Security (UNU-EHS), Bonn, Germany. [online] Available from: http://www.ehs.unu.edu/file/get/8335 (Accessed 25 September 2013), 2006.

Tian, J. and Reinartz, P.: Fusion of multi-spectral bands and DSM from Worldview-2 Stereo imagery for building extraction, pp. 135-138, Sao Paulo, doi: 10.1109/JURSE.2013.6550684, 2013.

Trechsel, H. R., Ed.: Moisture Analysis and Condensation Control in Building Envelopes, American Society for Testing & Materials, West Conshohocken. [online] Available from: http://www.astm.org/DIGITAL_LIBRARY/MNL/SOURCE_PAGES/MNL40_foreword.pdf (Accessed 21 June 2013), ISBN 978-0-8031-7004-9, 2001.

Turbay, S., Alzate, C., Alvarez, O., Gomez, G. and Lopez, A.: La fauna de la depresión momposina, Lealón, Colombia, ISBN: 9589679714, 2000.

UNFPA: Linking Population, Poverty and Development, United Nations Population Fund, New York. [online] Available from: http://www.unfpa.org/pds/urbanization.htm (Accessed 21 June 2013), 2008.

UNGRD: Formatos para la recolección de información sectorial sobre daños y necesidades, Never published but used for the collection of data, Unidad Nacional para la Gestion del Riesgo de Desastres, Bogotá, Colombia, 2008.

UNISDR: Terminology: Basic terms of disaster risk reduction, in Living with Risk: A Global Review of Disaster Reduction Initiatives, Geneva, United Nations. [online] Available from: http://www.unisdr.org/we/inform/publications/657 (Accessed 25 September 2013), 2004.

UNISDR: Hyogo Framework for Action 2005-2015: Building the Resilience of Nations and Communities to Disasters, Extract from the final report of the World Conference on Disaster Reduction (A/CONF.206/6), International Strategy for Disaster Reduction, Geneva. [online] Available from: http://www.unisdr.org/files/1037_hyogoframeworkforactionenglish.pdf (Accessed 21 June 2013), 2007.

UNISDR: Linking disaster risk reduction and poverty reduction: good practices and lessons learned, United Nations International Strategy for Disaster Reduction Secretariat, United Nations. [online] Available from: http://papers.ssrn.com/sol3/papers.cfm?abstract_id=1783159 (Accessed 21 June 2013), 2008.

Vedaldi, A. and Fulkerson, B.: An Open and Portable Library of Computer Vision Algorithms, [online] Available from: http://www.vlfeat.org/, 2008.

Velasquez, J.: International approaches for the derivation of depth-damage functions in flood risk management, Master thesis, TU-Dresden, Dresden, Germany, 2011.

Veregin, H.: Unit 100 - Data Quality Measurement and Assessment, [online] Available from: http://www.geo.upm.es/postgrado/CarlosLopez/materiales/cursos/www.ncgia.ucsb.edu/education/curricula/giscc/units/u100/u100_toc.html (Accessed 30 September 2013), 1998.

Villagrán, J. C.: Vulnerability a conceptual and methodological review, Studies of the University: Research, Counsel, Education, UNU Institute for Environment and Human Security (UNU-EHS), Bonn, Germany. [online] Available from: http://www.ehs.unu.edu/file/get/3904 (Accessed 25 September 2013), 2006.

Vu, T. T. and Ban, Y.: Context-based mapping of damaged buildings from high-resolution optical satellite images, International Journal of Remote Sensing, 31(13), 3411-3425, doi:10.1080/01431161003727697, 2010.

Ward-Harvey, K.: Fundamental Building Materials: Fourth Edition, Universal Publishers, Boca Raton, Florida, USA. ISBN: 9781599429540, 2009.

Weller, B., Naumann, T. and Jakubetz, S.: Gebäude unter den Einwirkungen des Klimawandels, Rhombos-Verlag, Berlin. ISBN: 978-3-941216-96-9, 2012.

WHO: Guidelines for indoor air quality: dampness and mould, World Health Organization, Copenhagen, Denmark. [online] Available from: http://www.euro.who.int/__data/assets/pdf_file/0017/43325/E92645.pdf (Accessed 25 September 2013), 2009.

Wieland, M., Pittore, M., Parolai, S., Zschau, J., Moldobekov, B. and Begaliev, U.: Estimating building inventory for rapid seismic vulnerability assessment: Towards an integrated approach based on multi-source imaging, Soil Dynamics and Earthquake Engineering, 36(0), 70-83, doi:10.1016/j.soildyn.2012.01.003, 2012.

Winsemius, H. C., Van Beek, L. P. H., Jongman, B., Ward, P. J. and Bouwman, A.: A framework for global river flood risk assessments, Hydrology and Earth System Sciences, 17(5), 1871-1892, doi:10.5194/hess-17-1871-2013, 2013.

World Bank: Climate Resilient Cities: 2008 Primer Reducing Vulnerabilities to Climate Change Impacts and Strengthening Disaster Risk Management in East Asian Cities, FGDRR and UNISDR, Washington, DC: World Bank. [online] Available from: http://www.unisdr.org/files/3483_climatecitiesfullreport.pdf (Accessed 25 September 2013), 2008.

WMO: Atlas of mortality and economic losses from weather, climate and water extremes (1970–2012). [online] Available from: https://www.wmo.int/pages/mediacentre/press_releases/pr_998_en.html, (Accessed 25 June 2015), 2014.

Xiao, J., Gerke, M. and Vosselman, G.: Building extraction from oblique airborne imagery based on robust façade detection, ISPRS Journal of Photogrammetry and Remote Sensing, 68(0), 56-68, doi:10.1016/j.isprsjprs.2011.12.006, 2012.

Yi, C.-S., Lee, J.-H. and Shim, M.-P.: GIS-based distributed technique for assessing economic loss from flood damage: pre-feasibility study for the Anyang Stream Basin in Korea, Natural Hazards, 55(2), 251-272, doi: 10.1007/s11069-010-9524-7, 2010.

Young, O. R.: The Institutional Dimensions of Environmental Change: Fit, Interplay, and Scale, Mit Press, Massachusetts. ISBN: 9780262740241, 2002.

Zamir, A. and Shah, M.: Accurate Image Localization Based on Google Maps Street View, in Computer Vision – ECCV 2010, vol. 6314, edited by K. Daniilidis, P. Maragos and N. Paragios, pp. 255-268, Springer Berlin Heidelberg. [online] Available from: http://dx.doi.org/10.1007/978-3-642-15561-1_19, 2010.

Zevenbergen, C., Gersonius, B., Veerbeek, W. and Van Herk, S.: Challenges in Urban Flood Management: travelling across spatial and temporal scales, Journal of Flood Risk Management, 1(2), 81-88, doi:10.1111/j.1753-318X.2008.00010.x, 2008.

Zhang, K. Z. K., Yan, J. Y. J. and Chen, S.-C.: Automatic Construction of Building Footprints From Airborne LIDAR Data, doi :10.1109/TGRS.2006.874137 , 2006.

Zhang, M., Li, X., Yang, Z. and Yang, Y.: A novel zero-crossing edge detection method based on multi-scale space theory, in 2010 IEEE 10th International Conference, pp. 1036-1039, Beijing, doi: 10.1109/ICOSP.2010.5655905, 2010.

Zhang, Y. and Maxwell, T.: Roof Mapping Using Fused Multiresolution Optical Satellite Images, in Remote Sensing of Impervious Surfaces, CRC Press. [online] Available from: http://dx.doi.org/10.1201/9781420043754.ch16, 2007.

Zhitov, D.: Calculation of construction materials, construction calculators, and designers. Free service calculation of building materials, [online] Available from: http://www.zhitov.ru/en/, 2013.

Zhou, F., Peng, B., Cui, Y., Wang, Y. and Tan, H.: A novel laser vision sensor for omnidirectional 3D measurement, Optics & Laser Technology, 45(0), 1-12, doi:10.1016/j.optlastec.2012.08.005, 2013.

Zhu, J., Humphreys, G., Koller, D., Steuart, S. and Wang, R.: Fast Omnidirectional 3D Scene Acquisition with an Array of Stereo Cameras, in Sixth International Conference on 3-D Digital Imaging and Modeling, pp. 217-224, Montreal, Quebec, Canada, doi: 10.1109/3DIM.2007.25, 2007.

Zhu, J., Zhou, L. and Zhang, D.: Identification for building surface material based on hyperspectral remote sensing, in 19th International Conference on Geomatics, pp. 1-5, Iran., doi: 10.1109/GeoInformatics.2011.5980687, 2011.

Index of figures

Index of tables

Appendices

The next scheme displays the structure of digital appendices

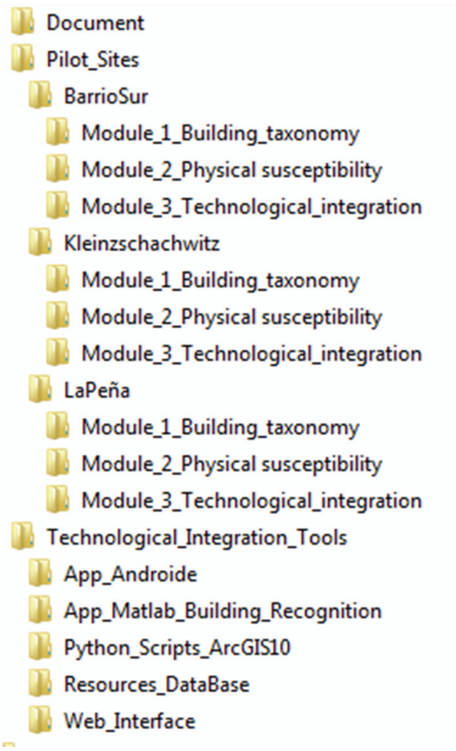

Appendix A: Summary information for damage models in some countries (Velasquez, 2011)

COUNTRY	DAMAGE MEASUREMENT METHODS	VARIABLES	SOURCE OF DATA	TYPE OF DATA	TYPE OF DAMAGE	MEASURMENT PROCESS	UNITS	TOOLS	AGENCIES INVOLVED
USA (Scawthorn et al., 2006)	HAZUS	Flood time % Expected damage Water Depth	Inventory (cadastre, questioners and insurance databases) Depreciation of assets United States Army Corps of Engineers (USACE) DTMs	Synthetic (from synthesis of many data objects) DEMs	-Damage to buildings and communal facilities - Damage to lifeline systems - Damage to vehicles - Agricultural loss - Direct/indirect economic loss (social loss)	Remote sensing, update depth-damage functions from USACE from 1993 and FIA (Federal Insurance Administrations)	Direct damage Total damage (depreciated) (estimated % damage).Replacement value (total or depreciated) Synthetic	GIS (Geographic Information System) based HAZUS-99 SR2 currently has MapInfo® and ArcView® versions	Developed by FEMA, under a cooperative agreement with NIBS. National Institute of Building Sciences
Germany (Neubert et al., 2014)	HOWAD (Flood Damage Simulation Model)	Expected damage Depth structure type Erecting time of building Original use Constructive details Vulnerability	Surveys ATKIS Database Topographical maps DTMs	Synthetic data from land use maps and Urban Structure Types	Damage by water and moisture, contamination, damages to load bearing construction	Remote sensing Topographical maps ATKIS data base	Damage cost per spatial unit	HOWAD LISFLOOD, SMS, WAVOS	The VERIS-Elbe research project. (BMBF)
Germany (Kreibich et al., 2010)	FEMOps FLEMOcs	Water depth Building type Building quality Contamination of the floodwater Private precaution	Surveys questionnaire, census, telephone calls, cadastral data	Empirical real surveyed data	Due to flood depth	Independent data set with less information. Comparison of repair costs from banking information	Damage cost per spatial unit	GIS data set of building Municipal cadastres	Centre for Natural Hazard Management Ltd., Innsbruck, Austria Engineering Hydrology Section, GeoForschungs Zentrum Potsdam, Germany
England and Wales (Penning-Rowsell, 2010)	Multicolored Manuals Residential properties	Water depth, market Values of assets Taxation Flood probability Flood time Warning time Content Use.	Updated price reports, consumer price index, field survey, contact to company for asset value estimation, DTMs	Synthetic and real loss data Property value	Moisture damage depending on the susceptibility level	Depth-damage function for inventories and for buildings	Percentage of property value Weighted averages, Area, value/m² British Pounds	HEC-RAS	Department for Environment, Food and Rural Affairs (DEFRA) Environmental Agency (EA) Flood and Coastal Erosion Risk Management R&D Program

Continuation of appendix A: Summary information for damage models in some countries (Velasquez, 2011).

COUNTRY	DAMAGE MEASUREMENT METHODS	VARIABLES	SOURCE OF DATA	TYPE OF DATA	TYPE OF DAMAGE	MEASURMENT PROCESS	UNITS	TOOLS	AGENCIES INVOLVED
England and Wales	Multicolored Manuals Non-residential properties	Water depth, market values of assets, taxation, flood probability, flood time, warning time, content, use	Company surveys	Susceptibility analysis according to commercial contents	Moisture damage depending on the susceptibility level	A database created in 2005. Formerly the 1990 DB is updated, surveys	British Pounds Value from susceptible assets.	HEC-RAS	
Australia (Middelmann-Fernandes, 2010)	ANUFLOOD	Velocity Water depth Repair or replacement costs	Contour maps, DTMs, statistical data	Synthetic data from land use maps	Water and moisture foundation damage	Depth-damage function for inventories and for buildings	Value in Australian dollars	HEC-RAS ANUFLOOD	Commonwealth of Australia (Geoscience Australia) Center for Resource and Environmental Studies (CRES)
Argentina (Corzo, 2010)	Post event assessment	Population, constructed area, socio-economic data, flood area	Census	Real surveyed data	None (risk assessment)	Questionnaires	Total damage cost	Mathematical equations	Economic Commission for Latin America and the Caribbean (CEPAL), various NGOs
Japan (Dutta et al., 2003)	Numerical Model	Flows: interception and evapotranspiration, river, overland, unsaturated zone and saturated zone. Depth Duration	DTMs, Contour maps, LANDSAT imagery.	Synthetic data gathered from governmental agencies	Urban, rural and infrastructure	Reports from governmental institutions	Total values, value/m^2 for households	Mathematical equations coupled with geographical data	Ministry of agriculture, forestry and fisheries of the government of Japan Ministry of transportation, Japan. Settlements
China (Kang et al., 2005)	Synthetic Database with geo-information system	Water depth Structure type	DTMs and flood potential map, building type, location and living styles, zoning maps	Synthetic data gathered from governmental agencies	Direct Indirect Tangible Intangible	Reports from governmental institutions	Total monetary cost of loss	Hydrology studies, hydraulic simulations, land use and economy studies, regional damages, risk analysis	Taipei Building administrations office Taipei Metropolitan regions Office

Appendix B: Parameters required for the component's volume calculation

Building components	Graphic	Parameters	Formula Volume
Gable roof	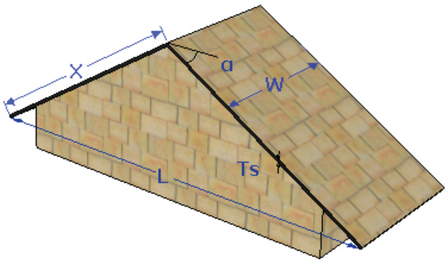	X= L / 2 cos α Measured in the field: ▪ Ts= Thickness roofing sheet ▪ La = Lapping of the roofing sheet	Vr = 2*X *W*Ts*(1+La)
Roof rafter		L =Length of the building ▪ Wr = Width of the rafters ▪ Tr = Thickness of the rafter ▪ Dr = Distance between the rafters	Vra= 2.5 Lr*Tr*(L/Dr)
Mansard	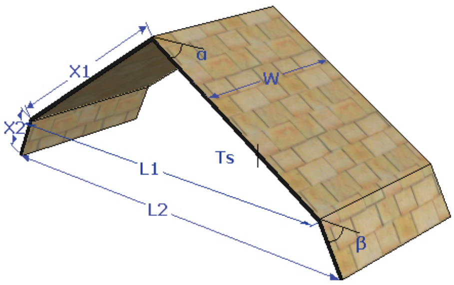	X_1=L_1 / 2 cos α X_2=L_2 / 2 cos β Measured in the field: ▪ Ts= Thickness roofing sheet ▪ La = Lapping of the roofing sheet	Vrm = 2X_1 **Ts*(1+La)+ 2X_2 *W*Ts*(1+La)
Beams	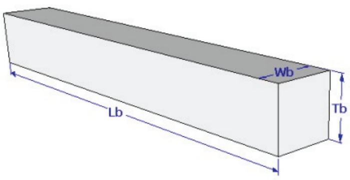	▪ Wb = Width of the beam ▪ Tb =Tthickness of the beam ▪ Lb = Largeness of the beam ▪ Ab = Amount of external beams	Vb = ∑Lb*Tb*Wb
Ceiling	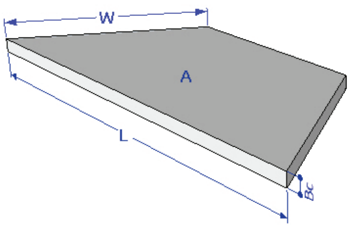	A = Area Measured in the field: ▪ Bc = Panel height	Vc = A*Bp
Slabs and plates	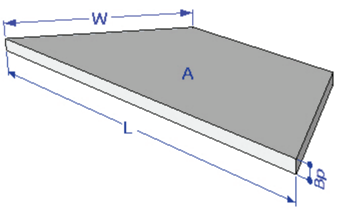	A= Area Measured in the field: ▪ Bp = Panel height of the slabs	Vsp= A*Bp

Building components	Graphic	Parameters	Formula Volume
External window frames	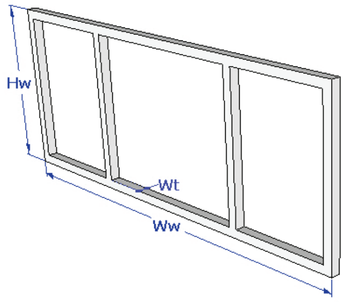	Measured in the field: ▪ Hw = Height of the window ▪ Ww = Width of the window ▪ Wt = Thickness of the window ▪ Wb = Width of the bar ▪ Nvc = Number of vertical crossbars ▪ New = Number of external windows	$New_{I} = Hw_i*Wb_i*Wt_i$ $+Nvc_i (Ww_i*Wb_i*Wt)$ $Vew = \sum New$
External doors	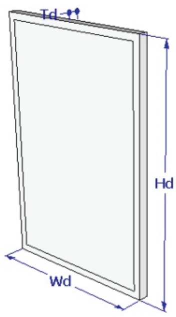	Measured in the field: ▪ Hd = Height of the door ▪ Wd = Width of the door ▪ Td = Thickness of the door ▪ Ned = Number of external doors	$Ned_{I} = Hd_i *Wd_i*Td_i$ $Ved = \sum Ned$
External walls type 1	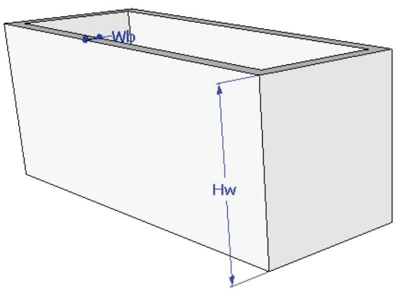	P = Perimeter Measured in the field: ▪ Wb = Thickness of walls ▪ Hw = Wall height	Vw1=P*Wb*Hw – (Vep +Vew)
External walls type 2	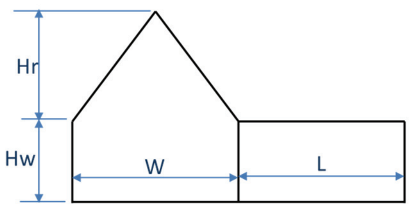	P = Perimeter Measured in the field: ▪ Wb = Thickness of walls ▪ Hw = Wall height ▪ Hr = H-Hw	Vw2 = (P*Wb*Hw) + (W*Hr*Wb) – (Vw +Vd)
External walls type 3	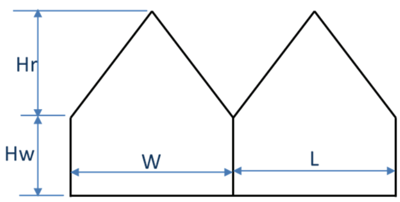	P = Perimeter Measured in the field: ▪ Wb = Thickness of walls ▪ Hw = Eaves height Hr = H-Hw	Vw3 = (P*Wb*Hw) + (W*Hr*Wb)+ (L*Hr*Wb – (Vw +Vd)

Building components	Graphic	Parameters	Formula Volume
Concrete stairs	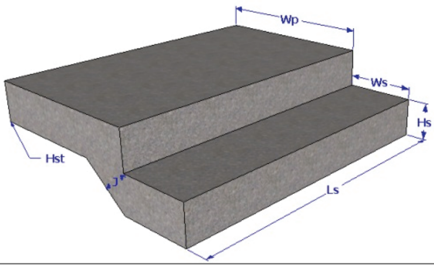	▪ Ns = Number of steps ▪ Ls= Length of the stair ▪ Hs = Height of the step ▪ Ws = Width of stairs ▪ Hst= Height of the stairs ▪ J= Extra thickness	$Vs = Ns^* (Ls^*Hs^*Ws/2)+J^* (\sqrt{Hst^2+(Ws^*Ns)^2}) ^*Ls+(Wp^*Ls^*Hs)$
Wood stairs	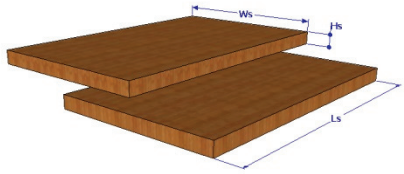	Measured in the field: ▪ Ns = Number of steps ▪ Ls= Length of the stair ▪ Hs = Height of the step ▪ Ws = Width of stairs	$Vs = Ls^*Hs^*Ws^*Ns$
Floor	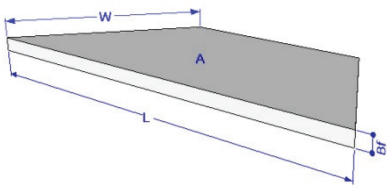	A = Area Measured in the field: ▪ Tf = Thickness of the floor	$V = A^*Bf$
Columns	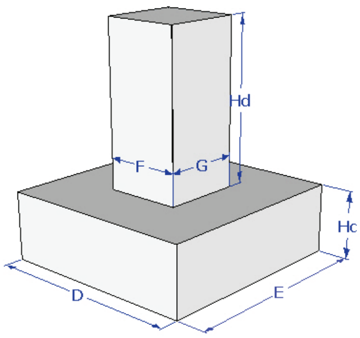	Measured or estimated in the field: ▪ D = Length of the rectangular base ▪ E = Width of the base ▪ Hc = Base height pillar ▪ Hd = Height of the main part ▪ F = Width of the main part ▪ G = Length of the main part	$Vc = D^*E^*Hc + F^*G^*Hd$
Foundation type 1	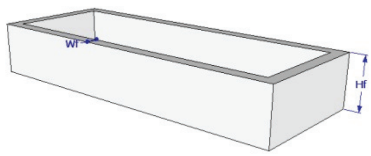	▪ P = Perimeter Measured in the field: ▪ Wf = Thickness of foundation ▪ Hf = Foundation height	$Vf1= P^*Wf^*Hf$
Foundation type 2	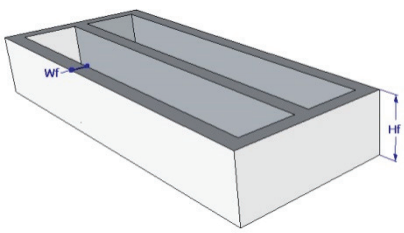	▪ P = Perimeter Measured in the field: ▪ Wf = Thickness of foundation ▪ Hf = Foundation height ▪ Tf = Type of the foundation	$Vf2 = P^*Wf^*Hf + (L-2Wf^* Wf^*Hf)$

Appendix C: List of materials with their value of resistance

Component	Material	Qualification of resistance	Institution
Bolts, hinges nails & fittings	Brass, nylon/stainless steel, removable pin hinges	5	AUS - Committee and Resources
Bolts, hinges nails & fittings	Galvanised steel, aluminium	4	AUS - Committee and Resources
Bolts, hinges nails & fittings	Mild steel	1	AUS - Committee and Resources
Building material	Brick-– Engineering bricks (Classes A and B)	5	UK - CIRIA
Building material	Brick – facing bricks (wire cut, sand facing)	3	UK - CIRIA
Building material	Handmade bricks	1	UK - CIRIA
Building material	Blocks – Concrete blocks	3	UK - CIRIA
Building material	Blocks – Aircrete blocks	3	UK - CIRIA
Building material	Timber boars, 11 mm thick	1	UK - CIRIA
Building material	Timber boars, 18 mm thick	1	UK - CIRIA
Building material	Gypsum Pasterboards, 9 mm thick	1	UK - CIRIA
Building material	Mortars below DPC 1:3 (cement: sand)	5	UK - CIRIA
Building material	Mortars below DPC 1:6 (cement: sand)	5	UK - CIRIA
Building material	Lime	5	GER - Hochwasserschutzfibel
Building material	Gypsum	1	GER - Hochwasserschutzfibel
Building material	Cement	5	GER - Hochwasserschutzfibel
Building material	Burned materials (bricks)	5/3	GER - Hochwasserschutzfibel
Building material	Stoneware goods	5	GER - Hochwasserschutzfibel
Building material	Bitumen	5	GER - Hochwasserschutzfibel
Building material	Metals (depending on type)	5/3	GER - Hochwasserschutzfibel
Building material	Plastic (depending on type)	5/3/1	GER - Hochwasserschutzfibel
Building material	Wood (depending on type)	5/3	GER - Hochwasserschutzfibel
Building material	Textile	1	GER - Hochwasserschutzfibel
Doors	Wood frames	1	GER - Hochwasserschutzfibel
Doors	Coated aluminium or metal	5	GER - Hochwasserschutzfibel
Doors	Steel frames	5	GER - Hochwasserschutzfibel
Doors	Slates	3	GER - Hochwasserschutzfibel
Doors	Wood doors	1	GER - Hochwasserschutzfibel
Doors	Stainless steel doors	5	GER - Hochwasserschutzfibel
Doors	Solid panel with waterproof adhesive	5	AUS - Committee and Resources
Doors	Flush marine ply with closed cell foam	5	AUS - Committee and Resources
Doors	Aluminium or galvanised steel frame	5	AUS - Committee and Resources
Doors	Flush or single panel marine ply with waterproof adhesive	4	AUS - Committee and Resources
Doors	Painted metal construction	4	AUS - Committee and Resources
Doors	Timber frame, full epoxy sealed	4	AUS - Committee and

Component	Material	Qualification of resistance	Institution
	before assembly		Resources
Doors	Standard timber frame	2	AUS - Committee and Resources
Doors	Standard flush hollow core with PVA adhesives and honeycomb paper core	1	AUS - Committee and Resources
Floor covering	Clay/concrete tiles	5	AUS - Committee and Resources
Floor covering	Epoxy or cementitious floor toppings on concrete	5	AUS - Committee and Resources
Floor covering	Rubber sheets (chemically set adhesives)	5	AUS - Committee and Resources
Floor covering	Vinyl sheet (chemically set adhesive)	5	AUS - Committee and Resources
Floor covering	Terrazzo	4	AUS - Committee and Resources
Floor covering	Rubber tiles (chemically set adhesives)	4	AUS - Committee and Resources
Floor covering	Vinyl tiles (chemically set adhesive)	4	AUS - Committee and Resources
Floor covering	Polished floor & loose rugs	4	AUS - Committee and Resources
Floor covering	Ceramic tiles	4	AUS - Committee and Resources
Floor covering	Loose fit nylon or acrylic carpet (closed cell rubber underlay)	2	AUS - Committee and Resources
Floor covering	Wall to wall carpet	1	AUS - Committee and Resources
Floor covering	Wall to wall seagrass matting	1	AUS - Committee and Resources
Floor covering	Cork	1	AUS - Committee and Resources
Floor covering	Linoleum	1	AUS - Committee and Resources
Floor sub-floor structure	Slab-on-ground	5	AUS - Committee and Resources
Floor sub-floor structure	Suspended concrete	5	AUS - Committee and Resources
Floor sub-floor structure	Standard grade plywood	4	AUS - Committee and Resources
Floor sub-floor structure	Timber floor close to the ground and particle board	1	AUS - Committee and Resources
Floor sub-floor structure	Timber T&G (with ends only epoxy sealed and provision of side clearance board swelling or plywood)	4	AUS - Committee and Resources
Floors	Cement/latex, formed-in-place	4	USA - FEMA Structural Materials
Floors	Concrete, precast or cast-in-place	5	USA - FEMA Structural Materials
Floors	Oriented-strand board (OSB), Exterior grade	2	USA - FEMA Structural Materials
Floors	Oriented-strand board (OSB), Edge swell-resistant OSB	2	USA - FEMA Structural Materials
Floors	Oriented-strand board (OSB), All other types	1	USA - FEMA Structural Materials

Component	Material	Qualification of resistance	Institution
Floors	Particle board	1	USA - FEMA Structural Materials
Floors	Plywood Marine grade	5	USA - FEMA Structural Materials
Floors	Plywood Preservative-treated, alkaline copper quaternary (ACQ) or copper azole (C-A)	4	USA - FEMA Structural Materials
Floors	Plywood Preservative-treated, Borate	5	USA - FEMA Structural Materials
Floors	Plywood Exterior grade/Exposure1 (WBP – weather and boil proof)	4	USA - FEMA Structural Materials
Floors	Plywood All other types	1	USA - FEMA Structural Materials
Floors	Recycled plastic lumber (RPL), Commingled, with 80-90 % polyethylene (PE)	5	USA - FEMA Structural Materials
Floors	Recycled plastic lumber (RPL), Fibre-reinforced, with glass fibre strands	5	USA - FEMA Structural Materials
Floors	Recycled plastic lumber (RPL), High-density polyethylene (HDPE), up to 95 %	5	USA - FEMA Structural Materials
Floors	Recycled plastic lumber (RPL), Wood-filled, with 50 % sawdust or wood fibre	3	USA - FEMA Structural Materials
Floors	Stone, natural or artificial non-absorbent solid or veneer, waterproof grout	5	USA - FEMA Structural Materials
Floors	Structural Building Components Floor trusses, wood, solid (2x4s), decay-resistant or preservative-treated	4	USA - FEMA Structural Materials
Floors	Structural Building Components Floor trusses, steel3	5	USA - FEMA Structural Materials
Floors	Structural Building Components I-joists	2	USA - FEMA Structural Materials
Floors	Wood Solid, decay-resistant4	5	USA - FEMA Structural Materials
Floors	Absorbing material	1	GER - Hochwasserschutzfibel
Floors	Waterproof concrete	5	GER - Hochwasserschutzfibel
Floors	Screed	5/3	GER - Hochwasserschutzfibel
Floors	Wooden beams	3	GER - Hochwasserschutzfibel
Floors	Natural stone (granite, dolomite)	5	GER - Hochwasserschutzfibel
Floors	Sandstone	1	GER - Hochwasserschutzfibel
Floors	Marmol	1	GER - Hochwasserschutzfibel
Floors	Artificial stone	5	GER - Hochwasserschutzfibel
Floors	Tiles (depending on the type)	5/3	GER - Hochwasserschutzfibel
Floors	Epoxy resin surfaces	5	GER - Hochwasserschutzfibel
Floors	Parquet/Laminate	1	GER - Hochwasserschutzfibel
Floors	Solid wood	1	GER - Hochwasserschutzfibel
Floors	Cork	1	GER - Hochwasserschutzfibel

Component	Material	Qualification of resistance	Institution
Floors	Textile covering (carpets)	1	GER - Hochwasserschutzfibel
Floors	Linoleum	1	GER - Hochwasserschutzfibel
Insulation	Plastic/polystyrene boards	5	AUS - Committee and Resources
Insulation	Closed cell solid insulation	5	AUS - Committee and Resources
Insulation	Reflective foil perforated with holes to drain water if used under timber floors	4	AUS - Committee and Resources
Insulation	Materials which store water and delay drying	1	AUS - Committee and Resources
Insulation	Open celled insulation (batts etc.)	1	AUS - Committee and Resources
Roof structure	Galvanised metal construction	5	AUS - Committee and Resources
Roof structure	Timber trusses with galvanised connections	4	AUS - Committee and Resources
Roof structure	Traditional timber roof construction	2	AUS - Committee and Resources
Roof structure	Traditional timber roof construction	1	AUS - Committee and Resources
Roof structure	Unsecured roof tiles	1	AUS - Committee and Resources
Roof structure	Reinforced concrete	5	AUS - Committee and Resources
Walls	Cavity insulation – Mineral fibre	1	UK - CIRIA
Walls	Cavity insulation – Blown-in	1	UK - CIRIA
Walls	Cavity insulation – Rigid PU foam	1	UK - CIRIA
Walls	Renders/Plaster – Cement render external	5	UK - CIRIA
Walls	Renders/Plaster –Cement/lime render-external	5	UK - CIRIA
Walls	Renders/Plaster – Gypsum plasterboard	1	UK - CIRIA
Walls	Renders/Plaster – Lime plaster	1	UK - CIRIA
Walls	Limestone	5	GER - Hochwasserschutzfibel
Walls	Fired solid brick	5	GER - Hochwasserschutzfibel
Walls	Perforated brick	3	GER - Hochwasserschutzfibel
Walls	Clinker	5	GER - Hochwasserschutzfibel
Walls	Concrete	5	GER - Hochwasserschutzfibel
Walls	Concrete (Gas)	3	GER - Hochwasserschutzfibel
Walls	Drywall partitions (plasterboard)	1	GER - Hochwasserschutzfibel
Walls	Wood (planks, chipboard, dividers)	1	GER - Hochwasserschutzfibel
Walls	Glass block	5	GER - Hochwasserschutzfibel
Walls and ceilings	Asbestos-cement board	5	USA - FEMA Structural Materials
Walls and ceilings	Brick face or glazed	5	USA - FEMA Structural Materials
Walls and ceilings	Brick common (clay)	4	USA - FEMA Structural Materials

Component	Material	Qualification of resistance	Institution
Walls and ceilings	Cast stone (in waterproof mortar)	5	USA - FEMA Structural Materials
Walls and ceilings	Cement board/fibre-cement board	5	USA - FEMA Structural Materials
Walls and ceilings	Clay tile, structural glazed	5	USA - FEMA Structural Materials
Walls and ceilings	Concrete, precast or cast-in-place	5	USA - FEMA Structural Materials
Walls and ceilings	Concrete block1	5	USA - FEMA Structural Materials
Walls and ceilings	Gypsum products – Paper-faced gypsum board	3	USA - FEMA Structural Materials
Walls and ceilings	Gypsum products – Non-paper-faced gypsum board	4	USA - FEMA Structural Materials
Walls and ceilings	Gypsum products – Greenboard	2	USA - FEMA Structural Materials
Walls and ceilings	Gypsum products – Keene's cement or plaster	3	USA - FEMA Structural Materials
Walls and ceilings	Gypsum products – Plaster, otherwise, including acoustical	2	USA - FEMA Structural Materials
Walls and ceilings	Gypsum products – Sheathing panels, exterior grade	3	USA - FEMA Structural Materials
Walls and ceilings	Gypsum products – Water-resistant, fibre-reinforced gypsum exterior sheathing	4	USA - FEMA Structural Materials
Walls and ceilings	Hardboard (high-density fibreboard) – Tempered, enamel or plastic coated	2	USA - FEMA Structural Materials
Walls and ceilings	Hardboard (high-density fibreboard) – All other types	1	USA - FEMA Structural Materials
Walls and ceilings	Mineral fibreboard	1	USA - FEMA Structural Materials
Walls and ceilings	Oriented-strand board (OSB) – Exterior grade	2	USA - FEMA Structural Materials
Walls and ceilings	Oriented-strand board (OSB) – Edge swell-resistant OSB	2	USA - FEMA Structural Materials
Walls and ceilings	Oriented-strand board (OSB) – All other types	1	USA - FEMA Structural Materials
Walls and ceilings	Plywood Marine grade	5	USA - FEMA Structural Materials
Walls and ceilings	Plywood Preservative-treated, alkaline copper quaternary (ACQ) or copper azole (C-A)	4	USA - FEMA Structural Materials
Walls and ceilings	Plywood – Preservative-treated, Borate	5	USA - FEMA Structural Materials
Walls and ceilings	Plywood – Exterior grade/Exposure1 (WBP – weather and boil proof)	4	USA - FEMA Structural Materials
Walls and ceilings	Plywood – All other types	1	USA - FEMA Structural Materials
Walls and ceilings	Stone – Natural or artificial non-absorbent solid or veneer, waterproof grout	5	USA - FEMA Structural Materials
Walls and ceilings	Stone – All other applications	3	USA - FEMA Structural Materials
Walls and ceilings	Structural Building Components Floor trusses, wood, solid (2x4s),	4	USA - FEMA Structural Materials

Component	Material	Qualification of resistance	Institution
	decay-resistant or preservative-treated		
Walls and ceilings	Structural Building Components Floor trusses, steel3	5	USA - FEMA Structural Materials
Walls and ceilings	Structural – Headers and beams, solid (2x4s) or plywood, exterior grade or preservative-treated	4	USA - FEMA Structural Materials
Walls and ceilings	Structural Building Components Headers and beams, OSB, exterior grade or edge-swell resistant	2	USA - FEMA Structural Materials
Walls and ceilings	Structural Building Components Headers and beams, steel3	5	USA - FEMA Structural Materials
Walls and ceilings	Structural Building Components I-joists	2	USA - FEMA Structural Materials
Walls and ceilings	Structural Building Components Wall panels, plywood, exterior grade or preservative-treated	4	USA - FEMA Structural Materials
Walls and ceilings	Structural Building Components Wall panels, OSB, exterior grade or edge-swell resistant	2	USA - FEMA Structural Materials
Walls and ceilings	Structural Building Components Wall panels, steel3	4	USA - FEMA Structural Materials
Walls and ceilings	Wood Solid, standard, structural (2x4s)	4	USA - FEMA Structural Materials
Walls and ceilings	Wood Solid, standard, finish/trim	3	USA - FEMA Structural Materials
Walls and ceilings	Wood Solid, decay-resistant4	5	USA - FEMA Structural Materials
Walls and ceilings	Wood Solid, preservative-treated, ACQ or C-A	4	USA - FEMA Structural Materials
Walls and ceilings	Wood Solid, preservative-treated, Borate2	4	USA - FEMA Structural Materials
Walls and ceilings	Face brick or blockwork	5	AUS - Committee and Resources
Walls and ceilings	Common bricks	4	AUS - Committee and Resources
Walls and ceilings	Glass and glass blocks	5	AUS - Committee and Resources
Walls and ceilings	Fibre cement	5	AUS - Committee and Resources
Walls and ceilings	Ceramic wall tiles	5	AUS - Committee and Resources
Walls and ceilings	Galvanised steel sheet	5	AUS - Committee and Resources
Walls and ceilings	Gypsum plaster	1	AUS - Committee and Resources
Walls and ceilings	Hardboard	2	AUS - Committee and Resources
Walls and ceilings	Plastic sheeting or tiles with waterproof adhesive	5	AUS - Committee and Resources
Walls and ceilings	Exterior grade plywood	4-2	AUS - Committee and Resources
Walls and ceilings	Standard plywood	1	AUS - Committee and Resources
Walls and ceilings	Plasterboard	2	AUS - Committee and Resources

Component	Material	Qualification of resistance	Institution
Walls and ceilings	Stone, solid or veneer	5	AUS - Committee and Resources
Walls and ceilings	Cloth wall	1	AUS - Committee and Resources
Walls and ceilings	Solid wood with allowance for swelling	2	AUS - Committee and Resources
Walls and ceilings	Exterior grade particleboard	2	AUS - Committee and Resources
Walls and ceilings	Solid wood, fully sealed	4	AUS - Committee and Resources
Walls and ceilings	Non-ferrous metals	4	AUS - Committee and Resources
Walls and ceilings	Fibreboard or strawboard	1	AUS - Committee and Resources
Walls and ceilings	Wallpaper	1	AUS - Committee and Resources
Walls support structure	Full brick/block masonry cavity brick	4	AUS - Committee and Resources
Walls support structure	Brick block veneer with venting (stud frame)	2	AUS - Committee and Resources
Walls support structure	Reinforced or mass concrete	5	AUS - Committee and Resources
Windows	Wood (depending on the type)	3/1	GER - Hochwasserschutzfibel
Windows	Plastic	5/3	GER - Hochwasserschutzfibel
Windows	Aluminium	5	GER - Hochwasserschutzfibel
Windows	Galvanized steel	5	GER - Hochwasserschutzfibel
Windows	Aluminium frame with stainless steel or brass rollers	5	AUS - Committee and Resources
Windows	Timber frame, full epoxy sealed before assembly with stainless steel or brass fittings	4	AUS - Committee and Resources
Windows	Timber with PVA glues	1	AUS - Committee and Resources
Windows	Mild steel fittings	1	AUS - Committee and Resources

Appendix D: Tools developed for every user

	User	Activity	Source
D1	**Administrator**	Store data	Database in Postgresql
		Display data Connect to users	Web application
D2	**Data preparation expert**	Define elevation and vegetation thresholds for a semi-automatic building-regions outline extraction	Matlab
		Calculate the accuracy of the extracted polygon using reference data	Python script for ArcGIS 10
		Calculate building taxonomic code	Python script for ArcGIS 10
		Select representative buildings	Python script for ArcGIS 10
		Select samples of representative buildings	ArcGIS
		Export polygons of representative buildings to KML for visualising in Google Earth	Python script for ArcGIS 10
D3	**Field data collector**	Collect data in-situ of the representative buildings using mobile devices	App in android which is connected to the database
D4	**Analyst**	Derivate depth-physical impact functions	Template in Excel and a VBA function for interpolation using the tool of Mehta (2012)
D5	**Final user**	Integrate the sources for the calculation of impacts for every house	Python script for ArcGIS 10

Appendix D1: Tools for the administrator

Installation and configuration of a database for storing the data.
Resources:

- *Java SDK* is a program development environment for writing Java applets and applications. It consists of a runtime environment that "sits on top" of the operating system layer as well as the tools and programming that developers need to compile, debug, and run applets and applications written in the Java language. (http://www.oracle.com/technetwork/java/javase/downloads/jdk7-downloads-1637583.html)
- *Jboss* is an application server that implements the Java Platform, Enterprise Edition (Java EE): http://download.jboss.org/jbossas/7.1/jboss-as-7.1.1.Final/jboss-as-7.1.1.Final.zip
- *Postgresql* is an object-relational database management system (ORDBMS). The PostgreSQL License is an MIT-style license, and is thus free and open source software (http://www.postgresql.org/download/windows/)
- BuildingsSusceptibility.apk is the app for the android phone. It must be downloaded and installed in the mobile phone.

Installation and configuration:

- The Java must be installed following this guide:
  http://docs.oracle.com/javase/7/docs/webnotes/install/index.html
  And a JAVA_HOME environment variable in the computer must be set up.
- The computer as server must be configured like this:
  Open the file: …\jboss-as-7.1.1.Final\standalone\configuration\ standalone.xml
  Change the line: <inet-address value="127.0.0.1"/> by <any-address />
- Install Postgresql with the user: postgres, password:posgres and port: “default”. In Stack builder 3.1.x select in categories Database Driver: pgJDBC v 9.1.-901-1 and in Spatial Estension: PostGIS 1.5 Web and continue the installation with next.
  - Copy the file postgresql-8.4-701.jdbc4.jar in the folder …\PostgreSQL\pgJDBC and page in the
    …\jboss-as-7.1.1.Final\standalone\deployments
    This file allows the application connection to the database.
  - Create DataBase
    Open pgAdmin III in start/programms
    New Database
    Name: buildings
    Definition: Template postgis.
- Execute application server:
  Open a Command Prompt Commands (cmd)
  Go to the path {jboss.home} \jboss\bin
  Write standalone.bat
  Write standalone.conf.bat
  This allows unlocking the server.
- Create an admin user for the application
  Open a Command Prompt Commands (cmd)
  Go to the path {jboss.home} \jboss\bin
  Write add_user.bat
  In Management
  User: angela
  Password:angelablanco
  Yes
  Yes
  Exit
- Enable port 8080
  Go to Firewall
  Add Port
  Name Jboss
  8080
- Create datasources for log in the database
  Open a firefox window localhost.8080

In profile select Datasources Attributes
Datasources: buildings
Java: jboss/datasources/BuildingDS
Next
Connection protocol setting
jdbc:posgresql//197.0.0.1:5432/buildings
user: posgres
password: posgres
Active: buildings Enable

- Copy the application developed in java to the server.
  copy building_web.war in {jboss.home} \standalone\deployments

Note: Every time when the computer starts, the standalone.bat and standalone.conf.bat must be started in the cmd.
The following figure shows the schema browser of the database in Postgresql, where the data will be stored.

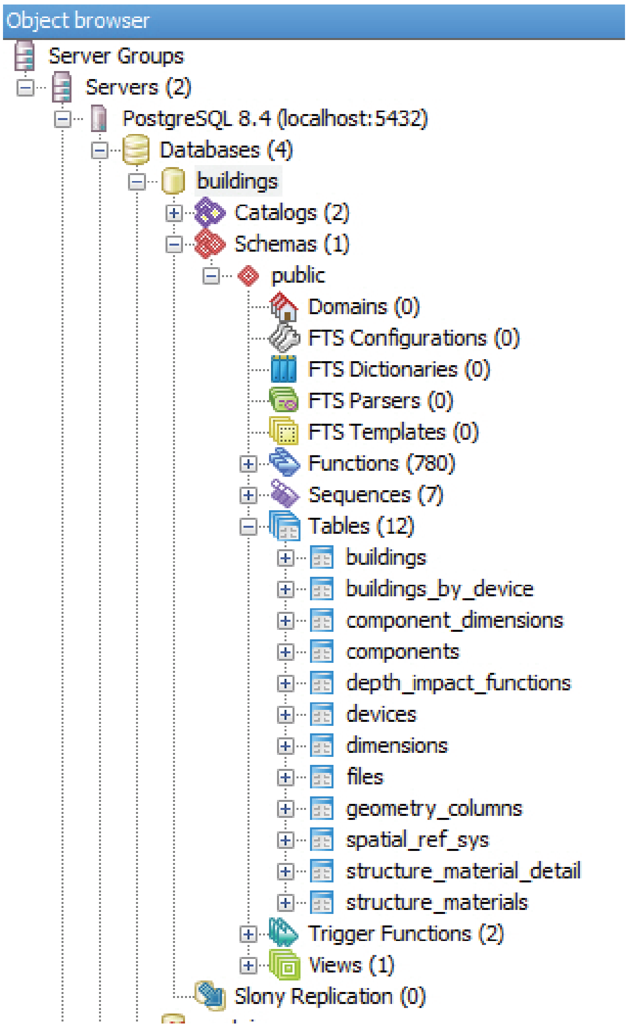

Figure D1.1: Schema browser of the database in Postgresql

The generated data from the different users must be converted in sql format before it its entered in the database. This conversion can be executed using one of the following links:
http://csv2sql.com/ http://www.withdata.com/csv/csv-to-sql/index.html http://netsource.hu/csv2sql/

Appendix D2: Tool for the data preparation expert

Appendix D2.1: Tool to define the threshold for a semi-automatic building-regions outlines extraction (digital annex).

A GUI is developed in Matlab for a semi-automatic building extraction, which can serve as an initial guide for advance processes of building outline extraction. The following semantic definition for building extraction in floodplain areas has been considered for the tool:

- Buildings have different spectral characteristics than vegetation.
- Floodplains are quite flat. It implies that the height variation of the terrain is very low, almost constant.
- Buildings are elevated.
- A building has a homogeneous roof texture or a defined pattern.

This tool has three windows. In the first one, the user can separate the vegetation based on a vegetation index threshold for RGB images with three layers.

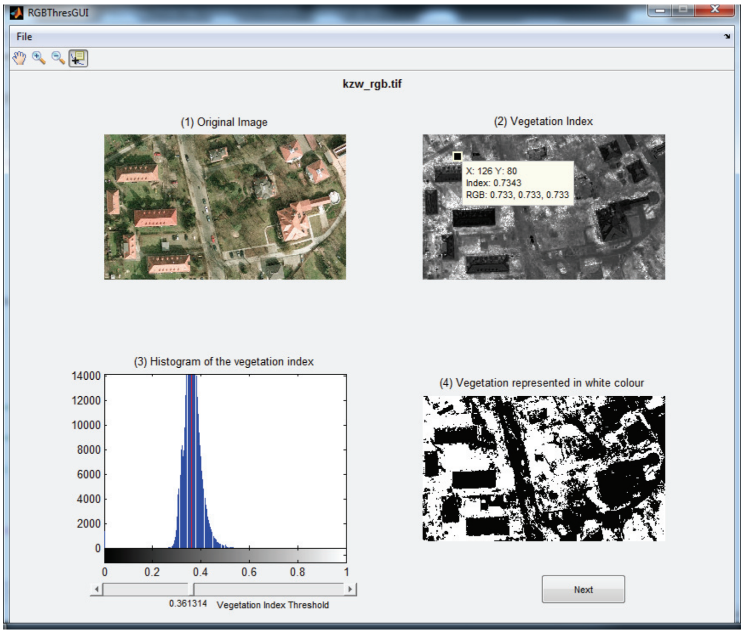

Figure D2.1.1: First window of the tool for semi-automatic building outlines

1) The first subplot of the window displays the original image RGB, which is loaded by the user.
2) The second subplot shows the vegetation index of the RGB image, which is calculated by the green ratio: Green / (Blue + Green + Red). Vegetated pixels appear brighter.
3) The third subplot displays the histogram of the vegetation index. Here the user can move the slide bar in order to separate vegetation from the other objects. The red line indicates the value of the threshold in the histogram.
4) The fourth subplot presents with colour the pixels characterised as vegetation and the other elements.

The next window of the tool allows the user to select the height for distinguishing between the terrain surface and elevated objects.

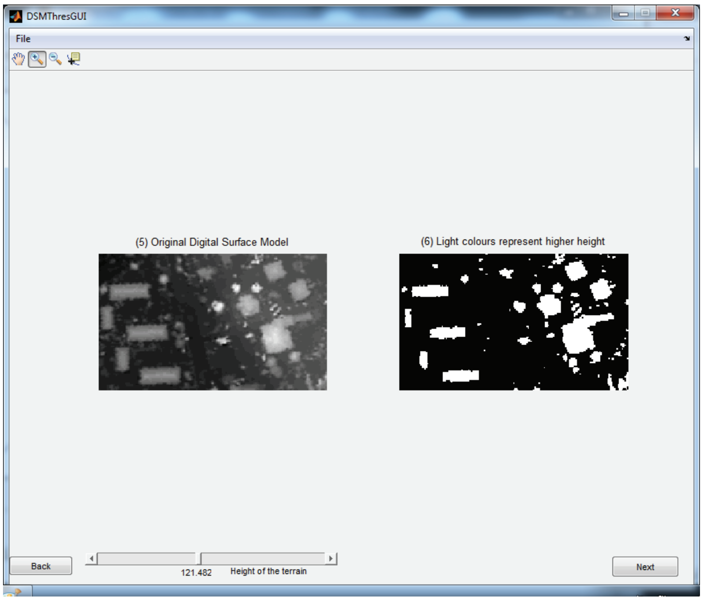

Figure D2.1.2: Second window of the tool for semi-automatic building outlines

1) The left subplot of this window displays the original digital surface model, which is loaded by the user.
2) The user can move the slide bar defining the height of the terrain. The user can observe in white colour the elevated object above the terrain in the right subplot.

In the third window, the results of the building extraction are displayed:

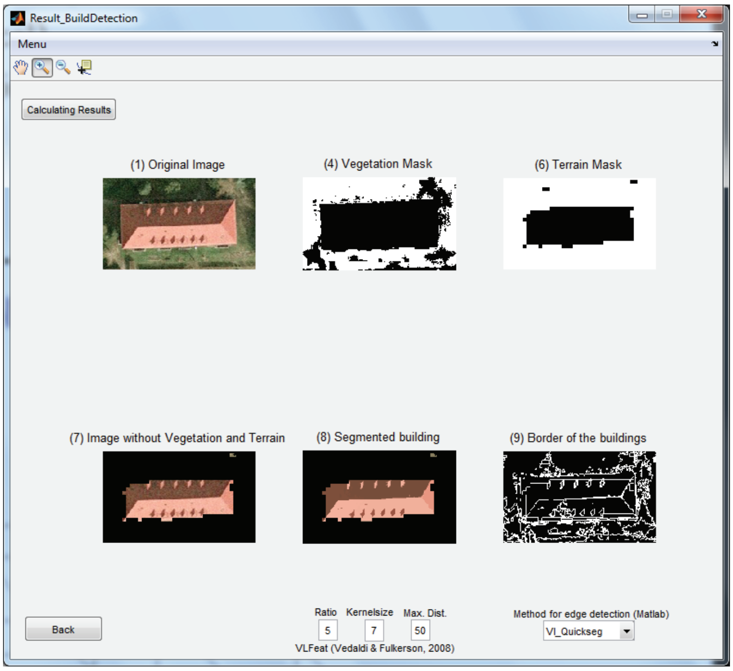

Figure D2.1.3: Third window of the tool for semi-automatic building outlines

The subplots (1), (4) and (6) are displayed again in the upper part of the window.

1) The pixels of the vegetation mask and terrain mask are subtracted from the original image.
2) The segmented buildings are calculated based on the quick shift algorithm (Vedaldi and Fulkerson, 2008). It links each pixel to its nearest neighbour which has an

increase in the estimate of the density. The user can modify the values of ratio, kernelsize and maxdist. The ratio is the tradeoff between colour importance and spatial importance (larger values give more importance to colour), kernelsize is the size of the kernel used to estimate the density, and maxdist is the maximum distance between points in the feature space that may be linked if the density is increased.

3) The user can select in the pop-up menu the method of the edge of the building.
4) The Sobel (Sobel and Feldman, 1968), Prewitt (Prewitt, 1970) and Roberts (Roberts, 1963) methods find edges using an approximation to the derivative. They return edges at those points where the gradient of the image is maximum. The gradient method detects the edges by looking for the maximum and minimum in the first derivative of the image.
5) The Canny method (Canny, 1986) finds edges by looking for local maxima of the gradient of image. The gradient is calculated using the derivative of a Gaussian filter. The method uses two thresholds, to detect strong and weak edges, and includes the weak edges in the output only if they are connected to strong edges. This method is therefore less likely than the others to be fooled by noise, and more likely to detect true weak edges.
6) The LoG method (Zhang et al., 2010) finds edges by looking for zero crossings after filtering the image with a Laplacian of Gaussian filter.
7) The tool allows the user to save in an image extension the results of (4), (6), (8) and (9).

Appendix D2.2: Tool for the calculation of the accuracy of the extracted polygon (digital annex)

The user enters the extracted polygons and the reference polygon in the next window and the calculation gives the error defined by Song and Haithcoat (2005).

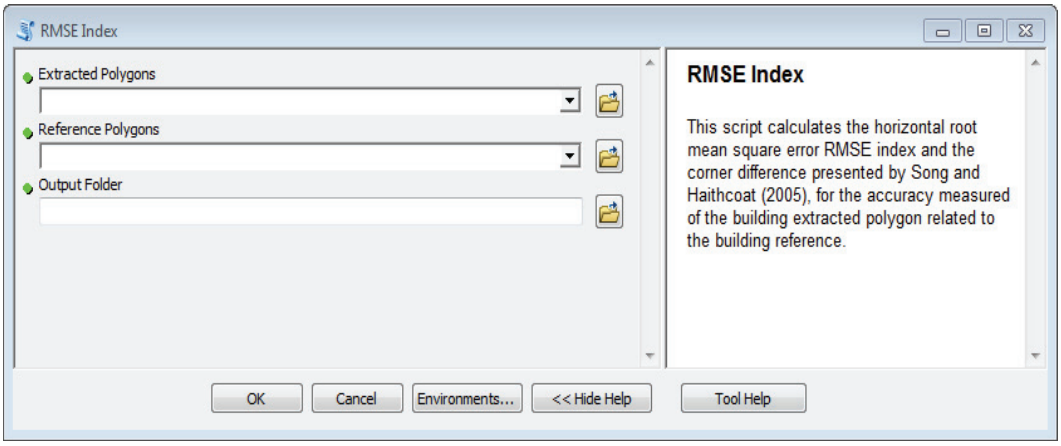

Figure D2.2.1: Input window for the calculation of the accuracy of the extracted polygon

Table D2.2.1: Indices of accuracy for building extraction (Song and Haithcoat, 2005)

Error	Description
Detection rate:	The percentage of correctly detected buildings to the total number of reference buildings.
Correctness:	The percentage of correctly detected buildings to the total number of detected buildings.
Matched Overlay:	The total area of overlapping building parts divided by the total area of the reference building.
Area Omission Error:	The percentage of the non-detected building parts to the total area of the reference data.
Area Commission Error:	The percentage of incorrectly detected building parts to the total area of detected buildings.
RMSE:	The horizontal RMSE is assessed using building corners as check points. For each corner point in the detected building polygon, the closest corresponding point in the reference data was found and a distance calculated. The horizontal RMSE was then obtained by summarizing these paired observations.
Corner Difference:	The average absolute building corner number difference between detected and reference buildings.
Area Difference:	The percentage of absolute area difference between detected buildings and reference data divided by the total reference area.
Perimeter Difference:	The percentage of absolute perimeter difference between detected buildings and reference data divided by the total reference perimeter.

Appendix D2.3: Tool for calculation of building taxonomic code (digital annex)

The script calculates the seven parameters: [Height_Code] & [Size_Code] & [Elongatedness_Code] & [Roof_form_Code] & [Roof_slope_Code] & [Compactness_Code] & [Adjacency_Code] and derives the taxonomic code. The user should enter the building polygons, DSM and DTM.

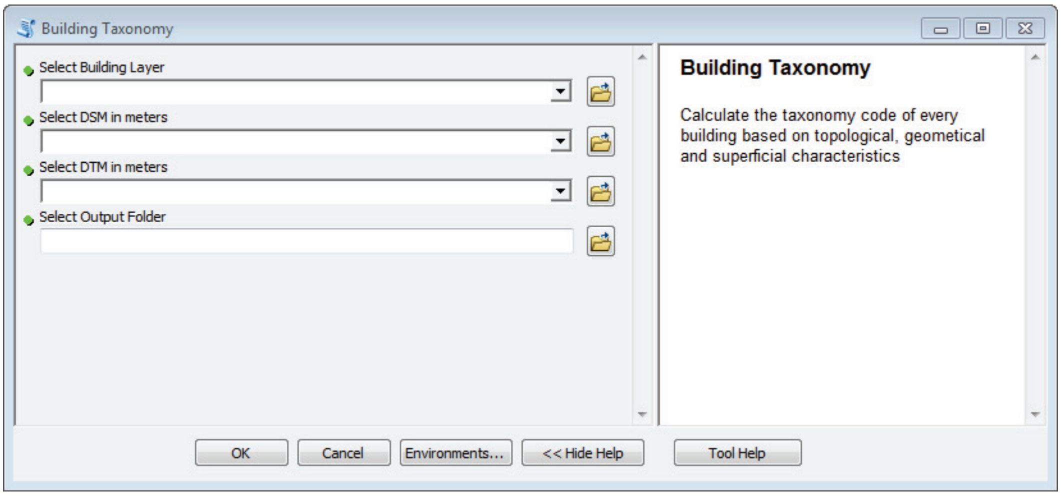

Figure D2.3: Input window for the calculation of the taxonomic code for buildings

Appendix D2.4: Tool for the automatic selection of representative buildings and the calculation of the matching using membership function (digital annex)

The script selects the building taxonomic code that has a frequency higher than the chosen threshold separating representative buildings from non-representative buildings. Then it calculates the matching percentage or membership between the non-representatives and the representatives. The user should enter the building with the taxonomic code, the threshold of representativeness and a folder for data output in the tool represented in the Figure D2.4.

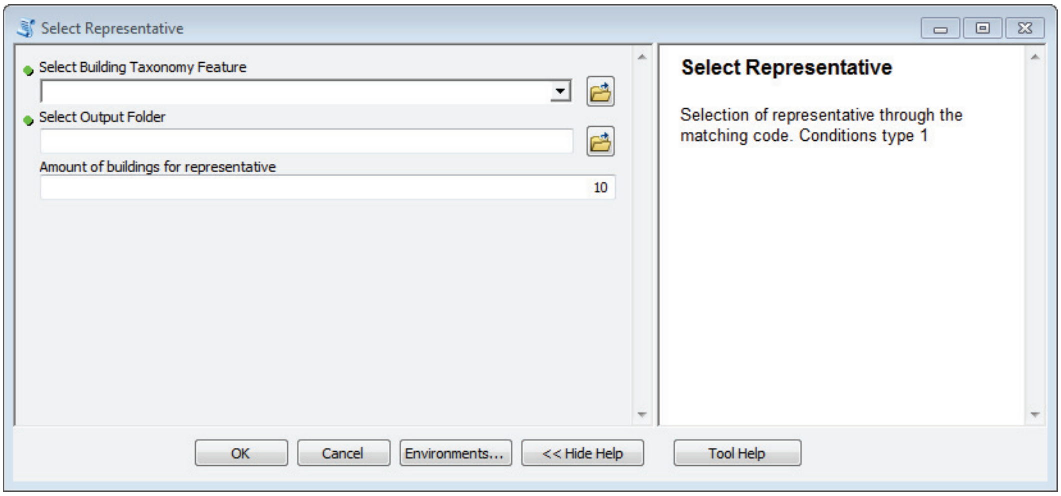

Figure D2.4: Input window for clustering RBT to NRBT

Appendix D2.5: Tool for building sampling

The selection of representative building samples can be carried out using the Sampling Design Tool for ArcGIS designed by NOAA (2012) (see Figure D2.5).

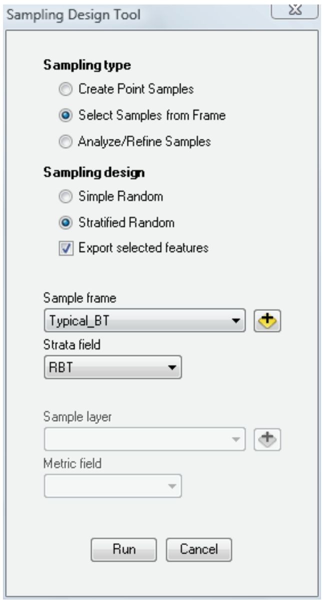

Figure D2.5: Input window for clustering RBT to NRBT

Appendix D3: Tool for the field data collector

The mobile device must first be connected to the server through the IP address of the server. The IP address is known with the command ipconfig in a cmd.

Table D3.1: Guide to the mobile device App

Steps	Displays	Description
1		The app "Buildings-Susceptibility" was developed for Android mobile devices. Once selected, the GPS function is active.
1.1		The app Smart Measure gets the distance and height of the objects. The server and the device mobile must be connected in the same net using Wi-Fi.
2	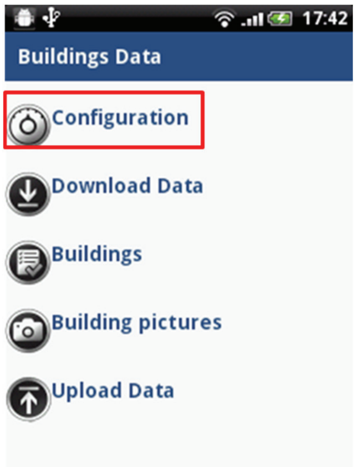	The first option of the app Buildings is configured.

2.1

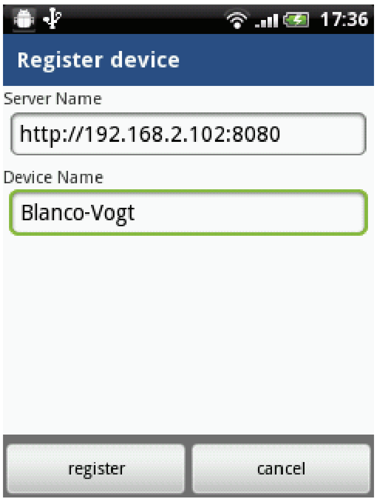

In *Server Name*, the IP address of the server with the port must be entered.

In *Device Name*, the identification of the mobile must be put in.

3

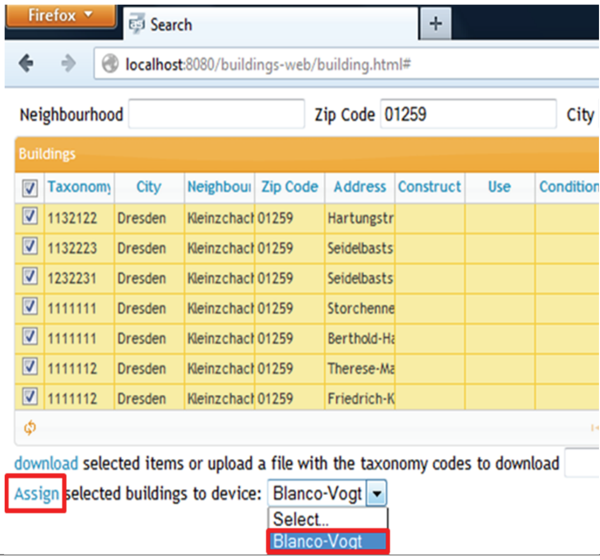

The administrator of the database selects the buildings, which will be assigned to the device.

4

The user downloads the data assigned in the mobile device.

4.1		Then the user selects the option Buildings and a list of the assigned buildings with the taxonomic code is displayed.
5	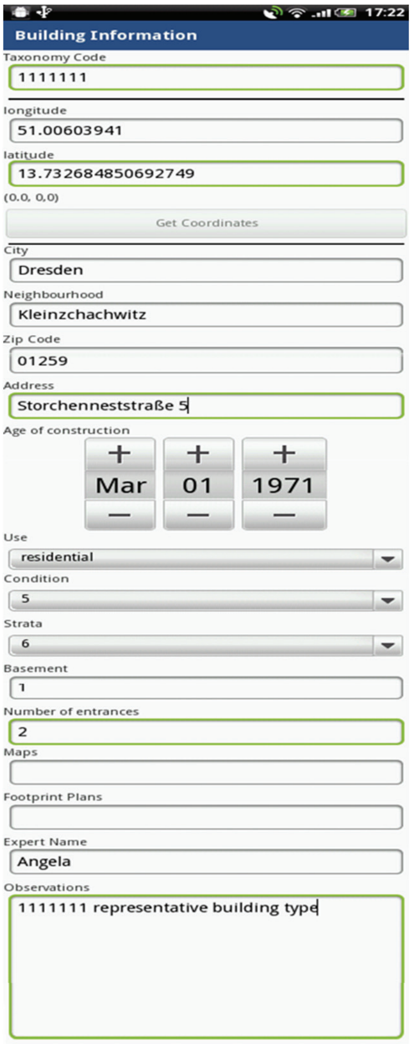	The expert in impact building assessment goes to the field and with *invasive method* fills the form.

6

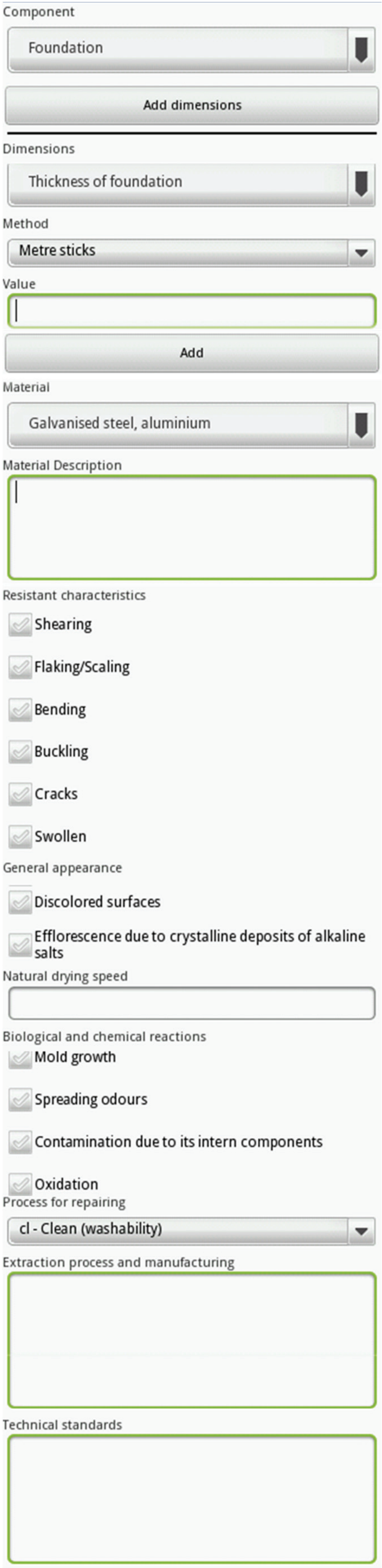

The expert adds the principal components of the building, assigns their structural material and susceptibility characteristics.

<table>
<tr><td>6.1</td><td>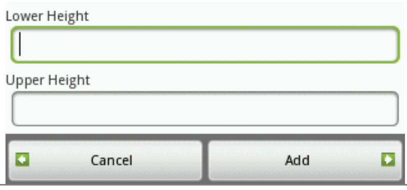
</td><td>For every component, its lower and upper height must be entered.</td></tr>
<tr><td>7</td><td>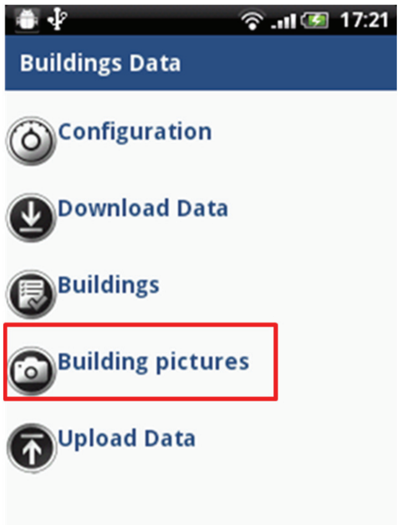
</td><td>The user can take the amount of pictures needed for the future description of materials and elements.</td></tr>
<tr><td>7.1</td><td>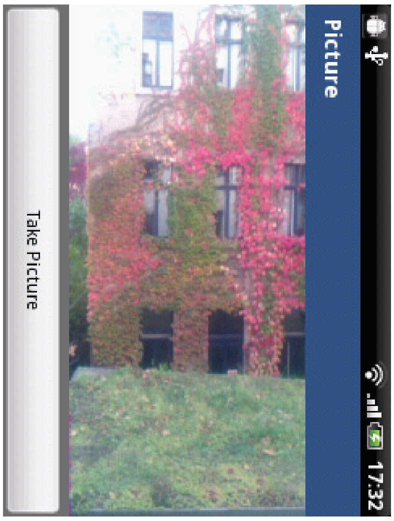
</td><td>The user can take the amount of pictures needs for the future description of materials and elements</td></tr>
<tr><td>8</td><td>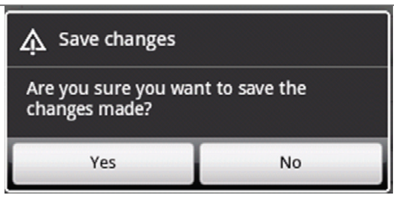
</td><td>Once the information is filled, the user saves the changes.</td></tr>
</table>

9		Then the user connects the device to the server through Wi-Fi and uploads the data collected in field.
10	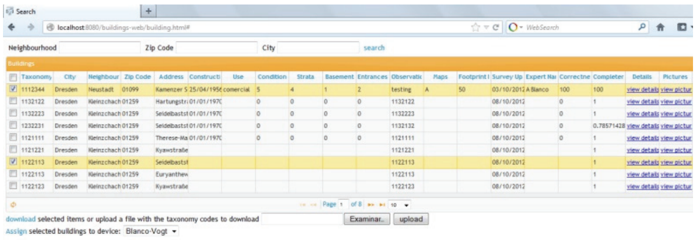	The final users can visualise and download the required information through the web application.

Appendix D4: Tools for the analysts

The following table shows the structure for storing the information of depth-physical impact function for a taxonomic code for every settlement; for every row, all fields should be filled. This table should be completed by the analyst expert and exported to a (plain) text format.

Table D4.1: Structure of the table for the input data of the depth-physical impact function

Fields of the table (flat text)	Definition	Type
Taxonomic_Code	Identification of the building type	*Text*
Height_Lower	Lower height of the component	*Double*
Height_Upper	Upper height of the component	*Double*
Susceptible_Volume	Susceptible volume for a water depth	*Double*
Volume_Building	Total volume material of the house	*Double*
Max_Susceptible_Vol	Maximum susceptible volume if the house is covered by water	*Double*
Perc_Susceptibility	Ratio of the susceptible volume for a water depth and the total volume material of the house	*Double*
Standard_Deviation	Standard deviation of susceptibility for a water depth	*Double*

Table D4.2:Example of the fields of the depth-physical impact function

Taxonomic_Code	Height_Upper	Height_Lower	Susceptible_Volume	Volume_Building	Max_Susceptible_Vol	Perc_Susceptibility	Standard_Deviation
'3222212'	-3.5	-3.6	1.00	629.04	348.00	0.00	0.05
'3222212'	-3.4	-3.5	3.51	629.04	348.00	0.01	0.05
'3222212'	-3.3	-3.4	6.02	629.04	348.00	0.01	0.05
'3222212'	-3.2	-3.3	8.53	629.04	348.00	0.01	0.05

Appendix D5: Tool for the end user

This script allows the user to integrate the data for the estimation of the potential degraded volume of every building for a water depth. For this aim, the user enters the building polygons with their taxonomic codes, the inundation scenario and the table with the information on the depth-physical impact function. The user should select the output folder for storing a geo-database. The user can download existing information on depth-physical impact functions from the database through the web application (see Appendix D3, Table D3.1, Step 3).

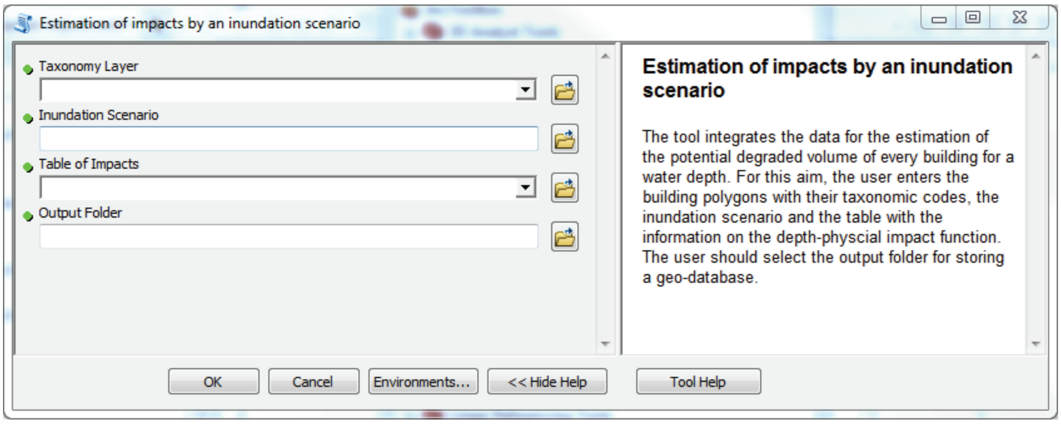

Figure D5.1: Input window for the estimation of building flood susceptibility

Appendix E: Relation of the taxonomic code to the urban structure types (IOER) – "Kleinzschachwitz"

	UST-IOER																								
Taxonomic code	**EE3**	**EE4**	**EE5**	**EE7**	**ER4**	**ER5**	**ER7**	**FOR**	**HH3**	**IP3**	**L2**	**ME3**	**ME4**	**ME7**	**MR3**	**MR4**	**MR5**	**MR7**	**SH3**	**SSP**	**TG**	**VE**	**VH**	**x**		**Total**
'1111111'	1	2	5	7			3							3			1							40	2	64
'1111211'	1	1	4	6																				17	4	33
'1121111'	1		5	11		2	4		6		1	1		2								2	1	91	7	134
'1121112'		5	6	4		22			3			1		1										17	2	61
'1121211'	8	4	6	5								4		1			1							46	4	79
'1122113'						22	3																	2		27
'1122114'						18	7					3			2									4		34
'2111211'	2	21	24	25		1	3					5	3	6				3						8		101
'2112211'	3	14	4	4	1							7	6	1												40
'2121111'		2	4	3		1	4	1	1		1	4		6										24	2	53
'2121211'	9	21	14	11	17	2	1		2		2	13	9	9	1		1				1			14	3	130
'2122211'	4	13	10	2	1							6	1	3	1									2		43
'2211111'				3								17	1	12										1		34
'2211211'	3	2	1	10	1		6					26	2	20										1		72
'2212211'	4	1	1	3					1	1		33	7	6	1											58
'2221211'	3	1		2	6	4	9			1	4	15	7	38	1	7		6		1				5		110
'2222211'	4	1	2	3	1	2	3				3	24	6	9	1			1						9		69
'3222211'	2			1							2	11		1	4			3	1							25
Total	**45**	**88**	**86**	**100**	**27**	**74**	**43**	**1**	**12**	**2**	**13**	**167**	**42**	**118**	**11**	**7**	**3**	**13**	**1**	**1**	**1**	**2**	**1**	**281**	**24**	**1167**

When comparing the building taxonomic code with the building types of UST, some matches were found. However the description of the UST classification does not match the building in the same category. UST contains the limit walls between properties and detailed forms of the building from the cadastral data.

Appendix F: Clustering of buildings to taxonomic codes – "Kleinzschachwitz"

'3222211' (25 buildings)	Three to four stories, footprint size 150-500 m^2, rectangular form in the terrain, complex form, steep roof; open space area larger than 66 % and single building

Berthold-Haupt-Straße 80
UST: ME 7
Taxonomic code 3322211
Representative building 3222211
Matching 92.8 %

Kleinzschachwitzer Ufer 70
UST: ME 3
Taxonomic code 3222211
Representative building 3222211
Matching 100 %

Zschierener Straße 5
UST: SH 3
Taxonomic code 3322211
Representative building 3222211
Matching 92.8 %

Inselstraße 4
UST: ME 3
Taxonomic code 3222211
Representative building 3222211
Matching 100 %

Peter-Schmoll-Straße 3
UST: EE 3
Taxonomic code 3222211
Representative building 3222211
Matching 100 %

Freystraße 1 b
UST: ME 3
Taxonomic code 3222211
Representative building 3222211
Matching 100 %

Kurhausstraße 16
UST: MR 3
Taxonomic code 3222211
Representative building 3222211
Matching 100 %

Kyawstraße 24
UST: EE 3
Taxonomic code 3222211
Representative building 3222211
Matching 100 %

Putjatinstraße 14
UST: MR 3
Taxonomic code 3222212
Representative building 3222211
Matching 92.8 %

Putjatinstraße 1
UST: MR 7
Taxonomic code 3322211
Representative building 3222211
Matching 92.8 %

Hartungstraße 2
UST: MR 3
Taxonomic code 3322111
Representative building 3222211
Matching 85.7 %

Putjatinstraße 24
UST: ME 7
Taxonomic code 3222211
Representative building 3222211
Matching 100 %

'*2211211*'[1] (72 buildings)	Two to three stories, footprint size 150-500 m^2, square form in the terrain, simple form, steep roof, open space area larger than 66 % and single building

Hosterwitzer Straße 20
UST: ME 3
Taxonomic code 2211211
Representative building 2211211
Matching 100 %

Hosterwitzer Straße 18
UST: ME 3
Taxonomic code 2211211
Representative building 2211211
Matching 100 %

Hosterwitzer Straße 16
UST: ME 3
Taxonomic code 2211211
Representative building 2211211
Matching 100 %

Kurhausstraße 25
UST: ME 3
Taxonomic code 3211211
Representative building 2211211
Matching 92.8 %

Freischützstraße 1
UST: ME 3
Taxonomic code 3211211
Representative building 2211211
Matching 92.8 %

Meußlitzer Straße 62
UST: ME 3
Taxonomic code 2211211
Representative building 2211211
Matching 100 %

Keppgrundstraße 10
UST: ME 7
Taxonomic code 2211211
Representative building 2211211
Matching 100 %

Keppgrundstraße 6
UST: ME 7
Taxonomic code 3211211
Representative building 2211211
Matching 92.8 %

Meußlitzer Straße 49
UST: ME 7
Taxonomic code 2211211
Representative building 2211211
Matching 100 %

[1] All the pictures of the buildings captured from Google Street View.

'2221211' (110 buildings)	Two to three stories, footprint size 150-500 m², rectangular form in the terrain, simple form, steep roof, open space area larger than 66 % and single building

Am Putjatinpark 2
UST: MR 7
Taxonomic code 2221211
Representative building 2221211
Matching 100 %

Putjatinstraße 9
UST: ME 7
Taxonomic code 2221211
Representative building 2221211
Matching 100 %

Kurhausstraße 6
UST: MR 3
Taxonomic code 3221211
Representative building 2221211
Matching 92.8 %

Fanny-Lewald-Straße 3
UST: ME 7
Taxonomic code 2221211
Representative building 2221211
Matching 100 %

Thömelstraße 14
UST: ME 7
Taxonomic code 2221211
Representative building 2221211
Matching 100 %

Fanny-Lewald-Straße 4
UST: ME 3
Taxonomic code 2221211
Representative building 2221211
Matching 100 %

Kyawstraße 1
UST: ME 3
Taxonomic code 2221211
Representative building 2221211
Matching 100 %

Meußlitzer Straße 47
UST: ME 7
Taxonomic code 2221211
Representative building 2221211
Matching 100 %

Meußlitzer Straße 76
UST: X
Taxonomic code 2221211
Representative building 2221211
Matching 100 %

'2121211' (128 buildings)	Two to three stories, footprint size lower than 150 m², rectangular form in the terrain, simple form, steep roof, open space area larger than 66 % and single building

August-Röckel-Straße 8
UST: ME 4
Taxonomic code 2121211
Representative building 2121211
Matching 100 %

August-Röckel-Straße 14
UST: ME 4
Taxonomic code 2121211
Representative building 2121211
Matching 100 %

Freischützstraße 24
UST: ME 4
Taxonomic code 2121211
Representative building: 2121211
Matching 100 %

Freischützstraße 19
UST: ME 4
Taxonomic code 2121211
Representative building 2121211
Matching 100 %

Meußlitzer Straße 20
UST: EE 7
Taxonomic code 2121211
Representative building 2121211
Matching 100 %

Meußlitzer Straße 56
UST: EE 4
Taxonomic code 2121211
Representative building 2121211
Matching 100 %

Meußlitzer Straße 63
UST: L 2
Taxonomic code 2121211
Representative building 2121211
Matching 100 %

Meußlitzer Straße 61
UST: M 4
Taxonomic code 2121211
Representative building 2121211
Matching 100 %

Zschierener Straße 14
UST: ME 3
Taxonomic code 2121211
Representative building 2121211
Matching 100 %

‘2111211’ (101 buildings)	One to two stories, footprint size lower than 150 m², square form in the terrain, simple form, steep roof , open space area larger than 66 % and single building

Neue Straße 22
UST: EE 4
Taxonomic code 2111211
Representative building 2111211
Matching 100 %

Kyawstraße 8a
UST: EE 3
Taxonomic code 2111211
Representative building 2111211
Matching 100 %

Berthold-Haupt-Straße 127
UST: EE 5
Taxonomic code 2111211
Representative building 2111211
Matching 100 %

August-Röckel-Straße 5
UST: EE 5
Taxonomic code 2111211
Representative building 2111211
Matching 100 %

Freischützstraße 18a
UST: EE 4
Taxonomic code 2111211
Representative building 2111211
Matching 100 %

Hosterwitzer Straße 40
UST: EE 3
Taxonomic code 2111211
Representative building 2111211
Matching 100 %

Oberonstraße 16f
UST: ER 7
Taxonomic code 2111211
Representative building 2111211
Matching 100 %

Meußlitzer Straße 77
UST: EE 4
Taxonomic code 2111211
Representative building 2111211
Matching 100 %

Euryantheweg 3
UST: EE 5
Taxonomic code 2111211
Representative building 2111211
Matching 100 %

'1111111' (64 buildings)	One storey, footprint size lower than 150 m², square form in the terrain, simple form, flat roof, open space area larger than 66 % and single building

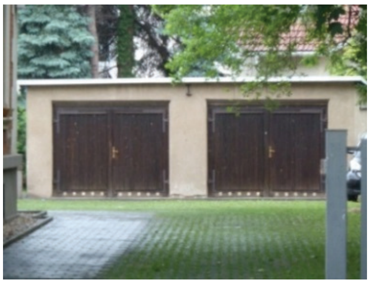

100 % matching

100 % matching

100 % matching

100 % matching

Taxonomic code: 1111112
Matching similarity: 92.3 %
Difference: Buidling is adjacent to another building

Taxonomic code: 1111125
Matching similarity: 78.5 %
Compacteness: Between 33-66 %
Building has more than three adjacent buildings

'1121111'[2] (134 buildings)	One storey, footprint size lower than 150 m², rectangular form in the terrain, simple form, flat roof, open space area larger than 66 % and single building

Am Sandberg 5

ER 5 News Siedlung

Zschierbachstrasse 5

Wilhelm-Weitling 22

Berthold-Haupt-Straße
Warehouse
One-story building

Therese-Malte-Straße 1

[2] Pictures captured from Google Street View

Appendix G: Fuzzy expert analyses for building material susceptibility – “Kleinzschachwitz”

Component	Material	y1	y2	y3	y4	Diff. y2-y1	Diff. y3-y2	Diff. y4-y3	∂	s1	s2	s3	y1*s1	y2*(s1+s2)/2	y3*(s2+s3)/2	y4*s3	sum	s1	(s1+s2)/2	(s2+s3)/2	s3	sum	b	u	a	c
Gründung	Streifenfundamente aus Natur-/Bruchstein (Sandstein/Granit)	0.40	0.50	0.50	0.60	0.1	0	0.1	0.06	- 0.73	1.00	-0.73	-0.29	0.07	0.07	-0.44	-.60	-.73	0.13	0.13	-.73	-1.2	0.50	-0.7	0.44	0.36
Gründung	Streifenfundamente aus Beton, Stampfbeton	0.20	0.30	0.30	0.40	0.1	0	0.1	0.06	-0.7	1.00	-0.73	-0.15	0.04	0.04	-0.29	-.36	-.73	0.13	0.13	-.73	-1.2	0.30	-0.7	0.24	0.36
Gründung	Flächengründung aus Stahlbeton (Bodenplatte)	0.00	0.10	0.10	0.20	0.1	0	0.1	0.06	-0.7	1.00	-0.73	0.00	0.01	0.01	-0.15	-.12	-.73	0.13	0.13	-.73	-1.2	0.10	-0.7	0.04	0.16
Fenster	Holzfenster/Holzsprossenfenster	0.80	0.90	0.90	1.00	0.1	0	0.1	0.06	-0.7	1.00	-0.73	-0.59	0.12	0.12	-0.73	- 1.08	-.73	0.13	0.13	-.73	-1.2	0.90	-0.7	0.84	0.96
Fenster	Kunststofffenster	0.80	0.90	0.90	1.00	0.1	0	0.1	0.06	-0.7	1.00	-0.73	-0.59	0.12	0.12	-0.73	- 1.08	-.73	0.13	0.13	-.73	-1.2	0.90	-0.7	0.84	0.96
Fenster	Metallfenster	0.40	0.50	0.50	0.60	0.1	0	0.1	0.06	-0.7	1.00	-0.73	-0.29	0.07	0.07	-0.44	- 0.60	-.73	0.13	0.13	-.73	-1.2	0.50	-0.7	0.44	0.56
Außenwände	Bruchsteinmauerwerk (Granit/Sandstein)	0.20	0.50	0.50	0.80	0.3	0	0.3	0.17	-0.7	1.00	-0.73	-0.15	0.07	0.07	-0.59	-.60	-.73	0.13	0.13	-.73	-1.2	0.50	-0.7	0.33	0.67
Außenwände	Stahlbeton (Weiße Wanne)	0.00	0.10	0.10	0.20	0.1	0	0.1	0.06	-0.7	1.00	-0.73	0.00	0.01	0.01	-0.15	-.12	-.73	0.13	0.13	-.73	-1.2	0.10	-0.7	0.04	0.16
Außenwände	Mauerwerk Sandstein	0.40	0.60	0.60	0.80	0.2	0	0.2	0.12	-0.7	1.00	-0.73	-0.29	0.08	0.08	-0.59	-.72	-.73	0.13	0.13	-.73	-1.2	0.60	-0.7	0.48	0.72
Außenwände	Mauerwerk Kalksandstein	0.40	0.50	0.50	0.60	0.1	0	0.1	0.06	-0.7	1.00	-0.73	-0.29	0.07	0.07	-0.44	-.60	-.73	0.13	0.13	-.73	-1.2	0.50	-0.7	0.44	0.56
Außenwände	Ziegelmauerwerk	0.40	0.50	0.50	0.60	0.1	0	0.1	0.06	-0.7	1.00	-0.73	-0.29	0.07	0.07	-0.44	-.60	-.73	0.13	0.13	-.73	-1.2	0.50	-0.7	0.44	0.56
Kellerdecke	Preußische Kappendecke	0.40	0.50	0.50	0.60	0.1	0	0.1	0.06	-0.7	1.00	-0.73	-0.29	0.07	0.07	-0.44	-.60	-.73	0.13	0.13	-.73	-1.2	0.50	-0.7	0.44	0.56
Kellerdecke	Stahlbetondecke	0.00	0.10	0.10	0.20	0.1	0	0.1	0.06	-0.7	1.00	-0.73	0.00	0.01	0.01	-0.15	-.12	-.73	0.13	0.13	-.73	-1.2	0.10	-0.7	0.04	0.16
Kellerdecke	Lagerhölzer und Schüttung	1.00	0.96	0.96	1.00	-.04	0	0.04	0.04	2.0	1.00	0.00	2.00	1.44	0.48	0.00	3.92	2.00	1.50	0.50	0.00	4.0	0.98	0.00	1.00	1.00
Kellerdecke	Füllkörperdecke (FB-Decke)	0.20	0.30	0.30	0.40	0.1	0	0.1	0.06	-0.7	1.00	-0.73	-0.15	0.04	0.04	-0.29	-.36	-.73	0.13	0.13	-.73	-1.2	0.30	-0.7	0.24	0.36
Kellerdecke	Stahlbetonhohldielendecke	0.40	0.36	0.42	0.40	-.04	0.06	-.02	0.05	1.7	- 0.13	1.38	0.70	0.29	0.26	0.55	1.81	1.76	0.81	0.62	1.38	4.6	0.40	-0.1	0.40	0.40
Kellertreppe	Stahlbeton Bodenfliesen	0.20	0.30	0.30	0.40	0.1	0	0.1	0.06	-0.7	1.00	-0.73	-0.15	0.04	0.04	-0.29	-.36	-.73	0.13	0.13	-.73	-1.2	0.30	-0.7	0.24	0.36
Kellertreppe	Betonstufen	0.20	0.16	0.24	0.20	-.04	0.08	-.04	0.07	1.6	- 0.15	1.58	0.32	0.11	0.17	0.32	0.92	1.58	0.71	0.71	1.58	4.58	0.20	-.15	0.20	0.20
Kellertreppe, Geschosstreppe	Sandstein	0.40	0.42	0.38	0.40	0.02	-.04	0.02	0.03	0.42	2.15	0.42	0.17	0.54	0.49	0.17	1.37	0.42	1.29	1.29	0.42	3.42	0.40	0.42	0.40	0.40
Fußboden	Vollziegel	0.40	0.50	0.50	0.60	0.1	0	0.1	0.06	-.73	1.00	-0.73	-0.29	0.07	0.07	-0.44	-.60	-.73	0.13	0.13	-.73	-1.2	0.50	-.73	0.44	0.56
Fußboden	Verbundestrich mit Schutzanstrich	0.20	0.16	0.24	0.20	-.04	0.08	-.04	0.07	1.58	- 0.15	1.58	0.32	0.11	0.17	0.32	0.92	1.58	0.71	0.71	1.58	4.6	0.20	-.15	0.20	0.20
Fußboden	Schwimmender Estrich auf Schüttung	0.80	0.76	0.84	0.80	- 0.04	0.08	- 0.04	0.07	1.58	- 0.15	1.58	1.26	0.54	0.60	1.26	3.66	1.58	0.71	0.71	1.58	4.6	0.80	- 0.15	0.80	0.80
Fußboden	Dielung auf Holzbalkendecke Fliesen- oder Holzbelag	1.00	0.96	0.98	1.00	- 0.04	0.02	0.02	0.03	2.15	0.42	0.42	2.15	1.24	0.41	0.42	4.23	2.15	1.29	0.42	0.42	4.29	0.99	0.42	1.01	1.01
Fußboden	Teppichbodenbelag	1.00	0.96	0.98	1.00	-.04	0.02	0.02	0.03	2.15	0.42	0.42	2.15	1.24	0.41	0.42	4.23	2.15	1.29	0.42	0.42	4.29	0.99	0.42	1.01	1.01
Fußboden	Laminat	1.00	0.96	0.98	1.00	-.04	0.02	0.02	0.03	2.15	0.42	0.42	2.15	1.24	0.41	0.42	4.23	2.15	1.29	0.42	0.42	4.29	0.99	0.42	1.01	1.01
Geschossdecke	Holzbalkendecke als Einschubdecke	0.80	0.76	0.84	0.80	-.04	0.08	- 0.04	0.07	1.58	- 0.15	1.58	1.26	0.54	0.60	1.26	3.66	1.58	0.71	0.71	1.58	4.58	0.80	- 0.15	0.80	0.80
Geschossdecke	Stahlbeton	0.00	0.10	0.10	0.20	0.1	0	0.1	0.06	-0.7	1.00	-0.73	0.00	0.01	0.01	-0.15	-.12	-.73	0.13	0.13	-.73	-1.2	0.10	-.73	0.04	0.16
Geschossdecke	Holzbalkendecke mit Dämmung und Dielung	0.80	0.76	0.84	0.80	-.04	0.08	-.04	0.07	1.58	- 0.15	1.58	1.26	0.54	0.60	1.26	3.66	1.58	0.71	0.71	1.58	4.58	0.80	-.15	0.80	0.80

Appendix H: Reconstruction of an inundation model in “Barrio Sur” and “La Peña”

A scenario of inundation is drawn up for the susceptibility analysis. The scenario allows to display the susceptibility values by a water depth. There are many approaches for flood modelling in one, two or three dimensions. All of them use digital terrain models in combination with the water level, and the values are commonly converted from discharge values. Hydraulic and hydrodynamic approaches for modelling the properties of the flowing water usually depend on different types of variables, such as water height, river bathymetric profiles, topographic contours, inclination and exposure of the terrain as well as roughness coefficients of the earth's surface (Krueger, 2009).

The hydraulic complexity of the Magdalena River in this sector with many tributaries, lakes, wetlands, swamps and marshes makes it difficult to collect the required variables for modelling a reliable flood scenario. Moreover, detailed information on the above-mentioned variables for a flood modelling are not available in this sector. A consistent flood model must be created in further works. Therefore, a simplified reconstruction scenario from water depth and flooded area was estimated taking into account the following data sources:

- Flooded area interpreted by SIAC et al. (2011) using satellite images (see Figure H.1).
- The return period of of maximum water levels (see Table H.1) and the water level gauge of the river provided (see Figure H.2) by IDEAM (2010b).
- A digital terrain model generated with the photogrammetric technique (see Figure 61 and Figure 80).
- The water depth reached at several houses in the pilot site, taken from pictures and measured with GPS in the field (see Figure H.2 and Figure H.3).

Flooded area interpreted using satellite images: The ICDE (2011) provides Web Map Services of the flood emergency 2010-2011. The red colour (see Figure H.1) displays the areas covered by water, as interpreted from satellite images.

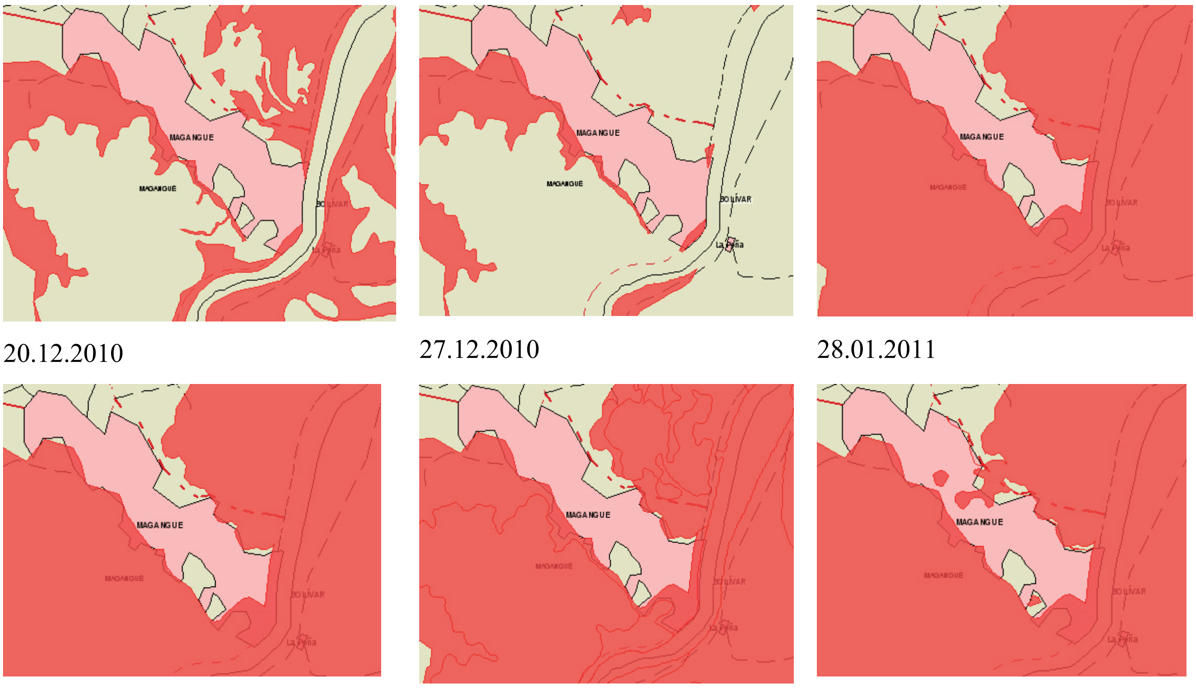

20.12.2010 27.12.2010 28.01.2011

23.02.2011 16.03.2011 06.06.2011

Figure H.1: Flooded areas in the pilot site of Colombia, source ICDE

The water level gauge *"Magangué":* According to Cormagdalena (2000), the water level gauge Magangué has the following description: coordinates 9°14'02.52695 N 74°44'35,28044 W, altitude 9.241 m[3], abscissa 257; water level: average daily 16.30 m ASL, maximum 18.94 m ASL and minimum 10.9 m ASL. The return periode is depicted in Table H.1 and the water level in Figure H.2.

Table H.1: Return period of maximum water levels – Magangué

Return period maximum levels	**Magangué [m]**
5	18.71
10	18.88
20	18.99
50	19.08
100	19.12

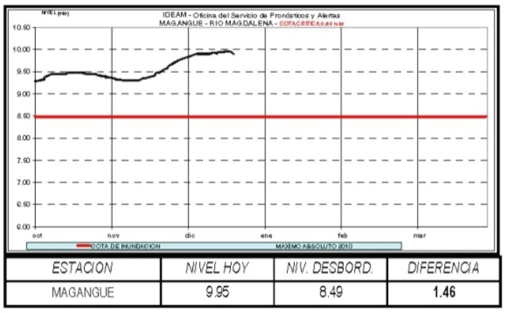

Date: 20.12.2010. Water level: 19.191 m.a.s.l.

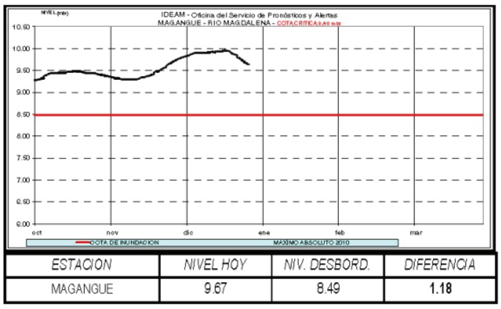

Date: 27.12.2010. Water level: 18.911 m.a.s.l.

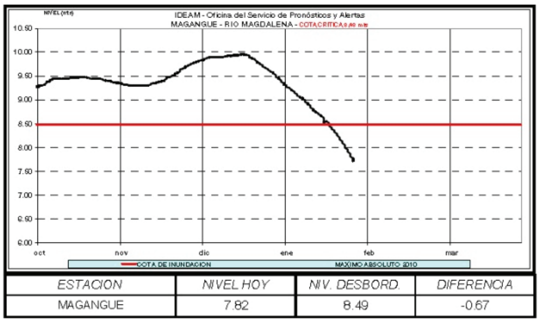

Date: 28.01.2011. Water level: 16.761 m.a.s.l.

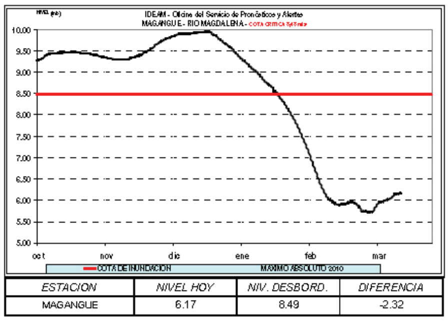

Date: 16.03.2011. Water level 15.411 m.a.s.l.

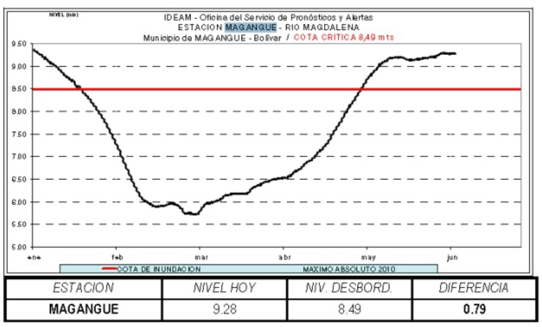

Date: 06.06.2011. Water level: 18.521 m.a.s.l.

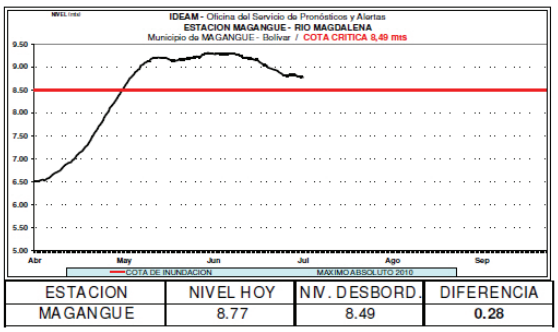

Date: 06.07.2011. Water level: 18.011 m.a.s.l

Figure H.2: Water level in Magangué gauge, source IDEAM

[3] Coordinates in Reference System Ellipsoid Bogotá, converted to Magna-SIRGAS Gauss-Krueger: 1512664.246 N, 927231.358 E, source: MagnaSirgas Pro 3-IGAC

The water level decreased in mid-December 2010, but increased again in mid-February 2011, leaving the prone areas inundated for about ten months.

Flood level rose to several houses: The following pictures show how the flood reached some houses.

Building 702

Building 712

Building 715

Building 728

Building 724

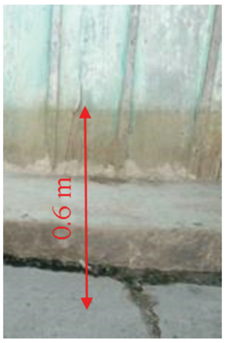

Building 706

Figure H.3: Flood level rose to some buildings – “Barrio Sur”

Building 776

Building 754

Building 756

Building 781

Figure H.4: Flood level rose to some buildings – “La Peña”

Reconstruction of a flood model: This is an attempt to reconstruct the water level on December 20th 2010 during the 100-year return period. The water depth at the houses is then converted to the altimeter values having the DTM as reference. After that, the values are interpolated using different interpolation models (Figure H.5).

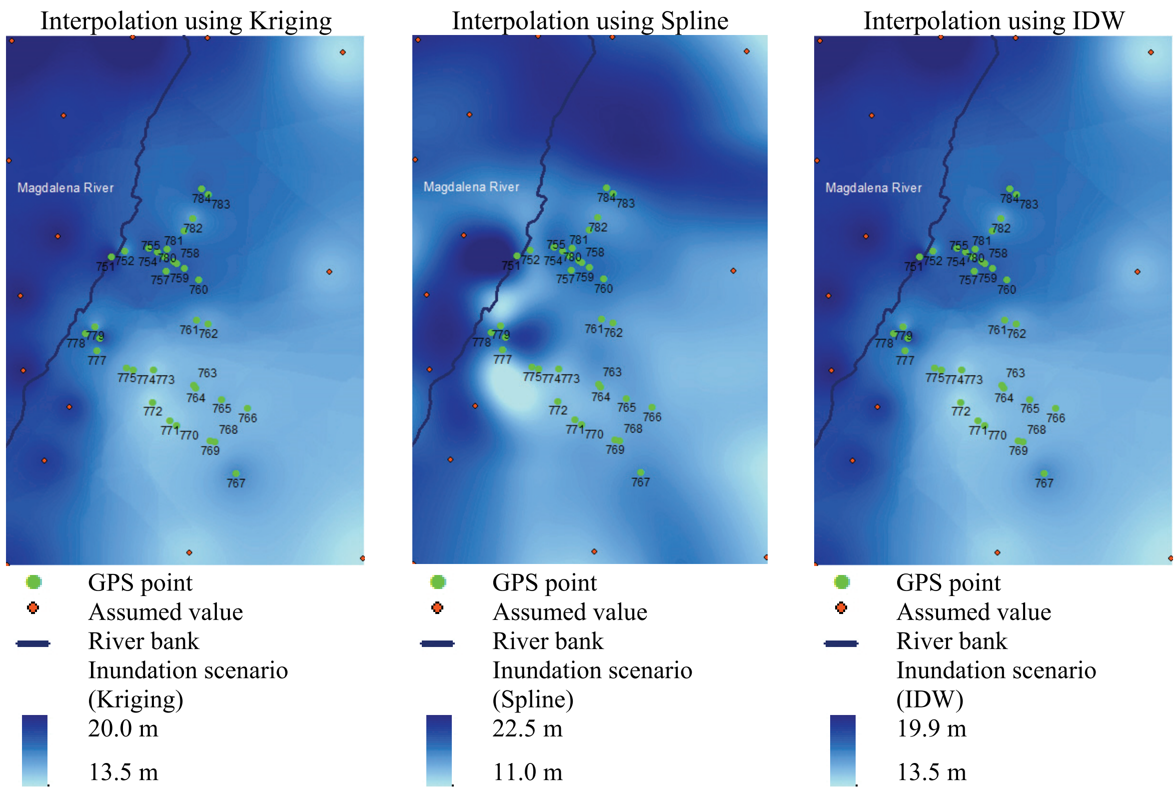

Figure H.5: Interpolation models for a water table – “La Peña”

The three models for a water table assumption show a different range of values. The IDW model is selected because it fits the range of values expected for a 100-year flood, taking into account that the slight differences in the water depth estimation can result in considerable inaccuracies in the estimation of potential impacts using depth-physical impact functions.

This approach is greatly simplified thanks to the high-resolution DTM. The variables for hydraulic or hydrodynamic calculations are disregarded in this approach in order to reconstruct the real conditions of the 2010/2011 flood. The water depth results from the subtraction of raster maps: the values of the DTM from the water table model (Figure H.6).

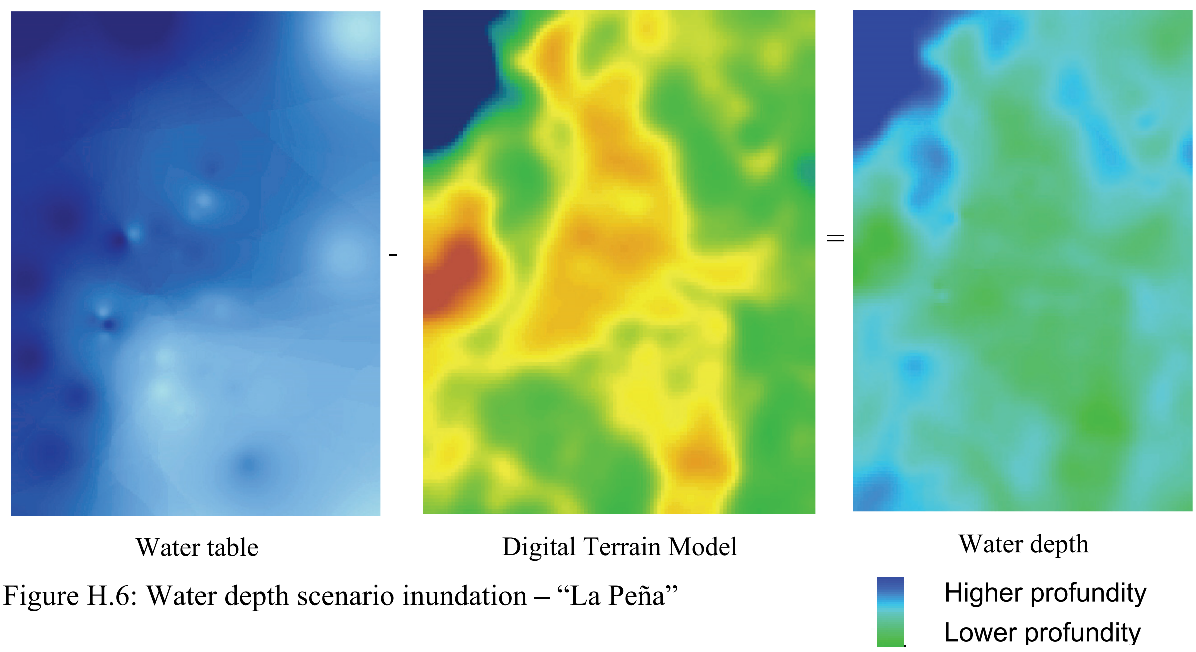

Figure H.6: Water depth scenario inundation – “La Peña”